DOT/FAA/TC-22/42

Federal Aviation Administration
William J. Hughes Technical Center
Aviation Research Division
Atlantic City International Airport
New Jersey 08405

Lift Rotor Control Power Assessment of a Lift+Cruise Configuration

September 2023

Final report

U.S. Department of Transportation
Federal Aviation Administration

NOTICE

Technical Report Documentation Page

Form DOT F 1700.7 (8-72) Reproduction of completed page authorized

1. Report No.	2. Government Accession No.	3. Recipient's Catalog No.
DOT/FAA/TC22/42		
4. Title and Subtitle Lift Rotor Control Power Assessment of a Lift+Cruise Configuration		5. Report Date September 2023
		6. Performing Organization Code
7. Author(s) Bossinger, Robert L.; Hoffler, Keith D.		8. Performing Organization Report No.
9. Performing Organization Name and Address Adaptive Aerospace Group, Inc. 1 Enterprise Parkway, Suite 340 Hampton, VA 23666		10. Work Unit No. (TRAIS)
		11. Contract or Grant No.
12. Sponsoring Agency Name and Address Federal Aviation Administration William J. Hughes Technical Center Aviation Research Division Atlantic City International Airport, NJ 08405.		13. Type of Report and Period Covered
		14. Sponsoring Agency Code

15. Supplementary Notes

FAA Sponsors: Ross Schaller and David Sizoo

16. Abstract

The recent advent of electric propulsion has freed designers to put propulsors in nonconventional locations and opened aircraft design space to novel configurations. Many electric Vertical Take-off and Landing (eVTOL) aircraft with multiple lift-rotors that require advanced control systems to manage the large number of control effectors are being presented to the FAA for certification. These aircraft generally have nonconventional fly-by-wire flight controls. Extensive understanding of the aircraft and their control effectors, their interactions, and how their use by the control system employs them is required to achieve desired aircraft response and ensure safety. Simultaneous commands to multiple axes can originate from pilot input or the flight controls even if the pilot is only commanding one axis. An understanding of the cross coupling of commands and available control power is needed. This report presents a methodology for assessing control power limitations and results from a limited application of the corresponding method to a representative multi-rotor vehicle. Some of the results emphasize the need for an extensive evaluation. One case shows that defeating envelope protection can occur due to lack of control power in an axis different from the one being commanded. Another case gives an example of a departure from controlled flight when control power priority was applied to the wrong axis for the situation. Specific and general lessons learned are presented and potential application of this method for aircraft evaluation is discussed.

17. Key Words	18. Distribution Statement
Control Power, eVTOL, Unified Flight Controls, certification, fly-by-wire, prioritization, rotor failure	This document is available to the U.S. public through the National Technical Information Service (NTIS), Springfield, Virginia 22161. This document is also available from the Federal Aviation Administration William J. Hughes Technical Center at actlibrary.tc.faa.gov.

19. Security Classif. (of this report)	20. Security Classif. (of this page)	21. No. of Pages	22. Price
Unclassified	Unclassified	177	

Contents

Figures

Tables

Acronyms

Acronym	Definition
AAG	Adaptive Aerospace Group
CMF	Cockpit Motion Facility
CP	Control Power
eVTOL	Electric Vertical Take-off and Landing
FAA	Federal Aviation Administration
FMT	Flight Mode Transition
FRT	Flight Region Transition
KGS	Knots Groundspeed
KIAS	Knots Indicated Airspeed
KTAS	Knots True Airspeed
LAT	Lateral
LCO	Limit Cycle Oscillation
LONG	Longitudinal
MSL	Mean Sea Level
NASA	National Aeronautics and Space Administration
PED	Pedal
RVLT	Revolutionary Vertical Lift Technology
UAM	Urban Air Mobility
VRS	Vortex Ring State

Symbols

Symbol	Definition	Units
AoA	Angle of attack	deg
A_Y	Y-axis Linear Acceleration	ft/s^2
g	Gravity Force	ft/s^2
hdot or $\dot{h}$	Altitude Rate	ft/s
L/W	Lift-Weight Ratio	g
L/W_{max}	Maximum Available Rotor L/W	g
N_X or n_x	Body X-axis Acceleration	g
N_Z or n_z	Body Z-axis Acceleration	g
P or p	Roll Rate	deg/s
Pdot or $\dot{p}$	Roll Acceleration	deg/s^2
Phi	Roll Angle	deg
Psi	Yaw Angle	deg
Q	Pitch Rate	deg/s
Qdot or $\dot{q}$	Pitch Acceleration	deg/s^2
R or r	Yaw Rate	deg/s
Rdot or $\dot{r}$	Yaw Acceleration	deg/s^2
Theta or θ	Pitch Angle	deg
V_{NE}	Never Exceed Velocity	ft/s
γ	Flight Path Angle	deg
$\dot{\gamma}$	Flight Path Angle Rate	deg/s

Executive summary

The recent advent of electric propulsion has freed designers to put propulsors in nonconventional locations and opened aircraft design space to novel configurations. Many Electric Vertical Take-off and Landing (eVTOL) aircraft with multiple lift-rotors that require advanced control systems to manage the large number of control effectors are being presented to the Federal Aviation Administration (FAA) for certification. These aircraft generally have nonconventional fly-by-wire flight controls. Extensive understanding of the aircraft control effectors, their interactions, and their use by the control system is required to achieve desired aircraft response and ensure safety. Simultaneous commands to multiple axes can originate from pilot input or the flight controls even if the pilot is only commanding one axis. An understanding of the cross coupling of commands and available control power is needed. This report presents a methodology for assessing control power limitations and results from a limited application of the corresponding method to a representative multi-rotor vehicle. Some of the results emphasize the need for an extensive evaluation. One case shows that defeating envelope protection can occur due to lack of control power in an axis different from the one being commanded. Another case gives an example of a departure from controlled flight when control power priority was applied to the wrong axis for the situation. Specific and general lessons learned are presented and potential application of this method for aircraft evaluation is discussed.

1 Introduction

The recent advent of electric propulsion has freed designers to put propulsors in nonconventional locations and opened aircraft design space to novel configurations. Many eVTOL aircraft with multiple lift-rotors that require advanced control systems to manage the large number of control effectors are being presented to the FAA for certification. Extensive understanding of the aircraft control effectors, their interactions, and their use by the control system is required to achieve desired aircraft response and ensure safety.

This report presents a methodology for evaluating the control power authority of a full authority fly-by-wire aircraft. A limited application of the method is applied to a multi-rotor vehicle model originally developed by Adaptive Aerospace Group (AAG) and used to evaluate means of compliance for certification of aircraft with nonconventional flight controls (Hoffler, Duerksen, Bossinger, Martos, & Mitchell, 2022). The reference also describes the vehicle and simulation in more detail. The model was loosely based on NASA's Revolutionary Vertical Lift Technology (RVLT) Lift+Cruise concept vehicle shown in Figure 1. The nonconventional controls implemented were similar to the F-35B unified flight controls (Denham Jr & Paines, 2008). Initial analysis of the Lift+Cruise vehicle model indicated rotor control authority was insufficient for maneuvering and handling qualities. The rotor control power was increased for the means of compliance work to ensure the maneuvers could be performed. However, an assessment was not made to evaluate the control power margin trade space or to determine a minimum control power that would be sufficient. This report addresses control power requirements in more detail.

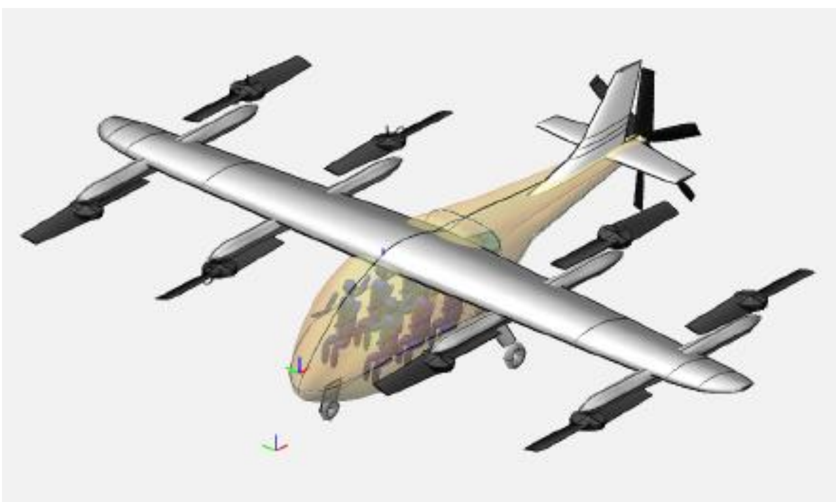

Figure 1. NASA's RVLT Lift+Cruise concept vehicle

Generally, fixed-wing aircraft will have consistent control power authority in each axis regardless of the magnitude of control power used in other axes for a given flight condition. As an example: aileron deflection does not impact elevator control authority; they are essentially decoupled. This independent control power authority for a single axis does not apply for single-rotor aircraft, multi-rotor aircraft, and some more complex fixed wing aircraft (e.g., flaperons and elevons). For most traditional single and multi-rotor aircraft, all rotors are used to generate the necessary lift to achieve the commanded forces and/or moments (control power) and therefore are interdependent. A control effector applied in any axis has a limiting effect on the control power authority of all other axes that may or may not be significant to aircraft controllability. The interaction of available control power between the primary and secondary axes is the focus of this paper. The primary axis refers to the axis to which the command is applied, and the secondary axes are all other axes.

This report describes an evaluation of lift rotor control power margin and its effect on vehicle performance for the subject multi-rotor aircraft. The approach is generic and applicable to any related vehicle. The specific results apply to only this vehicle, but general insights gained are presented that can be useful to designers and FAA evaluators.

2 Vehicle model

The vehicle control inceptors included a side stick with longitudinal (Long.) and lateral (Lat.) displacements, pedals (Ped.), and a longitudinal linear inceptor. Figure 2 shows the commands associated with each inceptor. These commands change slightly depending on current and commanded airspeed. This transition region generally occurs between ten knots groundspeed (KGS) and 35 knots indicated airspeed (KIAS). It will be referred to as the flight mode transition (FMT). Section one (Hoffler, Duerksen, Bossinger, Martos, & Mitchell, 2022) offers more detail on the aircraft and control system.

The control system was based on the F-35B's "Unified Control Law Concept" (Denham Jr & Paines, 2008) which aims to avoid the need for conscious mode changes between wing-borne and powered-lift flight regimes by ensuring that the axis of control associated with a given inceptor remains essentially the same for both flight regimes and across the flight envelope.

Figure 3 depicts how automatic transitions from rotor-borne to wing-borne flight are implemented in the control system. The transition region for aerodynamic surface control power is much wider and begins as low as 30 KIAS and ends at 105 KIAS and, along with the lift source transition, will collectively be referred to as the flight region transition (FRT). The figure shows the "mixing" region in blue which is the midpoint for FRT and where the most apparent switch in the predominent lift source is for the relevent time histories. The range for the aerodynamic surface control power portion of the FRT is not displayed because it is designed to go unnoticed by the pilot. Figure 3 also shows how pitch is used to accelerate and decelerate the aircraft when rotor-borne. This is not directly controlled by the pilot. The only way the pilot has control over these features is by commanding the speed associated with them. It is important to note that flight mode as shown in Figure 2 does not equate to flight region in Figure 3. Flight region indicates the source of control power for a given part of the flight envelope and will be important for reviewing the results of this analysis. This indicates the control system was designed to turn off the rotors at speeds the aircraft can fly on the wing. There are also envelope protections associated with the different flight regions. The protections are discussed in the Denham Jr. & Paines (2008) and addressed herein when applicable.

All transitions were automatic between the flight control modes depicted in Figure 2 and the physical flight mode, rotor, or wing lift depicted in Figure 3.

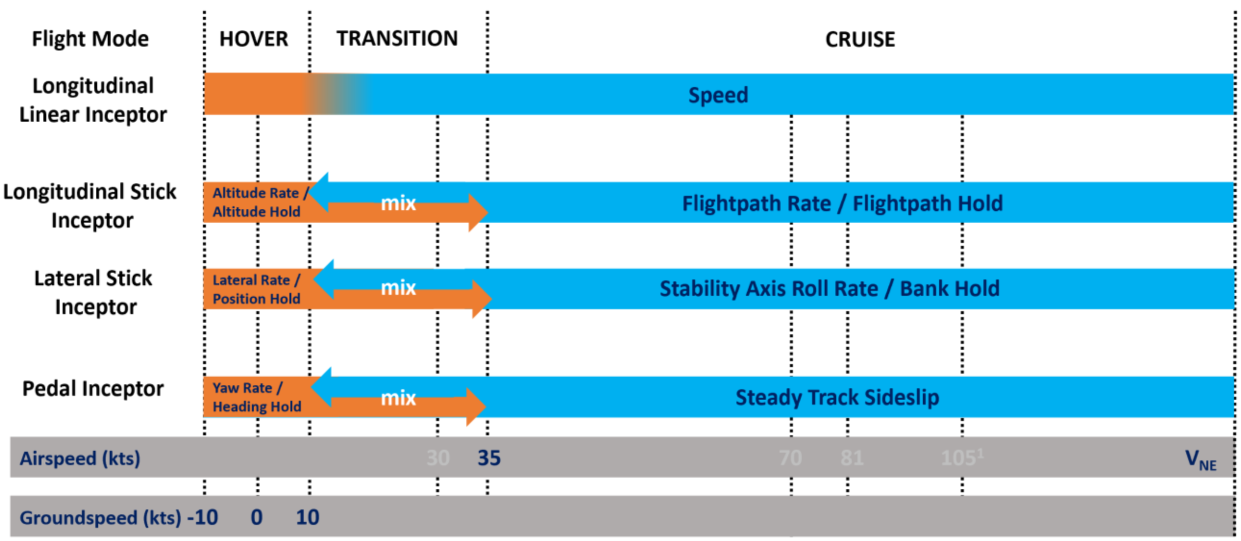

Figure 2. Flight control mapping

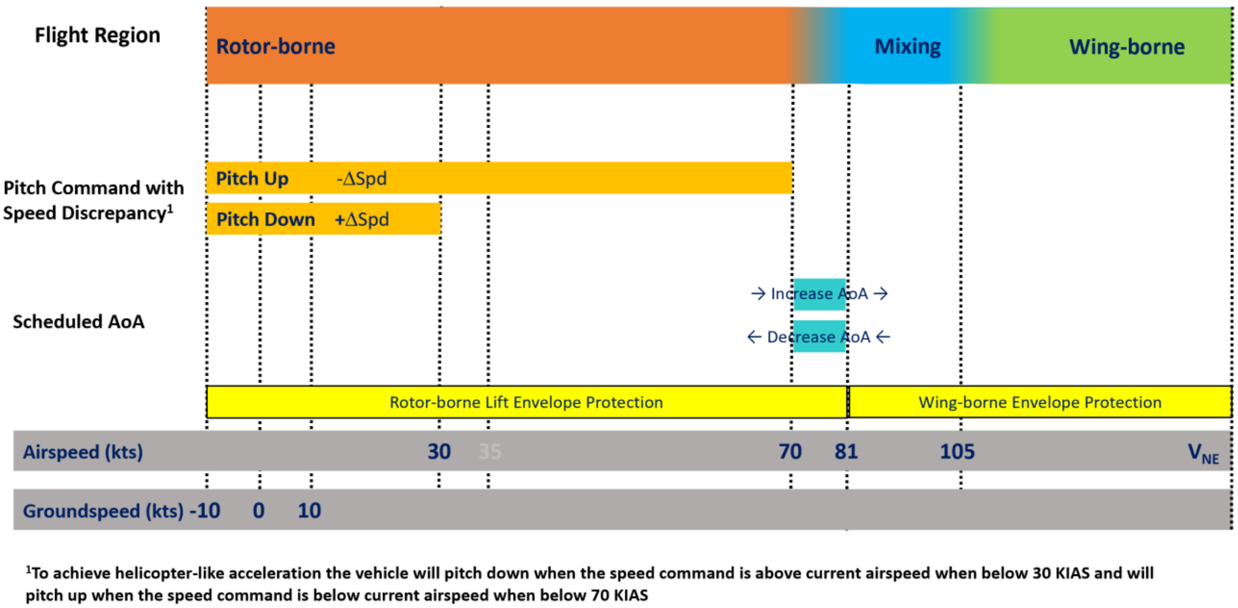

Figure 3. Lift mode and pitch changes associated with acceleration/deceleration commands

3 Method

3.1 Overview

The control power evaluation method flowchart is shown in Figure 4. The general principle can be broken down into three sections: developing the test matrix, running the test cases, and analyzing the results. The results of the analysis may justify the need to change the original test matrix and/or make changes to the vehicle or control system design. The test matrix should consider aircraft configuration, flight envelope, and command input factors. The factors explored can vary throughout the flight envelope to include normal operations. However, to evaluate the control power of the aircraft, test cases are necessary at the edges of the flight envelope and where configuration changes occur. Some examples of configuration changes are listed below and are originally found in section 3.1.2 of (Hoffler, Duerksen, Bossinger, Martos, & Mitchell, 2022).

- Landing gear retraction or extension
- Nacelle tilt
- Flap deployment or retraction
- Changing roll control from ailerons to rotors

- Control law changes
- Changing from an air mass referenced control system to an earth referenced control system
- Changing from a vertical speed command to a flight path angle rate ($\dot{\gamma}$) command
- Changing from "normal mode" to terrain protection
- Transition from "manual flying" to "coupled" on an approach

In essence, any change of the aircraft that can cause an alteration in the aircraft's operational characteristics is considered a configuration change. This definition of configuration is expanded beyond the definition in ADS-33E-PRF (2000) to include digital flight system mode changes that may have significant effects on aircraft behavior.

A limited application of the method is presented in this report highlighting significant discoveries. It would not be sufficient for full aircraft evaluation.

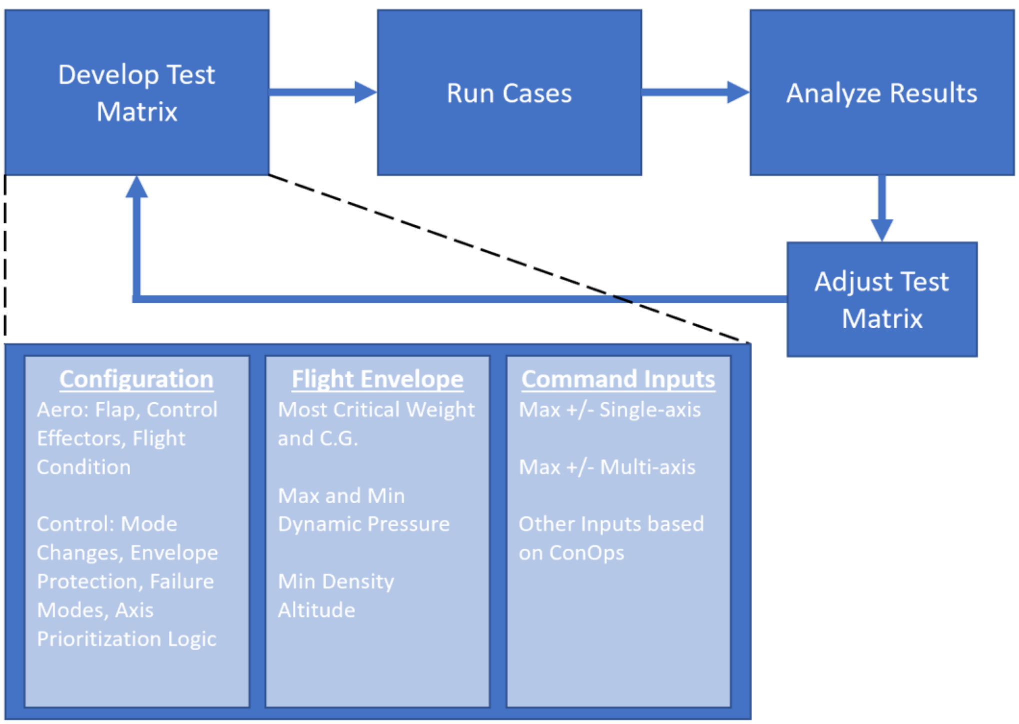

Figure 4. Control power analysis method

3.2 Limited application

Maximum available rotor Lift-Weight Ratio (L/W_{max}) and airspeed were the only two configuration and flight condition factors analyzed for this implementation of the control power analysis method. L/W_{max} was adjusted by changing the coefficient of thrust for each rotor, which maintains the same dimensions of the Lift+Cruise concept vehicle while varying rotor lift performance.

Airspeed was a factor tied directly with the control mapping for the vehicle. The Unified Control Law implementation used speed to trigger FMT and FRT. The range of speeds analyzed herein was stationary hover to 80 KIAS. Higher speeds were not analyzed due to the control system dedicating most of the commanded moments to the aerodynamic surfaces (Figure 3) as opposed to the rotors, which are the focus for this report. The control system begins allocating a small amount of control authority to the aerodynamic surfaces as low as the 40 KIAS test point but is still predominately in the rotor-borne region. When observing the response characteristics of the aircraft it is important to note when FMT occurs which can be observed in Figure 2. Mode changes alter the response type and duration.

Maximum step deflections were performed for every pilot inceptor. Longitudinal linear inceptor (speed command) also has step inputs equivalent to 26.5% of the total range above or below the initial speed. This value is the minimum deflection required to command a speed in the next adjacent flight mode from the initial speed. Lateral side stick and pedal vehicle response were symmetric for positive and negative commands so only positive inputs were made for the single-axis test matrix. A half-longitudinal stick deflection was also evaluated because pilots rarely used full deflections.

Rotor failures can be triggered in the simulation at any point during flight and with any variation of failure configuration. Multiple rotors can be failed simultaneously but the maximum number of failures evaluated was two (Hoffler, Duerksen, Bossinger, Martos, & Mitchell, 2022). Failing two rotors almost always resulted in settling to the ground and sometimes in departure from controlled flight even with 2 g L/W_{max}. Only single rotor failures were investigated for this report, i.e., rotors one and two were failed individually (Figure 5). The limited number of rotor failures was suitable for demonstrating this analysis method. However, for a full evaluation this aircraft would require assessment of all rotor failures on one side. It should be noted that these assumptions about rotor failure redundancy are highly dependent on the vehicle configuration. A designer or evaluator must have a detailed understanding of the aircraft to exclude redundant rotor failure test-points. For example, an aircraft with rotors that are not counter rotating on opposite sides of the aircraft would need failures of all rotors to be investigated because of a lack of symmetry.

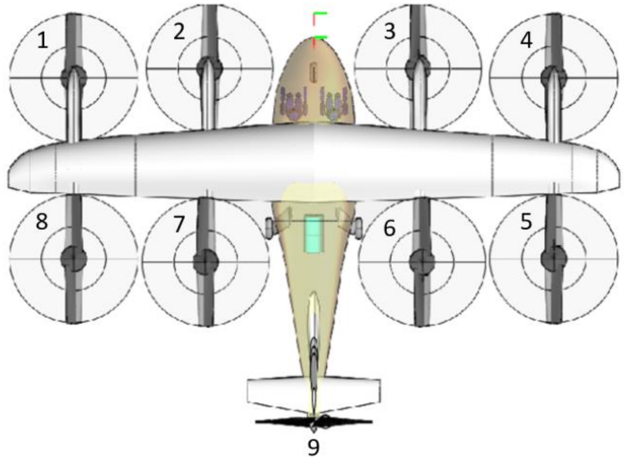

Figure 5. Lift+Cruise rotor identification

The original implementation did not include control power prioritization between the axes for the lift-rotor control allocation. Due to an observation during this work, a single-axis prioritization was implemented to correct an issue that was found. However, this simple prioritization corrected the targeted issue but caused another. All time history plots and results tables, unless otherwise specified, are run without prioritization.

The full test matrix is shown below. All cases were run at 1000 ft mean sea level (MSL) unless otherwise noted.

Single-axis test matrix: 185 test points

- Pilot inputs:
- Long. Max. Step Pos.
- Long. Max. Step Neg.
- Long. Half Step Pos.
- Lat. Max. Step Pos.
- Ped. Max. Step Pos.
- Th. Step Pos. (26.5%)

- Th. Step Neg (26.5%)
- Max. Accel. (only uses 0 KIAS speed)
- Max. Decel. (only uses 150 KIAS speed)
- Speeds: 0 KGS, 20 KGS, 40 KIAS, 60 KIAS, 80 KIAS, 150 KIAS
- L/W_{max}: 2, 1.8, 1.6, 1.4, 1.2 g

Multi-axis test matrix: 54 test points

- Pilot inputs:
    - Long. Max. Pos. and Ped. Max. Pos. Step
    - Long. Max. Neg. and Ped. Max. Pos. Step
    - Long. Max. Pos. and Lat. Max. Pos Step
    - Long. Max. Neg. and Lat. Max. Pos. Step
    - Lat. Max. Pos. and Ped. Max. Pos. Step
    - Lat. Max. Pos. and Ped. Max. Neg. Step
- Speeds: 0 KGS, 20 KGS, 40 KIAS
- L/W_{max}: 2, 1.6, 1.2 g

Rotor failure: 104 test points

- Pilot inputs:
    - Long. Max. Step Pos.
    - Lat. Max. Step Pos.
    - Lat. Max. Step Neg.
    - Ped. Max. Step Pos.
    - Ped. Max. Step Neg.
    - Max. Accel.
    - Max. Decel.
    - Long. Max. Pos. and Ped. Max. Neg. Step
    - Long. Max. Pos. and Lat. Max. Neg. Step
    - Lat. Max. Neg. and Ped. Max. Neg. Step
- Speeds: 0 KGS, 20 KGS, 40 KIAS, 150 (only for Max. Decel.) KIAS
- L/W_{max}: 2, 1.8 g

- Rotors failed: one and two

4 Results

Time histories from cases that are control power limited and/or exhibit interesting responses are shown and discussed in this section. They are followed by tables showing the interaction between aircraft speed, aircraft rotor control power, and pilot inputs with response duration and control power limit severity for a broader set of cases.

Time history figures for most of the remaining elements of the test matrix can be found in Appendix ASelected additional . Tables associated with the additional time histories can be found in Appendix B.

4.1 Single-axis input results

The time history plots for each test point show control power limits for key parameters. These include propeller thrust on the Body X-axis Acceleration (n_x) plot, direct lift on the Body Z-axis Acceleration (n_z) plot, Roll Acceleration ($\dot{p}$) plot, Pitch Acceleration ($\dot{q}$) plot, and Yaw Acceleration ($\dot{r}$) plot. Each of these plots include a rotor or propeller control power limit curve in red, an aerodynamic control power limit curve in green, and a total control power curve, which is the sum of the two, in purple. The red rotor control power curve represents the control power allowed by the control system. Whereas the green aerodynamic surface control power curve is the currently available control power but is not necessarily being used by the control system.

4.1.1 Maximum positive longitudinal steps

The time history from a maximum positive longitudinal step pilot input at 0 KGS (hover) with the L/W_{max} of 2 g is shown in Figure 6. The time history shows that none of the vehicle state accelerations reaches the control power limits. The “rotor thrust” and “thrust error” plots in the time histories are specific to the rotor model. The rotor thrust plot depicts all eight rotors along with the maximum static thrust available to each rotor for the given flight condition. All eight rotors generated the same amount of thrust, thus the single line. The rotor thrust plot is useful in identifying when a rotor is saturated. The thrust error plot is the difference between the incoming thrust commands from the control system and the maximum currently available rotor thrust. The thrust error is calculated prior to rotor dynamics while the rotor thrust plot is calculated afterwards. In this run, the control system is asking for nearly 8000 pounds of thrust more than the maximum thrust available for each rotor initially. The error then goes back to zero as the commanded rate is achieved.

In contrast to the $L/W_{max} = 2$ g time history (Figure 6), Figure 7 shows the same input and flight condition but with $L/W_{max} = 1.2$ g. Not surprisingly, the vehicle takes longer to achieve the commanded altitude rate ($\dot{h}$). All four axes controlled by the rotors are limited due to the primary axis (n_z) hitting the upper control power limit. Each of the rotors also reach the maximum rotor thrust as seen in the rotor thrust plot. The thrust error takes longer to return to zero.

This analysis assessed the control system, configuration, and control effectors as a system to reflect operating control power of the entire vehicle and not any single element. This must be considered when reviewing the results. As expected, there is more control power saturation as L/W_{max} decreases. However, this does not directly correlate with response duration. As mentioned in the method section, the vehicle control system was designed to start phasing out the rotors during FRT. Figure 8 shows the response with an L/W_{max} of 1.2 g at 60 KIAS. A sustained flight path rate is achieved in approximately one second, but the rotors start becoming saturated due to a decrease in Angle of Attack (AoA), which results in negative lift for which the rotors must compensate.

At 80 KIAS the aerodynamic surfaces are contributing nearly all the acceleration necessary to achieve the maximum positive longitudinal step command, so varying the L/W_{max} has no effect on the response duration. Figure 9 shows the 80 KIAS with an L/W_{max} of 1.2 g.

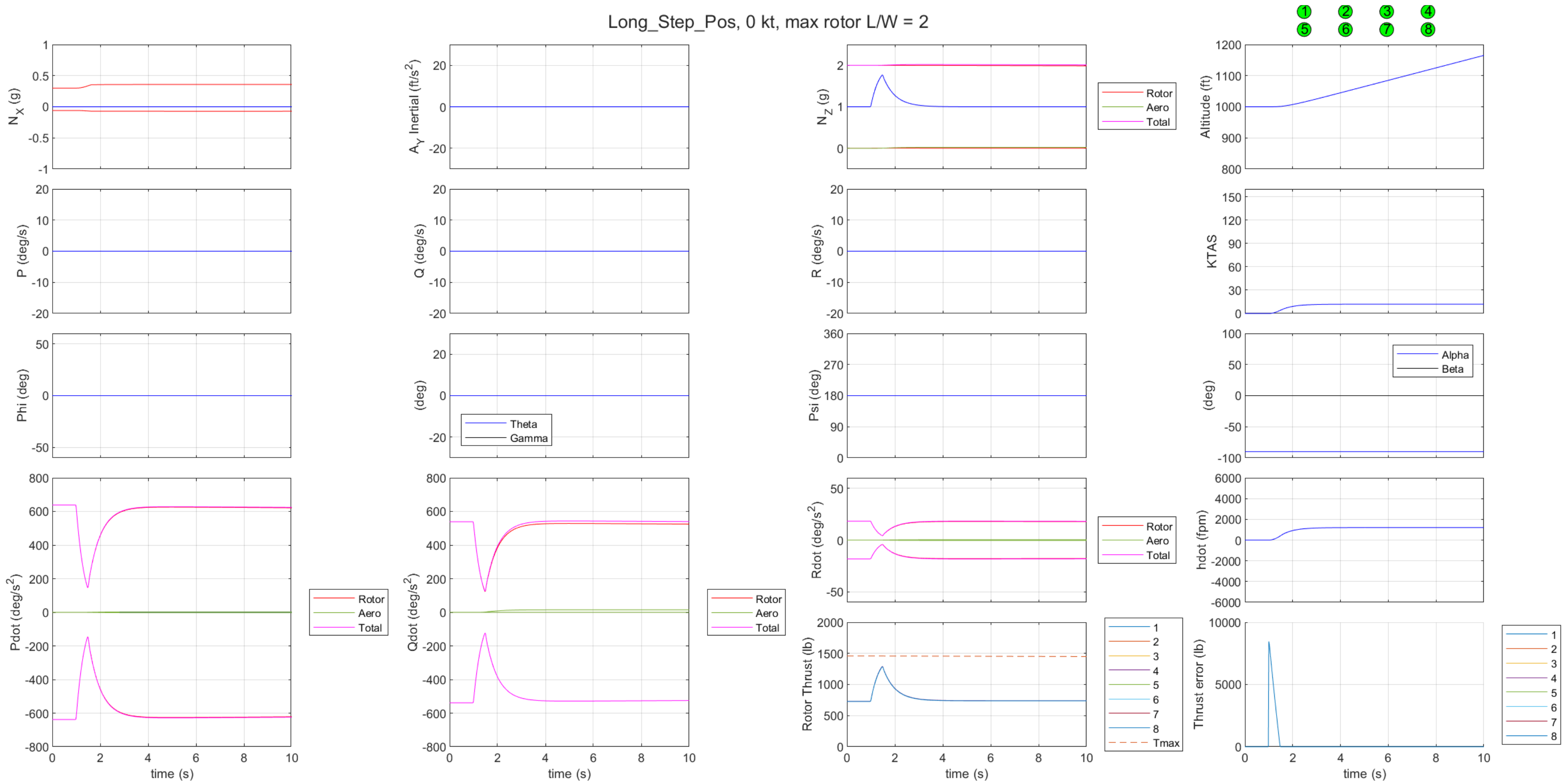

Figure 6. Max Pos. Long. step trimmed at 0 KGS with an L/Wmax = 2 g

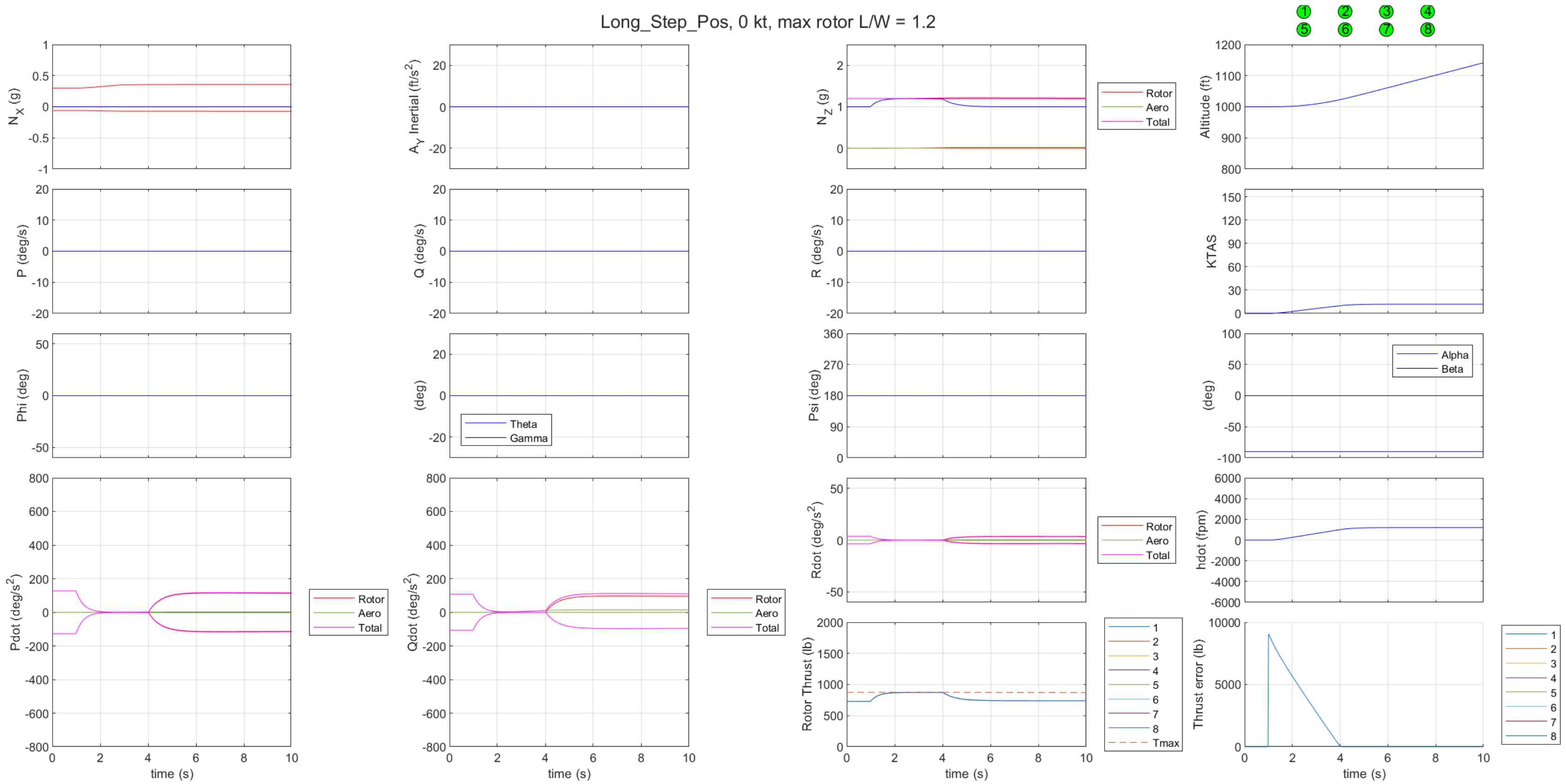

Figure 7. Max Pos. Long. step trimmed at 0 KGS with an L/Wmax = 1.2 g

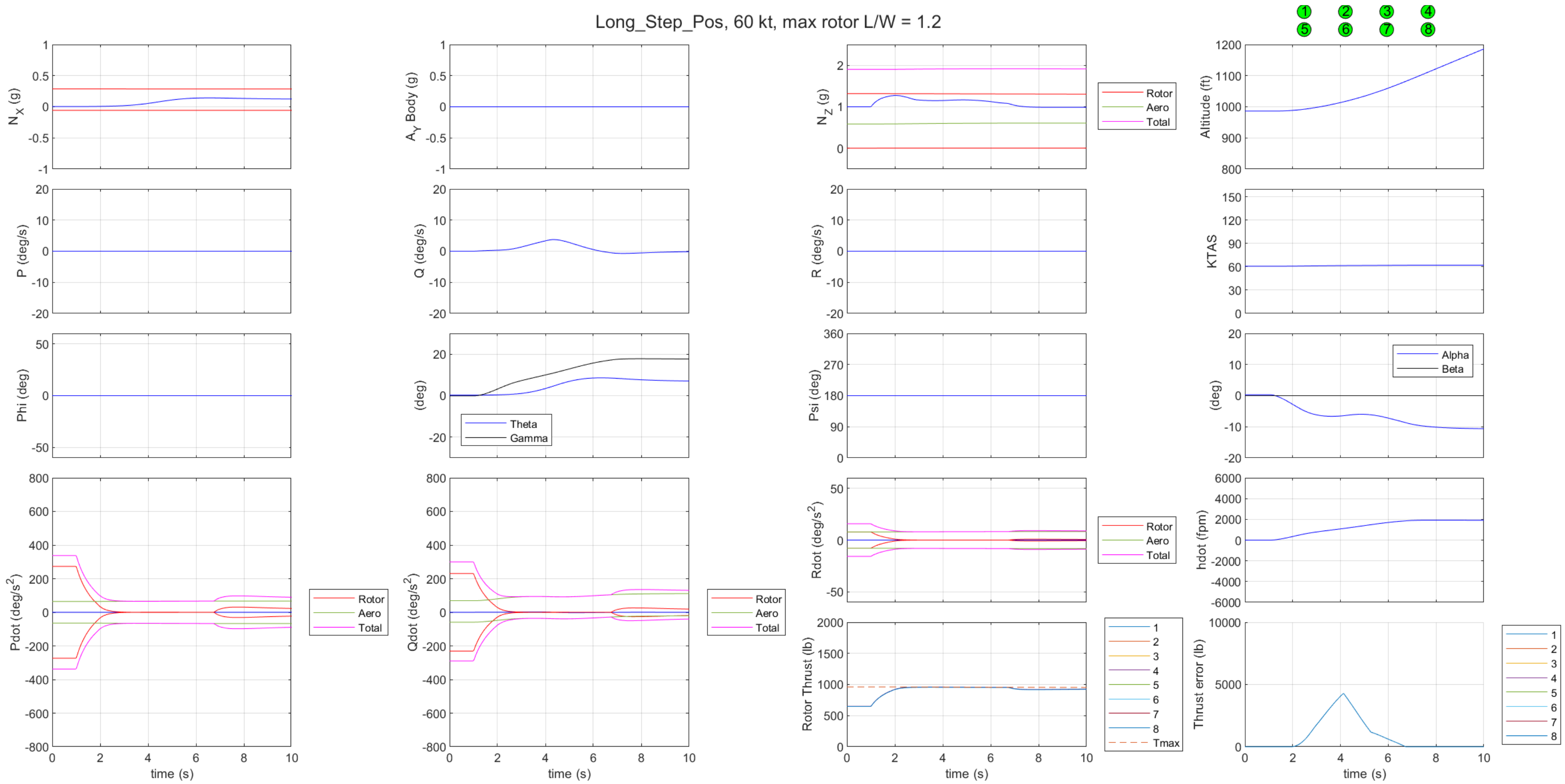

Figure 8. Max Pos. Long. step trimmed at 60 KIAS with an L/Wmax = 1.2 g

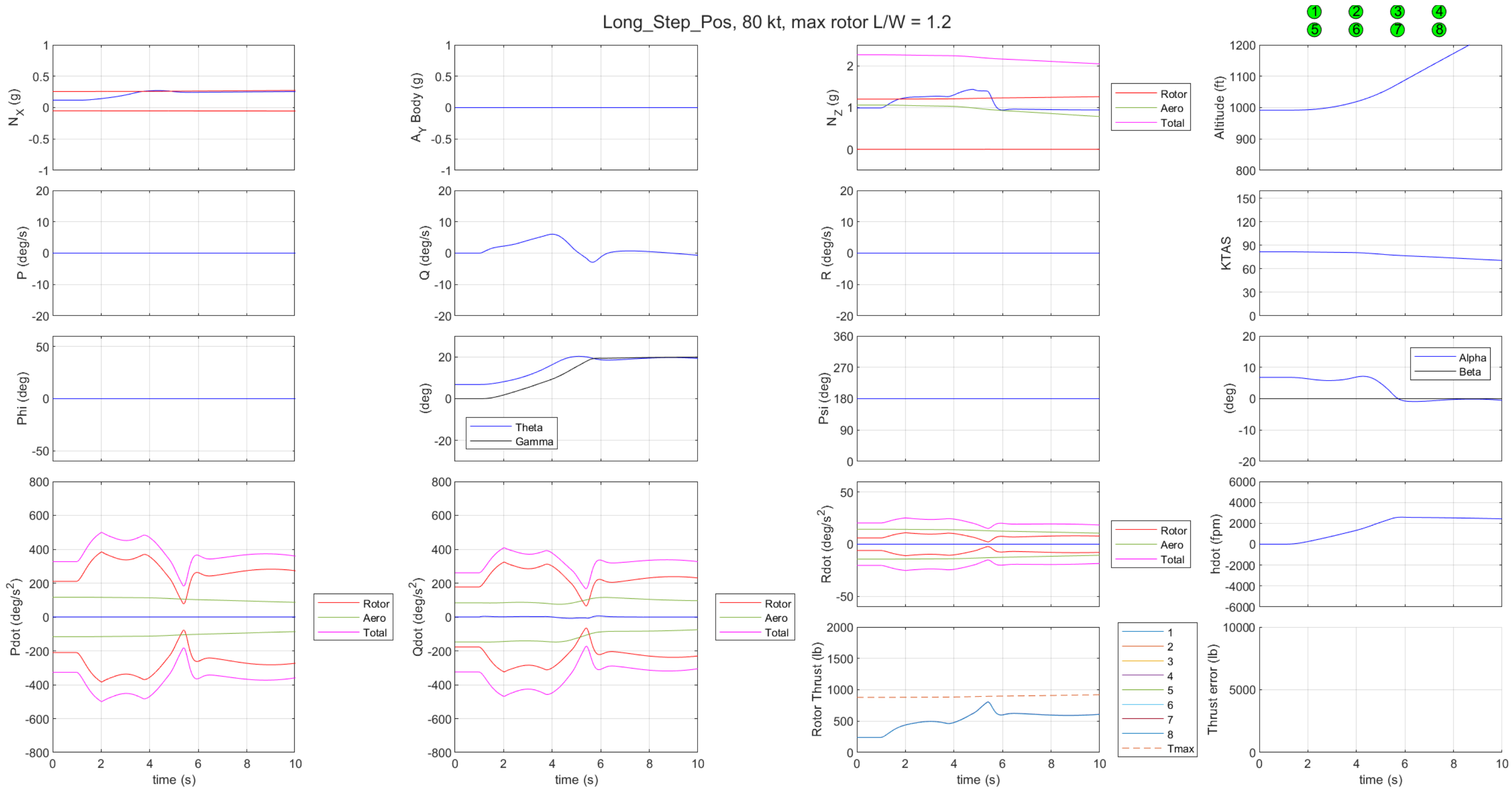

Figure 9. Max. Pos. Long. step trimmed at 80 KIAS with an L/Wmax = 1.2 g

Table 1 shows maximum positive longitudinal step results. The table serves two purposes. The fourth column provides the duration of the primary axis response required to achieve the commanded rate. The next four columns (five through eight) describe the limiting severity of the rotor and total control power of the primary axis and secondary axes. The colors in the Control Power (CP) status columns represent the CP being: "never limited" in green; "significantly limited" in yellow; and "completely limited" in red. "Significantly limited" indicates the axis was using over 90% of its available control power at some point during the run. Completely limited indicates the axis is against its respective control power limit at some point during the run. When a test point is "completely limited," the duration the axis was limited is given in seconds.

The diminished rotor control power authority effect on the response duration from lowering L/W_{max} is seen in Table 1 for the 60 KIAS cases. There are some time histories for the maximum positive longitudinal step, such as the 60 KIAS case with 1.4 g L/W_{max}, where the response duration appears unaffected at higher speeds, but the rotors become saturated. This is a result of the vehicle being in the middle of FRT. At and below 60 KIAS the vehicle is still primarily using powered lift. Part of the implementation included maintaining 0 deg pitch (θ) below 60 KIAS unless a change in speed is commanded. One side effect of this method is that the vehicle uses direct lift from the rotors to achieve a commanded positive $\dot{\gamma}$ resulting in a large negative AoA and thereby generating an increasing negative lift force from the wing. The rotor control power is completely limited for over four seconds in the L/W_{max} of the 1.2 g test point, but the vehicle has available aerodynamic surface control power that the control system does not fully utilize at this state of the FRT. The response duration still increased slightly because of the decreased rotor control power since a large majority of the lift generated is from the rotors. However, at these higher speeds where $\dot{\gamma}$ is commanded, response duration is minimally affected from decreased control power compared to lower speeds due in part to having some available aerodynamic surface control power and the nature of the commanded rate. The rotor CP status column will still indicate if the rotors are being saturated even if the vehicle has available total control power.

The change in command type of the control system because of FMT has a significant effect on the response duration of the maneuver. The maximum positive longitudinal step case switches from $\dot{h}$to a $\dot{\gamma}$ when going from hover to cruise. The transition happens automatically and is relatively intuitive but requires some pilot familiarization. The time to achieve a commanded $\dot{h}$ from powered lift takes longer than it does to achieve a commanded $\dot{\gamma}$ which is reflected in the response durations found in Table 1.

Table 1. Max Pos. Long. step results

Pilot Input	Trim Speed (kt)	Max Rotor L/W	Response Duration (s)	Primary Axis Rotor CP Status	Secondary Axis Rotor CP Status	Primary Axis Total CP Status	Secondary Axis Total CP Status
Long. Pos. Step	0	1.2	5.68	2.00	2.00	2.00	2.00
		1.4	4.42	0.50	0.50	0.50	0.50
		1.6	4.08				
		1.8	3.94				
		2	3.88				
	20	1.2	4.94	1.72	1.72	1.72	1.72
		1.4	2.90	0.52	0.52	0.52	0.52
		1.6	2.42				
		1.8	2.24				
		2	2.16				
	40	1.2	0.88	2.04	2.04		
		1.4	0.78				
		1.6	0.78				
		1.8	0.78				
		2	0.78				
	60	1.2	1.06	4.20	4.20		
		1.4	0.98	1.16	1.16		
		1.6	0.98				
		1.8	0.98				
		2	0.98				
	80	1.2	1.36				
		1.4	1.36				
		1.6	1.36				
		1.8	1.36				
		2	1.36				

Completely Limited
Significantly Limited
Never Limited

4.1.2 Half positive longitudinal step

The saturation caused by an increase in negative lift as flight path angle (γ) increases is easier to see because it happens slower with a half positive longitudinal step at 40 KIAS with an L/W_{max} of 1.2 g which is shown in Figure 10. As the vertical γ of the vehicle increases while maintaining level attitude, the AoA becomes more negative. The direct lift from the rotors increases to compensate for the negative lift being generated by the wing and becomes control power limited at the end of the maneuver. Although the commanded $\dot{\gamma}$ is achieved without any issue, the vehicle becomes control power limited before hitting the upper γ limit. The N_z plot in Figure 10 does not appear saturated. This is due to the vertical acceleration being a sum of the wing-borne negative lift and the compensation from the rotor-borne lift. The rotor saturation is most apparent from the rotor thrust plot where the increased compensation for the negative lift finally saturates the rotors when the AoA reaches approximately -17 deg. This may not be an ideal control system implementation. The alternative of pitching up steeply may not be comfortable to passengers and crew and would add drag due to a component of the rotor lift being pointed aft. A balance between the two approaches would likely be an optimum approach, but that detail was not important when the simulation was developed.

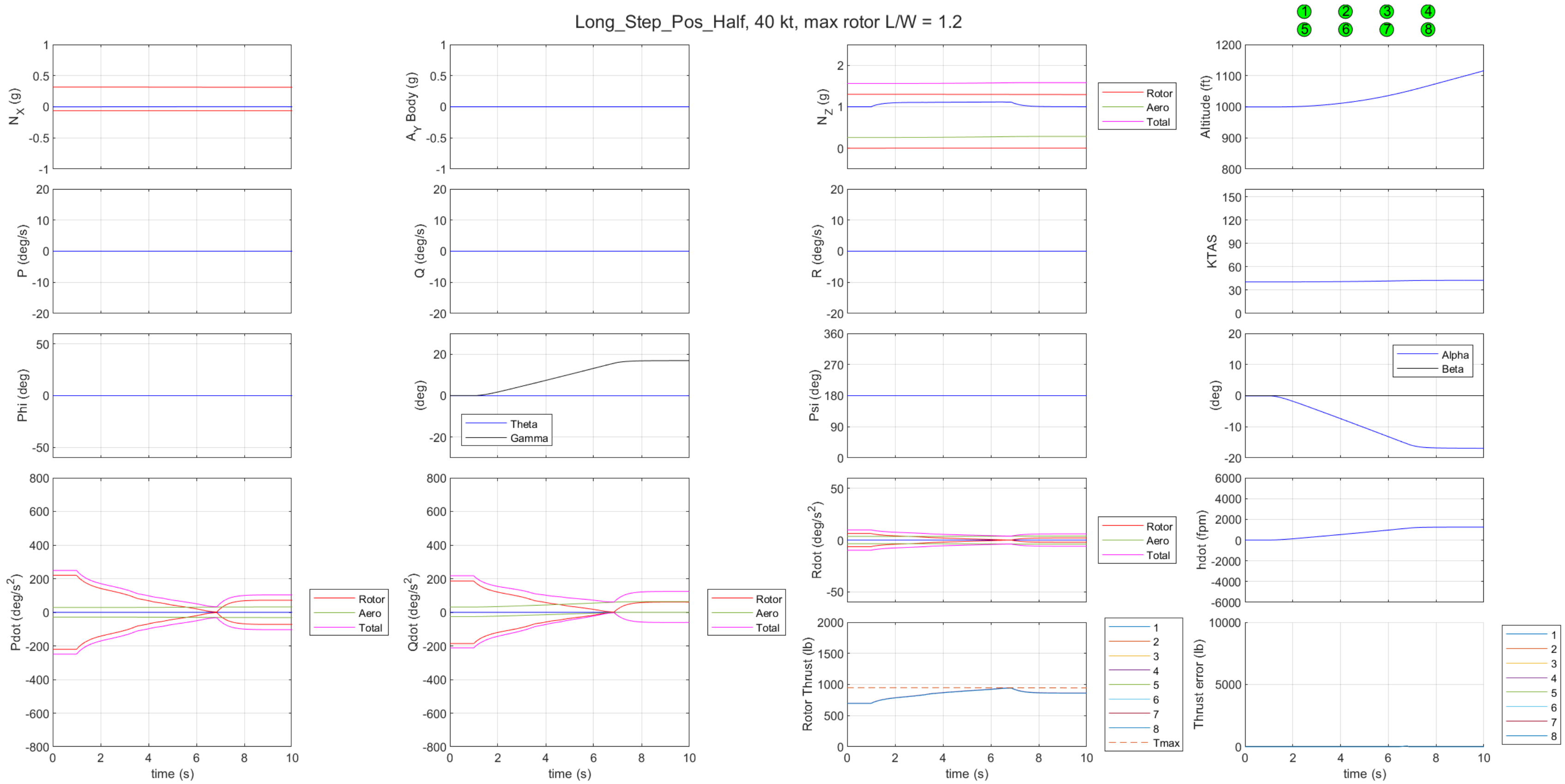

Figure 10. Half Long. Pos. step trimmed at 40 KIAS with an L/Wmax = 1.2

4.1.3 Maximum positive pedal step

Yaw acceleration commands to the rotors resulted in a small altitude loss. This was caused by the increased demand from the rotor control implementation, which generated yaw control power from the slightly canted inboard rotors. This effect was more significant with lower total control power. It was most prevalent with the high body axis $\dot{r}$ commanded in hover. With the full 2 g L/W_{max}, the loss in altitude is not noticeable on the time histories. However, as shown below in Figure 11, at 1.2 g L/W_{max} nearly 10 feet is lost during the $\dot{r}$. Although not a significant loss from many flight conditions, the phenomenon is important in identifying potential deficiencies. This effect was persistent throughout the analysis and was determined to be the cause of a flight condition that defeated the control system's envelope protection in a case detailed in Section 4.2.3.

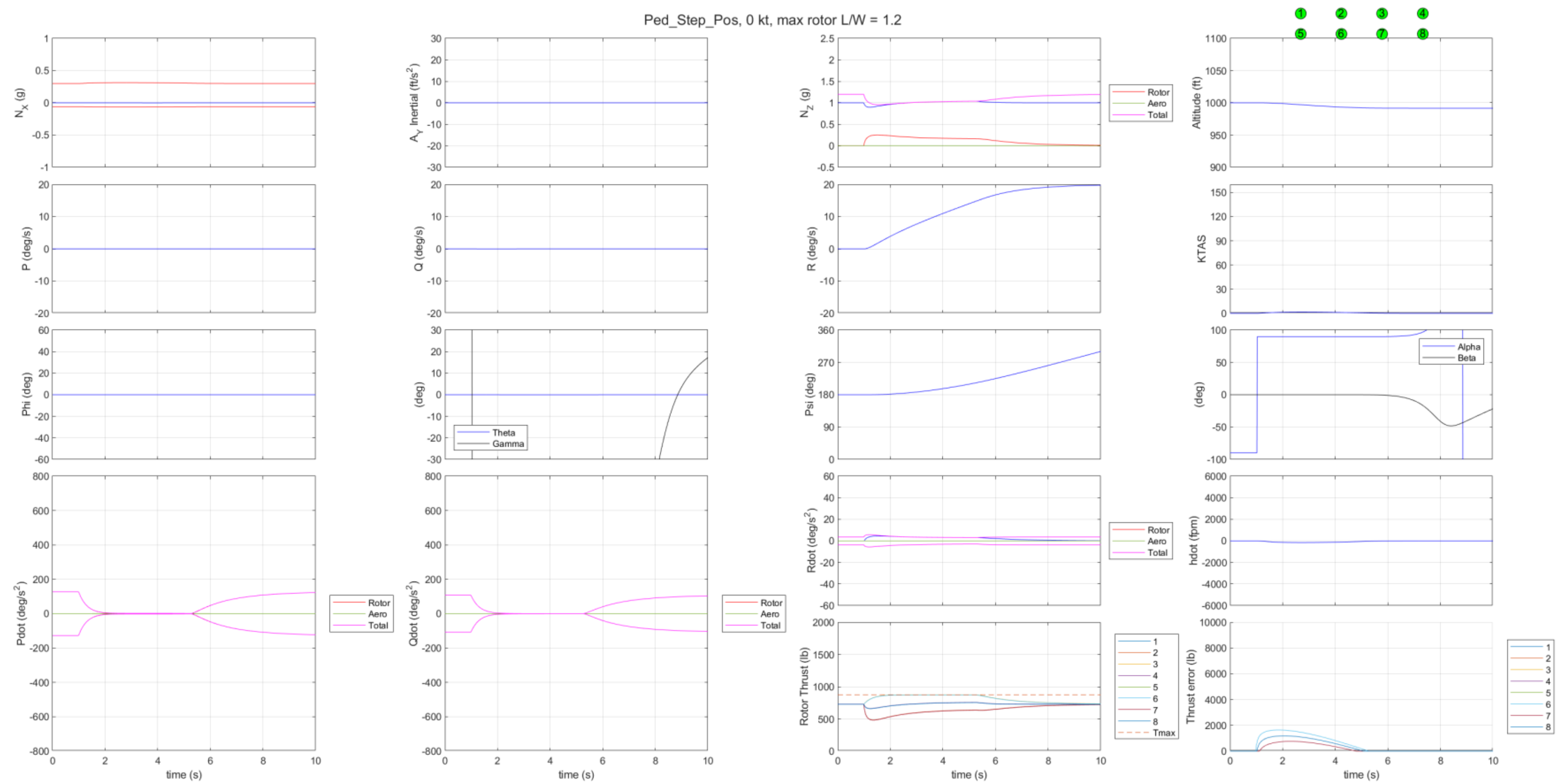

Figure 11. Max Pos. pedal step trimmed at 0 KGS with an L/Wmax = 1.2 g

The pedal input results can be found in Table 2. Uniquely to this case, every completely limited test point had the same loss in altitude behavior as observed in Figure 11. The maximum commanded $\dot{r}$ takes up a smaller portion of that axis' available control power than the n_z maximum command. Unlike other saturation cases, L/W$_{max}$ of 1.6 or higher exhibited no control power saturation.

Table 2. Max Pos. ped. step results

Pilot Input	Trim Speed (kt)	Max Rotor L/W	Response Duration (s)	Primary Axis Rotor CP Status	Secondary Axis Rotor CP Status	Primary Axis Total CP Status	Secondary Axis Total CP Status
Ped. Pos. Step	0	1.2	6.74	3.26	2.66	3.26	2.66
		1.4	5.08	0.78	0.78	0.78	0.78
		1.6	4.78				
		1.8	4.70				
		2	4.70				
	20	1.2	>9.00	2.36	3.02	2.08	3.02
		1.4	>9.00	0.4	0.4	0.4	0.4
		1.6	8.02				
		1.8	7.96				
		2	7.94				
	40	1.2	1.44				
		1.4	1.36				
		1.6	1.32				
		1.8	1.28				
		2	1.26				
	60	1.2	1.2				
		1.4	1.2				
		1.6	1.2				
		1.8	1.2				
		2	1.2				
	80	1.2	1				
		1.4	1				
		1.6	1				
		1.8	1				
		2	1				

Completely Limited
Significantly Limited
Never Limited

Figure 12 shows the time history for a 20 KIAS maximum positive pedal step input with a L/W$_{max}$ of 1.2 g. The response duration increased significantly compared to the hover case as seen in Table 2. This is a result of the different dynamic response characteristics in the hover to cruise transition region. Note the $\dot{r}$ and $\dot{p}$ in this case versus only $\dot{r}$ in the hover case. There is a minimal loss in rotor thrust at 20 KIAS, but it is not the primary reason for the change in response duration.

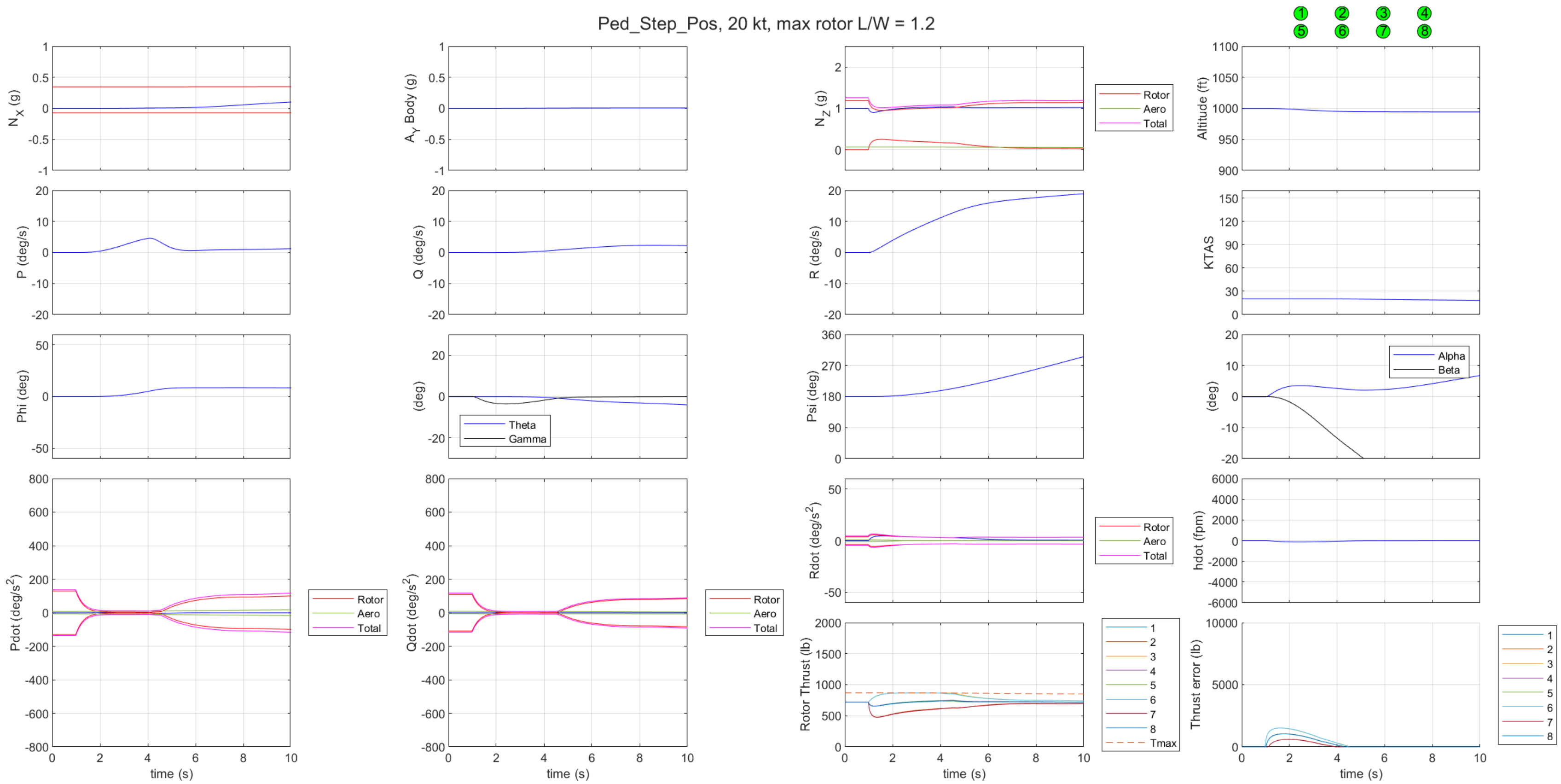

Figure 12. Max Pos. pedal step trimmed at 20 KIAS with an L/Wmax = 1.2 g

4.1.4 Maximum acceleration and deceleration

Two pilot commands in the test matrix were representative inputs commonly used by pilots in simulation evaluations. They were maximum acceleration (Accel.) and the maximum deceleration (Decel.) inputs starting from a hover or maximum commanded speed. The first command started the aircraft in a hover and accelerated to 150 KIAS. The second started at 150 KIAS and decelerated back to a hover. The FRT and the use of pitch to accelerate and decelerate is most apparent from these time histories. These input maneuvers are run for 60 seconds instead of 10 to show the entire duration of the maneuver with the commanded speeds reached before the end.

For the maximum acceleration, input shown in Figure 13 a significant drop in rotor control power authority can be seen at approximately 15 seconds as the vehicle accelerates through ~90 KIAS. This decrease is not a physical limitation but the scheduled FRT. The rotors can produce the necessary lift at high-speed flight conditions, but the control system does not use them. Figure 14 shows the maximum acceleration with an L/W_{max} of 1.2 g and is the only case between the maximum acceleration and deceleration pilot commands that exhibits limited control power. Figure 15 shows the time history for a maximum deceleration. The FRT can be seen at approximately 25 seconds into the time history. The rotor power demand increases at ~32 seconds as the vehicle pitches up to use the rotors to decelerate.

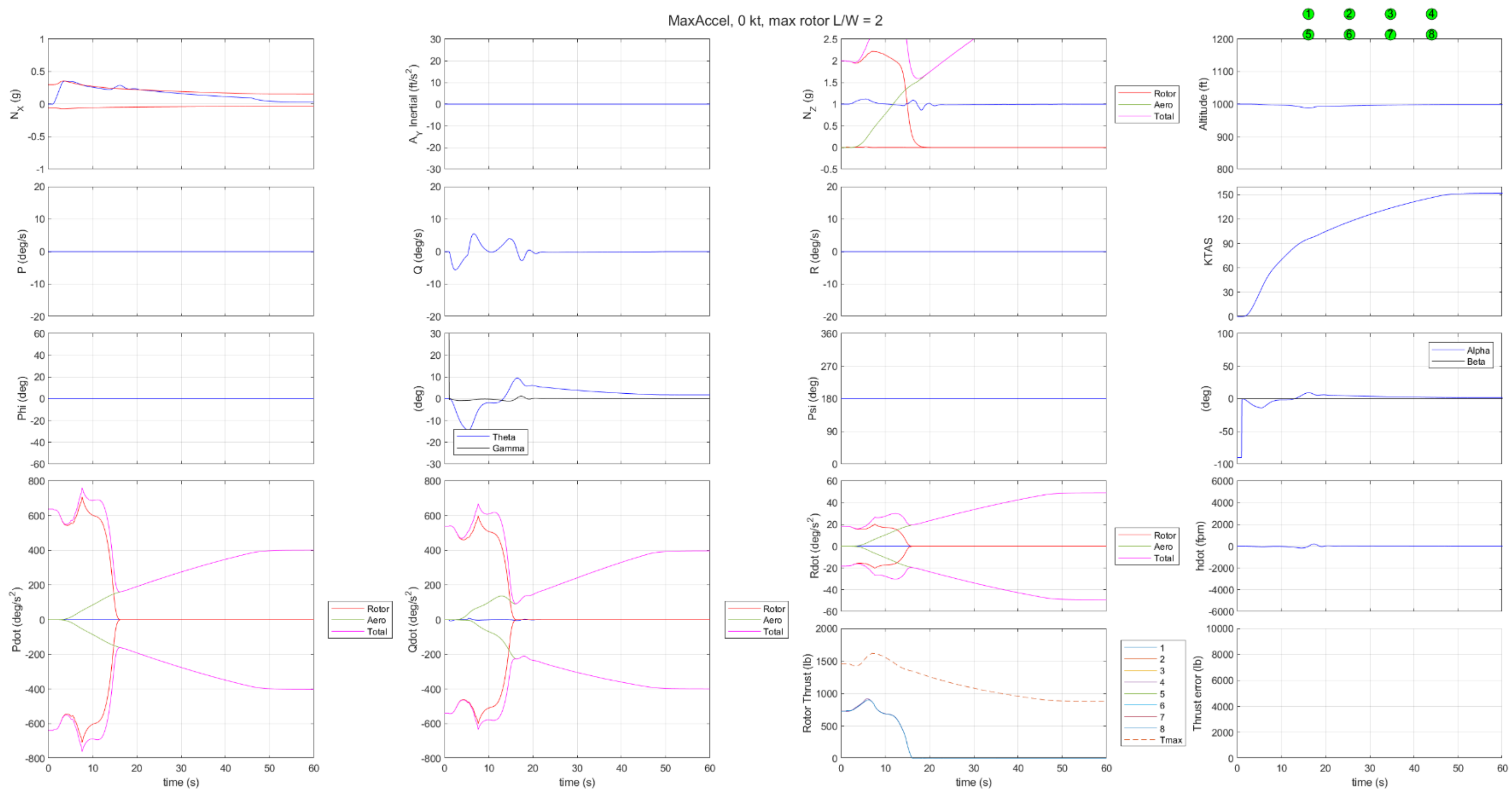

Figure 13. Max Accel. trimmed at 0 KGS with an L/Wmax = 2 g

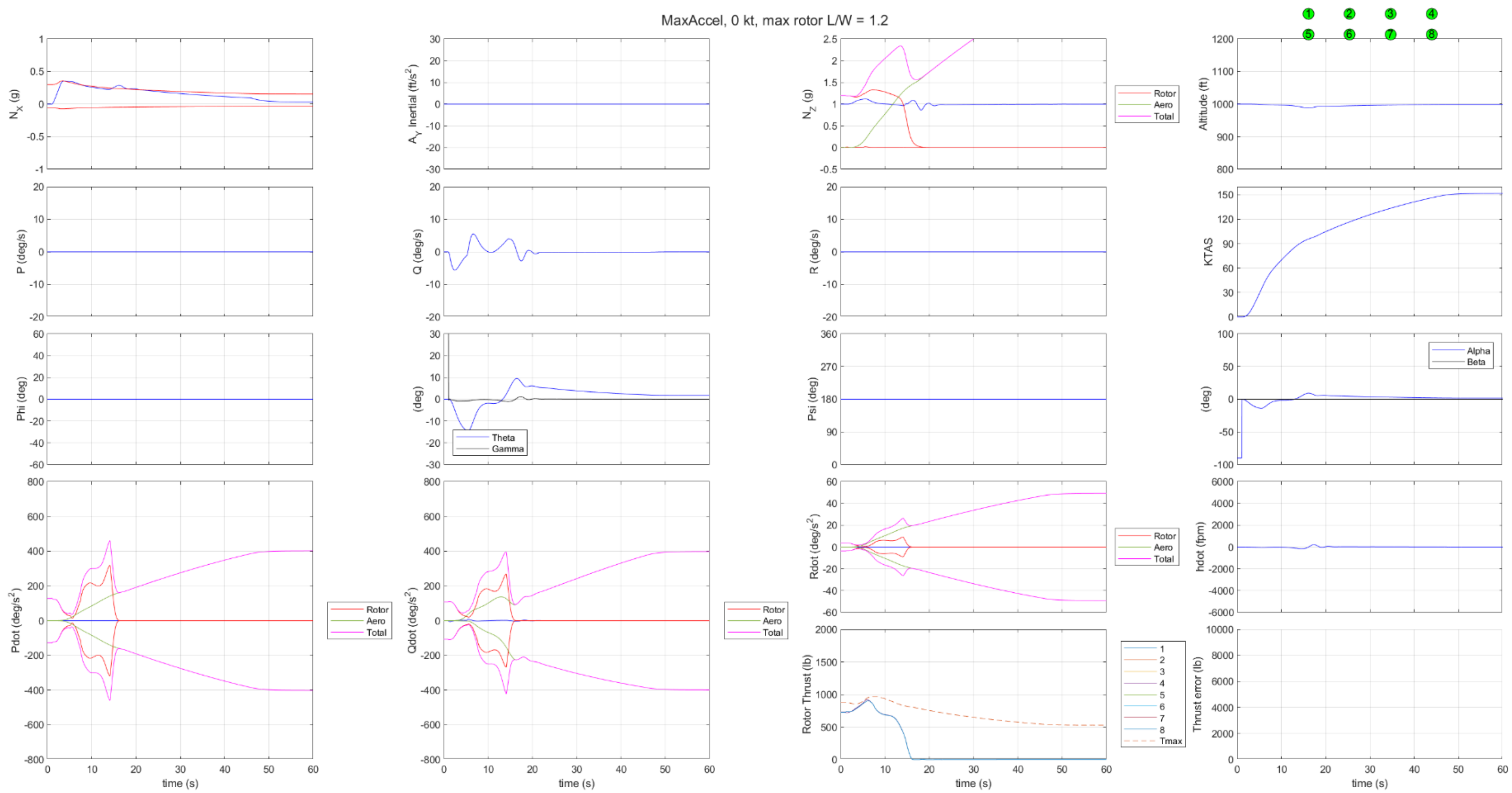

Figure 14. Max Accel. trimmed at 0 KGS with an L/Wmax = 1.2 g

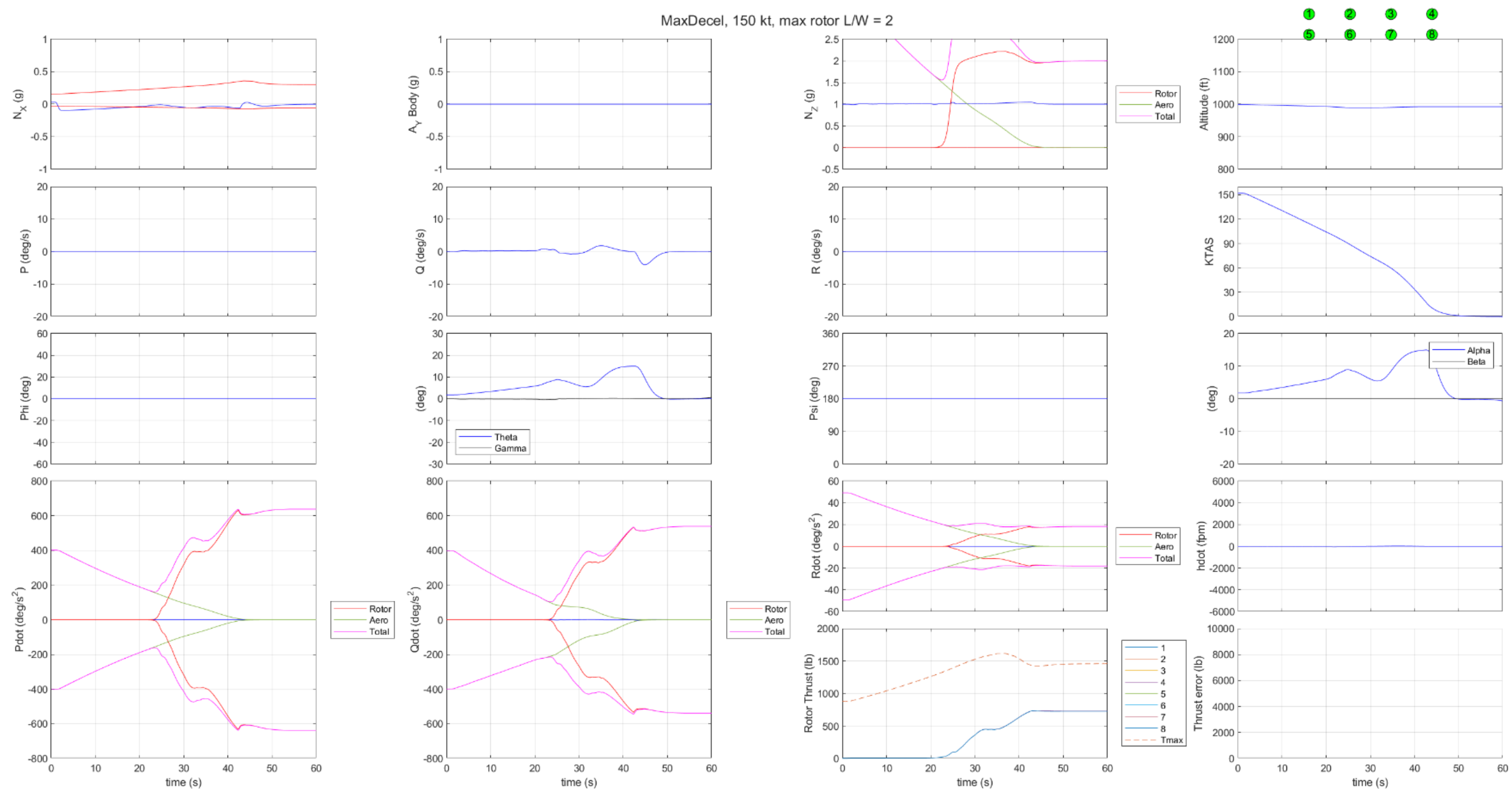

Figure 15. Max Decel. trimmed at 150 KIAS with an L/Wmax = 2 g

Results from the maximum acceleration and deceleration are given in Table 3 and Table 4. As previously stated, there were no completely limited cases and only the L/Wmax = 1.2 g case shows any significant limitation.

Table 3. Max acceleration results

Pilot Input	Trim Speed (kt)	Max Rotor L/W	Response Duration (s)	Primary Axis Rotor CP Status	Secondary Axis Rotor CP Status	Primary Axis Total CP Status	Secondary Axis Total CP Status
Max Accel	0	1.2	46.36				
		1.4	46.36				
		1.6	46.36				
		1.8	46.36				
		2	46.36				

Completely Limited
Significantly Limited
Never Limited

Table 4. Max acceleration results

Pilot Input	Trim Speed (kt)	Max Rotor L/W	Response Duration (s)	Primary Axis Rotor CP Status	Secondary Axis Rotor CP Status	Primary Axis Total CP Status	Secondary Axis Total CP Status
Max Decel	150	1.2	49.48				
		1.4	49.48				
		1.6	49.48				
		1.8	49.48				
		2	49.48				

Completely Limited
Significantly Limited
Never Limited

4.2 Multi-axis input results

Multi-axis commands typically resulted in more significant control power limits than single-axis commands given the interdependence of control power across axes. Residual force and moment error was prominent due to rotor saturation for multi-axis commands. The rotor control power allocator attempts to find a solution that provides the commanded forces and moments given the rotor geometry matrix and currently available maximum thrust from each rotor. The maximum available thrust of the rotors changes with speed and density altitude. When there is insufficient control power to meet all commands, the allocator biases the results based on how big the commands are. If the N_z command exceeds the available power by a factor of five and the others are exceeded by a factor of two, N_z receives priority. There was no intentional axis prioritization behind this allocation as it was not necessary for the purpose.

4.2.1 Maximum positive lateral and positive pedal step

The multi-input case for positive pedal and positive lateral stick step input with L/W_{max} of 1.2 g is shown in Figure 16. The loss in altitude due to the turn rate command in hover from a multi-axis command is more than the single axis turn rate command previously shown in Figure 11.

The difference between losses in altitude is small at only an additional foot of altitude lost but shows the increased total control power used from multi-input commands.

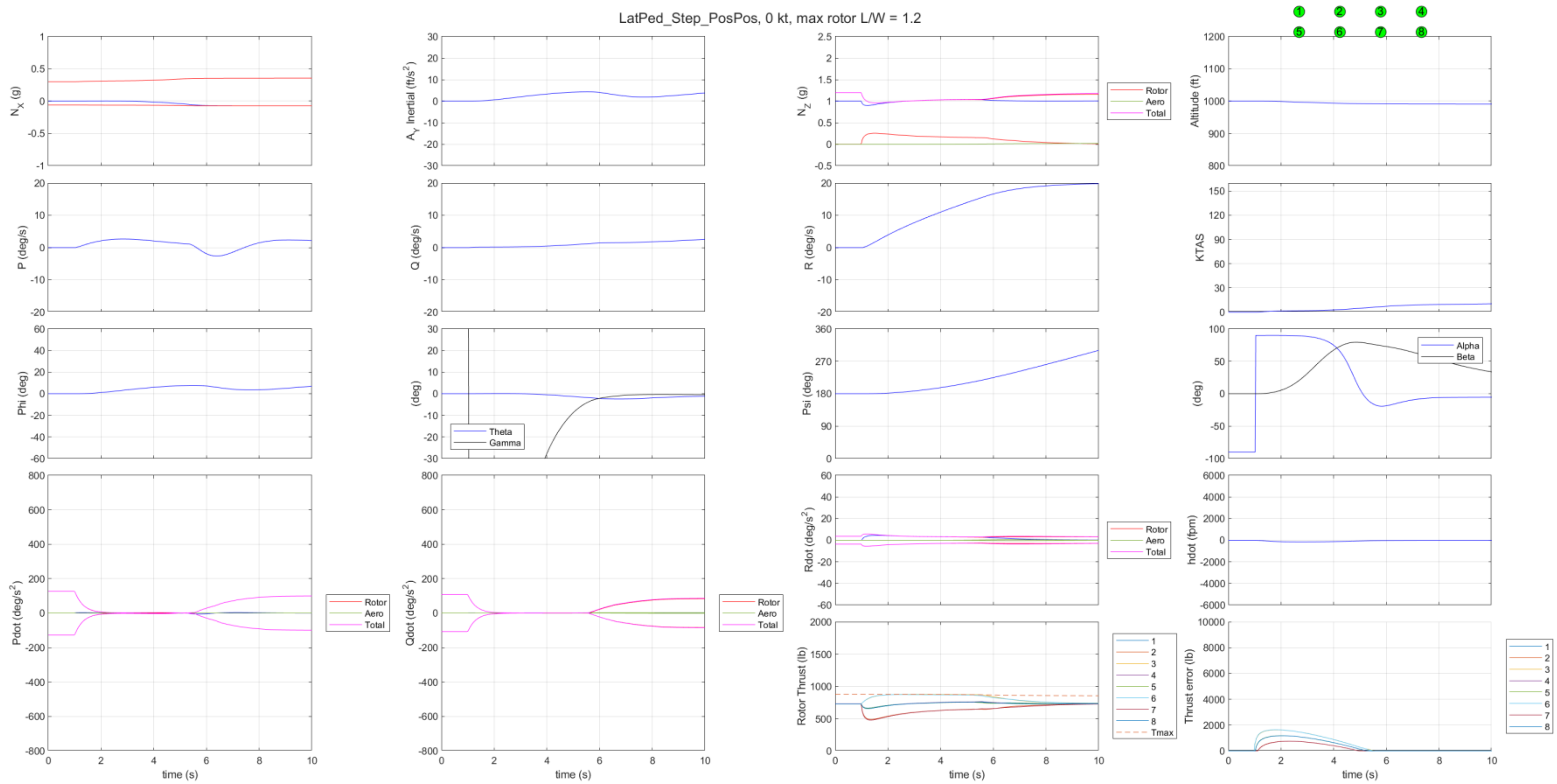

Figure 16. Max Pos. Lat and Pos. Ped step trimmed at 0 KGS with an L/Wmax = 1.2 g

The lateral and pedal step input command results summary is shown in Table 5. For multi-input results tables the axis is specified for the response duration columns. The two primary axes for the CP status columns are in the same order, as they appear in the response duration columns. The lateral stick command in hover does not require much control power due to the minimal bank angle required to begin accelerating laterally. The response and control power limit durations increased for the multi-input cases but only marginally. The rotors were saturated for four seconds with this multi-axis input, but the single-axis pedal input had rotor saturation for 3.26 seconds as seen in Table 2. This was due to more control power required to achieve the commanded forces and moments of both axes. Like the single-axis pedal input, the vehicle loses some altitude for each control power limited scenario.

Table 5. Max Pos. Lat. and Pos. Ped step results

Pilot Input	Trim Speed (kt)	Max Rotor L/W	Pdot Response Duration (s)	Rdot Response Duration (s)	Primary Axis 1 Rotor CP Status	Primary Axis 2 Rotor CP Status	Secondary Axis Rotor CP Status	Primary Axis 1 Total CP Status	Primary Axis 2 Total CP Status	Secondary Axis Total CP Status
Pos. Lat. & Pos. Ped Step	0	1.2	1.82	7.80	4.00	4.00	4.00	4.00	4.00	4.00
		1.6	1.18	5.80						
		2	1.08	5.72						
	20	1.2	1.80	>9	2.96	2.96	2.96		2.96	
		1.6	1.20	>9						
		2	1.10	>9						
	40	1.2	1.34	1.44						
		1.6	1.16	1.30						
		2	1.06	1.22						

Completely Limited
Significantly Limited
Never Limited

4.2.2 Maximum positive longitudinal and positive pedal step

Further indication of the interaction between n_z and $\dot{r}$ originally introduced in Section 4.1.2 is seen in a multi-axis maximum positive longitudinal and positive pedal step input. The time history shown in Figure 17 is full authority 2 g L/W_{max} in a hover. Even with full authority, the rotors become significantly limited. An L/W_{max} of 1.6 g will completely limit the control power of the aircraft for a significant duration as seen in Figure 18.

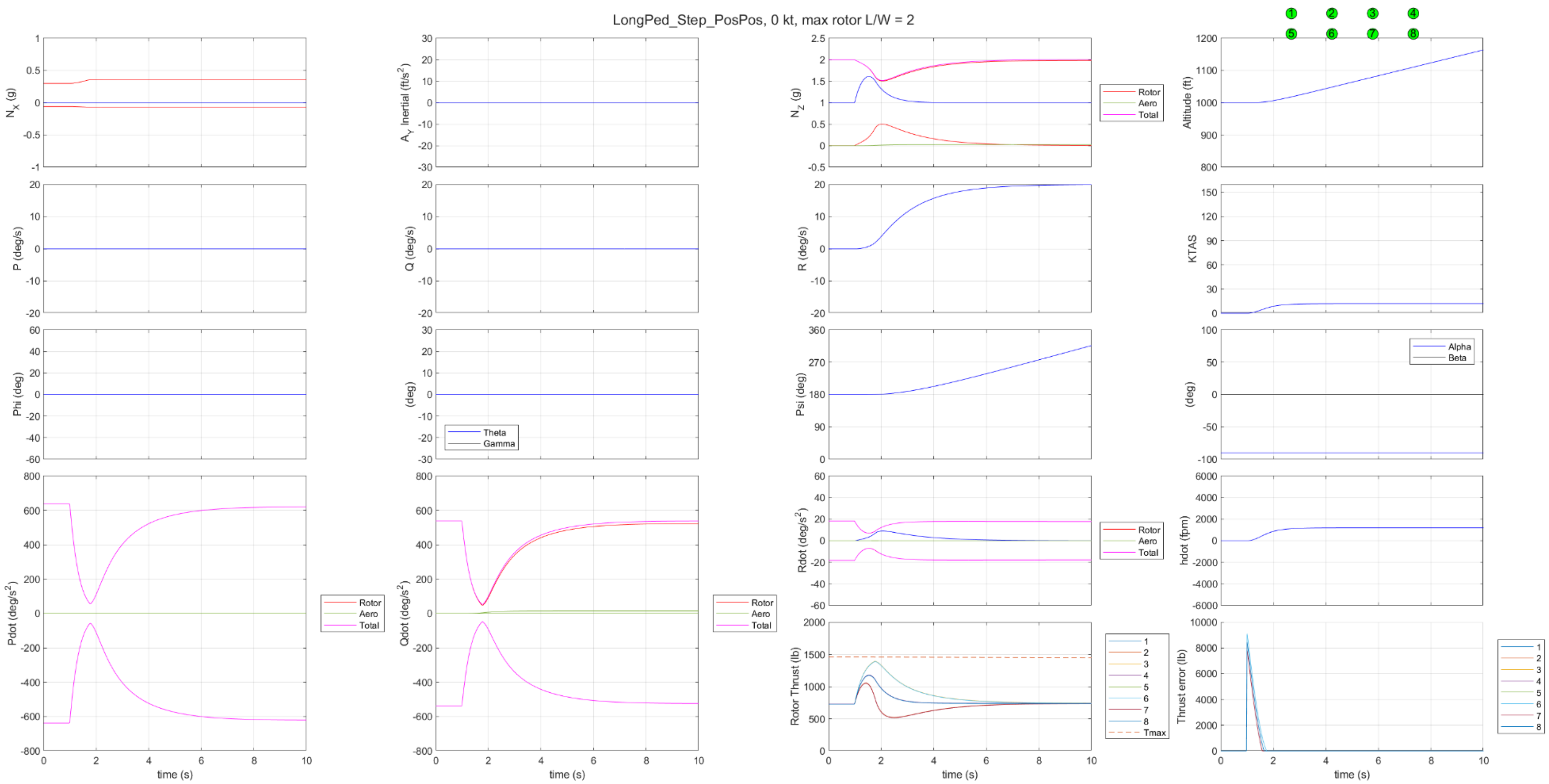

Figure 17. Max Pos. Long. and Max Pos. pedal step trimmed at 0 KGS with an L/Wmax = 2 g

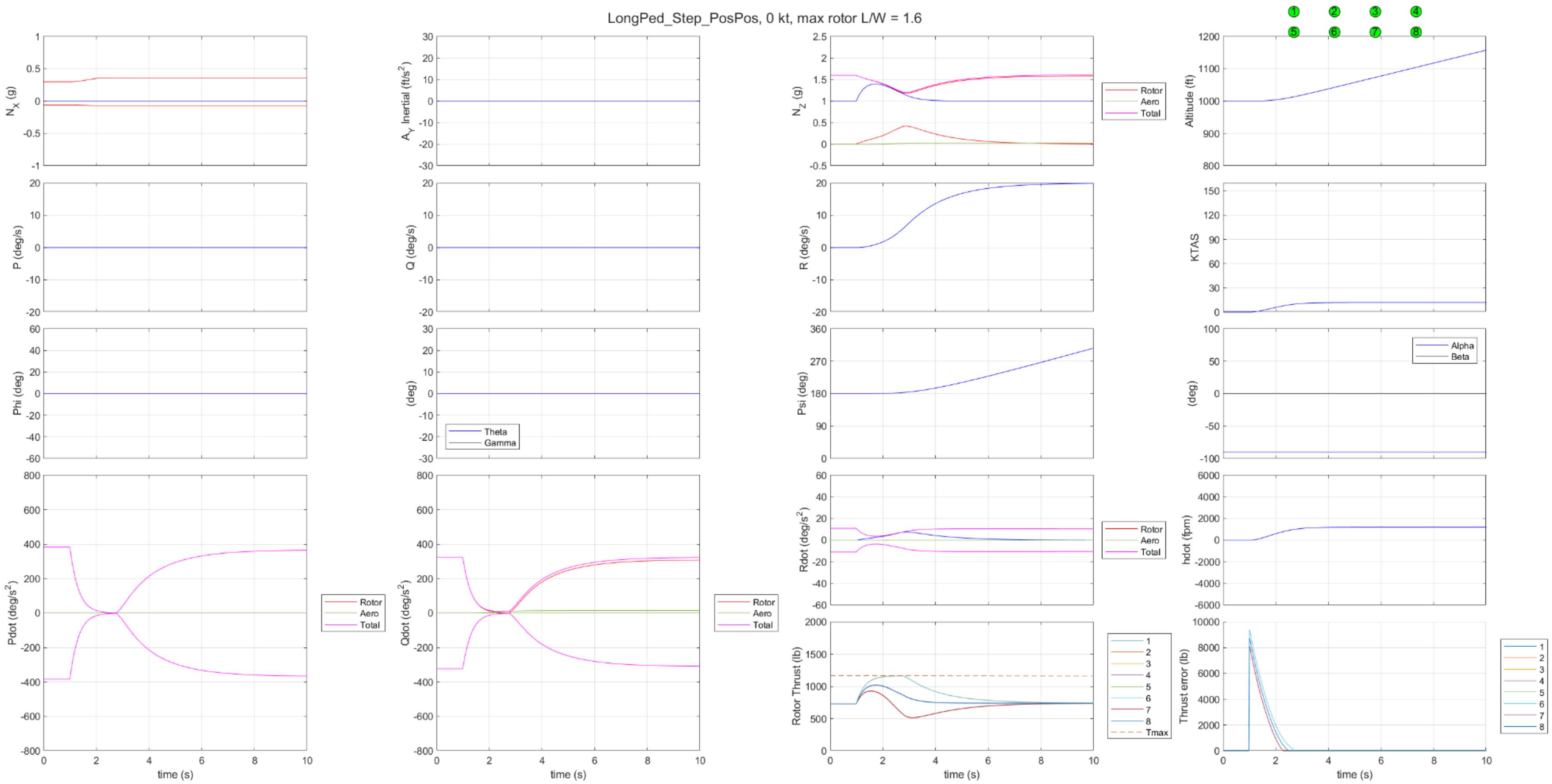

Figure 18. Max Pos. Long. and Pos. pedal step trimmed at 0 KGS with an L/Wmax = 1.6 g

The results from the maximum positive longitudinal and positive pedal step are shown in Table 6. This is the only command input that has a significantly limited case for the L/W_{max} of 2 g and that is not a rotor failure discussed in Section 4.3. Similarly, to the maximum positive lateral and pedal step, both response duration and control power status increase for their single-axis counterparts.

Table 6. Max Pos. Long. and Pos. ped. step results

Pilot Input	Trim Speed (kt)	Max Rotor L/W	Nz Response Duration (s)	Rdot Response Duration (s)	Primary Axis 1 Rotor CP Status	Primary Axis 2 Rotor CP Status	Secondary Axis Rotor CP Status	Primary Axis 1 Total CP Status	Primary Axis 2 Total CP Status	Secondary Axis Total CP Status
Pos. Long. & Pos. Ped Step	0	1.2	8.92	>9	6.46	6.46	6.46	6.46	6.46	6.46
		1.6	2.90	6.76	0.76	0.76	0.76	0.76	0.76	0.76
		2	2.22	6.18						
	20	1.2	7.50	>9	5.92	7.22	5.92	5.92	7.22	5.92
		1.6	2.44	4.94	0.76	0.76	0.76	0.76	0.76	0.76
		2	1.82	4.44						
	40	1.2	0.86	6.10	3.50	3.50	3.50			
		1.6	0.44	1.46						
		2	0.26	1.32						

Completely Limited
Significantly Limited
Never Limited

4.2.3 Defeated envelope protection

Upon further investigation of the n_z and $\dot{r}$ interaction it was discovered with some manual flying in the simulator that a yaw rate (r) commanded in hover while commanding maximum negative $\dot{h}$ command results in increased descent rate and defeating the envelope protection. The maximum descent rate envelop protection in hover prevents the vehicle from entering Vortex Ring State (VRS). Manual flying was used to quickly explore other input combinations and their results. This result is significant because it showed that unoptimized rotor allocation methods along with lower control power margins could potentially result in the aircraft entering hazardous or highly unstable flight conditions. Figure 19 shows the $\dot{h}$, longitudinal stick, pedal, n_z, and r for the manual staggered inputs. A dashed line is used to indicate the $\dot{h}$ limit for the VRS envelope protection. The VRS line is crossed each time there is $\dot{r}$.

Note that VRS is not modeled in this simulation. If modeled, the larger vertical rate seen when envelope protection was defeated would result in poor vehicle response and may result in an unrecoverable state.

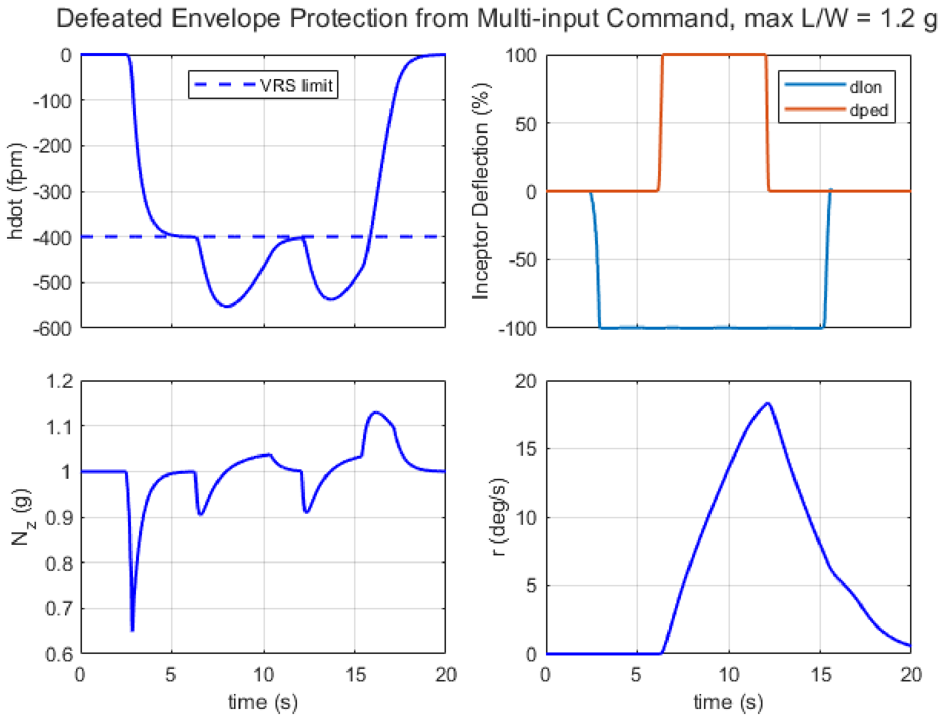

Figure 19. Defeated VRS envelope protection from manual multi-input commands

4.3 Rotor failure results

Most of the rotor failure test cases exhibited completely limited control power but most of them did not depart from controlled flight. One specific case where a departure does occur is discussed in this section. Both single-axis and multi-axis commands were used in the analysis. All time histories from the rotor failure cases can be found in Appendix A. The associated rotor that is failed is indicated in the small graphic at the top right of the figures with a red circle indicating the failed rotor. In all cases when the rotor was failed, the vehicle automatically restabilized before the pilot input was applied. All L/W_{max} values represent the value prior to the rotor failure.

4.3.1 Maximum positive longitudinal step with rotor failures

The time history in Figure 20 shows the maximum positive longitudinal step input applied after the vehicle self-stabilized following a failure of rotor 1. Figure 21 shows the results from rotor two being failed with the same input. Both start in a hover and have an L/W_{max} of 2 g. The rotor control power limits for the rotor failure plots are different from the single-axis and multi-axis results. These limits are static and give the total acceleration available to the aircraft while accounting for thrust allocations that prevent uncommanded forces or moments. Therefore, Figure 20 shows a static n_z limit closer to 1.15 g as opposed to the presumed available control power of 1.75 g (7/8 of the original L/W_{max}) given a single rotor failure. Unlike the previous cases, in these figures the control power limits do not update during the run based on the current state of the rotors.

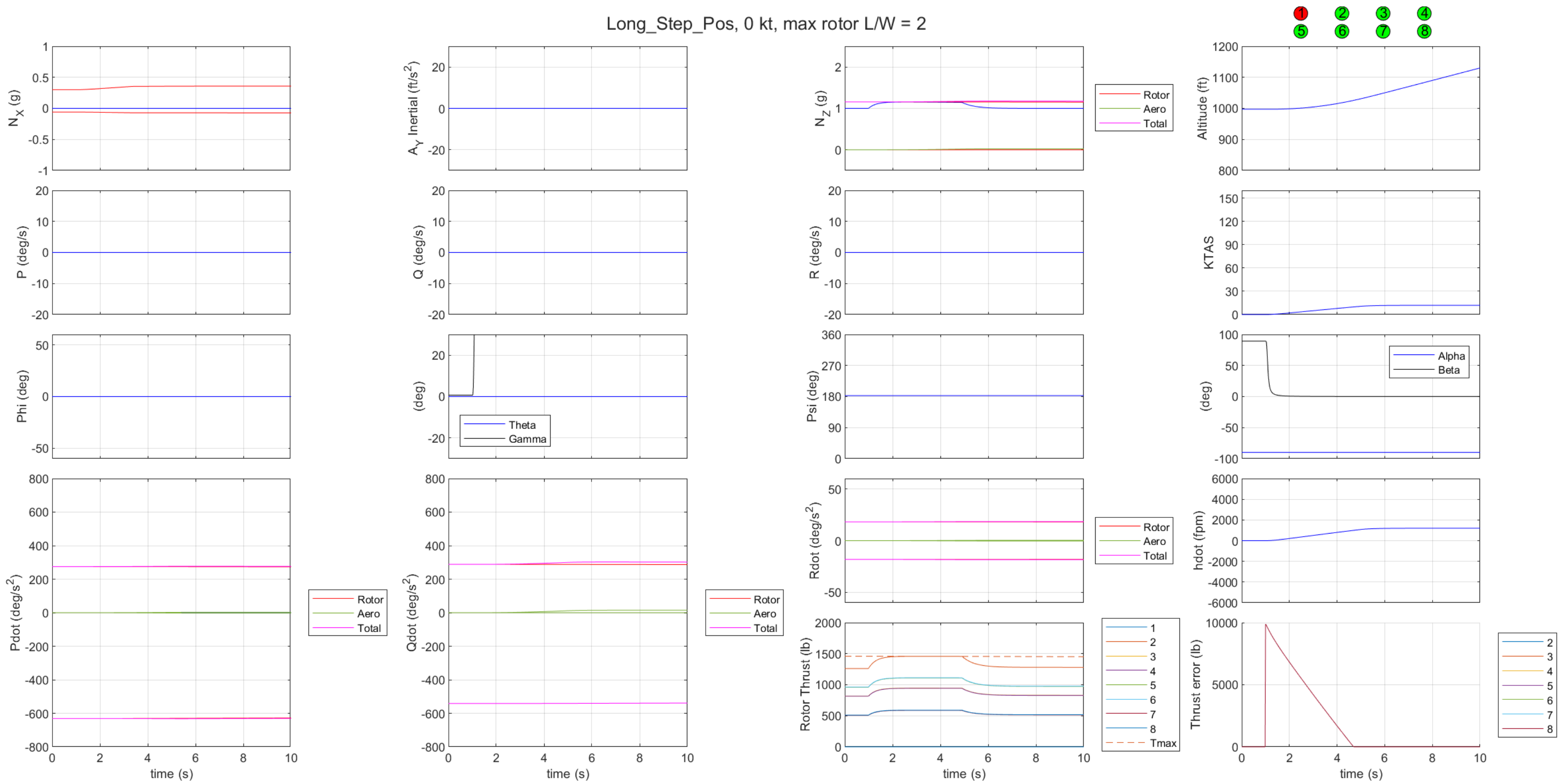

Figure 20. Max Pos. long. step trimmed at 0 KGS with an L/Wmax = 2 g and rotor one failed

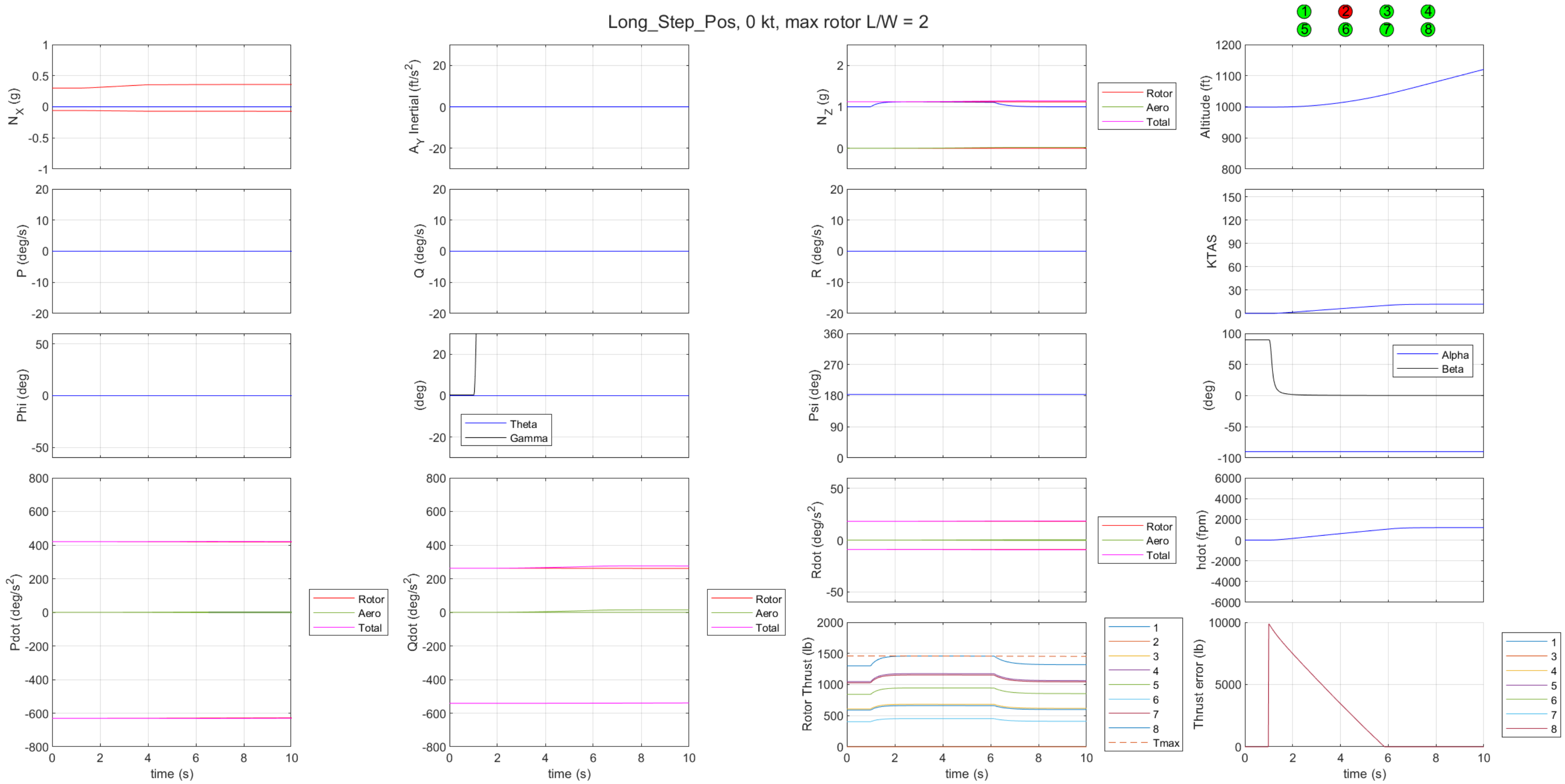

Figure 21. Max Pos. long. step trimmed at 0 KGS with an L/Wmax = 2 g and rotor two failed

The failure of rotor two has a slightly more significant effect on the vertical acceleration response of the vehicle as seen in the increased duration it takes to eliminate the thrust error. The increased duration of the limited vehicle response from either a rotor one failure or a rotor two failure can be observed in Table 7 and Table 8 respectively. The aircraft does not recover from a rotor two failure in a hover with L/W_{max} of 1.8 g but at all other conditions represented in both tables.

Table 7. Max Pos. Long. step rotor one failure results

Pilot Input	Trim Speed (kt)	Max Rotor L/W	Nz Response Duration (s)	Primary Axis Rotor CP Status	Secondary Axis Rotor CP Status	Primary Axis Total CP Status	Secondary Axis Total CP Status
Long. Pos. Step	0	1.8	>9	>9	>9	>9	>9
		2	5.38	3.00	3.00	3.00	3.00
	20	1.8	>9	>9	>9	>9	>9
		2	6.08	4.56	4.56	4.56	4.56
	40	1.8	0.64	>9	>9	>9	>9
		2	0.68	>9	>9	>9	>9

Rotor 1 Failure
Completely Limited
Significantly Limited
Never Limited

Table 8. Max Pos. Long. step rotor two failure results

Pilot Input	Trim Speed (kt)	Max Rotor L/W	Nz Response Duration (s)	Primary Axis Rotor CP Status	Secondary Axis Rotor CP Status	Primary Axis Total CP Status	Secondary Axis Total CP Status
Long. Pos. Step	0	1.8	Doesn't Recover				
		2	6.62	4.16	4.16	4.16	4.16
	20	1.8	>9	>9	>9	>9	>9
		2	8.48	6.82	6.82	6.82	6.82
	40	1.8	0.66	>9	>9	>9	>9
		2	0.20	6.58	6.58	6.58	6.58

Rotor 2 Failure
Completely Limited
Significantly Limited
Never Limited

4.3.2 Maximum pedal step with rotor failures

For lateral/directional axes, positive and negative inputs were performed to show the asymmetry resulting from a single rotor failure. The thrust allocation for the respective command is visible from the rotor thrust plot and provides a good visual tool in identifying the cause of the asymmetry. The time histories for a maximum pedal step in both directions are shown in Figure 22 and Figure 23. Rotor one was only failed for the L/W_{max} of 2 g cases. The rotor thrust plot in Figure 23 shows the saturation of rotor two and the resulting diminished $\dot{r}$ response while Figure 22 has no rotor saturation.

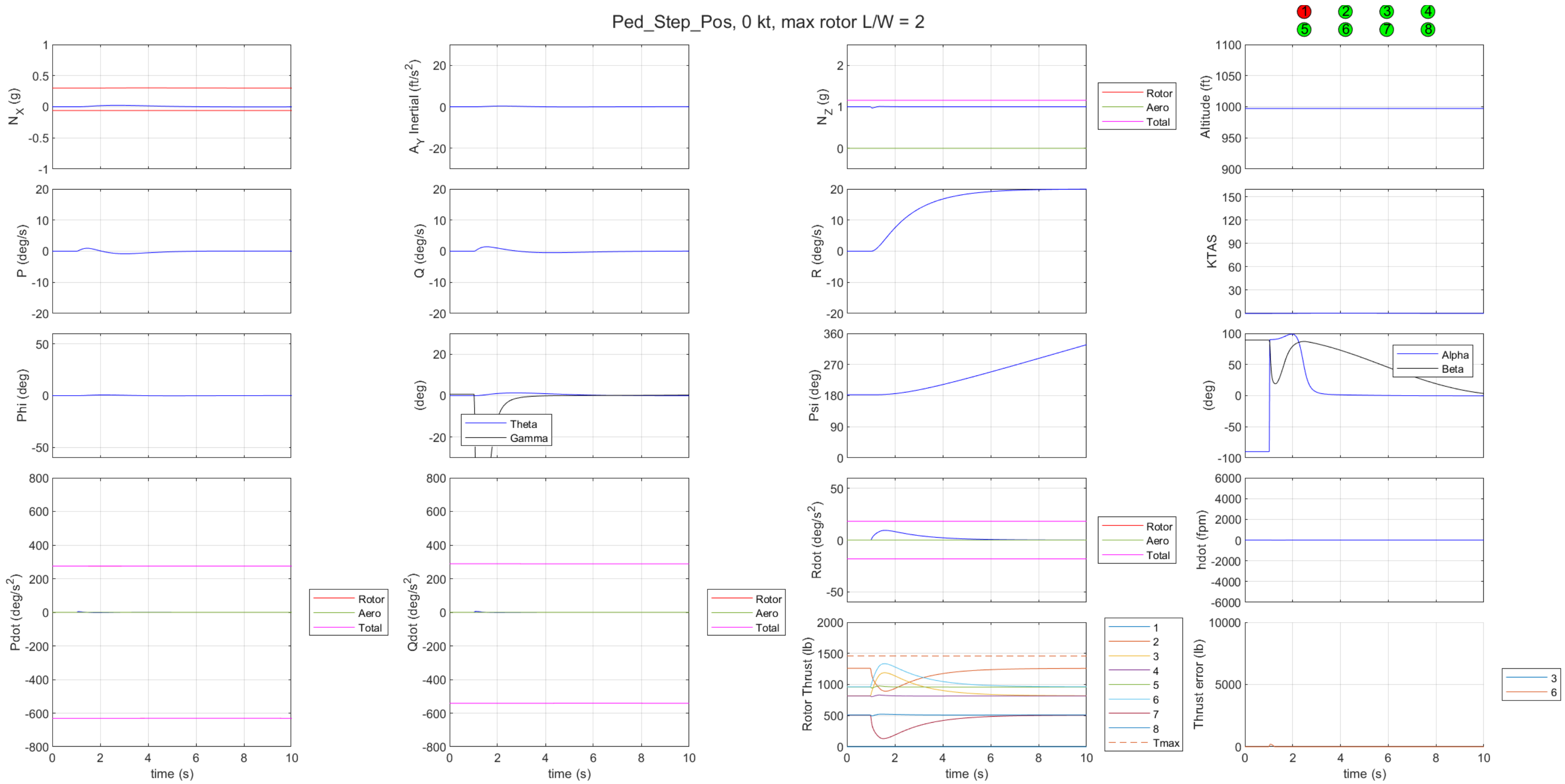

Figure 22. Max Pos. Ped. step trimmed at 0 KGS with an L/Wmax = 2 g and rotor one failed

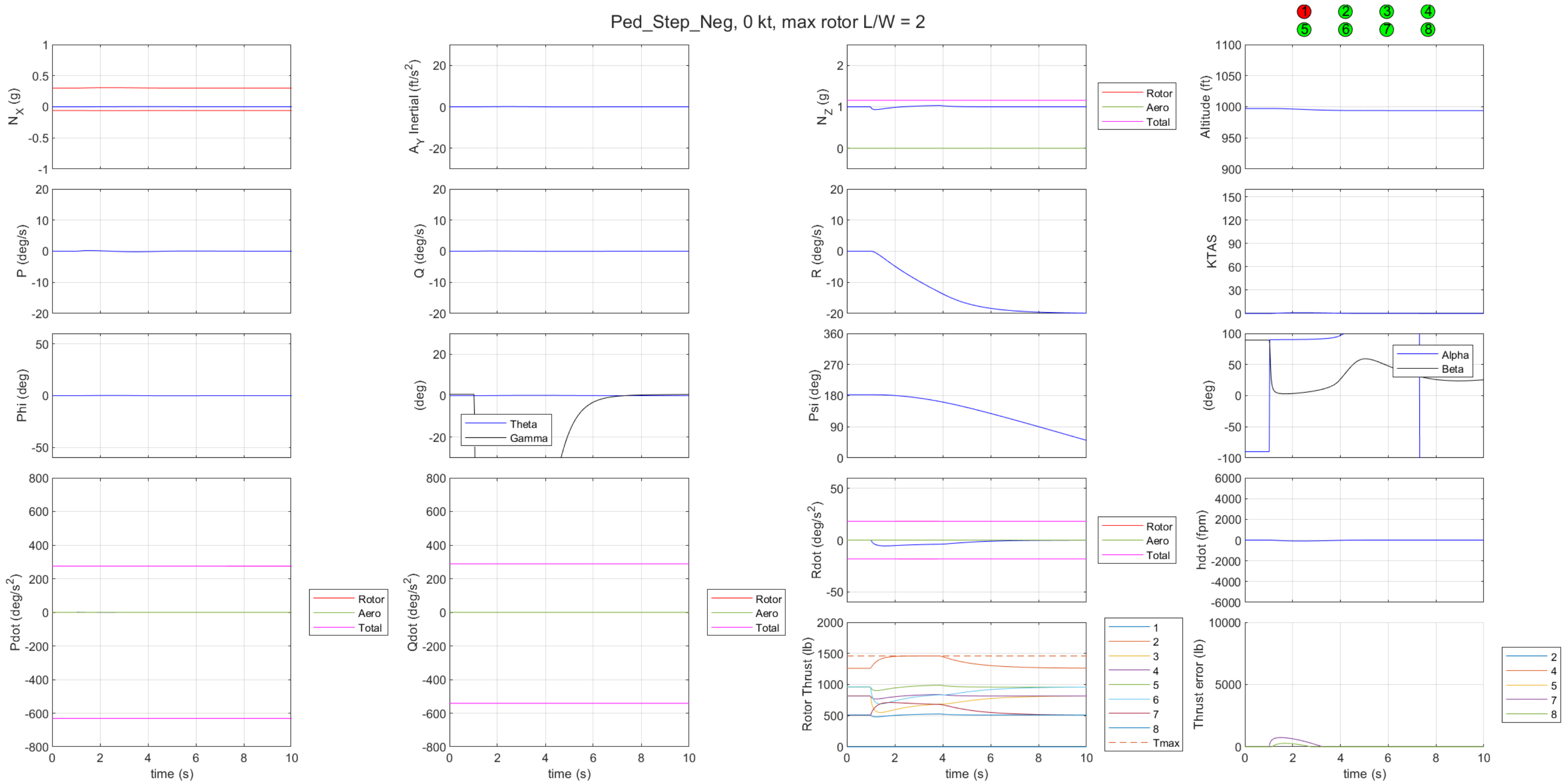

Figure 23. Max Neg. Ped. step trimmed at 0 KGS with an L/Wmax = 2 g and rotor one failed

The results of a positive and negative pedal step input with rotor one failed are shown below in Table 9 and Table 10 respectively. As mentioned, the difference in significance of control power limitations is apparent between positive and negative commands. The 40 KIAS and above test conditions were not evaluated because the vehicle did not recover to wings level after the rotor failure. The rotor failure caused an initial bank angle and the bank angle hold function in cruise mode held the bank angle. Since the aircraft was not designed to return to a bank angle of zero on its own, the lateral/directional response characteristics would be affected and a valid comparison in response durations between test cases could be compromised. For a full evaluation, a programmed input or autopilot control should return the vehicle to wings level before inputs are applied. That was not done for this limited study.

Table 9. Max Pos. Ped. step rotor one failure results

Pilot Input	Trim Speed (kt)	Max Rotor L/W	Rdot Response Duration (s)	Primary Axis Rotor CP Status	Secondary Axis Rotor CP Status	Primary Axis Total CP Status	Secondary Axis Total CP Status
Ped. Pos. Step	0	1.8	5.90				
		2	5.74				
	20	1.8	>9				
		2	>9				
	40	1.8	Control system is bank angle hold. Bank angle does not return to wings level after rotor failure				
		2					

Rotor 1 Failure
Completely Limited
Significantly Limited
Never Limited

Table 10. Max Neg. Ped. step rotor one failure results

Pilot Input	Trim Speed (kt)	Max Rotor L/W	Rdot Response Duration (s)	Primary Axis Rotor CP Status	Secondary Axis Rotor CP Status	Primary Axis Total CP Status	Secondary Axis Total CP Status
Ped. Neg. Step	0	1.8	>9	>9	>9	>9	>9
		2	6.76	1.94	1.94	1.94	1.94
	20	1.8	>9	>9	>9	>9	>9
		2	>9	1.32	1.32	1.32	1.32
	40	1.8	Control system is bank angle hold. Bank angle does not return to wings level after rotor failure				
		2					

Rotor 1 Failure
Completely Limited
Significantly Limited
Never Limited

4.3.3 Maximum positive longitudinal and negative lateral step with rotor failures

Multi-axis commands during rotor failures were the most severely control power-limited cases out of the entire analysis. Every input combination explored in the analysis of this type had at least four completely limited cases out of six for both rotor failures. Figure 24 and Figure 25 show a maximum positive longitudinal step with a simultaneous maximum negative lateral step for a rotor one and rotor two failure respectively. The runs start in a hover after the rotor failure and have the L/W_{max} of 2 g configuration. The increased significance of vehicle response to the rotor two failure is also noticeable for this multi-input case. While control power was completely limited for an extended period in both cases, the aircraft did not depart controlled flight. Given the lack of control margin, that may not be the case with external disturbances like turbulence.

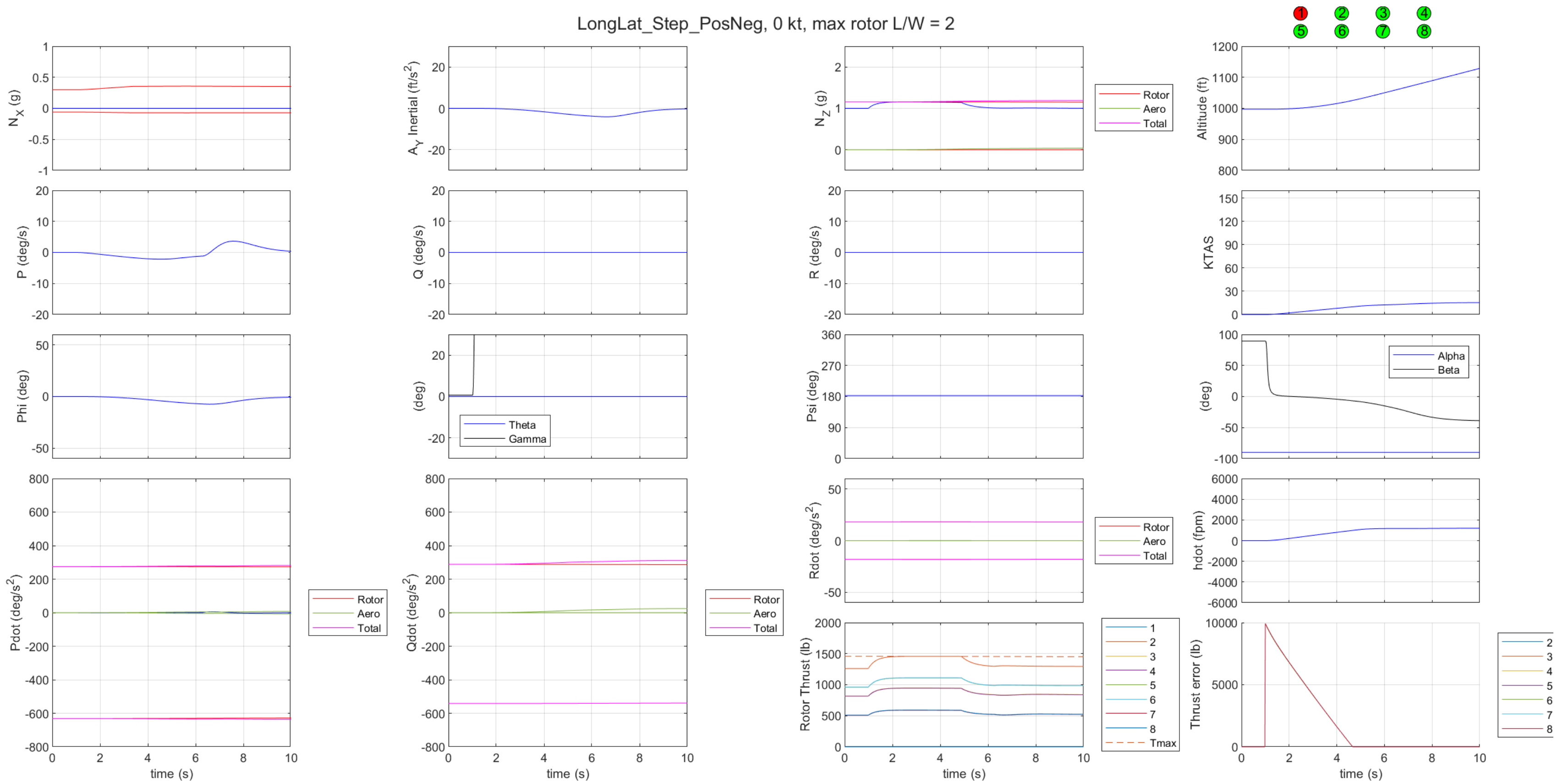

Figure 24. Max Pos. Long. and Neg. Lat. step trimmed at 0 KGS with an L/Wmax = 2 g and rotor one failed

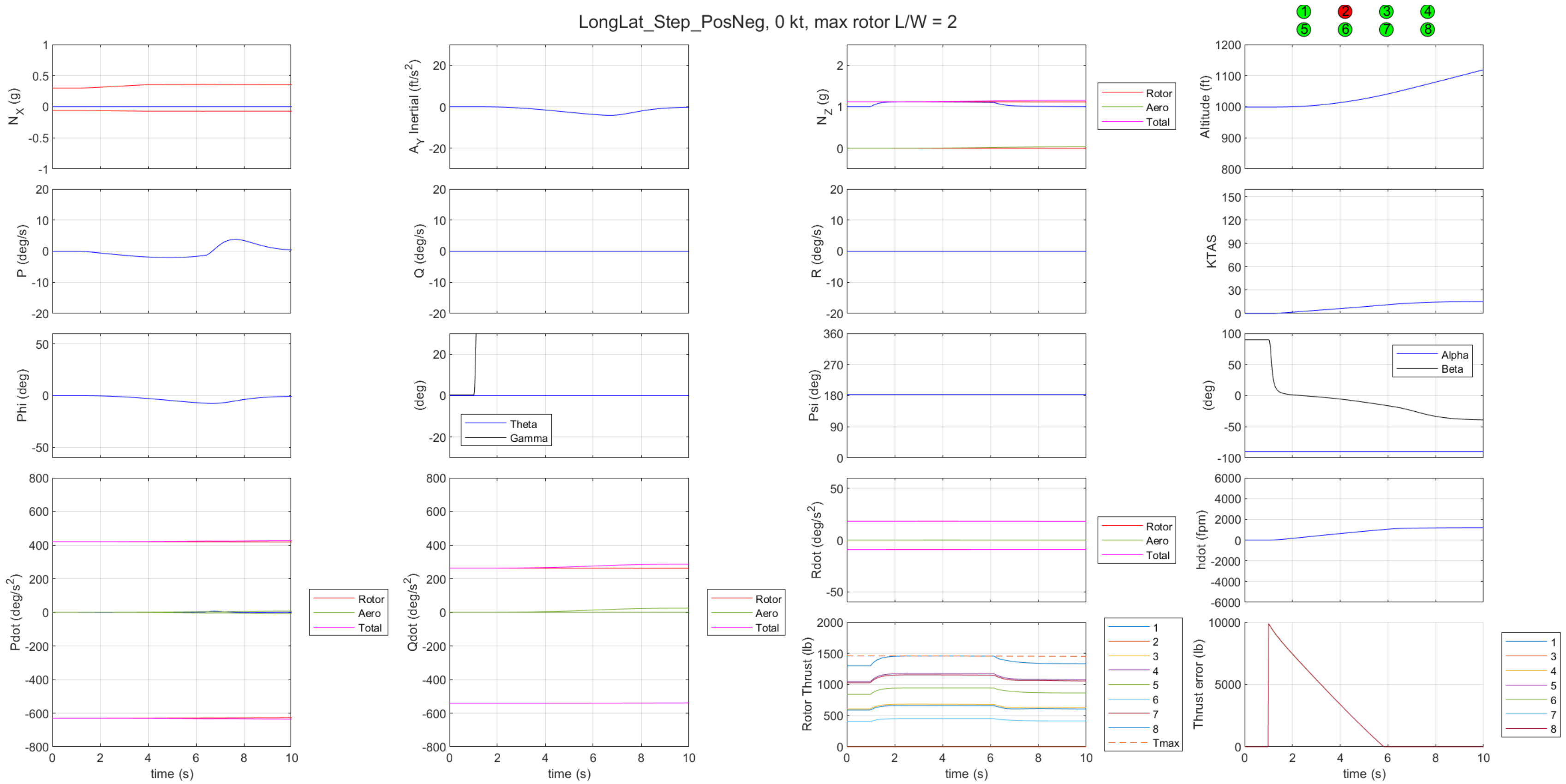

Figure 25. Max Pos. Long. and Neg. Lat. step trimmed at 0 KGS with a L/Wmax = 2 g and rotor two failed

Results from the simultaneous maximum positive longitudinal and negative lateral step command with a rotor one and rotor two failure is shown in Table 11 and Table 12 respectively. A unique result of this test case is the low-speed roll at 20 KIAS caused by the bank angle limiter not being tuned for the rotor failure and decreased control power authority. The aircraft enters a limit cycle oscillation (LCO) against the bank angle limit. This effect was not present during nominal flight with full control power authority; and therefore, the response duration was not recorded. This demonstrates the need to modify the control system for failure modes. Control system modifications were not part of this work. Runs for the 40 KIAS and above trim speed during a rotor 1 failure were not included for the same reason as discussed for Table 9 and Table 10.

Table 11. Max Pos. Long. and Neg. Lat. step rotor one failure results

Pilot Input	Trim Speed (kt)	Max Rotor L/W	Nz Response Duration (s)	Pdot Response Duration (s)	Primary Axis 1 Rotor CP Status	Primary Axis 2 Rotor CP Status	Secondary Axis Rotor CP Status	Primary Axis 1 Total CP Status	Primary Axis 2 Total CP Status	Secondary Axis Total CP Status
Pos. Long. & Pos. Lat Step	0	1.8	>9	6.96	>9	>9	>9	>9	>9	>9
		2	5.44	5.60	2.88	2.88	2.88	2.88	2.88	2.88
	20	1.8	Begins Low Frequency Limit Cycle Oscillation							
		2	8.22	3.98	7.08	7.08	7.08	7.08	7.08	7.08
	40	1.8	Control system is bank angle hold. Bank angle does not return to wings level after rotor failure							
		2								

Rotor 1 Failure
Completely Limited
Significantly Limited
Never Limited

Table 12. Max Pos. Long. and Neg. Lat. step rotor two failure results

Pilot Input	Trim Speed (kt)	Max Rotor L/W	Nz Response Duration (s)	Pdot Response Duration (s)	Primary Axis 1 Rotor CP Status	Primary Axis 2 Rotor CP Status	Secondary Axis Rotor CP Status	Primary Axis 1 Total CP Status	Primary Axis 2 Total CP Status	Secondary Axis Total CP Status
Pos. Long. & Pos. Lat Step	0	1.8	Doesn't Recover							
		2	7.78	5.68	4.32	4.32	4.32	4.32	4.32	4.32
	20	1.8	Begins Low Frequency Limit Cycle Oscillation							
		2	7.70	4.26	>9	>9	>9	>9	>9	>9
	40	1.8	0.70	1.56	>9	>9	>9	>9	>9	>9
		2	0.72	1.20	>9	>9	>9	>9	>9	>9

Rotor 2 Failure
Completely Limited
Significantly Limited
Never Limited

The cases where data was omitted due to a potential misrepresentation of the trend of the response and control power saturation durations from this limited analysis must still be considered. A complete evaluation would require running the cases that were omitted in this paper. The rotor failure cases at 40 KIAS and above could be run by first putting in a pilot input to take the bank angle out. The LCO case with a rotor failure indicates a control system modification is needed. Making such modifications was not part of this work, but the cases clearly need to be addressed for a full evaluation.

4.4 Prioritization results

Single-axis prioritization was implemented for the vertical axis to address the envelope protection failure discussed in Section 4.2.3. The failure resulted in a negative vertical rate that could defeat the envelop protection and enter VRS. The prioritization method was designed to scale down all other commands to ensure the commanded vertical lift command is achieved. The scaling down is done with up to 50 iterations within a single simulation timestep. It is possible a residual error would remain with this approach. However, that did not happen in the runs made. Importantly, the simple prioritization implemented made some control power limits less significant but resulted in loss of control in other cases, which is addressed later in this section.

Figure 26 shows two time histories from two batch runs plotted over each other with identical staggered step inputs shown in the inceptor deflection plot. The second plot shows a red line and a pink dashed line like the $\dot{h}$ departure from Figure 19 without prioritization. The blue line is the same case run with prioritization. Vertical lift prioritization prevented the maneuver from breaking through the VRS envelope protection.

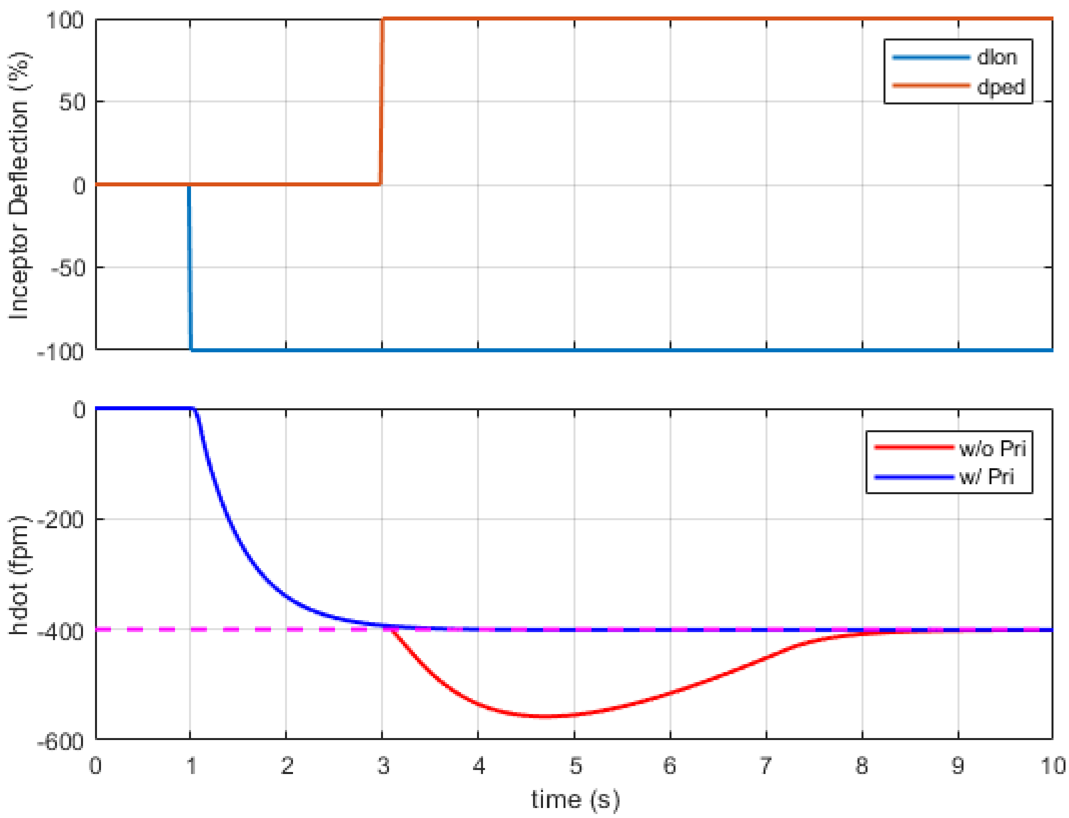

Figure 26. VRS envelope protection with and without prioritization

A limited analysis was performed to evaluate the effect of single-axis prioritization on rotor failure cases. It was found that the aircraft could not recover from a failure of rotor two at 1000 ft. The failure with vertical control prioritization resulted in combined roll and pitch departures even with the full 2 g L/W_{max} control power configuration. Running the same case at 50 ft MSL instead of the standard 1000 ft MSL was recoverable. It was determined that rotor one was being saturated trying to compensate for the loss of rotor two. During the saturation, the system prioritized altitude, not the pitch and roll departures that result from all rotor failure configurations. When the vehicle is prioritizing the vertical axis the control system is unable to command the moments necessary to washout the residual pitch rate (q) and roll rate (p). Despite the n_z prioritization, the vehicle was also unable to maintain altitude due to both the rotor saturation and the pitch and roll departure. If prioritization were applied to the pitch and roll axes during the aircraft reaction to a rotor failure the departure could likely have been avoided.

Rotor 1 is not saturated at 50 ft MSL because of the increased available control power due to the increased air density. The change in available thrust per rotor was only 2.76% between cases but it was enough to saturate rotor one and cause the departure. Four simulation runs are shown in Figure 27, which compare the failure of rotor two at one second for 50 ft MSL and 1000 ft MSL. Cases without and with prioritization are shown on the left and right respectively.

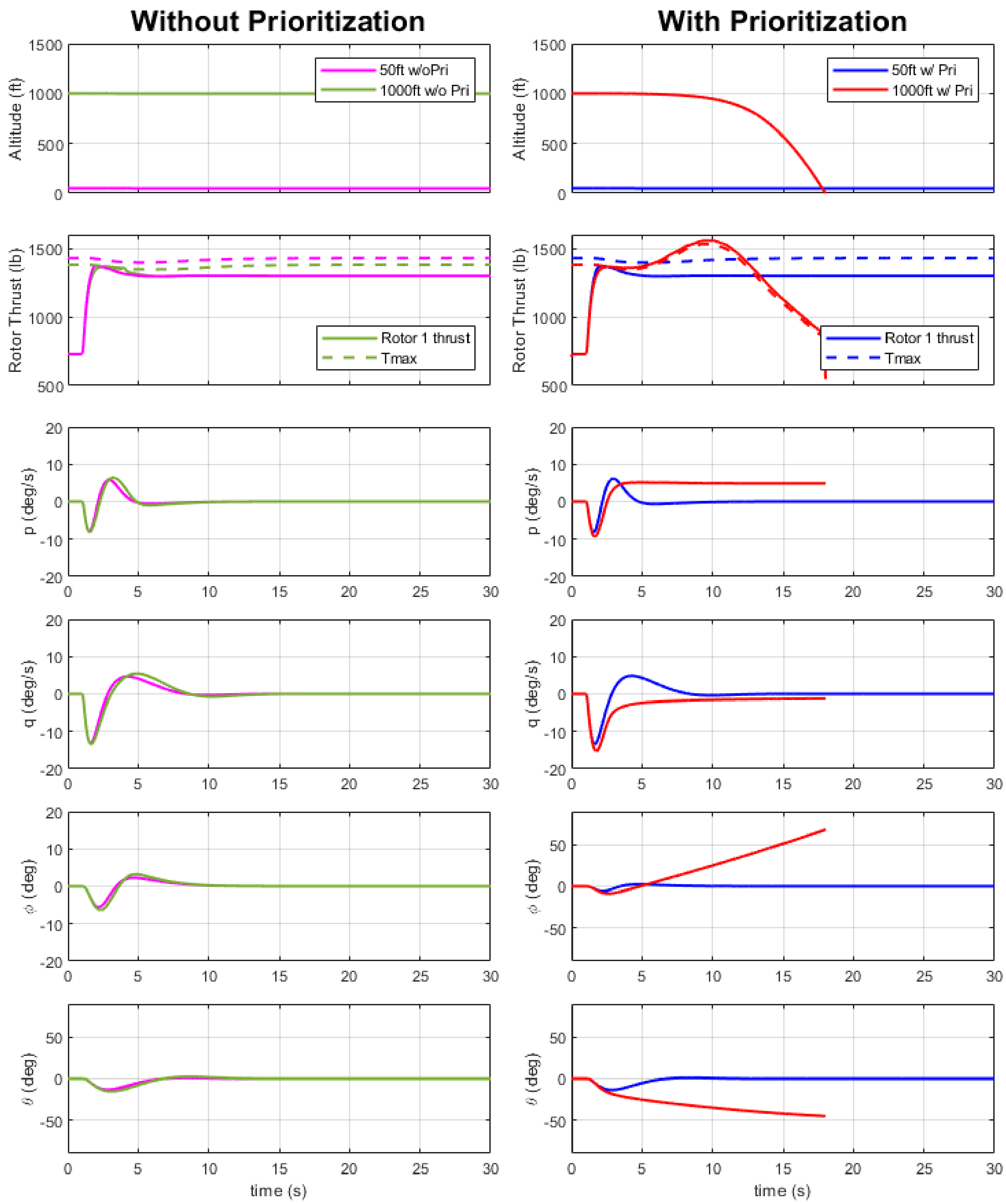

Figure 27. Time history after rotor failure at two altitudes without (left) and with (right) prioritization

5 Figure eight observations/lessons learned

The control power analysis method presented in this paper should be considered during aircraft design and evaluation. The following are lessons learned and observations from the work. Some are specific to the vehicle used in the study and some are generally applicable.

5.1 Secondary axis limitations

In this analysis, control inputs were applied from a steady state condition. The axis to which the command was applied was the primary axis and all other axes were considered secondary. The results from this analysis show that any kind of pilot input and rotor failure configuration can severely limit a vehicle's control power with a small control power margin. Multi-input commands and rotor failures resulted in the most significant control power limiting even with larger control power margins. This is applicable to most eVTOL rotorcraft, but significance of the limits will vary across configurations.

A single-axis command will significantly limit the secondary axis' control authority only if the primary axis itself is limited. Some configurations may have effectors that control a specific axis independently from the rest and therefore may have less primary and secondary axis coupling. Additionally, the Lift+Cruise configuration analyzed for this work is designed to function entirely as a fixed-wing aircraft at high speeds. Other configurations such as multirotor aircraft without aerodynamic surfaces may have their control power supplied by the rotors for the entire flight envelope. This would require adjustments to the speeds being tested to reflect the rotor-borne flight envelope.

5.2 Envelope protection

It is important to consider that control power allocation could be unoptimized and has the potential to defeat envelope protection for certain pilot inputs or flight conditions. Without control power prioritization it was shown that multiple command inputs can result in envelope protections being defeated. How and under what conditions this can occur should be carefully considered and evaluated. Additionally, it was demonstrated that a simple control power prioritization addressing a problem at one flight condition could cause a problem at another. Thus, the control power prioritization needs to consider flight condition and more than one parameter.

5.3 Control methods

Vehicle response from rotor failure can vary depending on which rotor fails and its role for a given control method. The Lift+Cruise model for this study used its inboard canted rotors to generate yawing moments. This contrasts with differential torque from variable rotor RPM used to generate a yawing moment. The insufficient performance from a speed-controlled variable rotor sized for urban air mobility (UAM) is determined in Malpica & Winthrow-Maser (2020). However, because of the inboard canted rotor control method used by the vehicle described in this paper any inboard rotor failure will significantly limit the yaw authority of the aircraft in a hover. This is due to the limited number of rotors available to achieve the commanded r while maintaining the lift required to hold altitude. This is very configuration specific but illustrates the need for testing failure modes for all rotors.

5.4 Configuration control authority

The Lift+Cruise configuration evaluated was found to have no significant single-axis control power limiting above 1.6 g L/W_{max} and negligible multi-axis limiting at 1.8 g. This is dependent on the rotor model and configuration, but could potentially be used as a rule of thumb with determining necessary control power margin for the rotors.

5.5 Prioritization

It was demonstrated that rotor control power axis prioritization is likely necessary. A single axis prioritization algorithm was added to the rotor allocation controller given inter-axis coupling observed between n_z and $\dot{r}$. The simple implementation was shown to be successful in preventing the uncommanded losses in altitude that was observed. However, with rotor failures, prioritization was found to result in loss of control under other conditions. The departure was sensitive to flight condition. A relatively small change in lift control power available due to an altitude change resulted in a departure in one case but not another. The change in control power in a real vehicle could be the result of different density altitude, lower battery energy state, among other things that may occur frequently under normal operations. This indicates that each case must be analyzed to determine, not just whether the test case is limited, but how close was the case to a catastrophic limit in control power. This consideration simply points to a need to conduct the evaluations at the most control power limited parts of the flight envelope.

The vehicle model had been flown for over a year in the Cockpit Motion Facility (CMF) and was shown to effectively recover from any single rotor failure at all tested flight conditions without prioritization. The level of nuance and care necessary for this analysis is apparent given that consequences from features such as this single-axis prioritization may go completely undiscovered if the vehicle is not extensively evaluated.

6 Conclusion

A method of control power analysis was described and partially applied to get a better understanding of the interaction of control power margin with vehicle performance along with primary and secondary axis control power authority. Results also provided a means of developing understanding of the vehicle and its various systems, quirks, and features. Some things discovered were unknown until the analysis. The extent of the evaluation using this method should be left to the discretion of the designer or evaluator having extensive knowledge of the vehicle and flight controls. All configuration change points should be explored by testing around them seeking a deeper understanding of vehicle behavior. A thorough understanding of the control power authority with respect to the operational envelope of the vehicle is necessary. Control power limited flight conditions and even some dangerous failure modes can be identified using this approach. The method described should be beneficial to designers and evaluators of new aircraft and existing aircraft with new or modified aerodynamics and/or flight controls.

7 References

Advanced Rotorcraft Technology, Inc. (2019). *Flight control models for a concept vehicle.* Sunnyvale: Research Activities Branch, National Aeronautics and Space Administration.

Aeronautical design standard performance specification handling qualities requirements for military rotorcraft [ADS-33E-PRF]. (2000). Redstone Arsenal, Alabama: United States Army Aviation And Missile Command Aviation.

Denham Jr, J. W., & Paines, J. (2008). *Converging on a precision hover control strategy for the F-35B STOVL aircraft.* Honolulu: AIAA.

Hoffler, K. D., Duerksen, N., Bossinger, R. L., Martos, B., & Mitchell, D. G. (2022). *Development and evaluation of mission task elements for certification of aircraft with non-conventional control interfaces, [DOT/FAA/TC-22/32]*. Federal Aviation Administration.

Malpica, C., & Withrow-Maser, S. (2020, January 21-23). Handling qualities analysis of blade pitch and rotor speed controlled eVTOL quadrotor concepts for urban air mobility. San Jose: VFS International Powered Lift Conference 2020.

A Selected additional cases

The time histories given in this appendix are all remaining individual test points from the test matrices that are not explicitly discussed in the Results section.

This appendix is organized by pilot input as followed:

A.1 Maximum positive longitudinal step

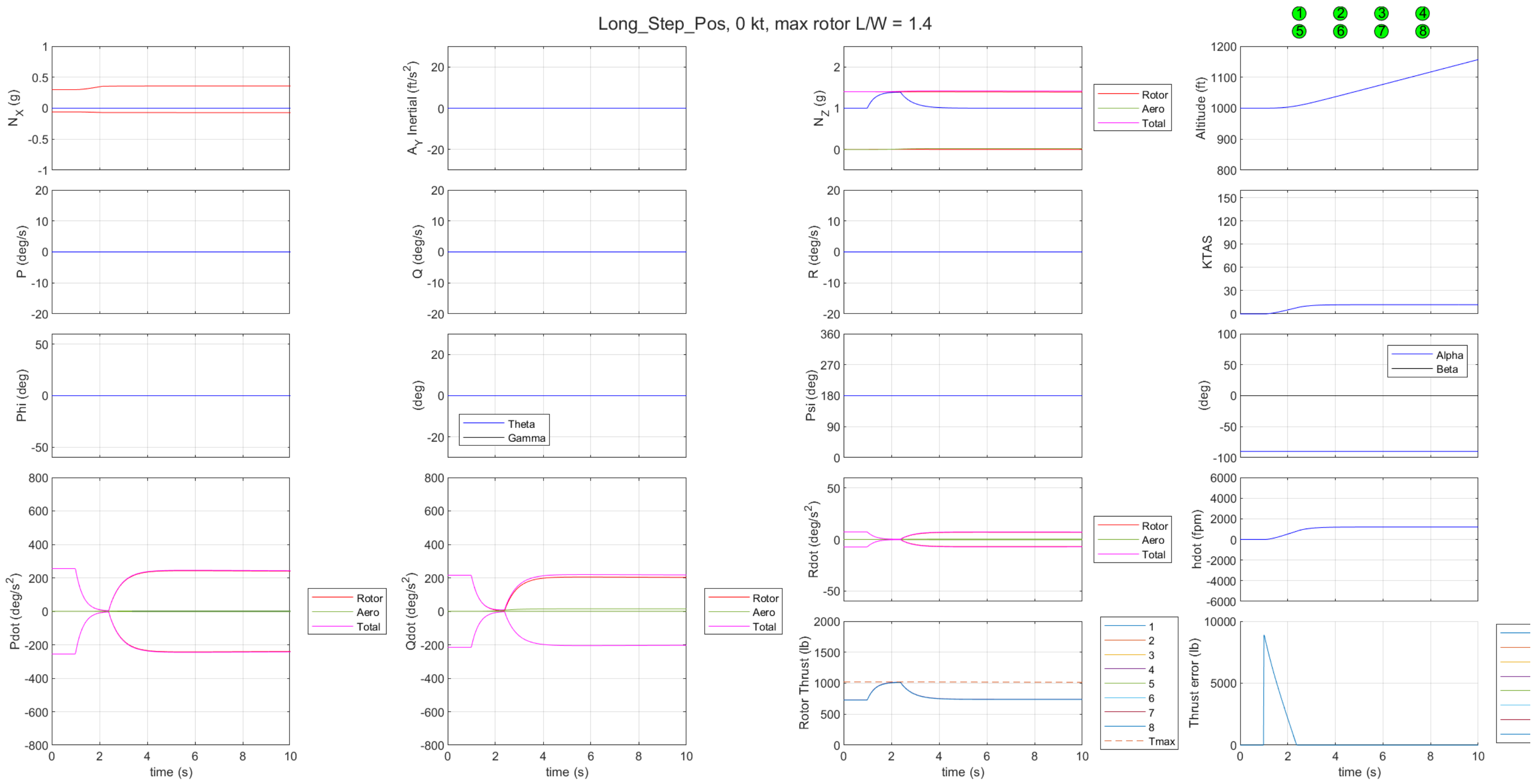

Figure A- 1. Max Long. Pos. Step trimmed at 0 KGS with an L/Wmax = 1.4 g

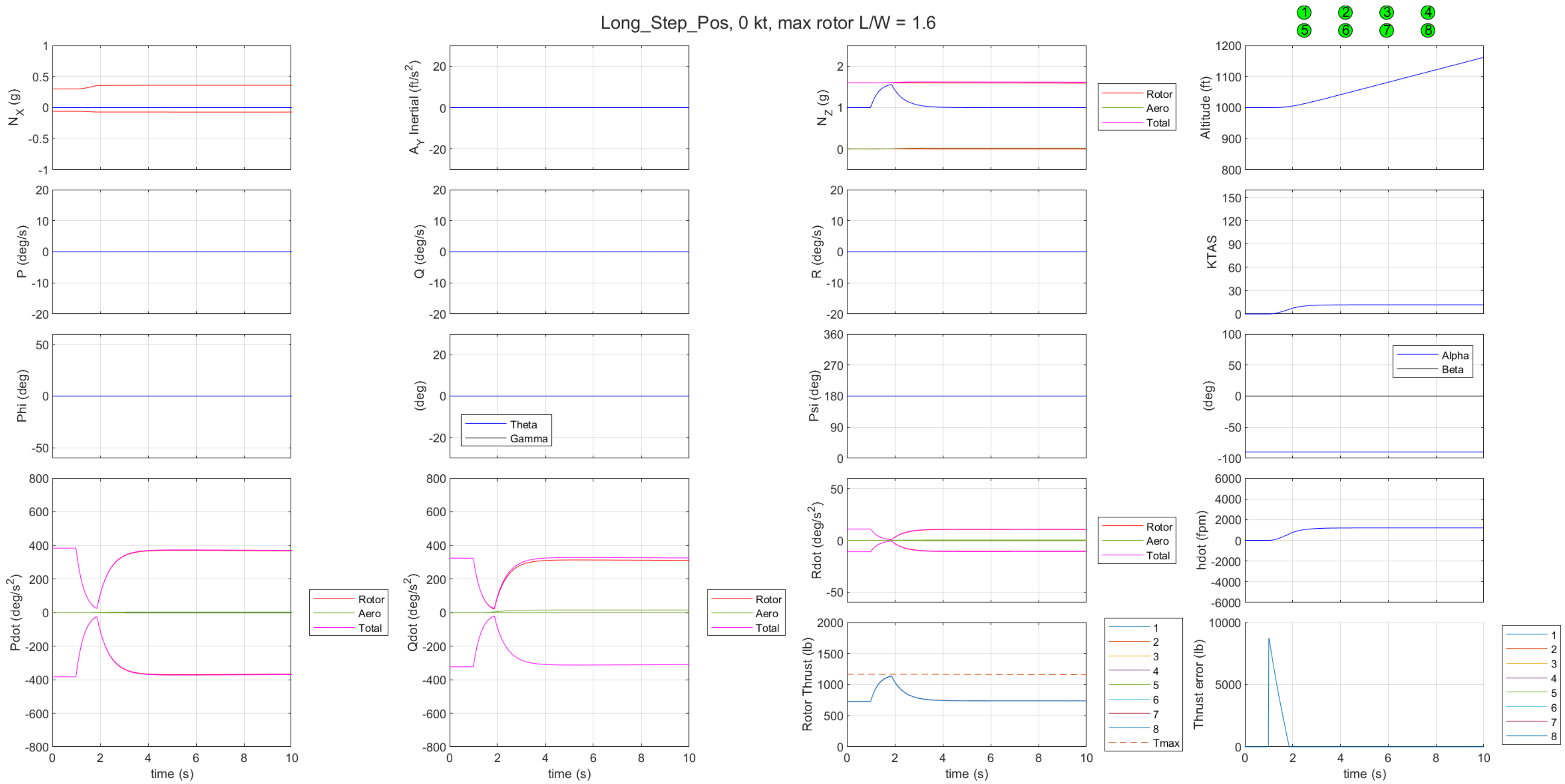

Figure A- 2. Max Pos. Long. Step trimmed at 0 KGS with an L/Wmax = 1.6 g

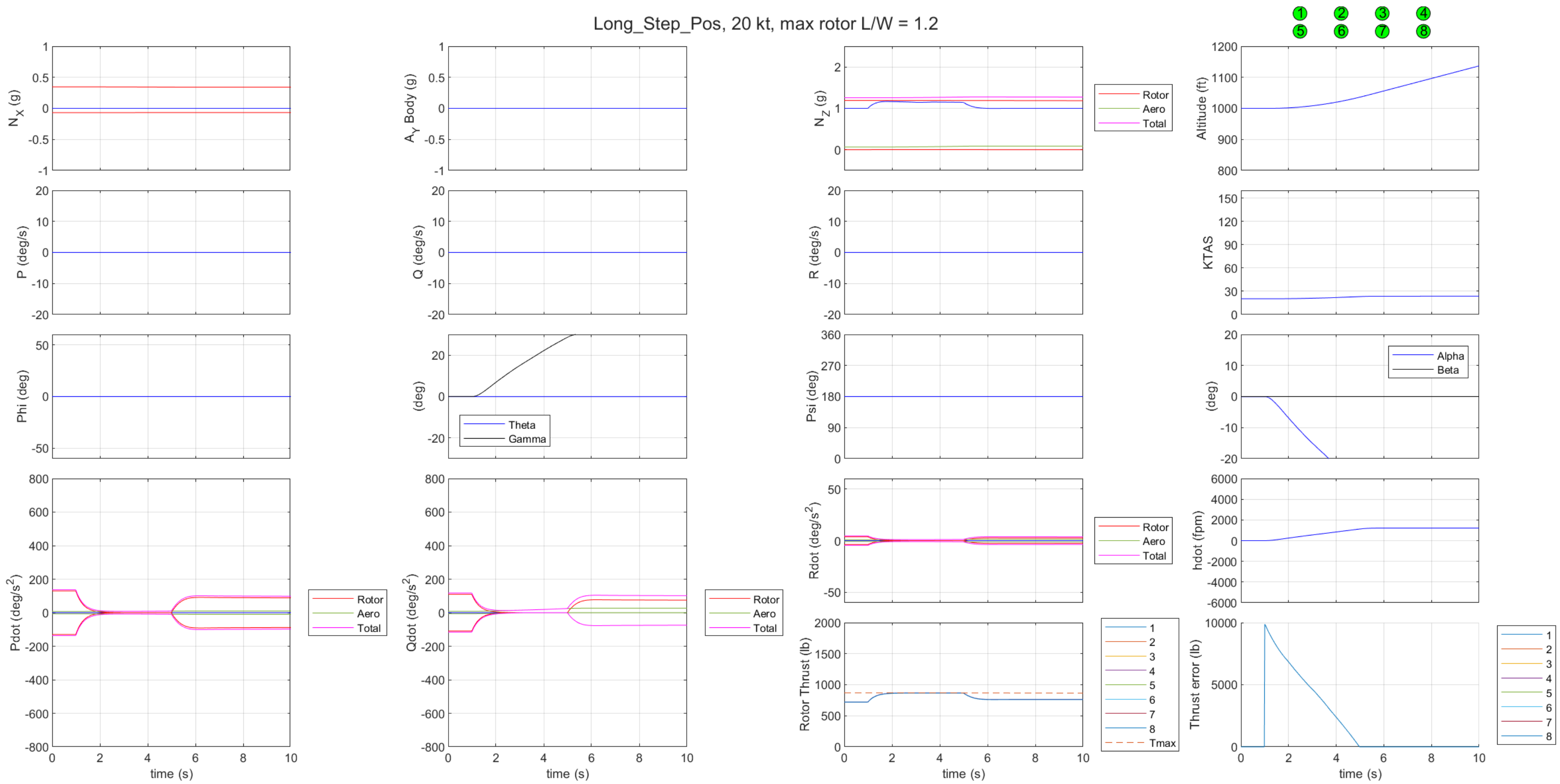

Figure A- 3. Max Pos. Long. Step trimmed at 20 KIAS with an L/Wmax = 1.2 g

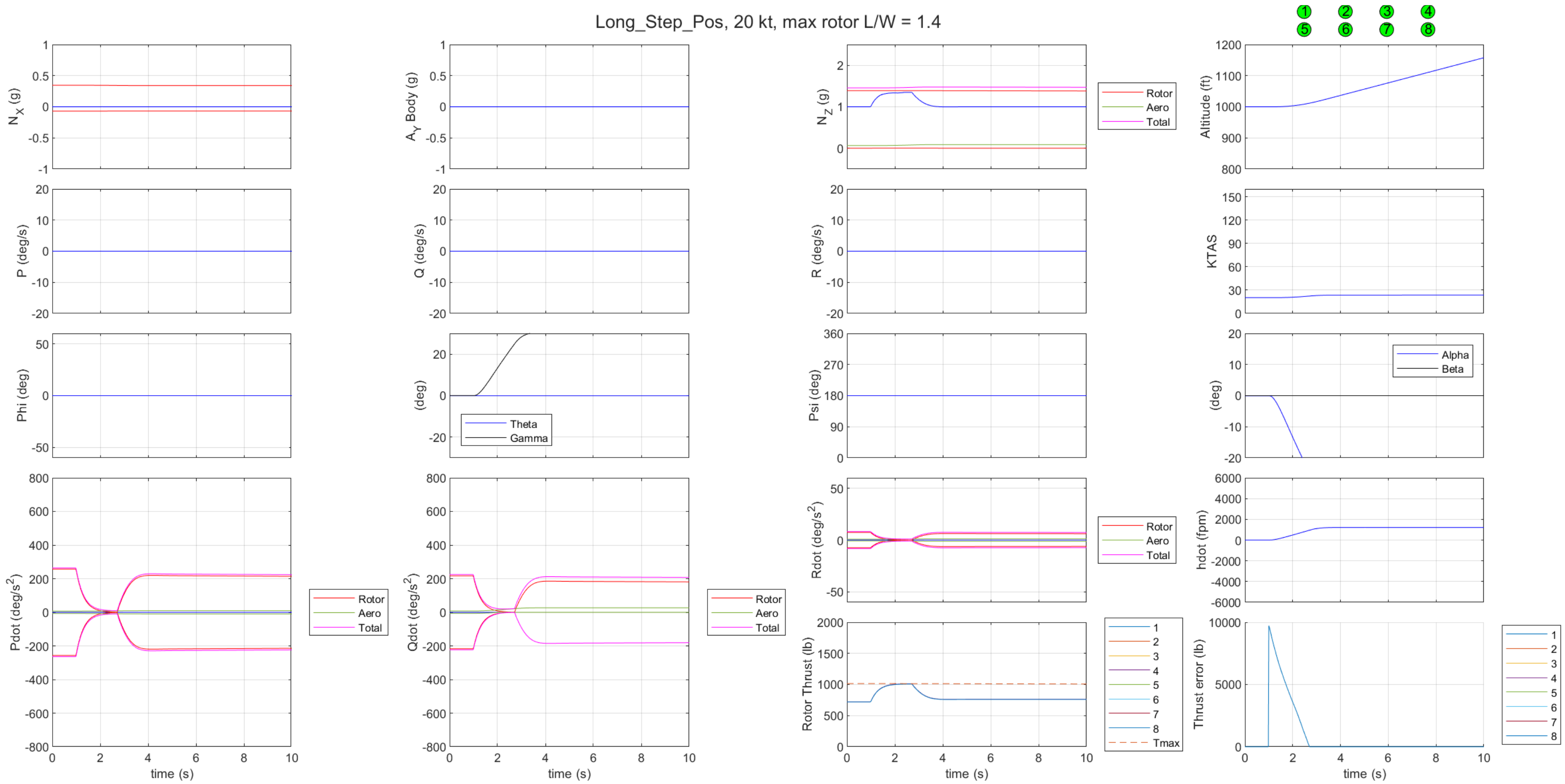

Figure A- 4. Max Pos. Long. Step trimmed at 20 KIAS with an L/Wmax = 1.4 g

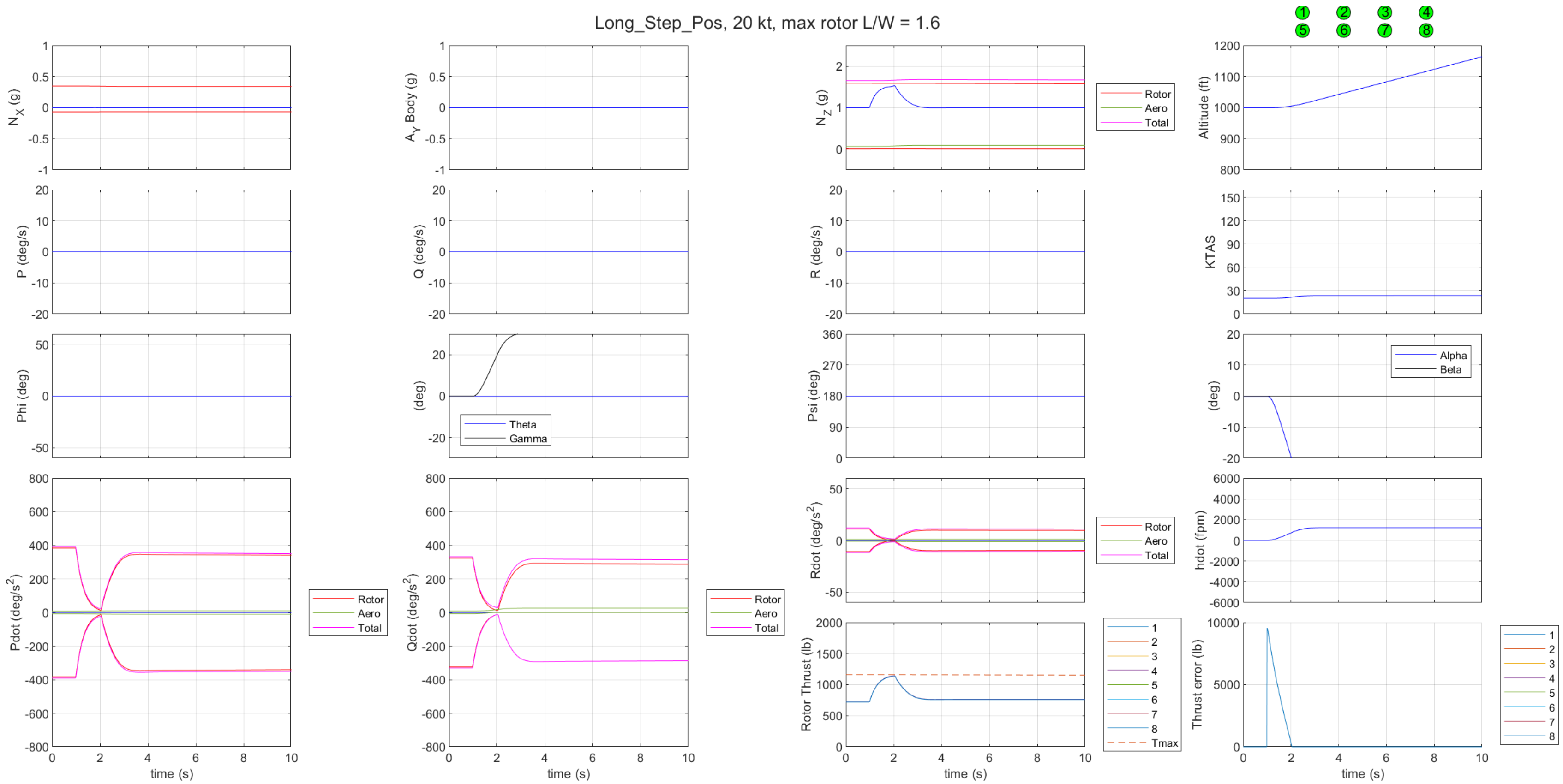

Figure A- 5. Max Pos. Long. Step trimmed at 20 KIAS with an L/Wmax = 1.6 g

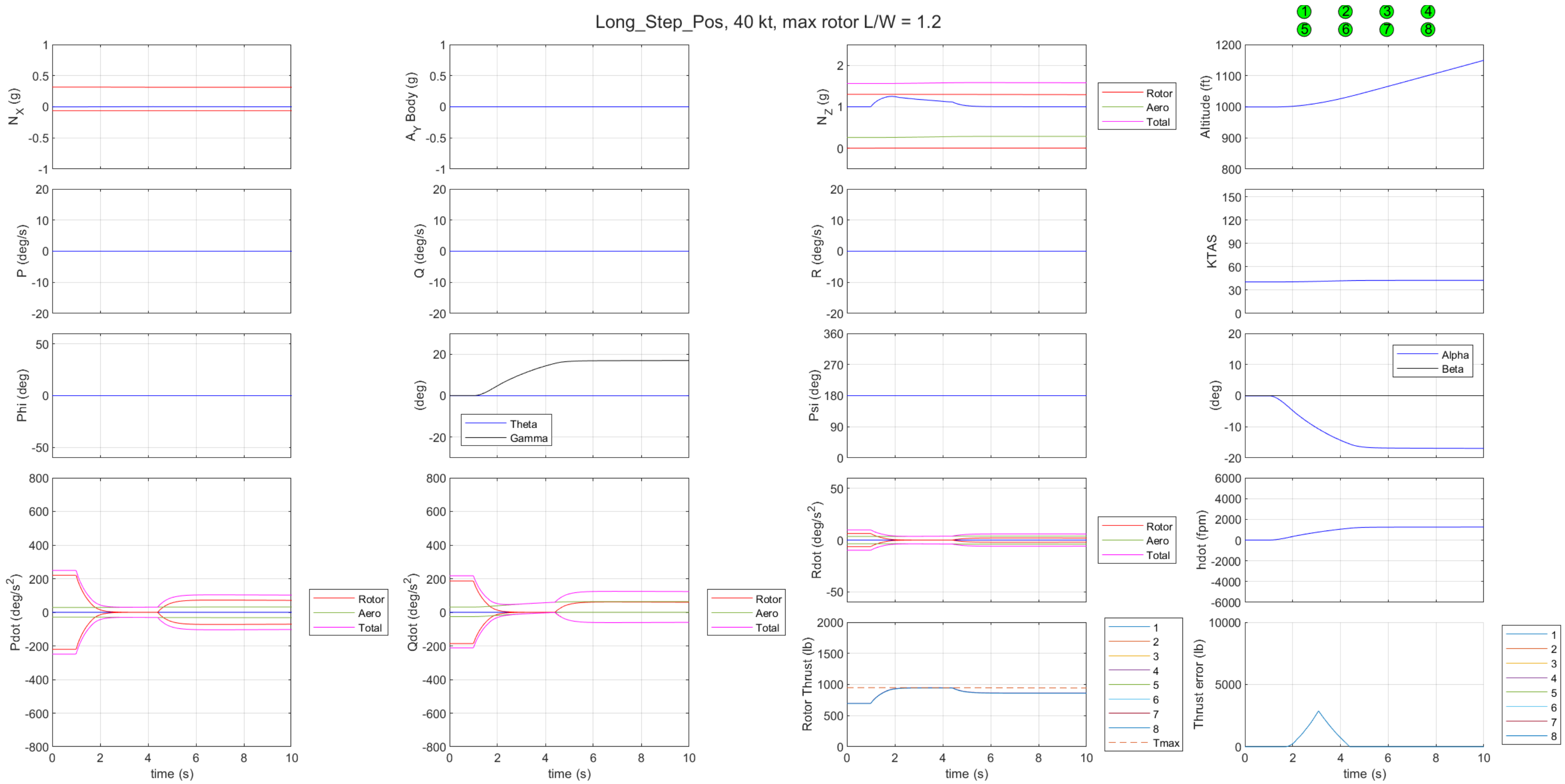

Figure A- 6. Max Pos. Long. Step trimmed at 40 KIAS with an L/Wmax = 1.2 g

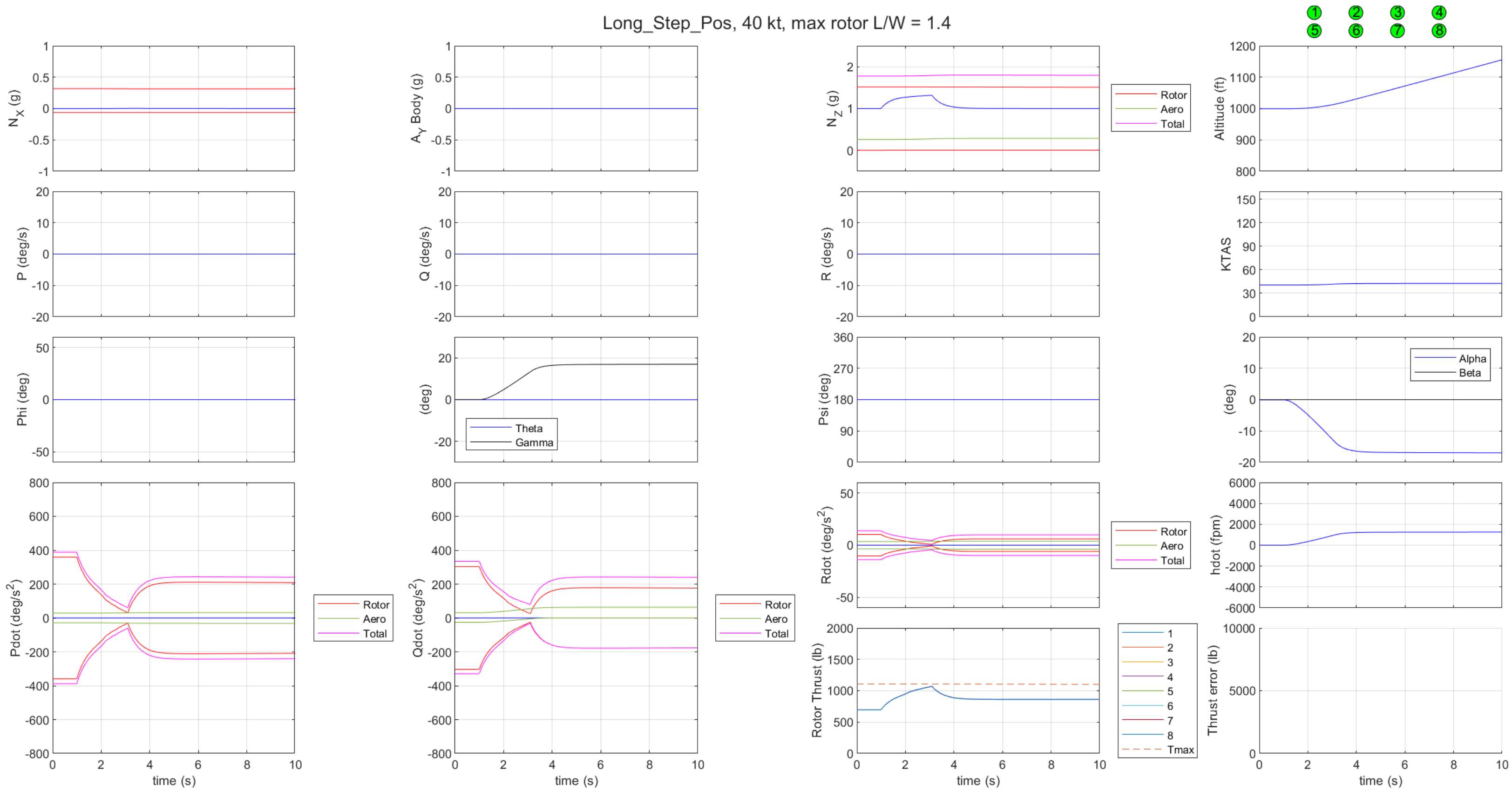

Figure A- 7. Max Pos. Long. Step trimmed at 40 KIAS with an L/Wmax = 1.4 g

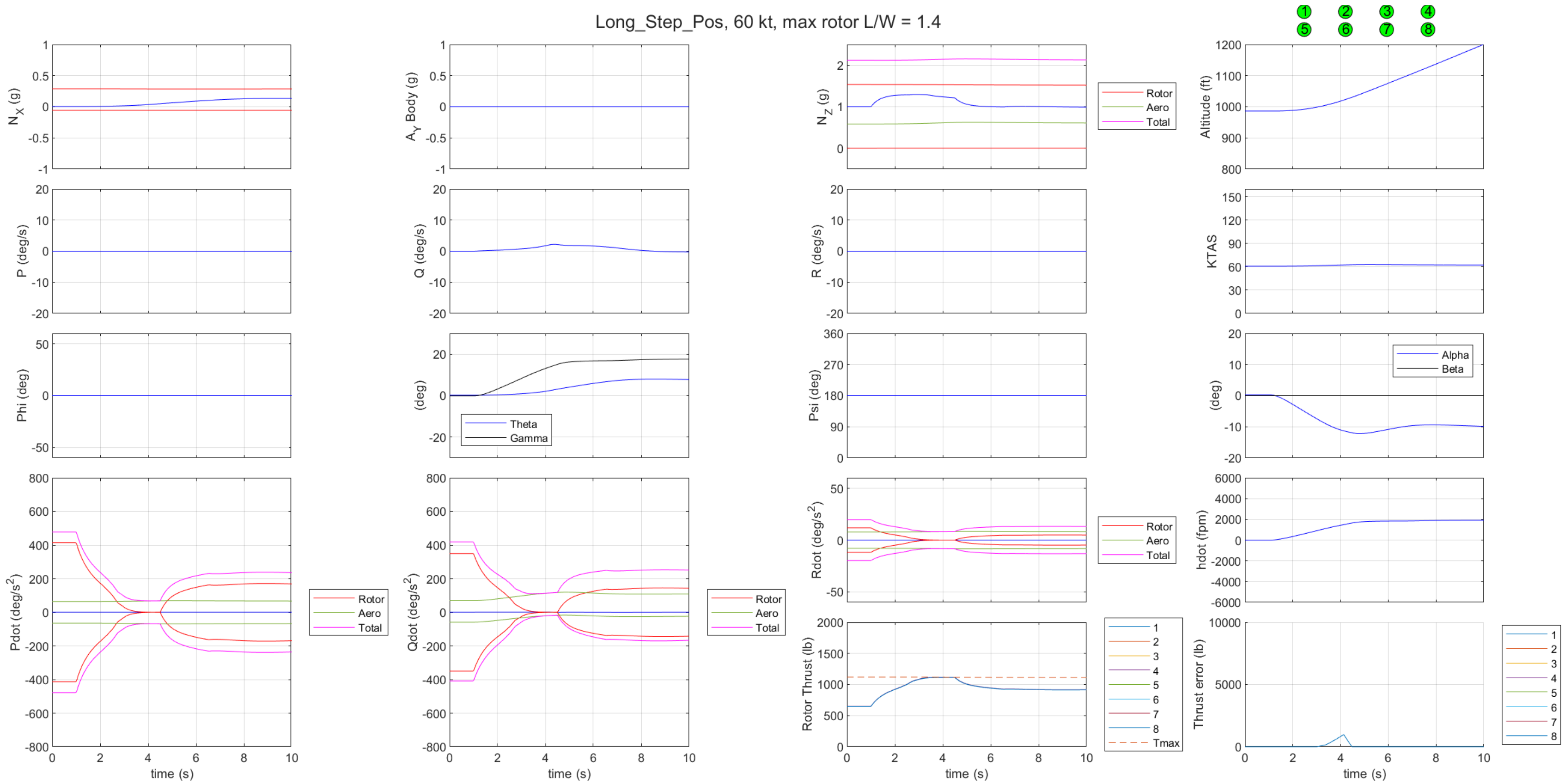

Figure A- 8. Max Pos. Long. step trimmed at 60 KIAS with an L/Wmax = 1.4 g

A.2 Half positive longitudinal step

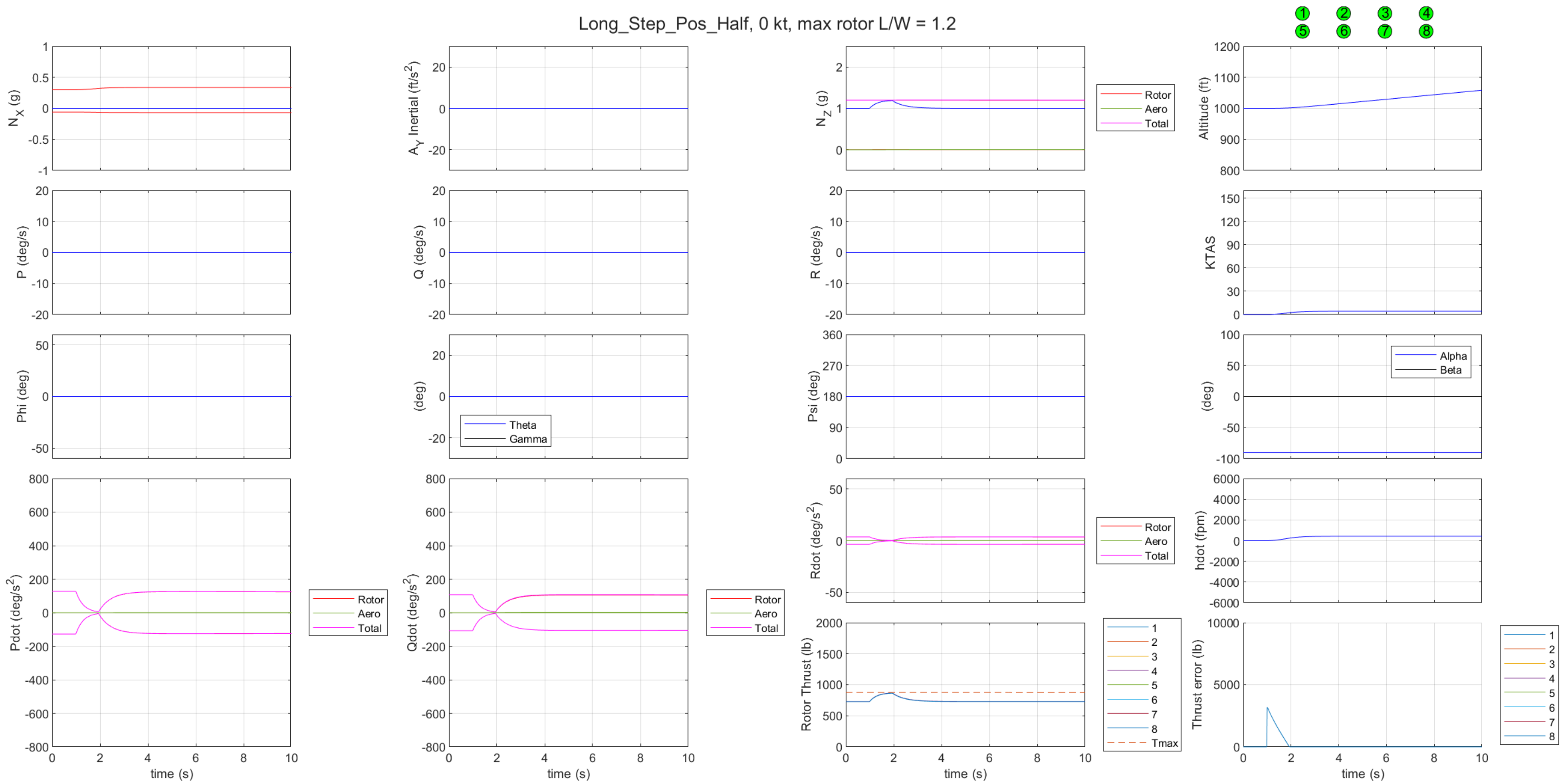

Figure A- 9. Half Pos. Long. step trimmed at 0 KGS with an L/Wmax = 1.2 g

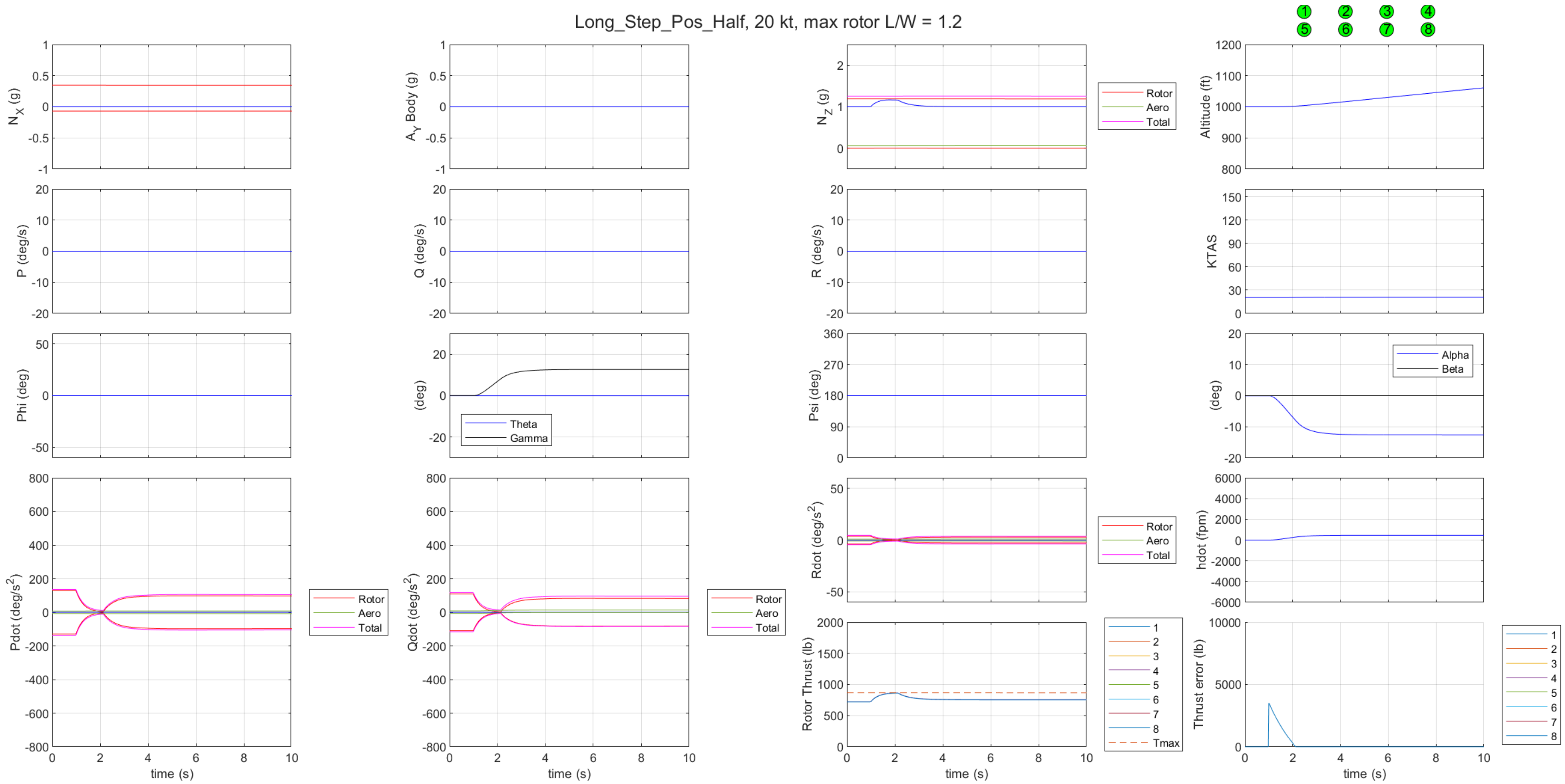

Figure A- 10. Half Pos. Long. step trimmed at 20 KIAS with an L/Wmax = 1.2 g

A.3 Maximum negative longitudinal step

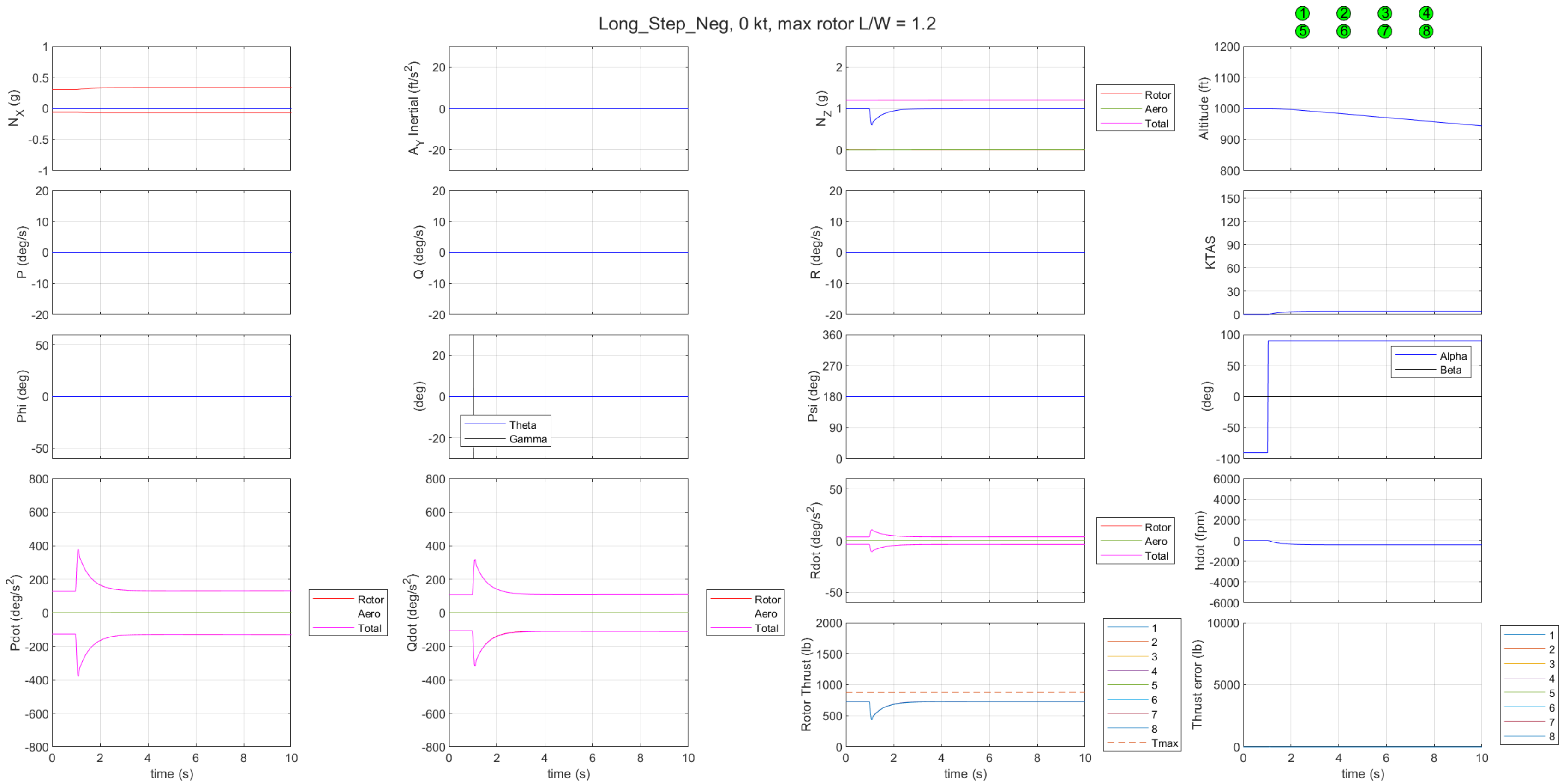

Figure A- 11. Max Neg. Long. step trimmed at 0 KGS with an L/Wmax = 1.2 g

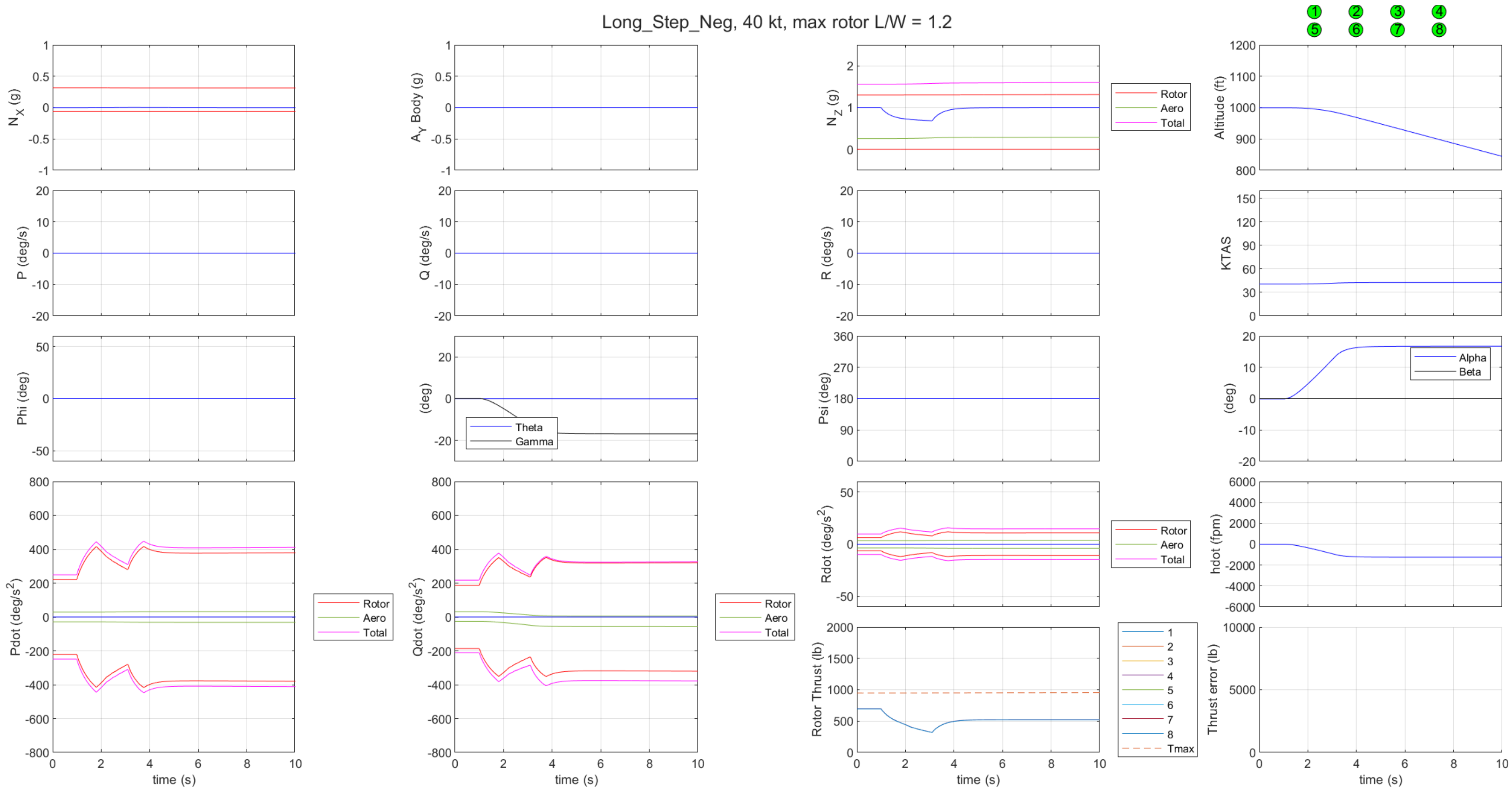

Figure A- 12. Max Neg. Long. step trimmed at 40 KIAS with an L/Wmax = 1.2 g

A.4 Maximum positive lateral step

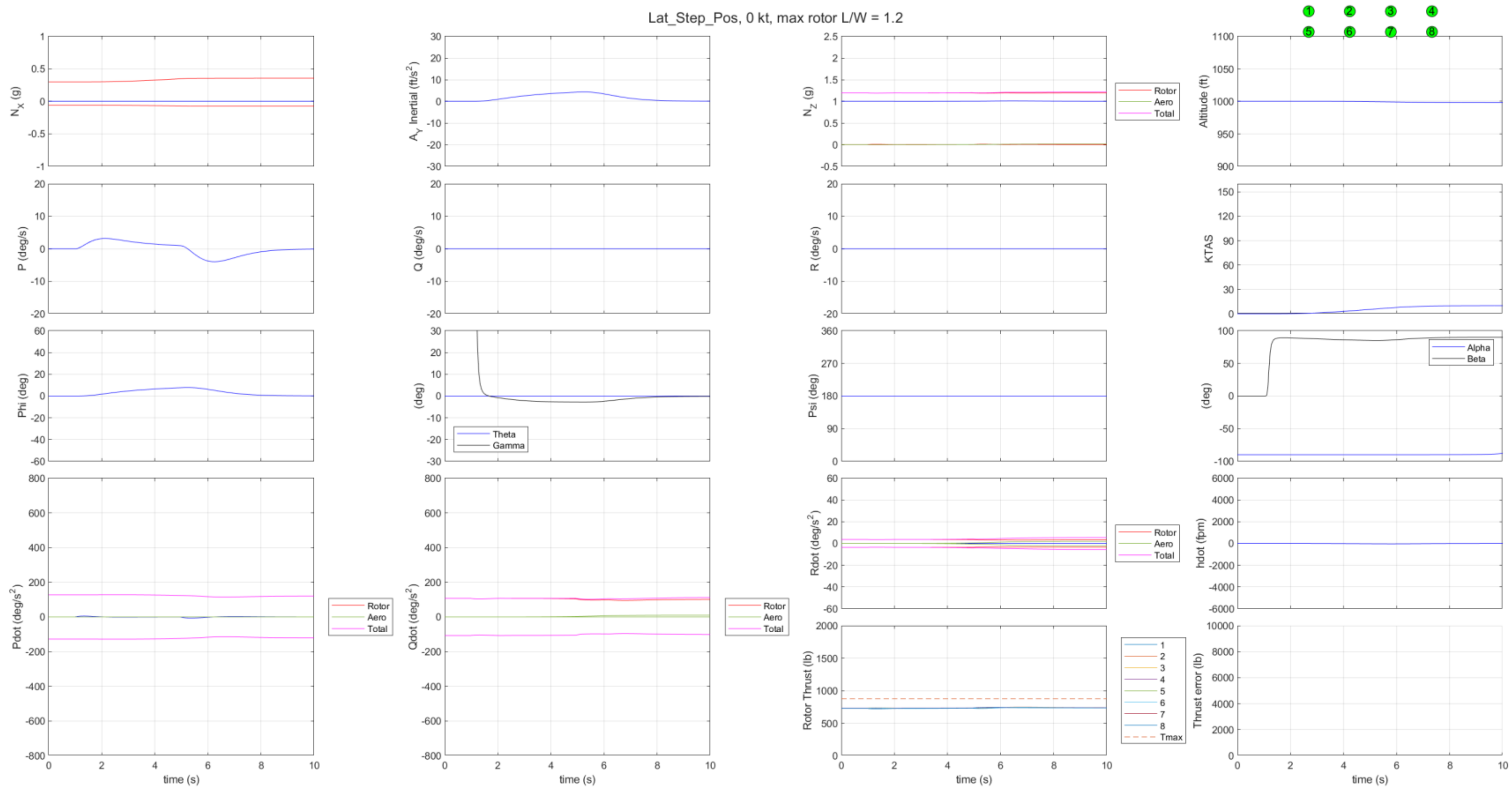

Figure A- 13. Max Pos. Lat. step trimmed at 0 KGS with an L/Wmax = 1.2 g

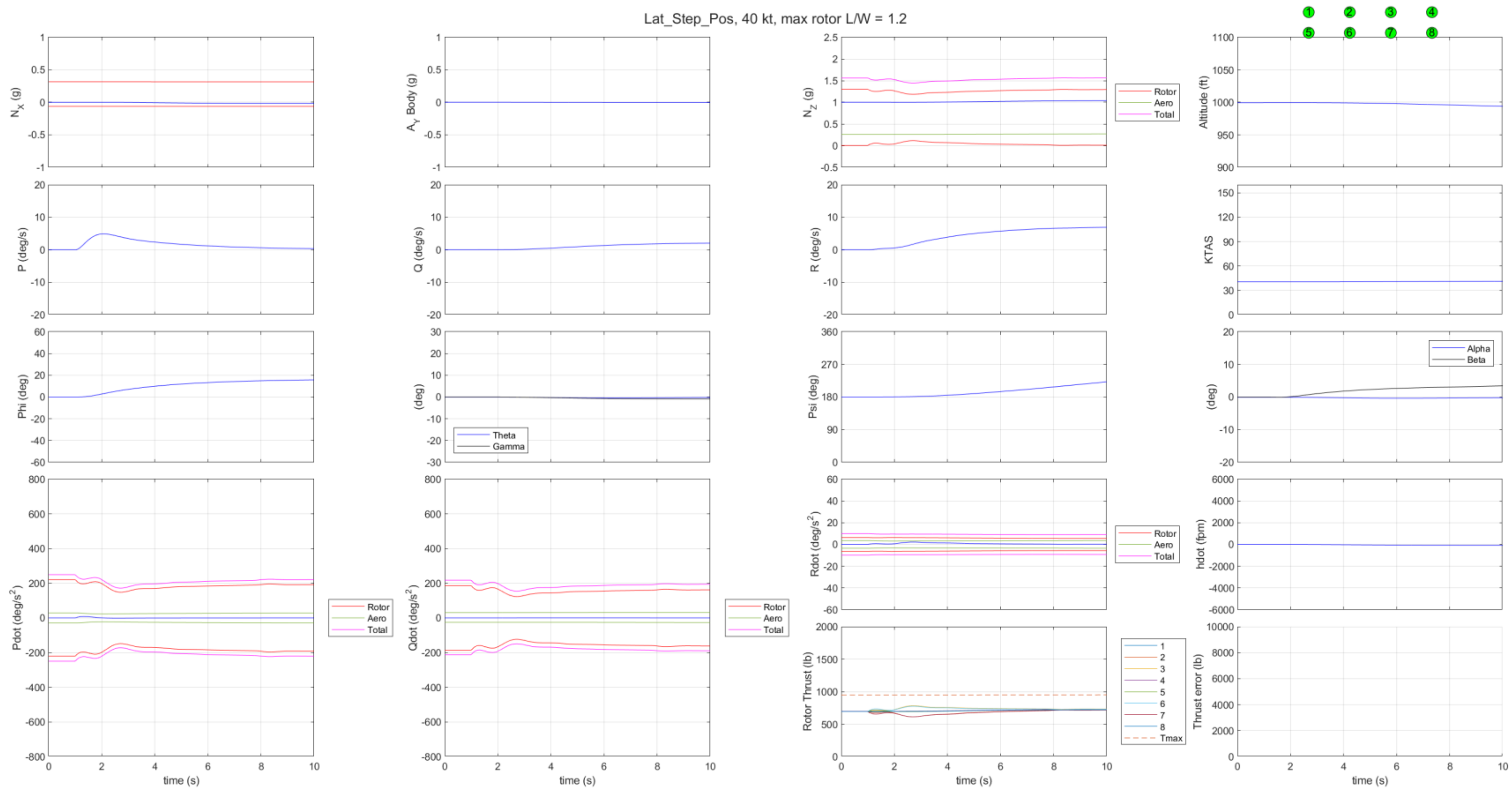

Figure A- 14. Max Pos. Lat. step trimmed at 40 KIAS with an L/Wmax = 1.2 g

A.5 Maximum positive pedal step

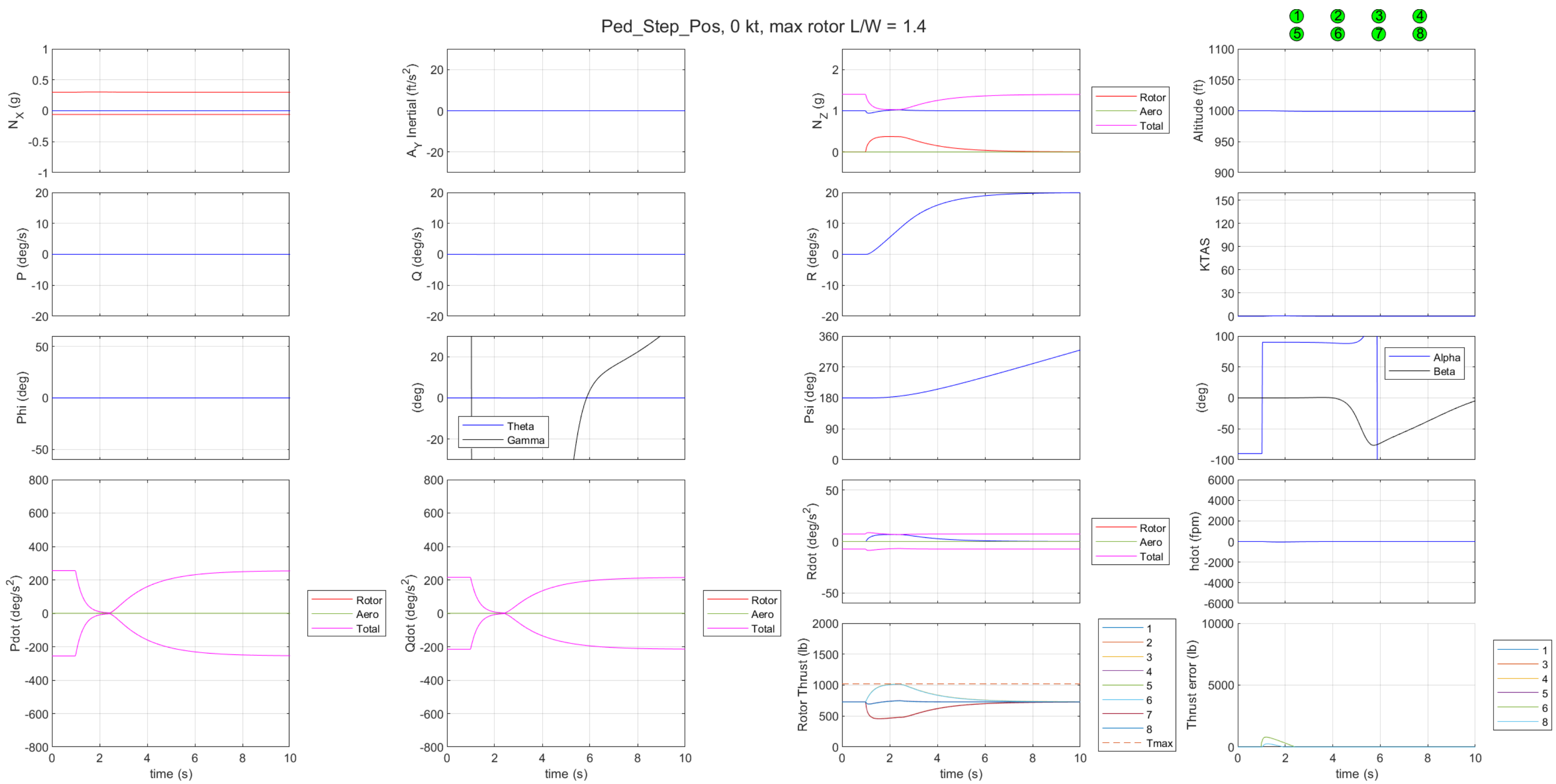

Figure A- 15. Max Pos. Ped. step trimmed at 0 KGS with an L/Wmax = 1.4 g

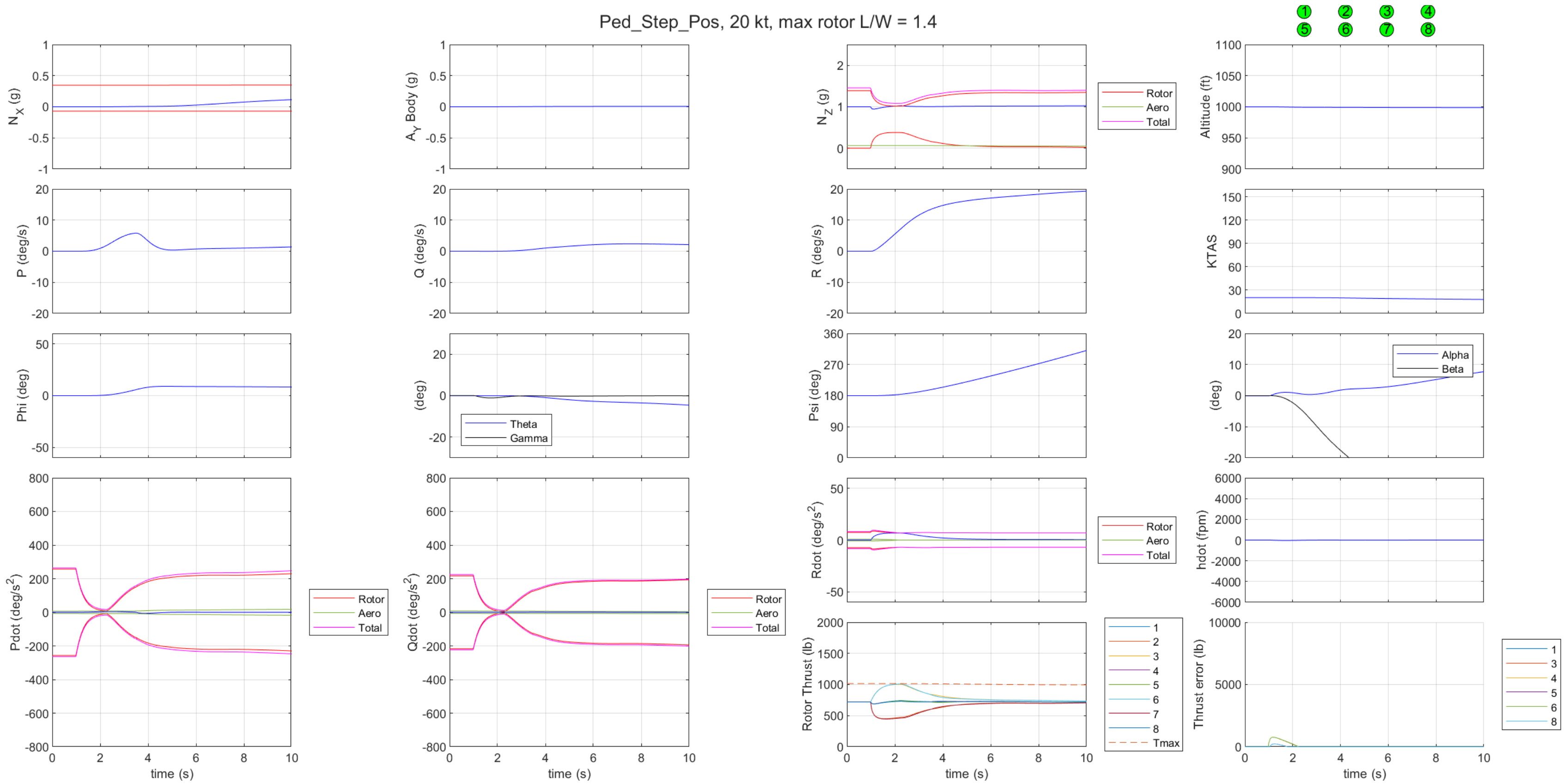

Figure A- 16. Max Pos. Ped. step trimmed at 20 KIAS with an L/Wmax = 1.4 g

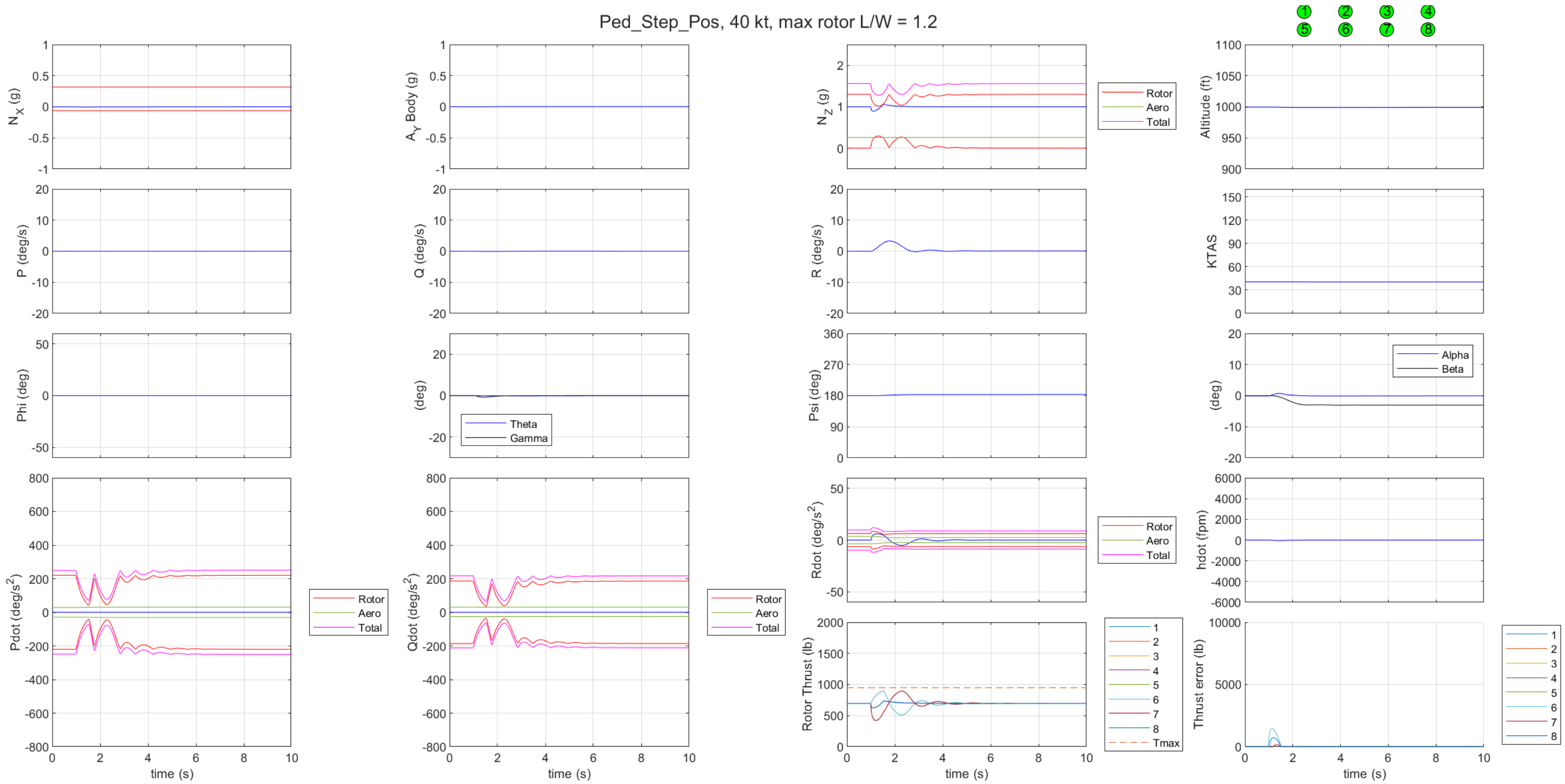

Figure A- 17. Max Pos. Ped. step trimmed at 40 KIAS with an L/Wmax = 1.2 g

A.6 Maximum positive longitudinal and positive pedal step

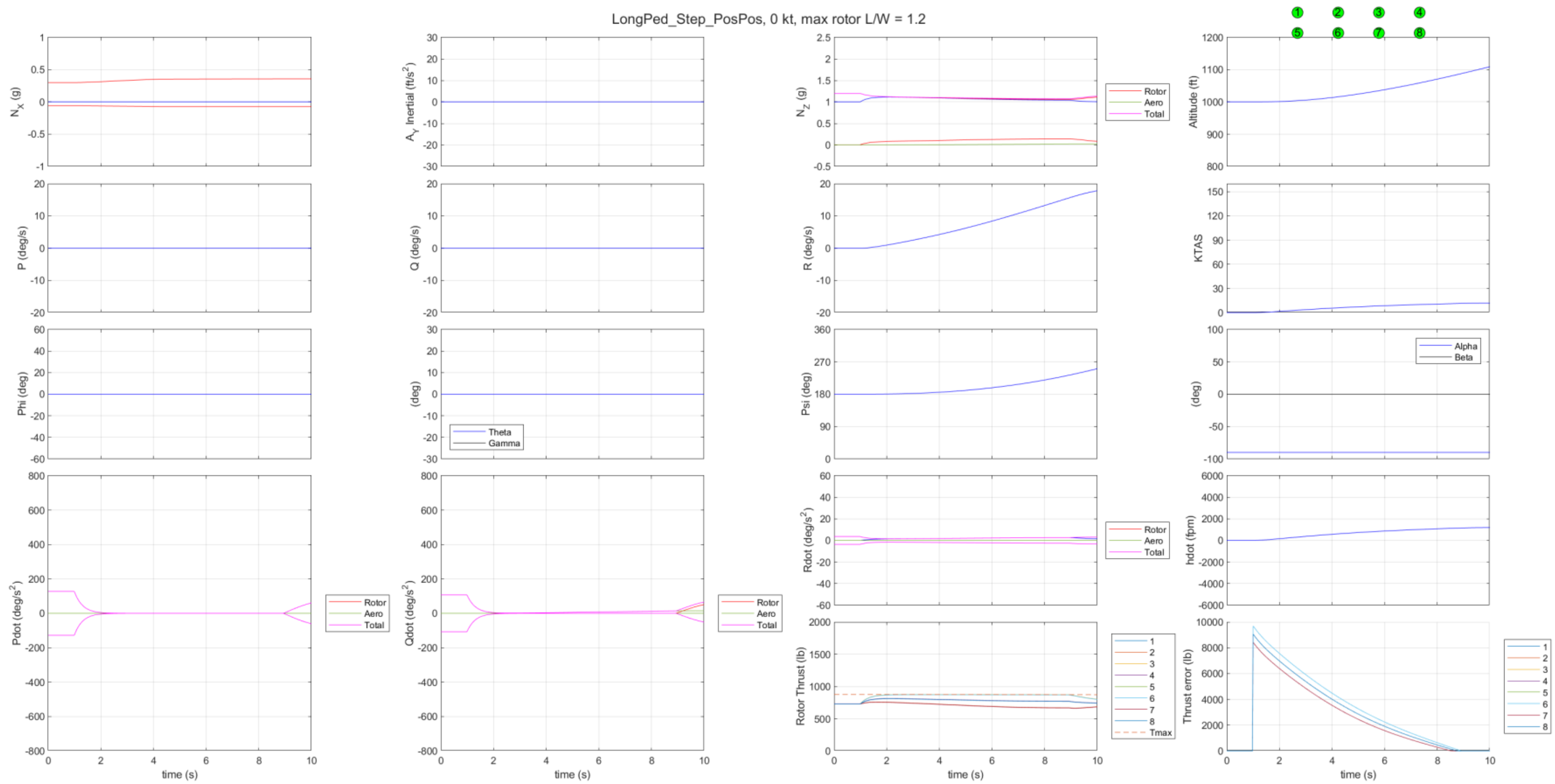

Figure A- 18. Max Pos. Long. and Pos. Ped. step trimmed at 0 KGS with an L/Wmax = 1.2 g

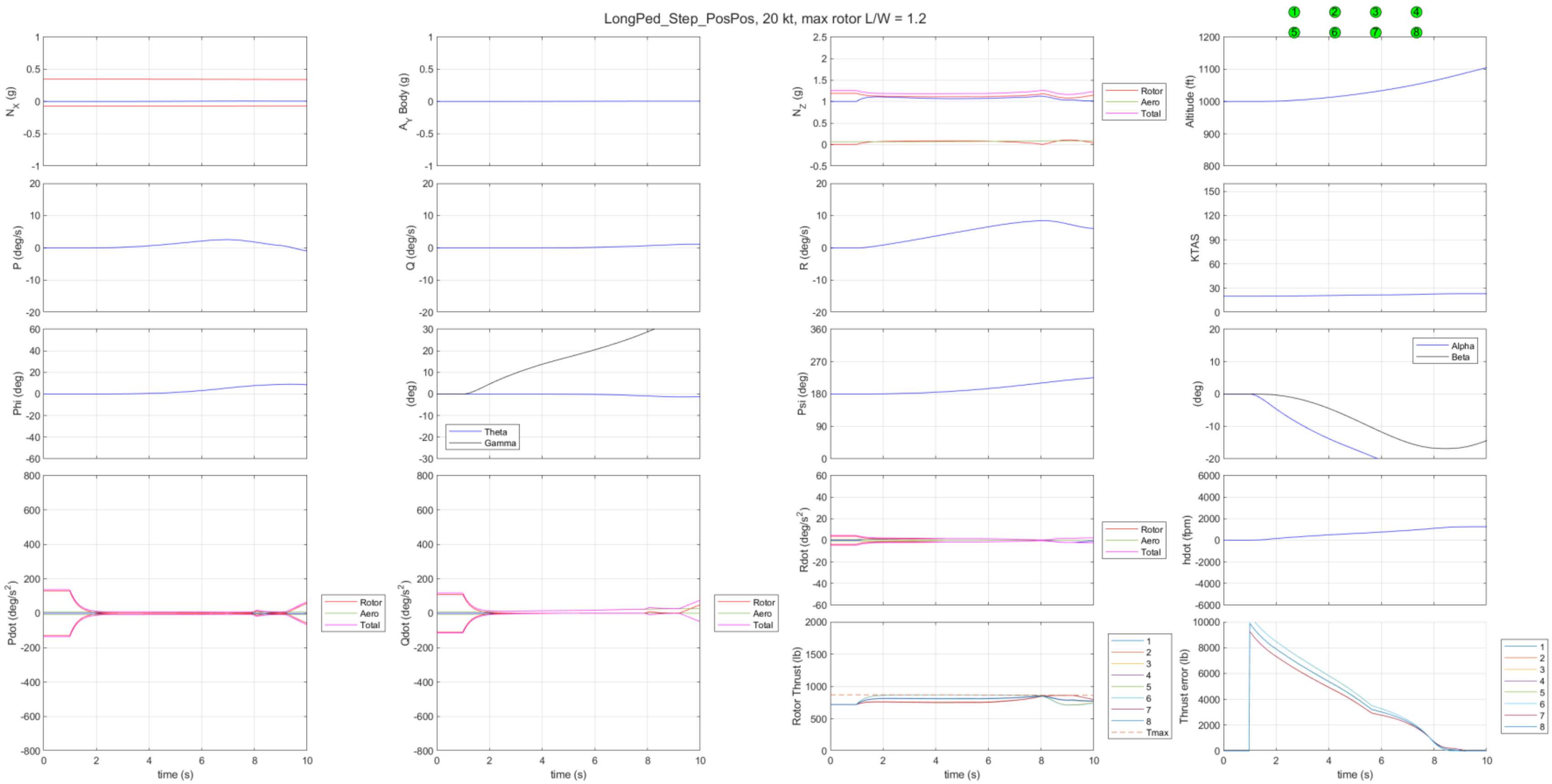

Figure A- 19. Max Pos. Long. and Pos. Ped. step trimmed at 20 KIAS with an L/Wmax = 1.2 g

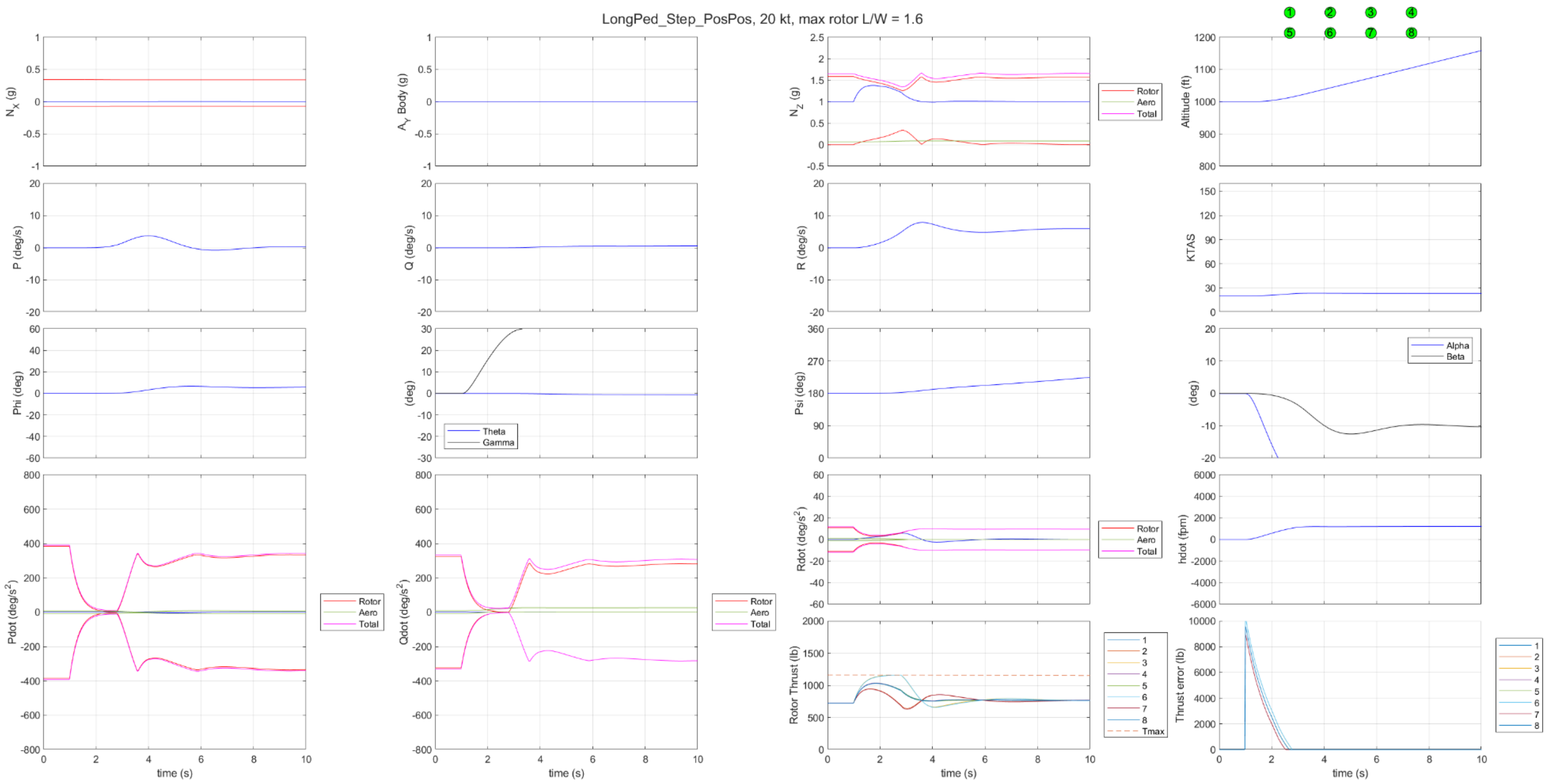

Figure A- 20. Max Pos. Long. and Pos. Ped. step trimmed at 20 KIAS with an L/Wmax = 1.6 g

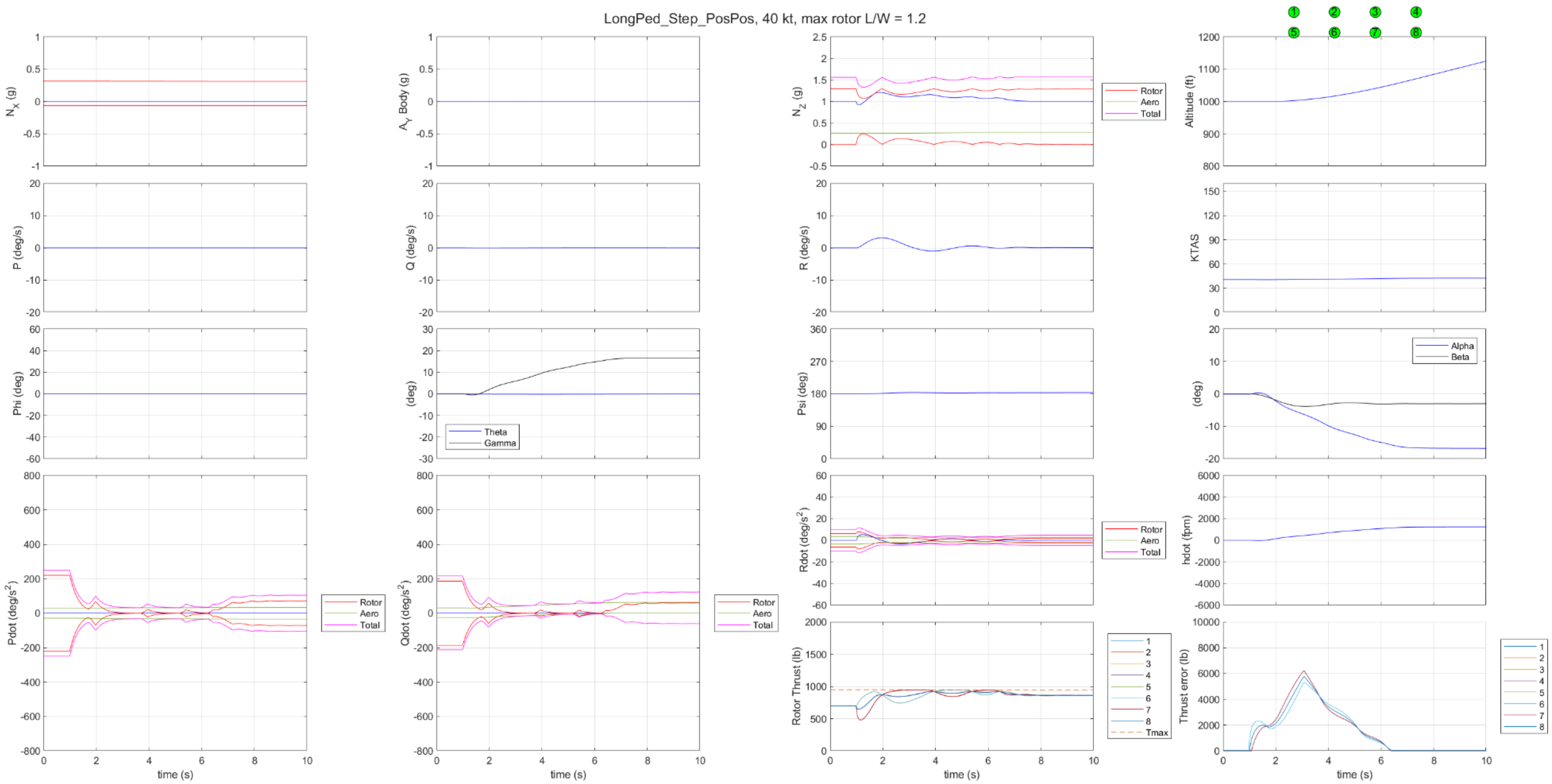

Figure A- 21. Max Pos. Long. and Pos. Ped. step trimmed at 40 KIAS with an L/Wmax = 1.2 g

A.7 Maximum negative longitudinal and positive pedal step

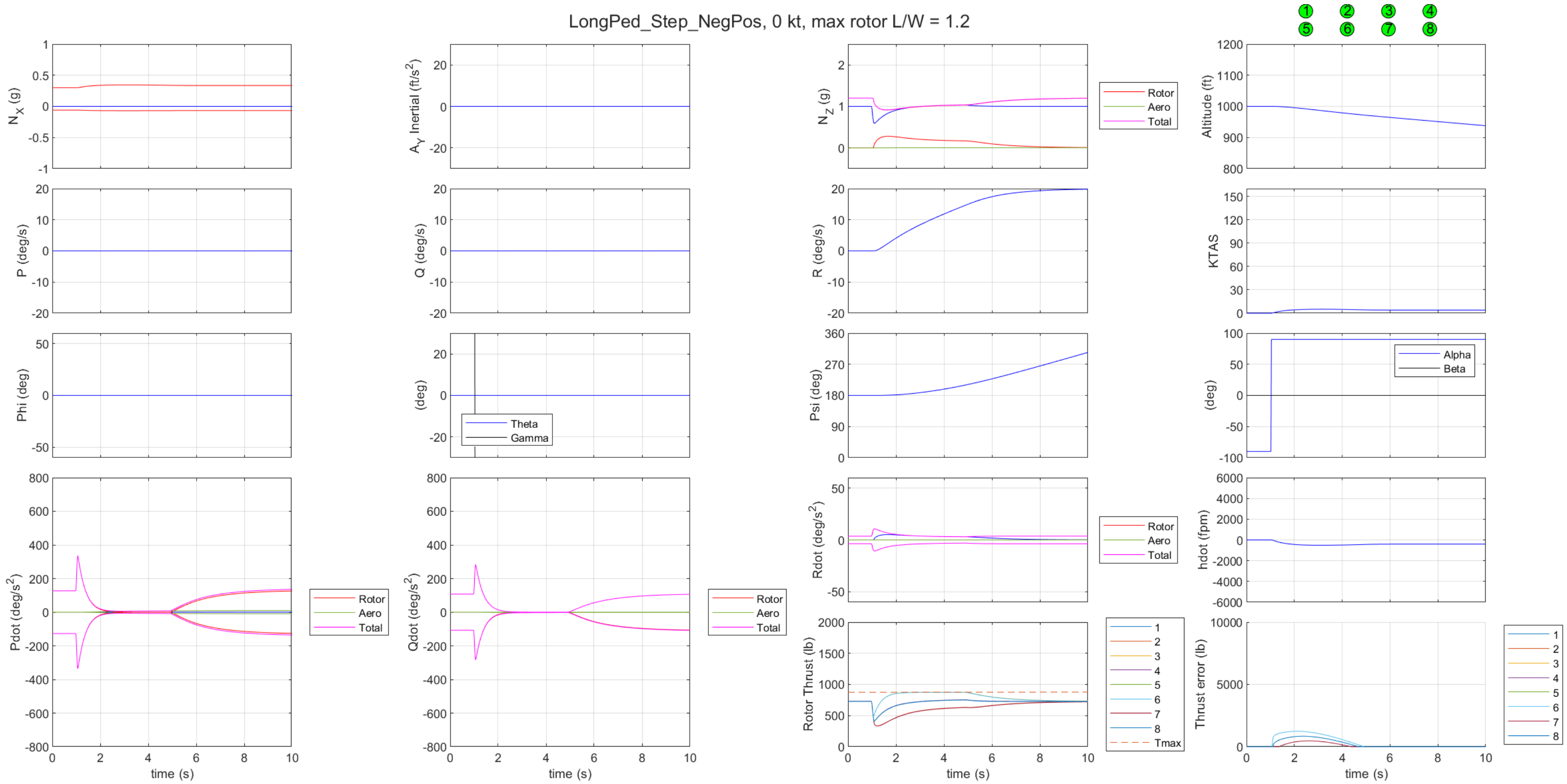

Figure A- 22. Max Neg. Long. and Pos. Ped. step trimmed at 0 KGS with an L/Wmax = 1.2 g

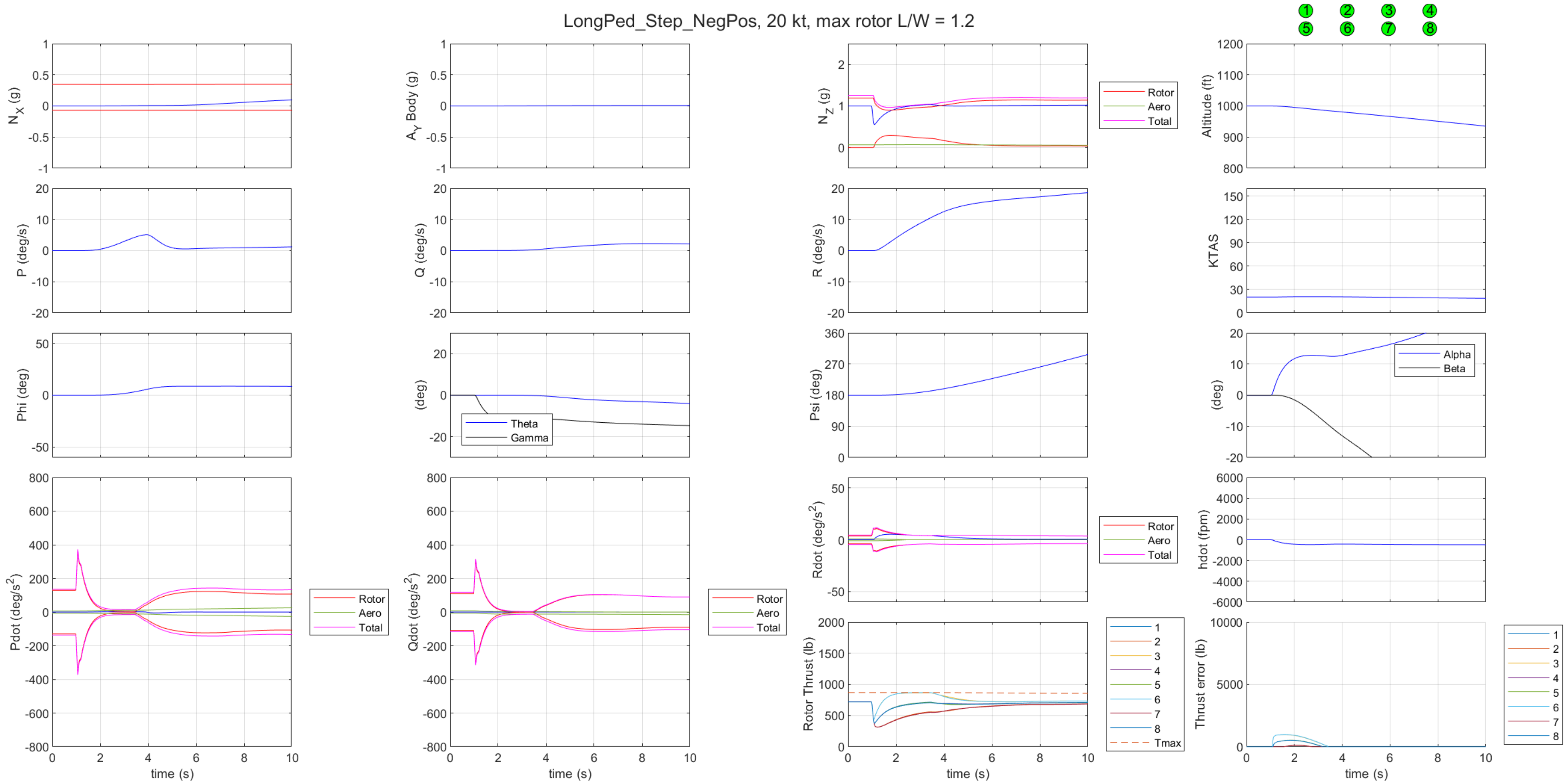

Figure A- 23. Max Neg. Long. and Pos. Ped. step trimmed at 20 KIAS with an L/Wmax = 1.2 g

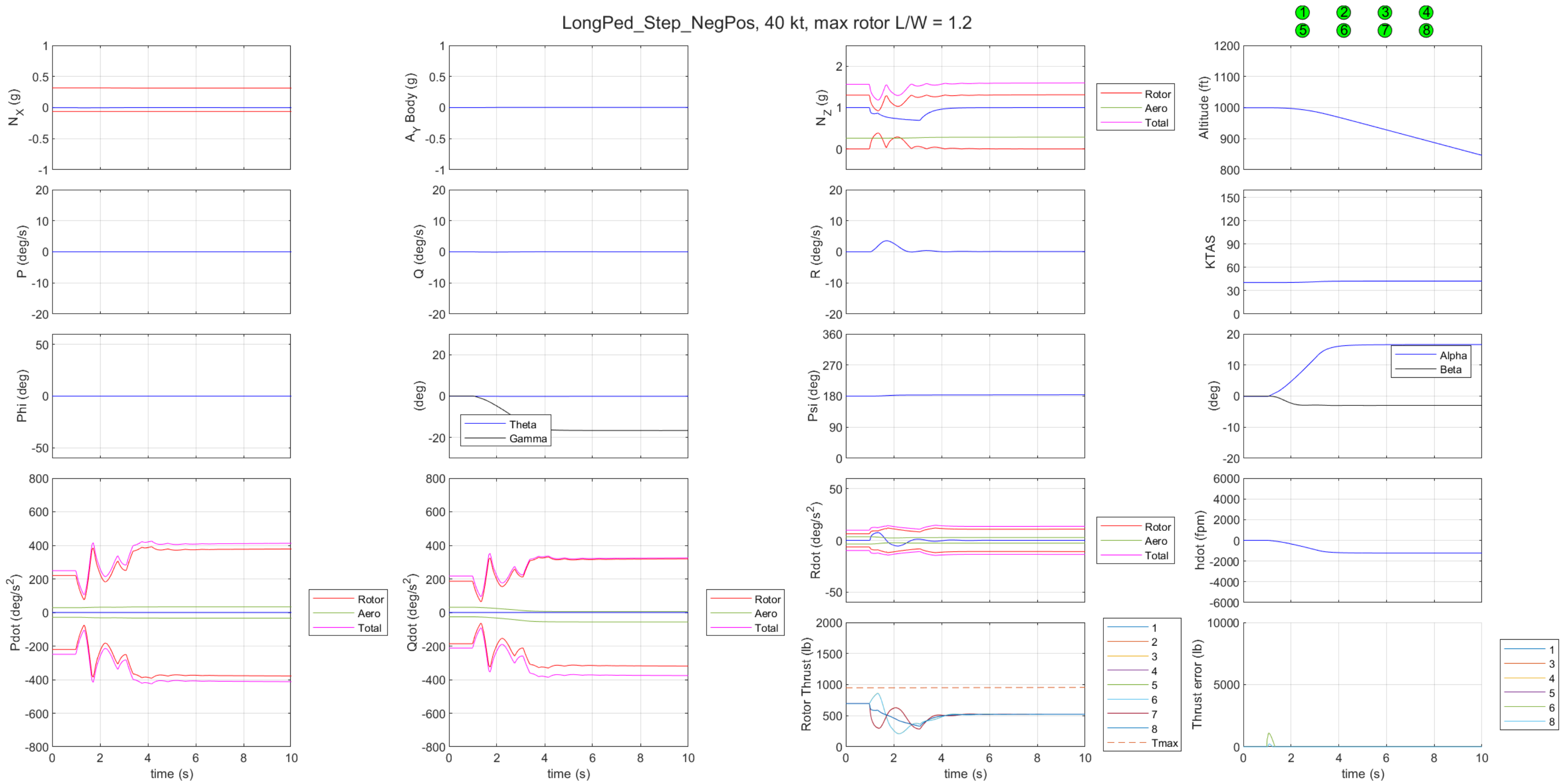

Figure A- 24. Max Neg. Long. and Pos. Ped. step trimmed at 40 KIAS with an L/Wmax = 1.2 g

A.8 Maximum positive longitudinal and positive lateral step

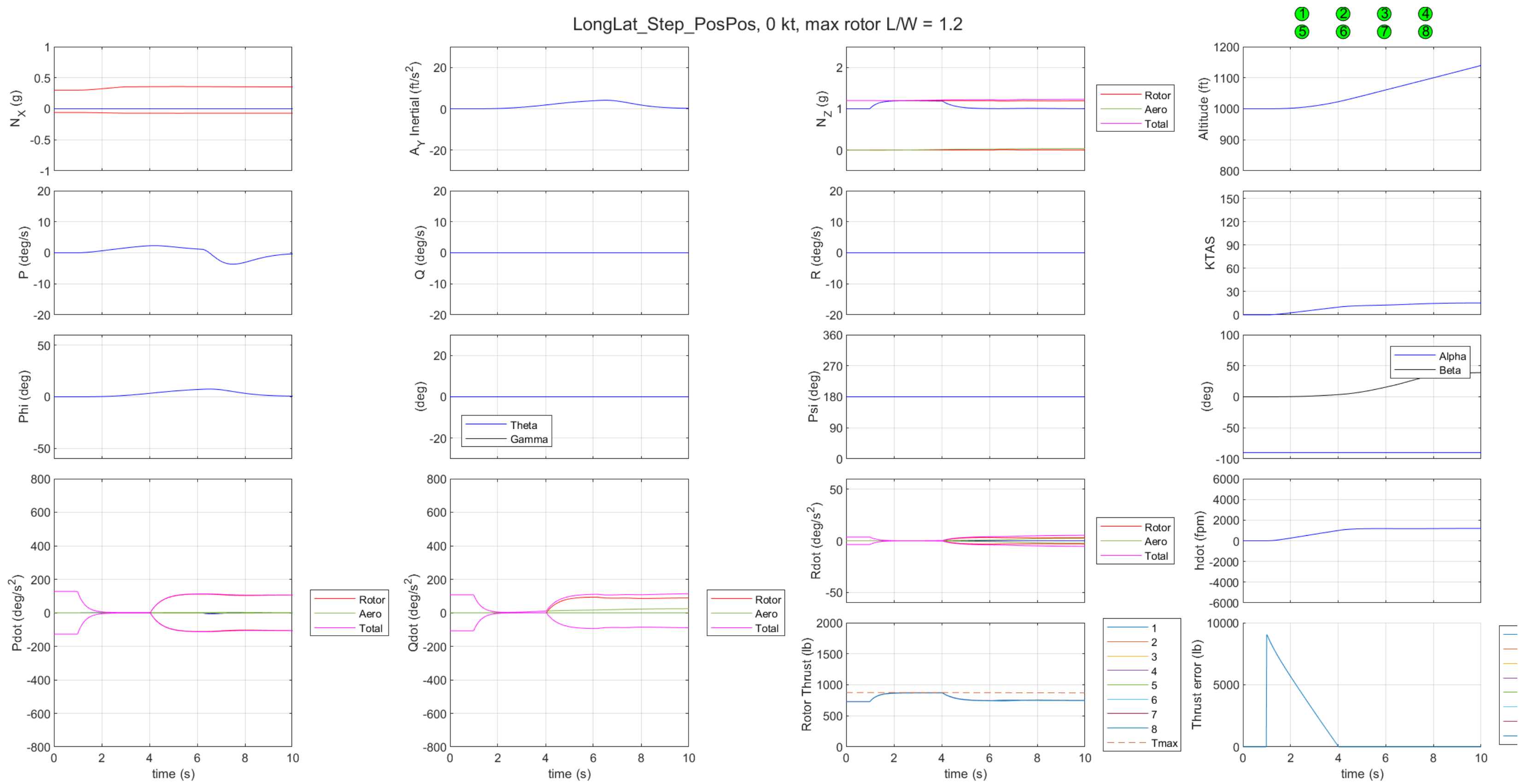

Figure A- 25. Max Pos. Long. and Pos. Lat. step trimmed at 0 KGS with an L/Wmax = 1.2 g

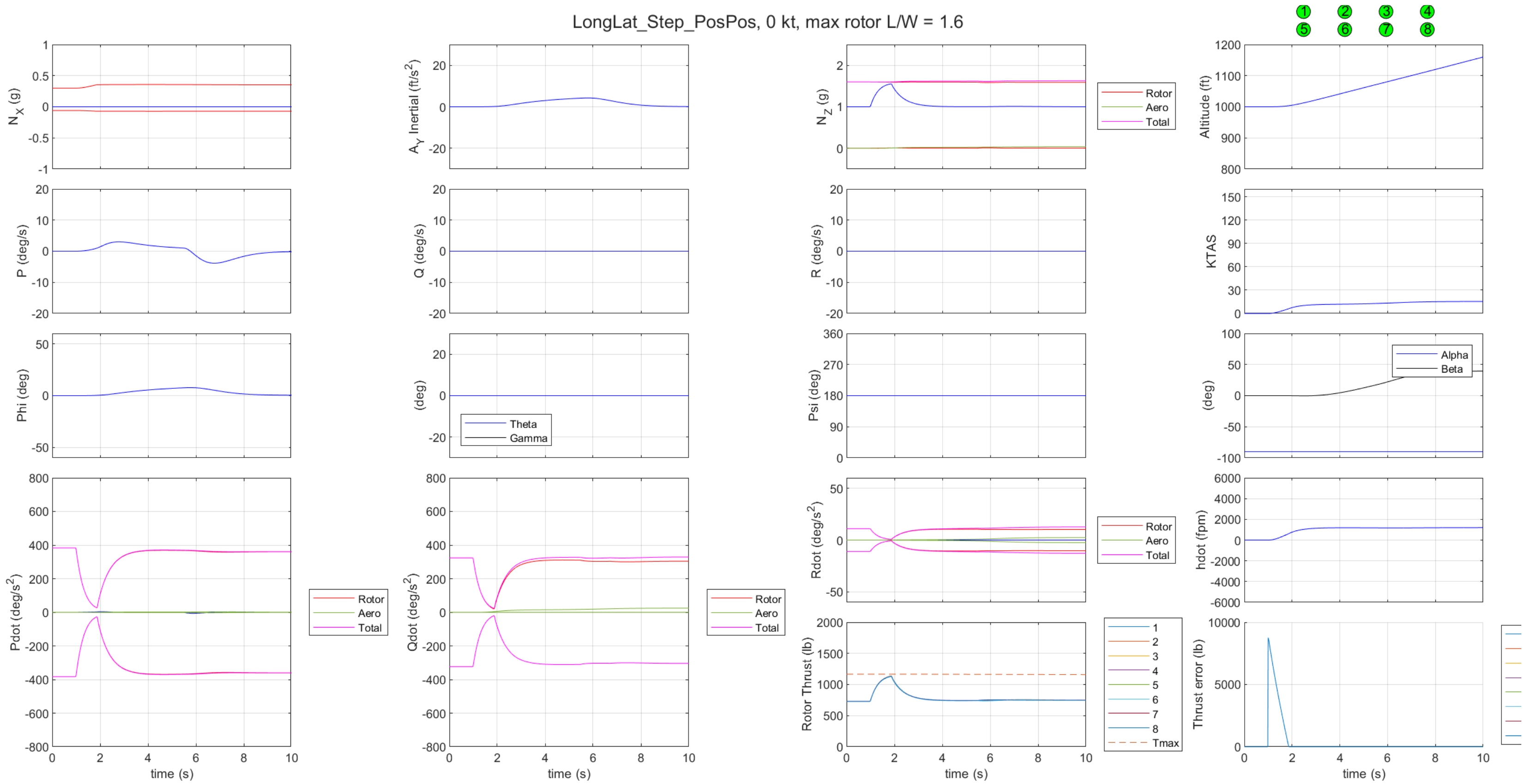

Figure A- 26. Max Pos. Long. and Pos. Lat. step trimmed at 0 KGS with an L/Wmax = 1.6 g

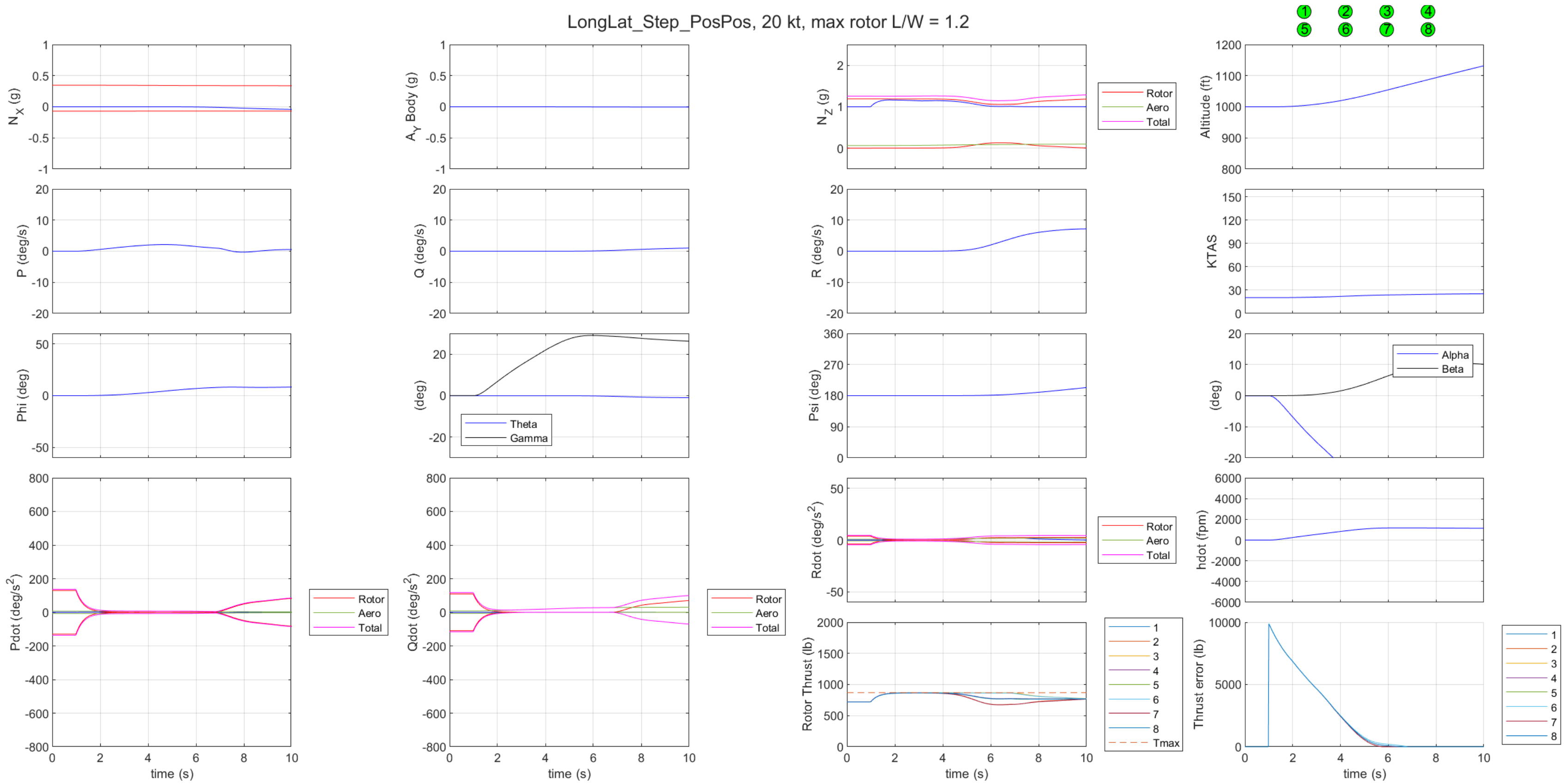

Figure A- 27. Max Pos. Long. and Pos. Lat. step trimmed at 20 KIAS with an L/Wmax = 1.2 g

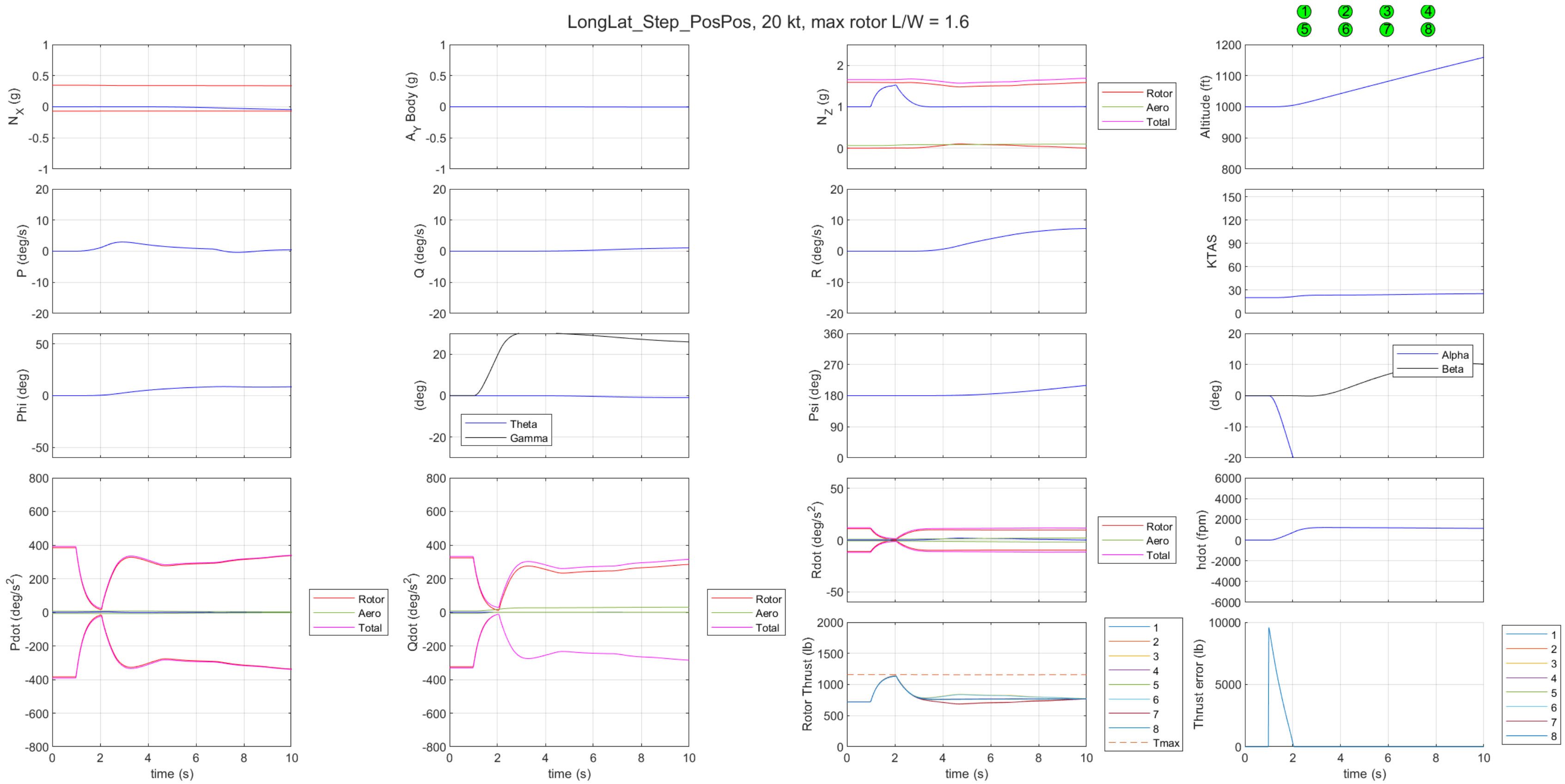

Figure A- 28. Max Pos. Long. and Pos. Lat. step trimmed at 20 KIAS with an L/Wmax = 1.6 g

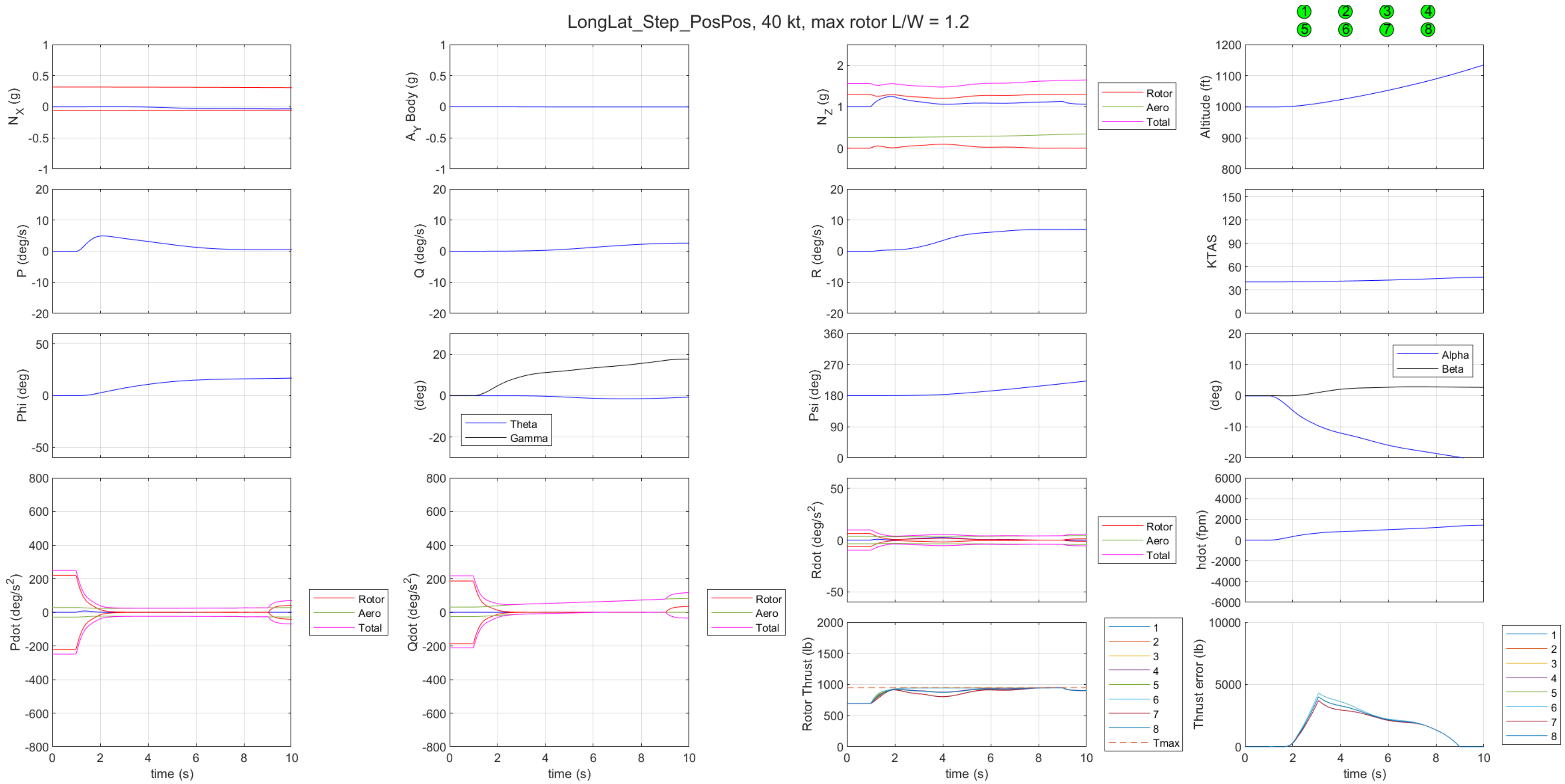

Figure A- 29. Max Pos. Long. and Pos. Lat. step trimmed at 40 KIAS with an L/Wmax = 1.2 g

A.9 Maximum negative longitudinal and positive lateral step

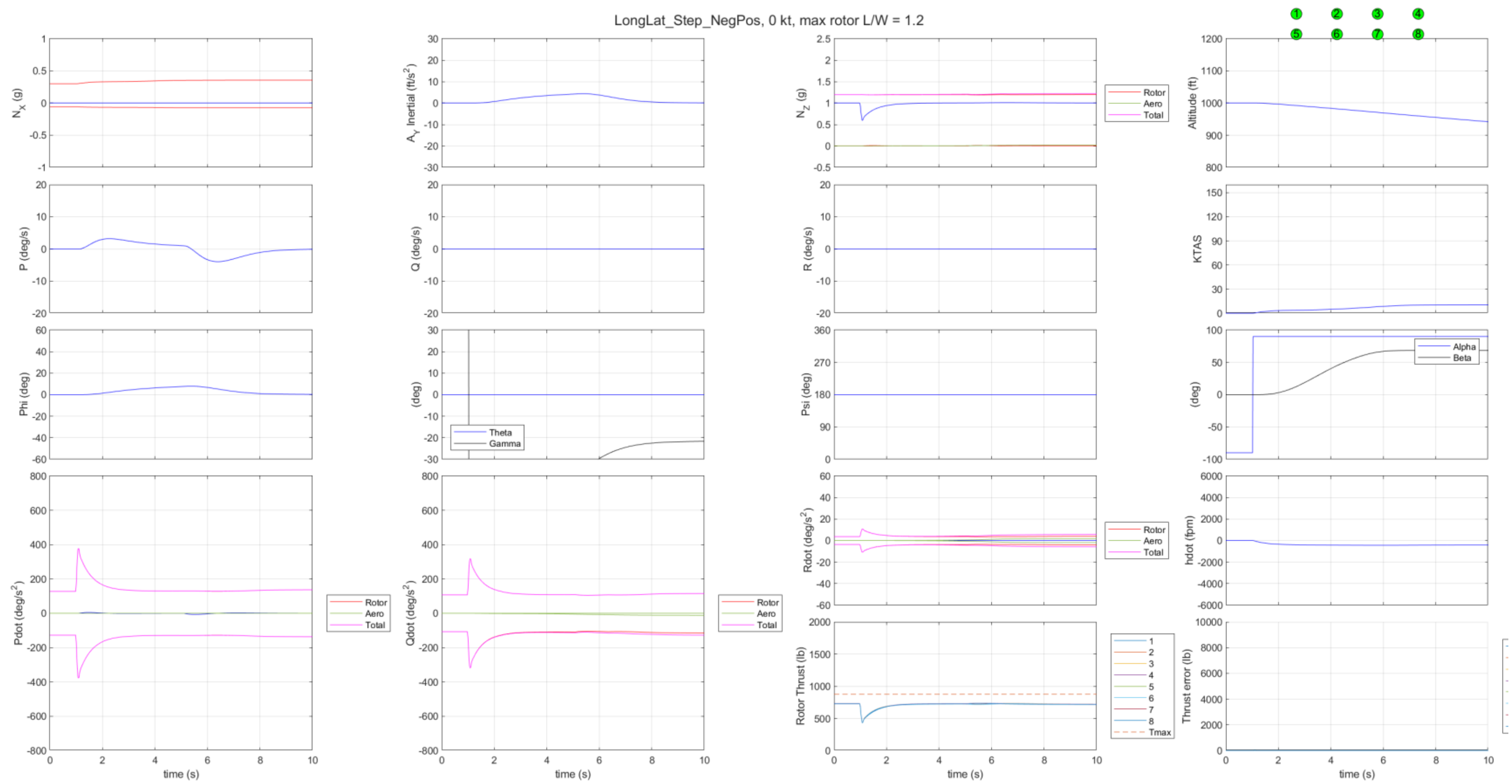

Figure A- 30. Max Neg. Long. and Pos. Lat. step trimmed at 0 KGS with an L/Wmax = 1.2 g

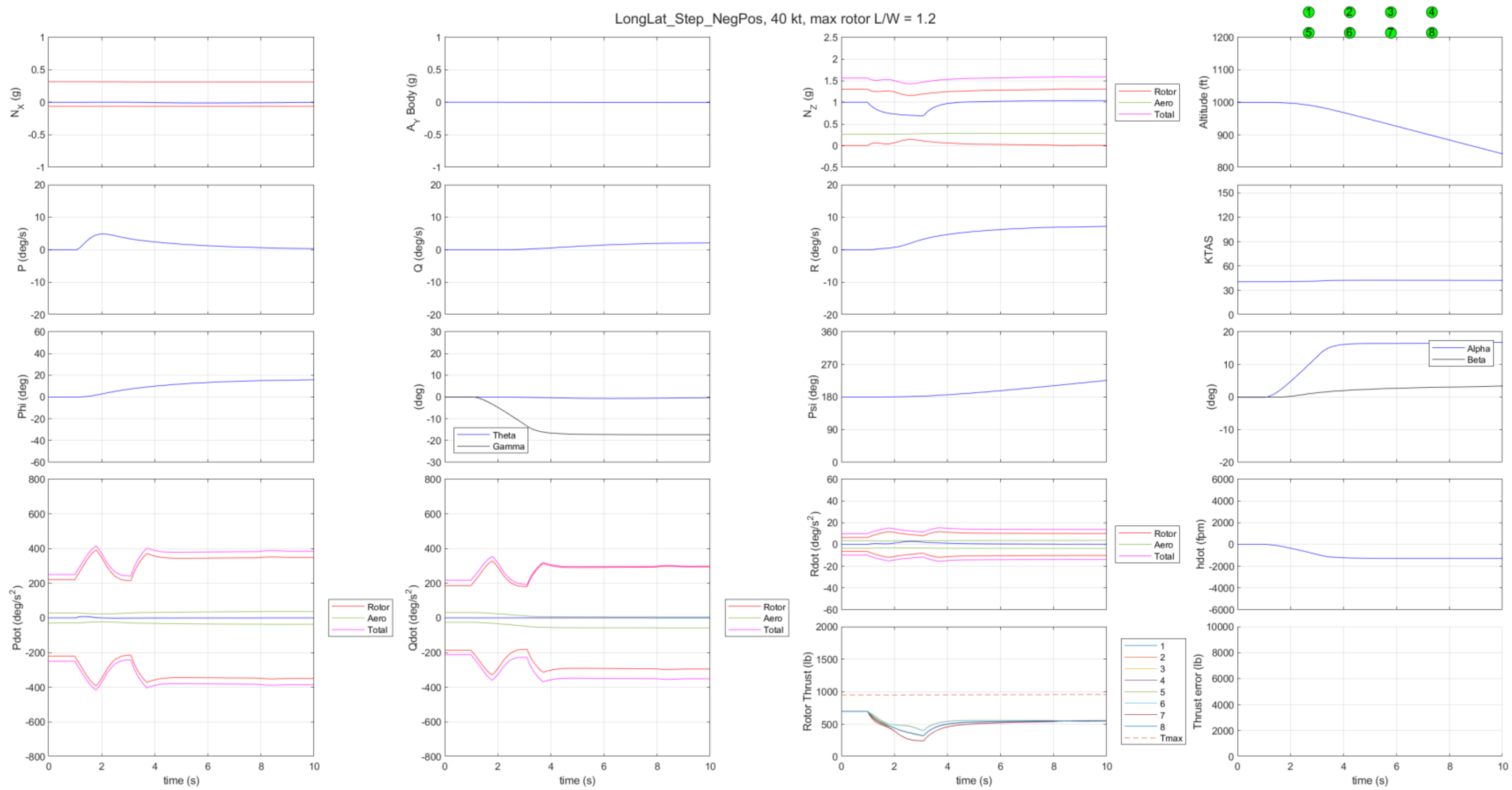

Figure A- 31. Max Neg. Long. and Pos. Lat. step trimmed at 40 KIAS with an L/Wmax = 1.2 g

A. 10 Maximum positive lateral and positive pedal step

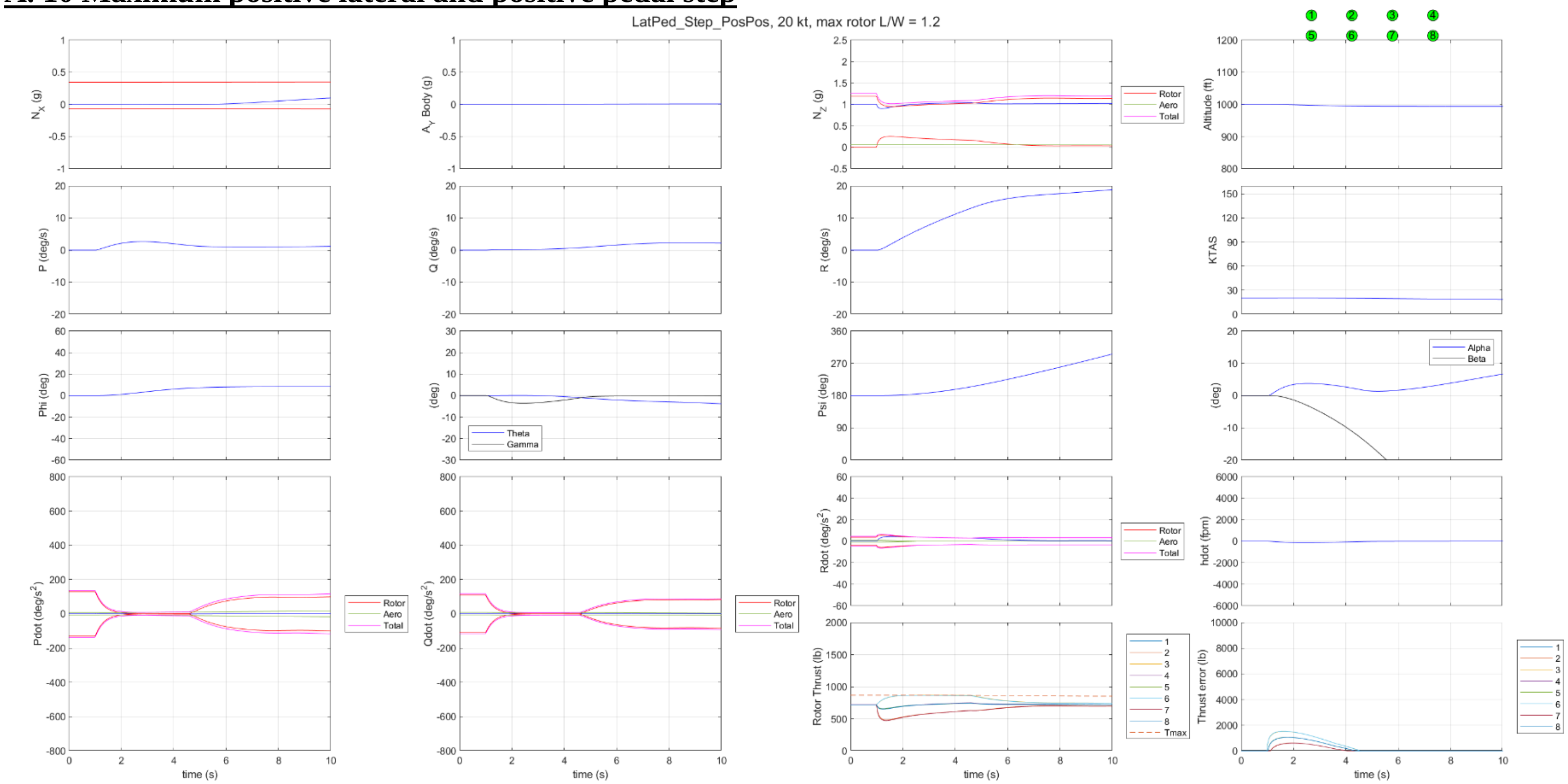

Figure A- 32. Max Pos. Lat. and Pos. Ped. step trimmed at 20 KIAS with an L/Wmax = 1.2 g

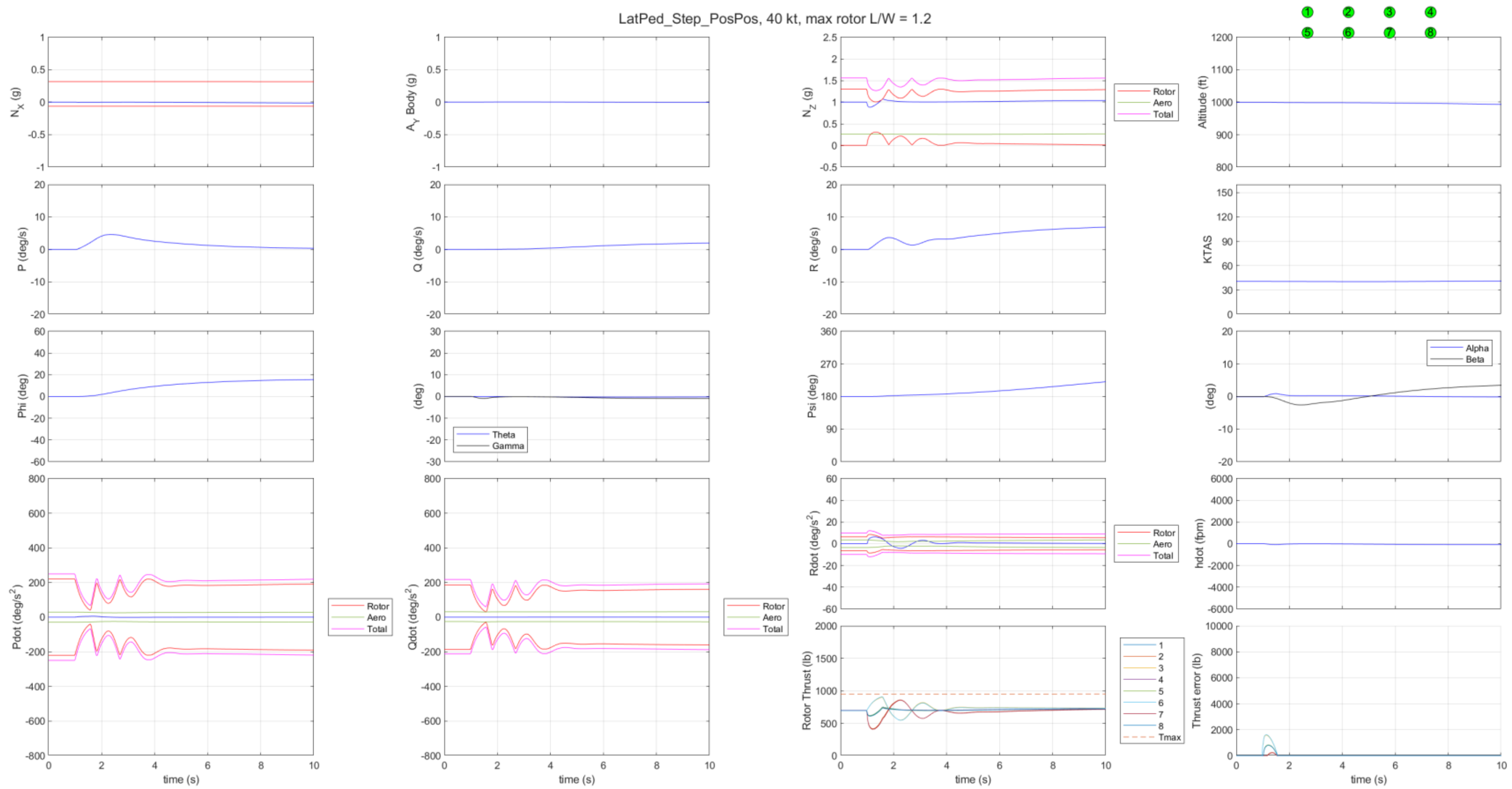

Figure A- 33. Max Pos. Lat. and Pos. Ped. step trimmed at 40 KIAS with an L/Wmax = 1.2 g

A.11 Maximum positive lateral and negative pedal step

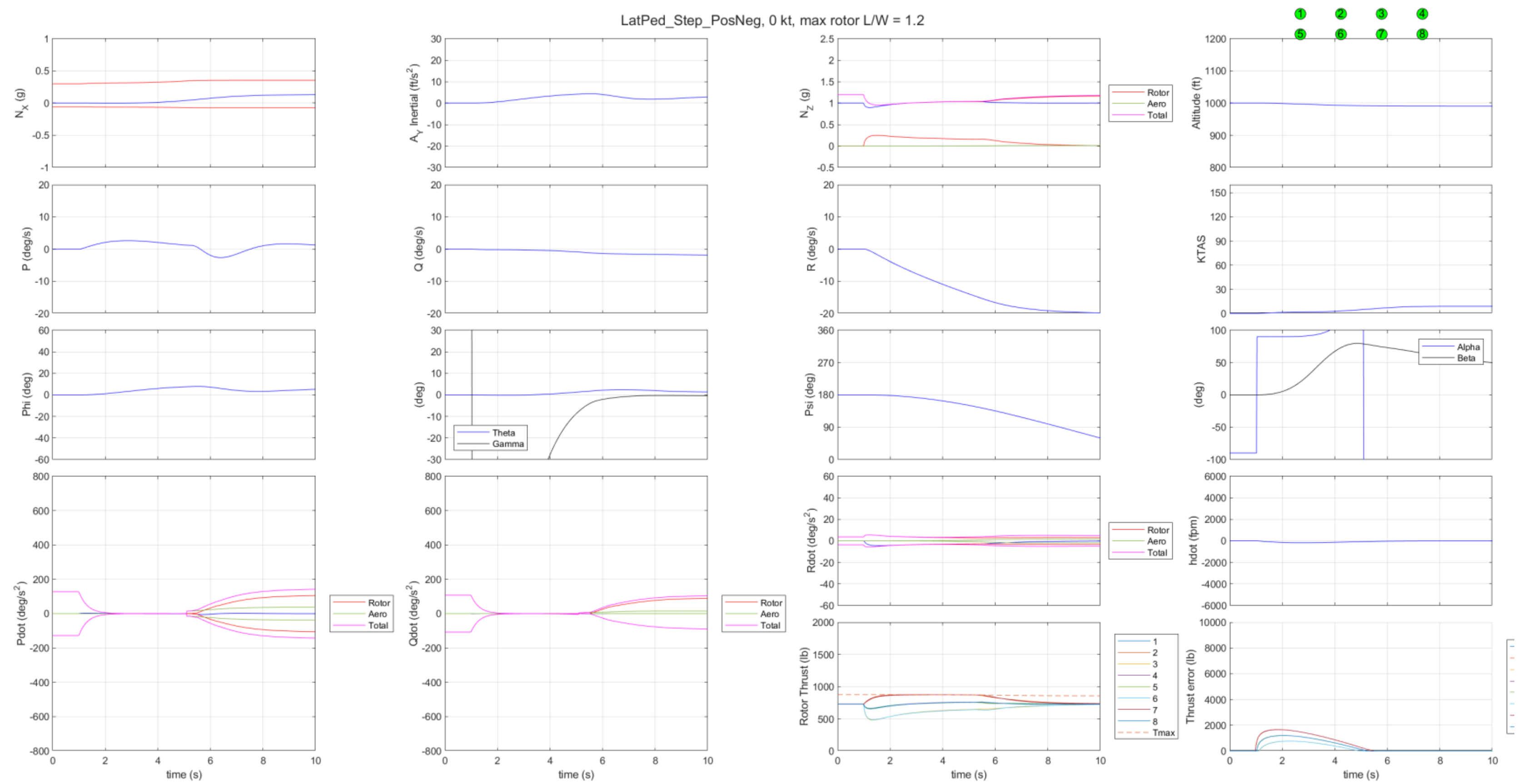

Figure A- 34. Max Pos. Lat. And Neg. Ped. step trimmed at 0 KGS with an L/Wmax = 1.2 g

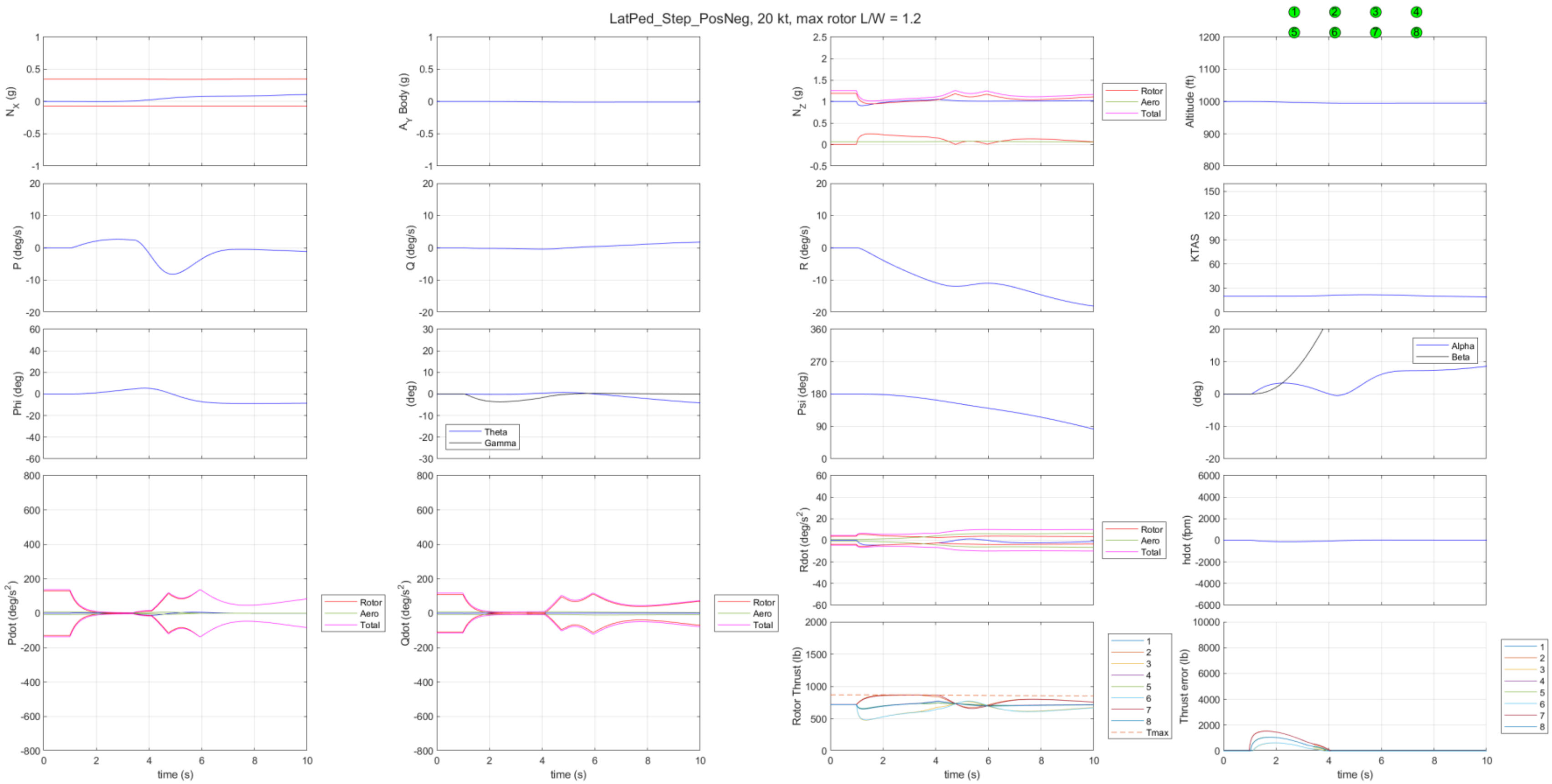

Figure A- 35. Max Pos. Lat. And Neg. Ped. step trimmed at 20 KIAS with an L/Wmax = 1.2 g

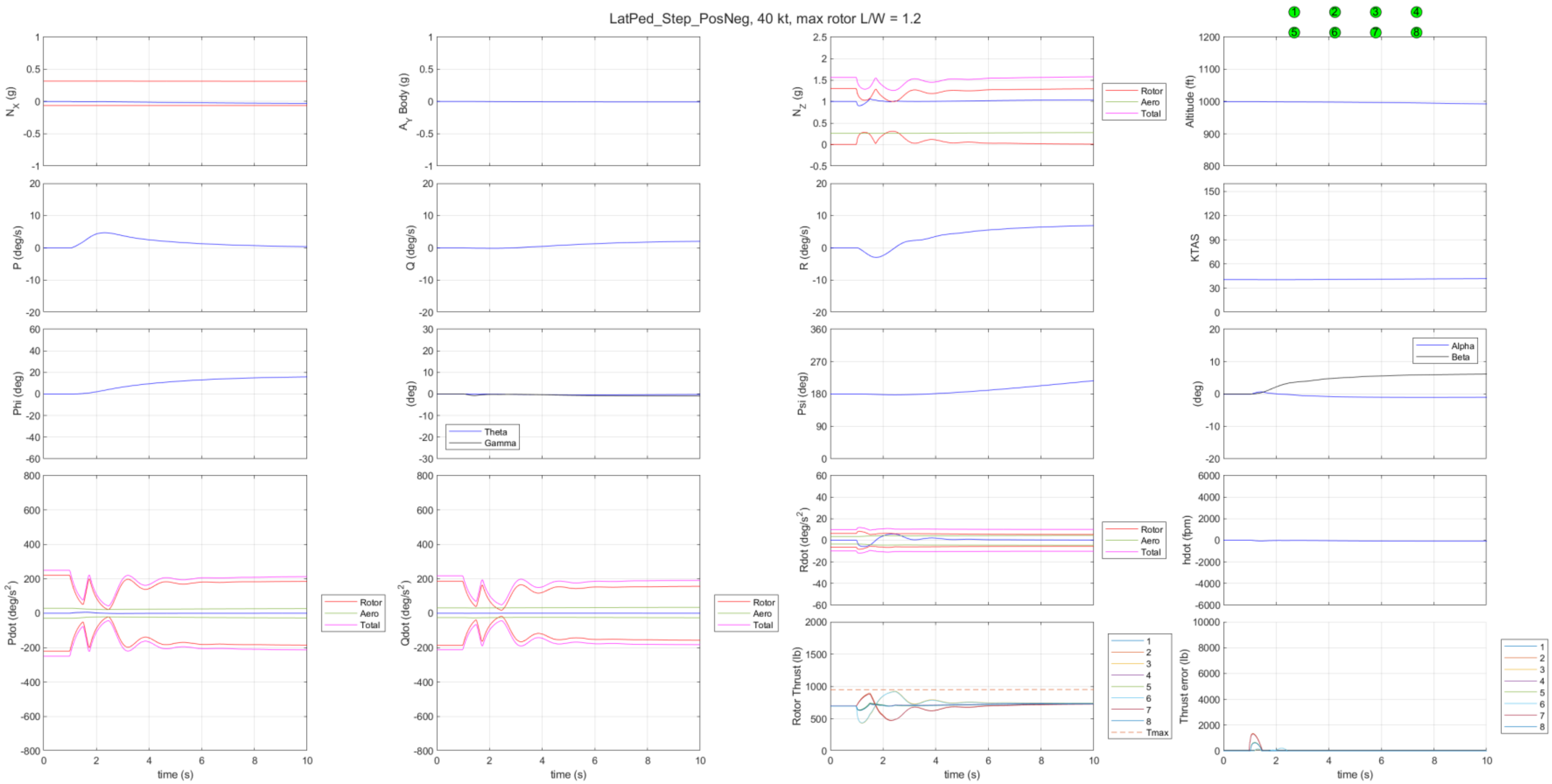

Figure A- 36. Max Pos. Lat. And Neg. Ped. step trimmed at 40 KIAS with an L/Wmax = 1.2 g

A.12 Maximum positive longitudinal step with rotor failures

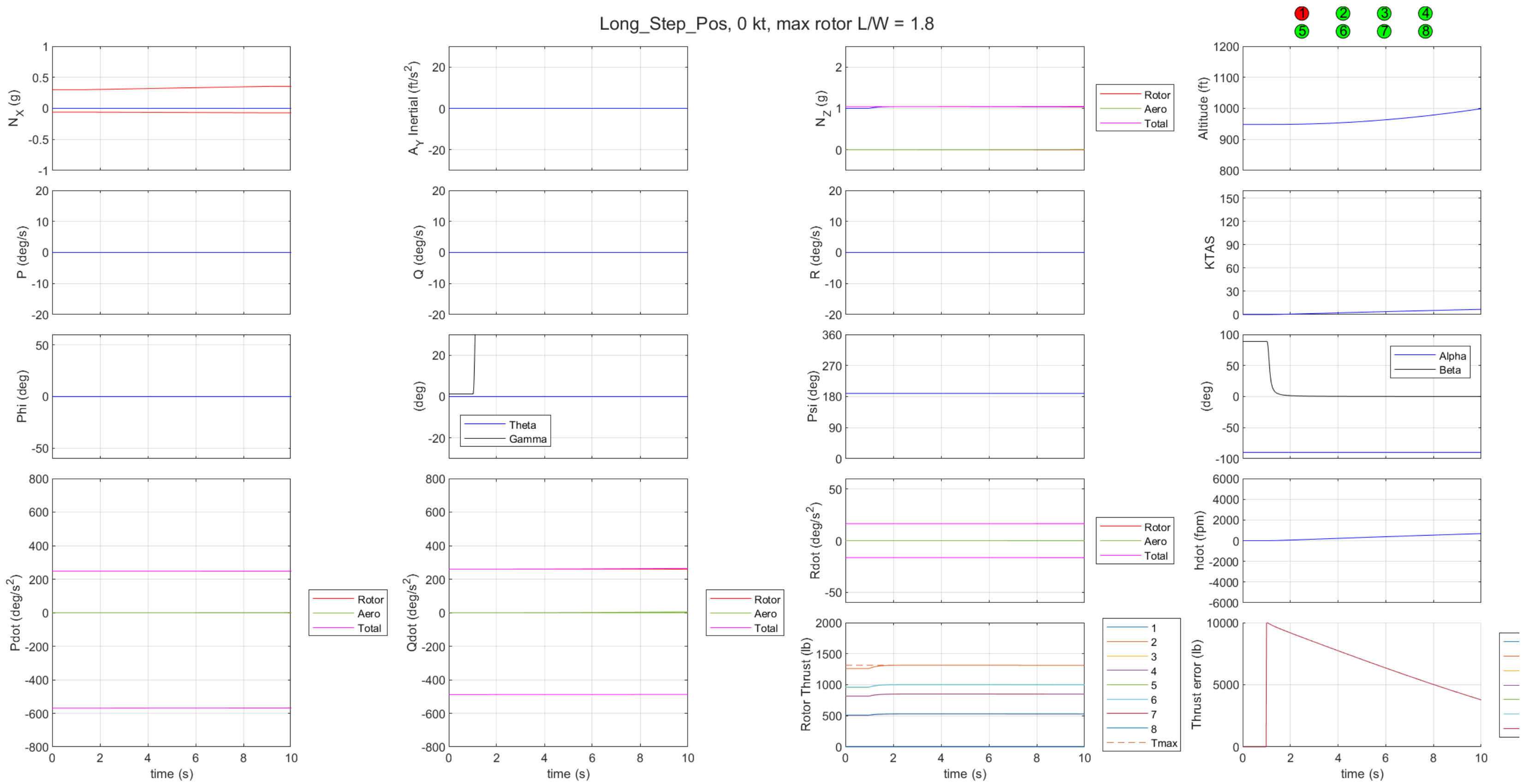

Figure A- 37. Max Pos. Long. step trimmed at 0 KGS with an L/Wmax = 1.8 g and rotor one failed

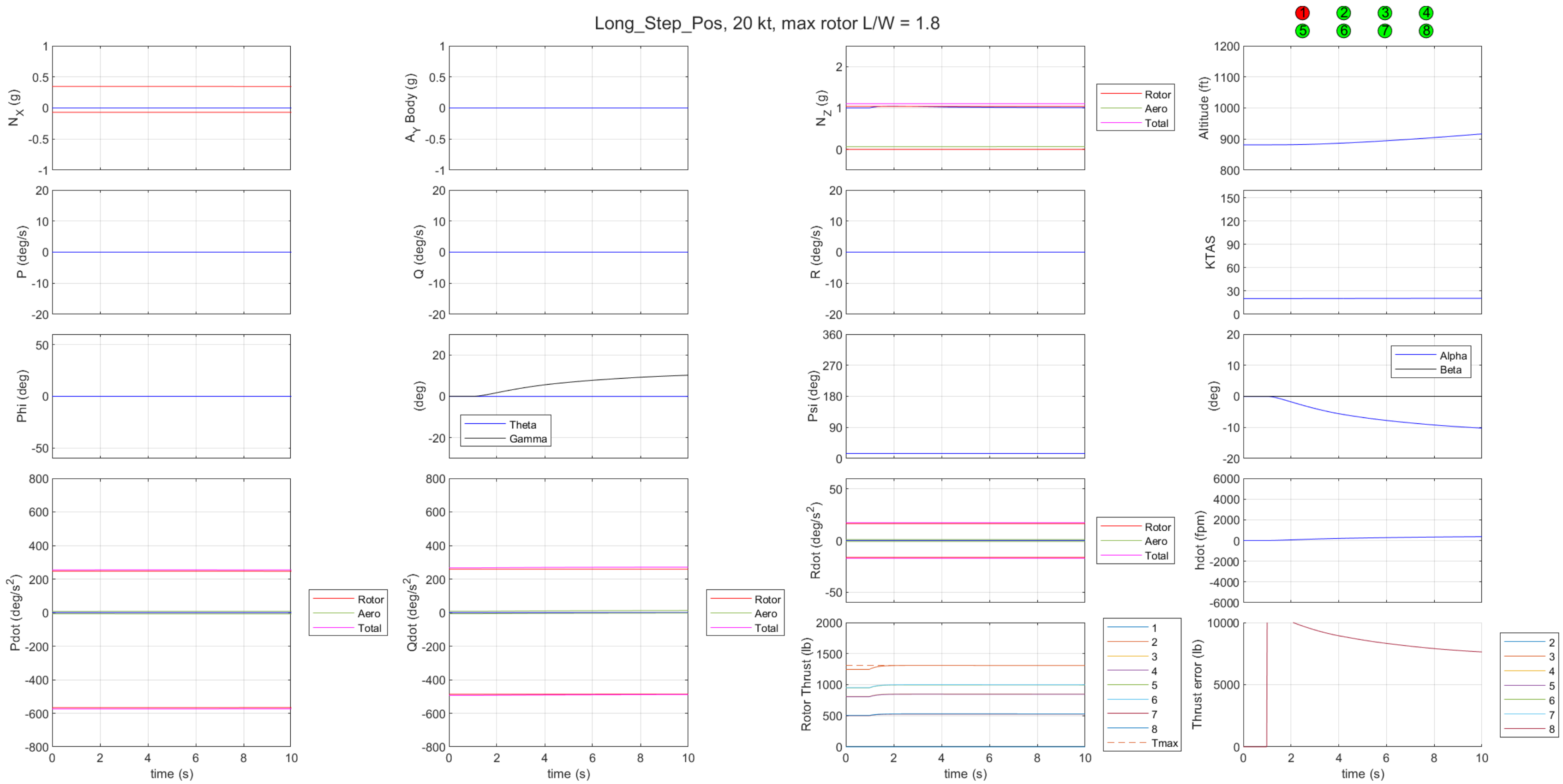

Figure A- 38. Max Pos. Long. Step trimmed at 20 KIAS with an L/Wmax = 1.8 g and rotor one failed

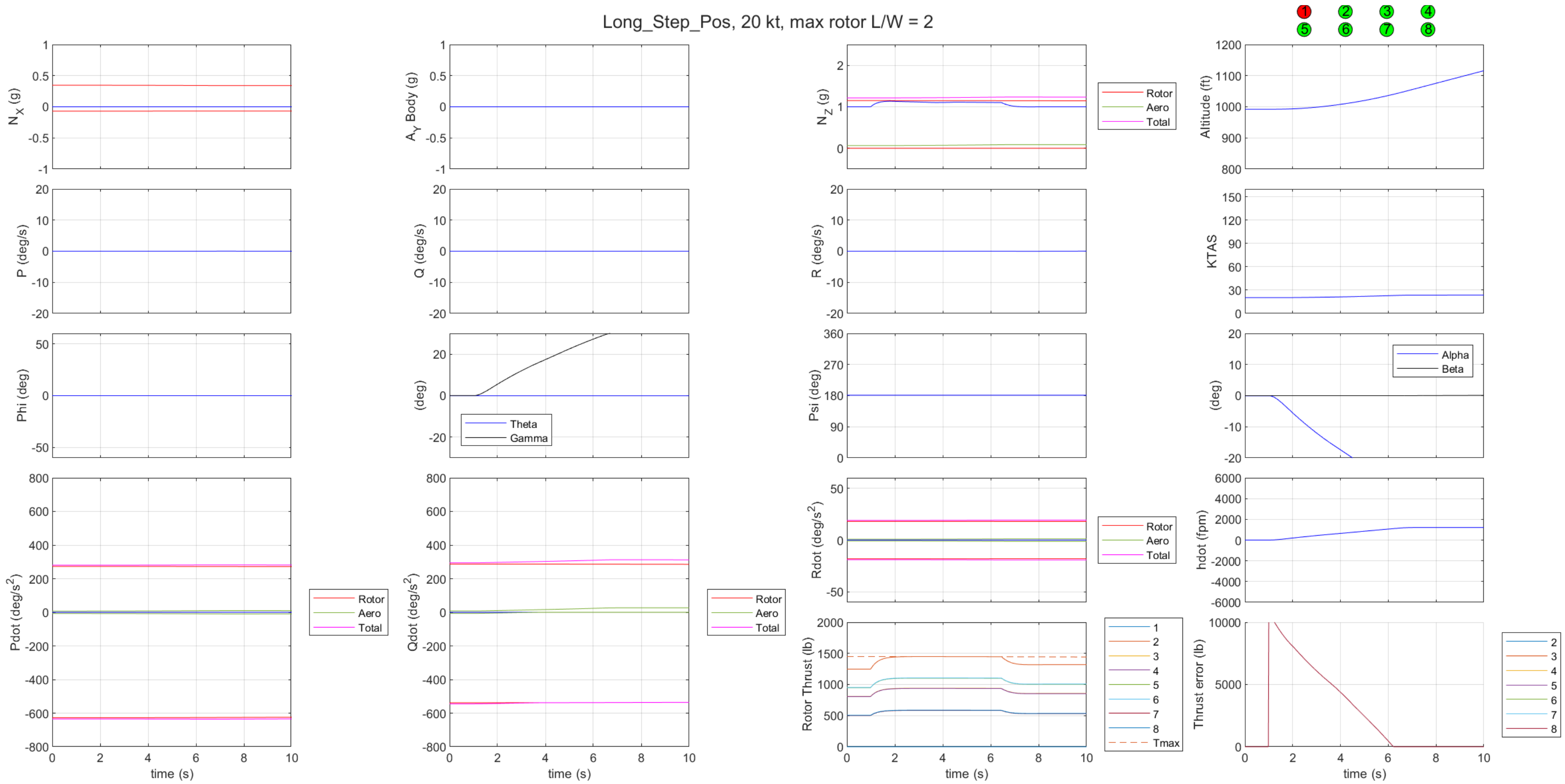

Figure A- 39. Max Pos. Long. step trimmed at 20 KIAS with an L/Wmax = 2 g and rotor one failed

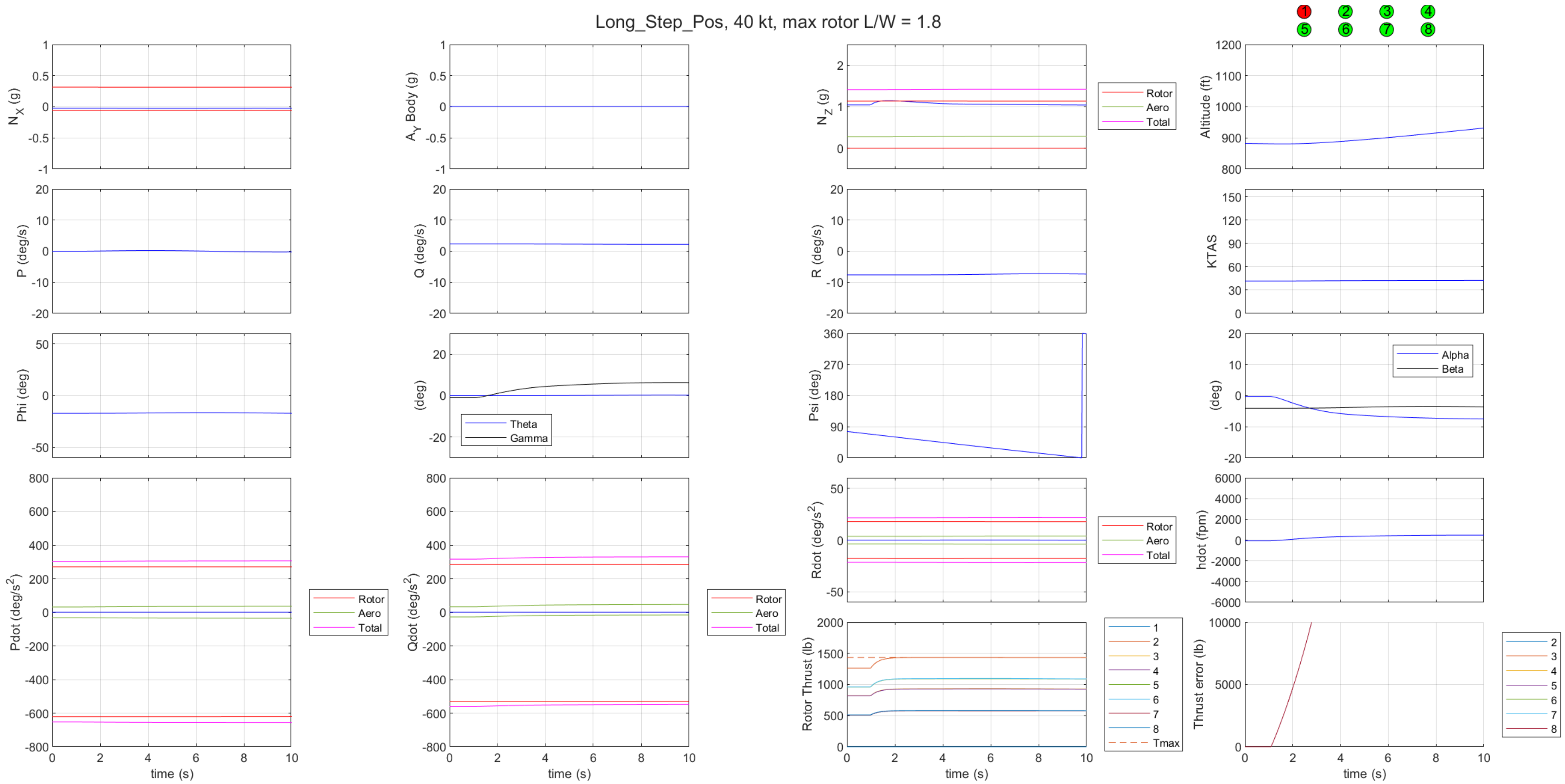

Figure A- 40. Max Pos. Long. step trimmed at 40 KIAS with an L/Wmax = 1.8 g and rotor one failed

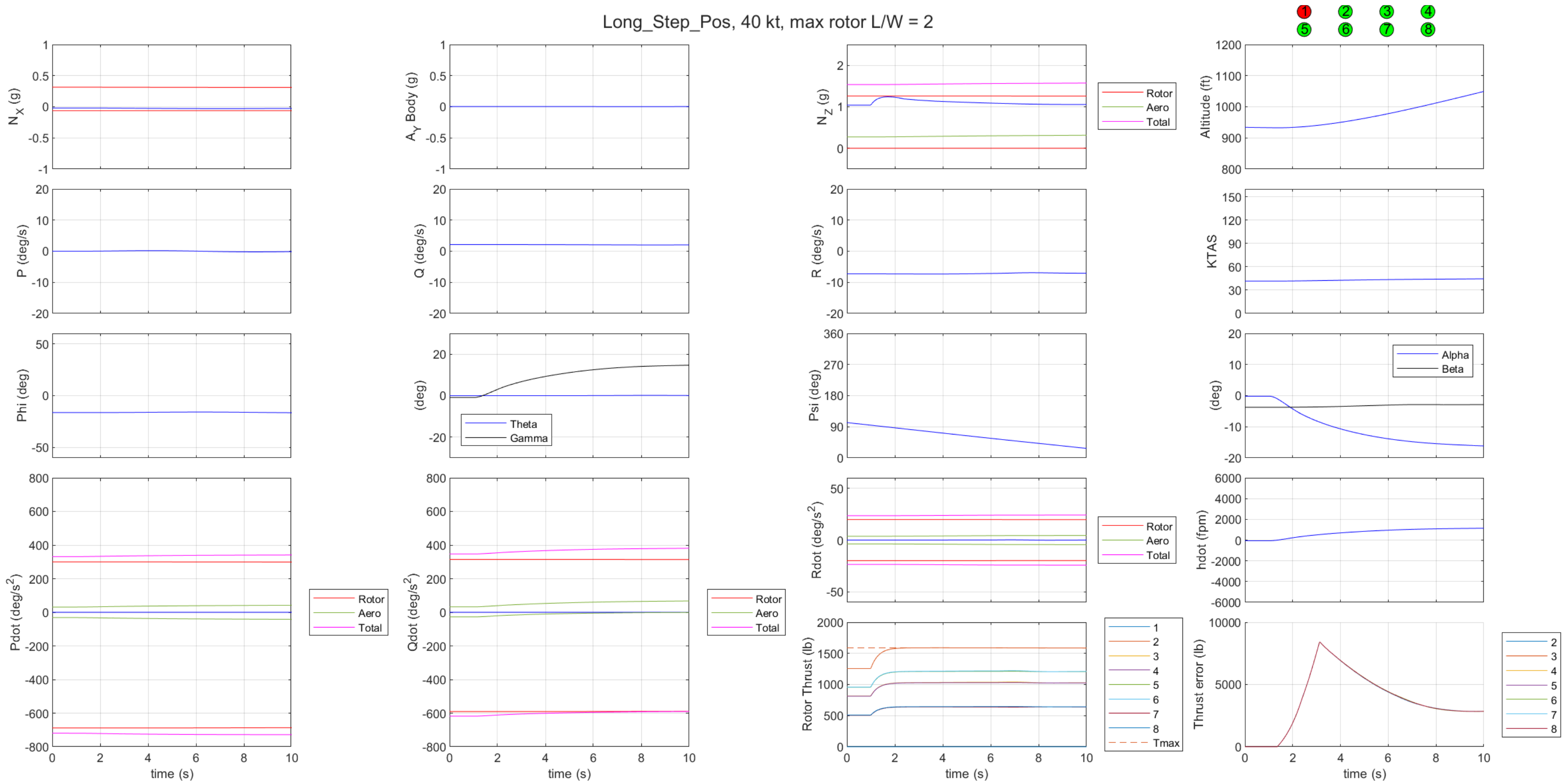

Figure A- 41. Max Pos. Long. step trimmed at 40 KIAS with an L/Wmax = 2 g and rotor one failed

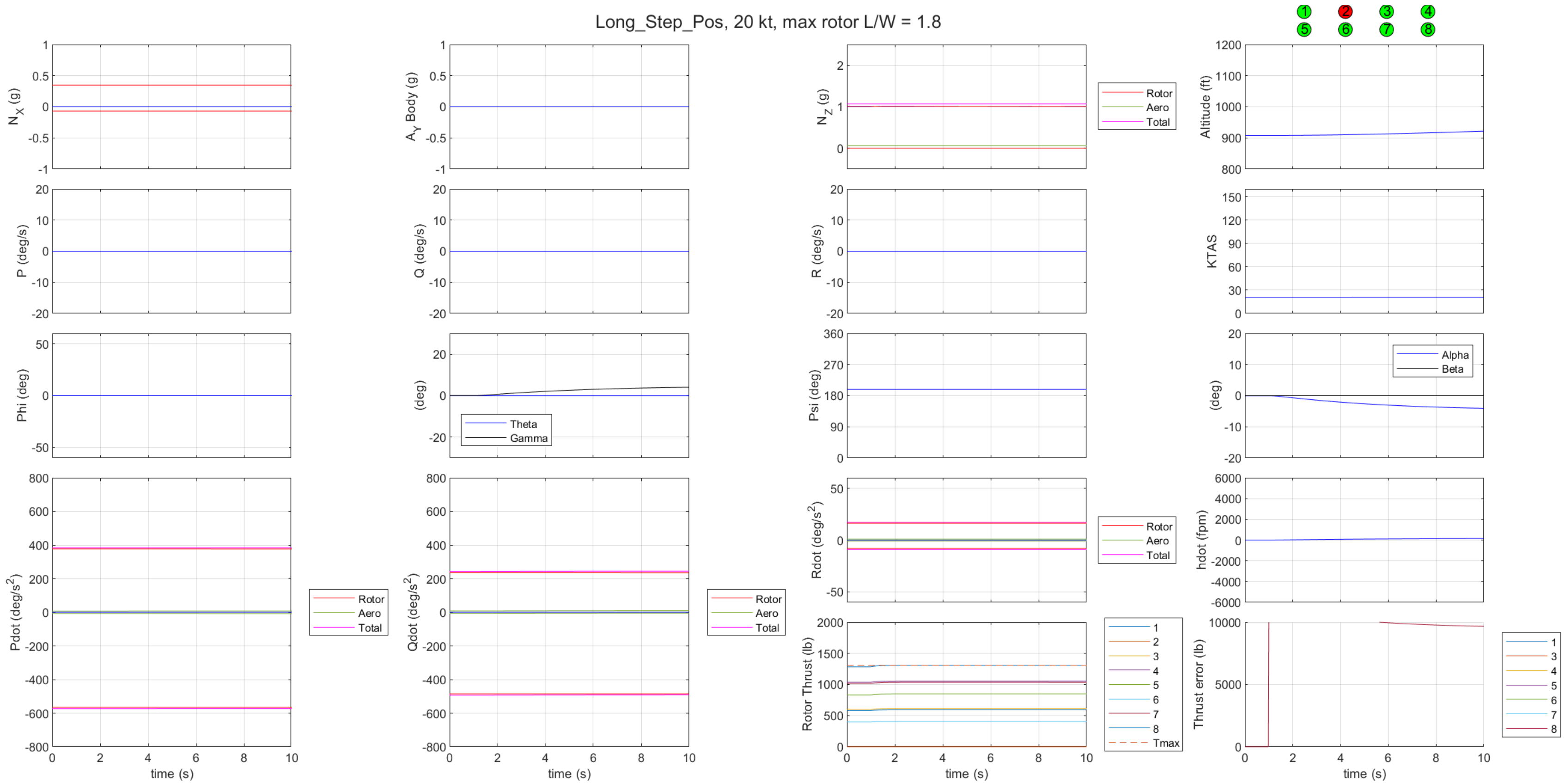

Figure A- 42. Max Pos. Long. step trimmed at 20 KIAS with an L/Wmax = 1.8 g and rotor two failed

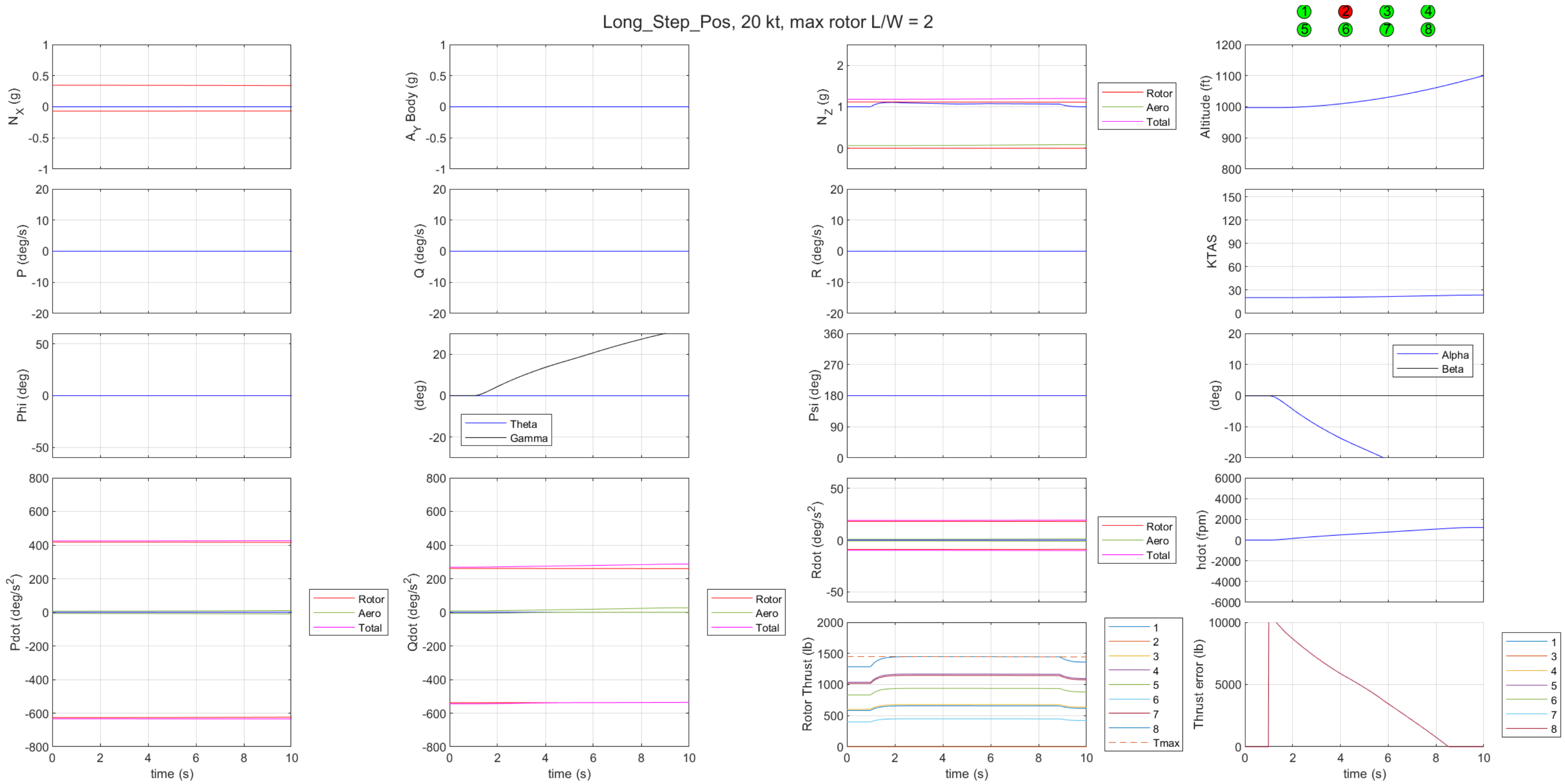

Figure A- 43. Max Pos. Long. step trimmed at 20 KIAS with an L/Wmax = 2 g and rotor two failed

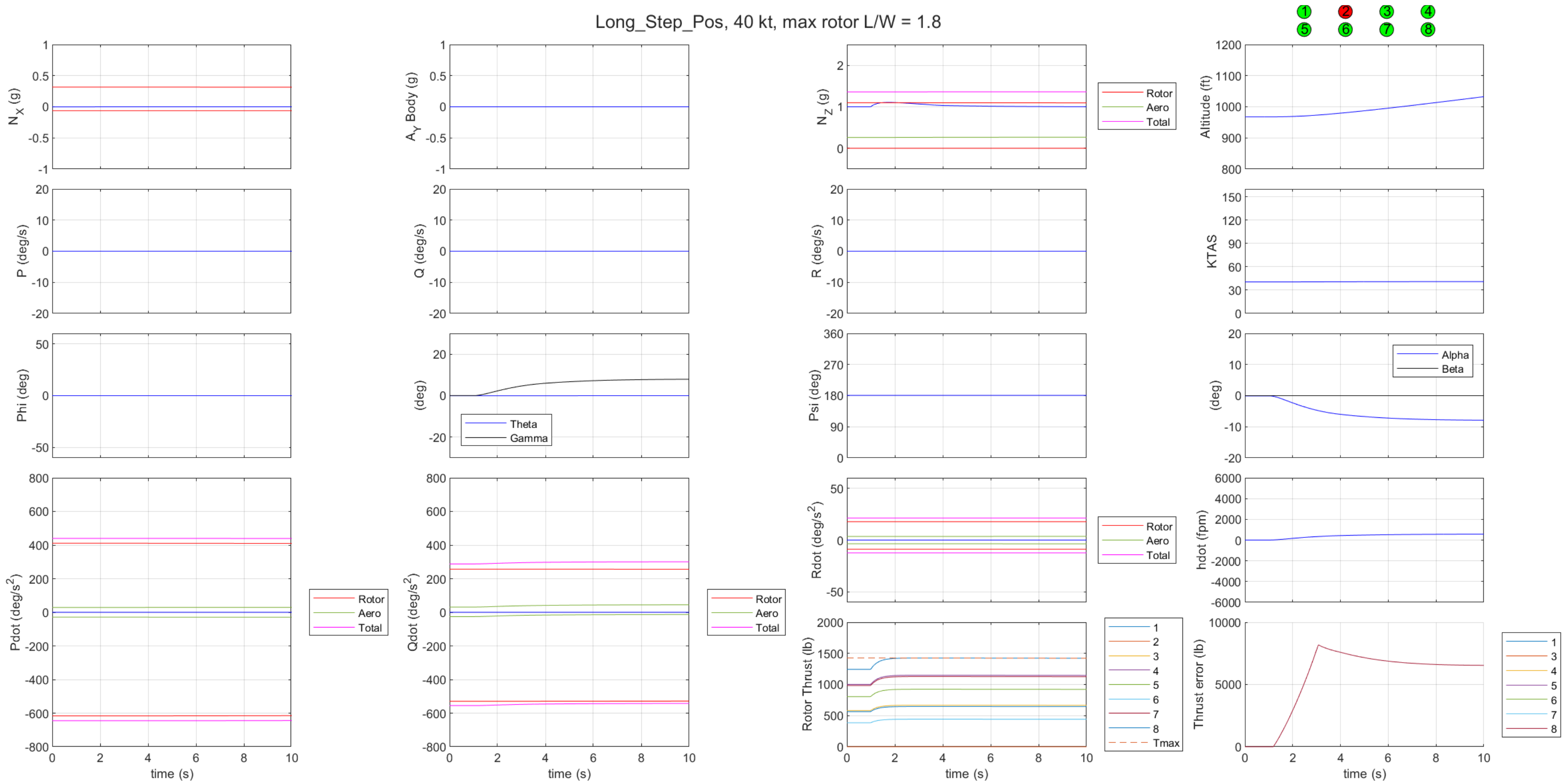

Figure A- 44. Max Pos. Long. step trimmed at 40 KIAS with an L/Wmax = 1.8 g and rotor two failed

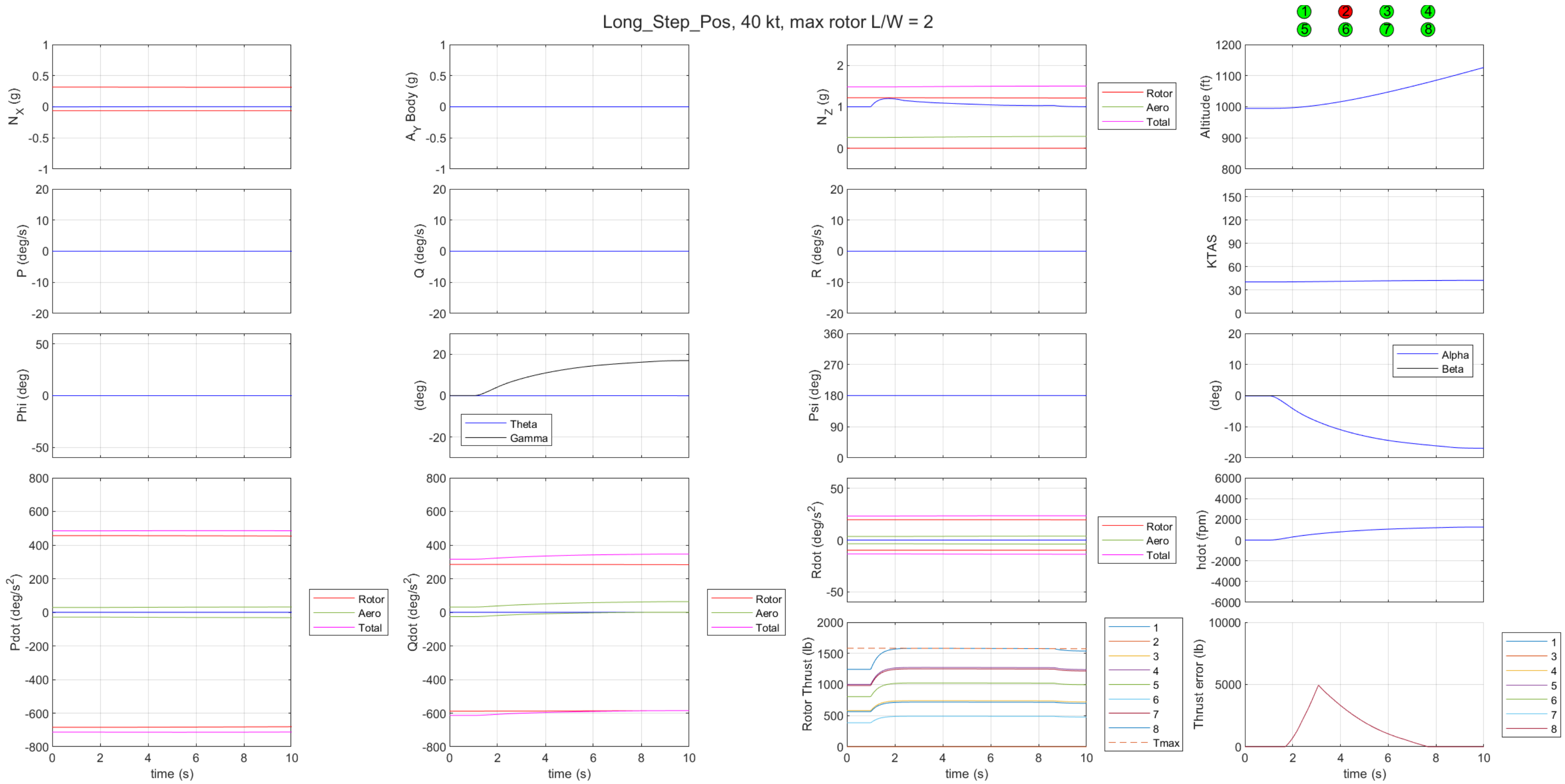

Figure A- 45. Max Pos. Long. step trimmed at 40 KIAS with an L/Wmax = 2 g and rotor two failed

A.13 Maximum positive lateral step with rotor failures

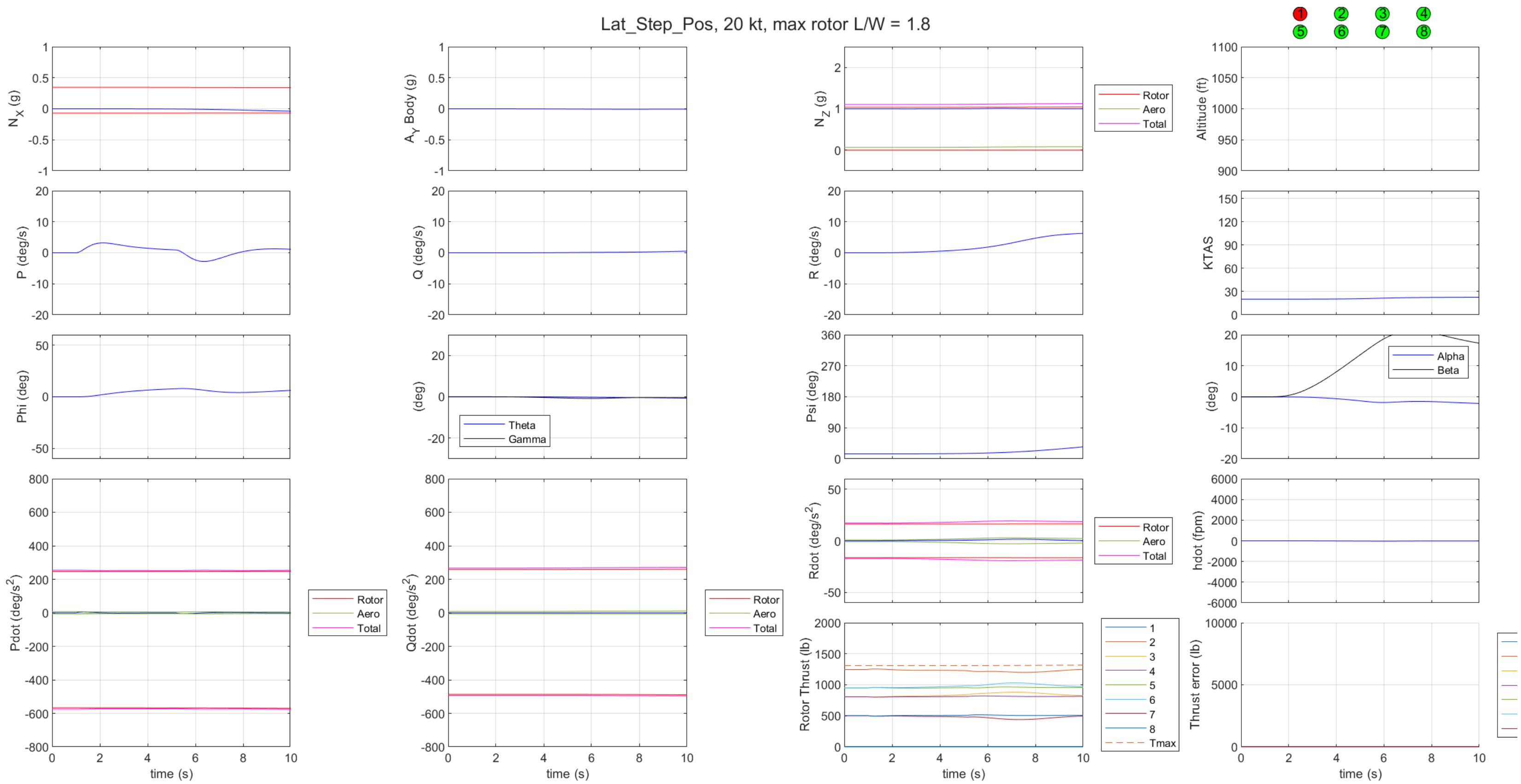

Figure A- 46. Max Pos. Lat. step trimmed at 20 KIAS with an L/Wmax = 1.8 g and rotor one failed

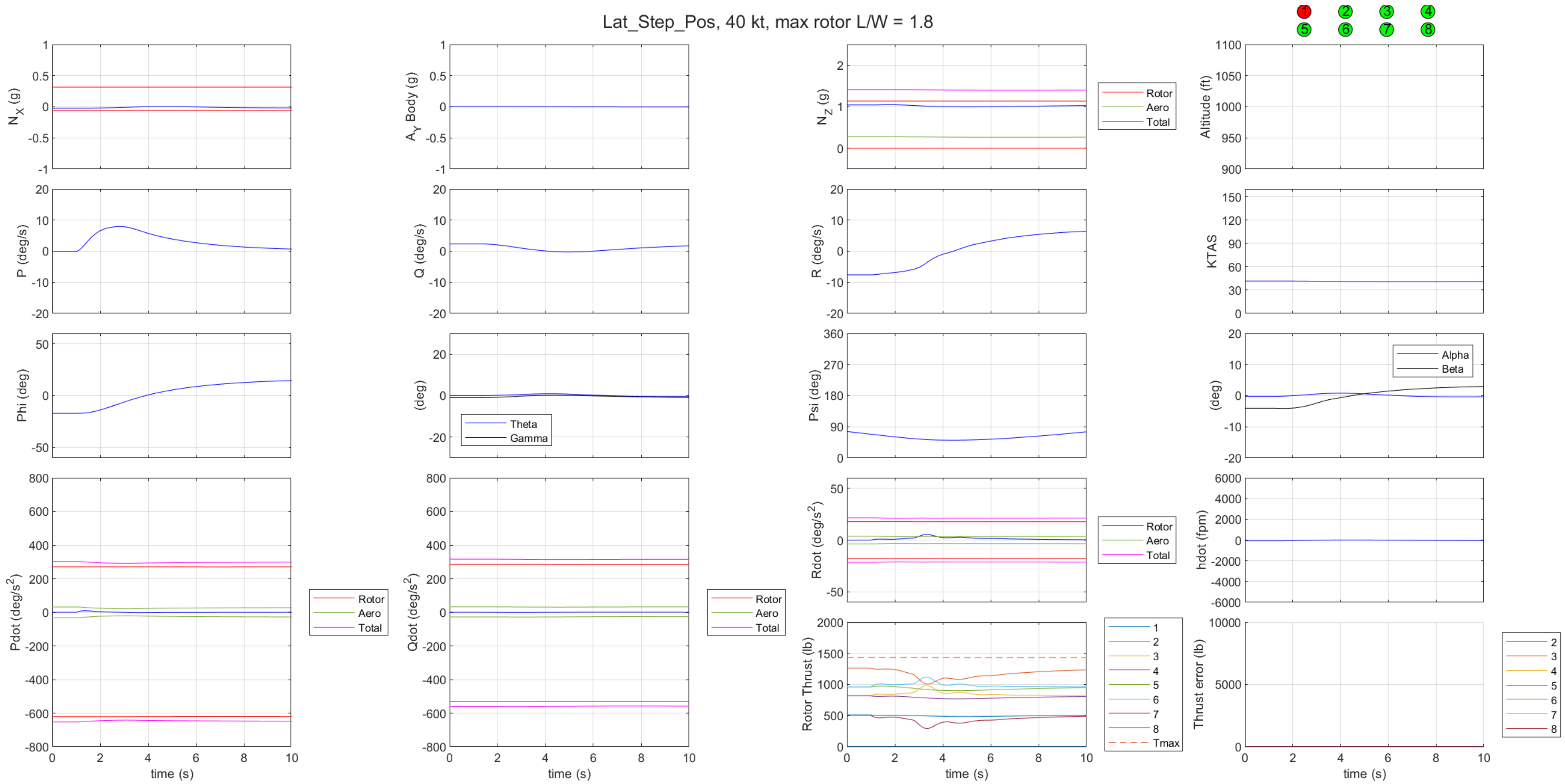

Figure A- 47. Max Pos. Lat. step trimmed at 40 KIAS with an L/Wmax = 1.8 g and rotor one failed

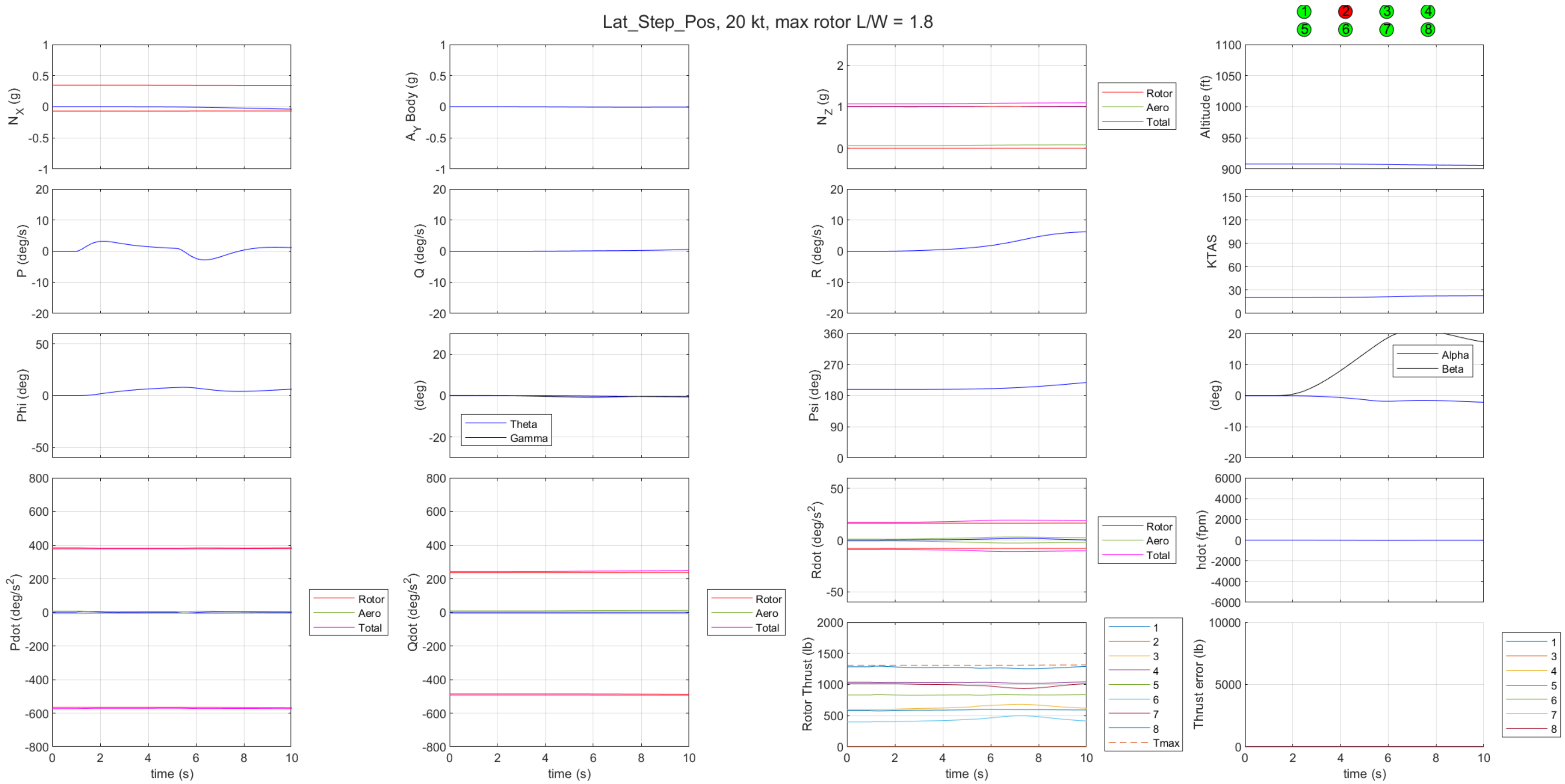

Figure A- 48. Max Pos. Lat. step trimmed at 20 KIAS with an L/Wmax = 1.8 g and rotor two failed

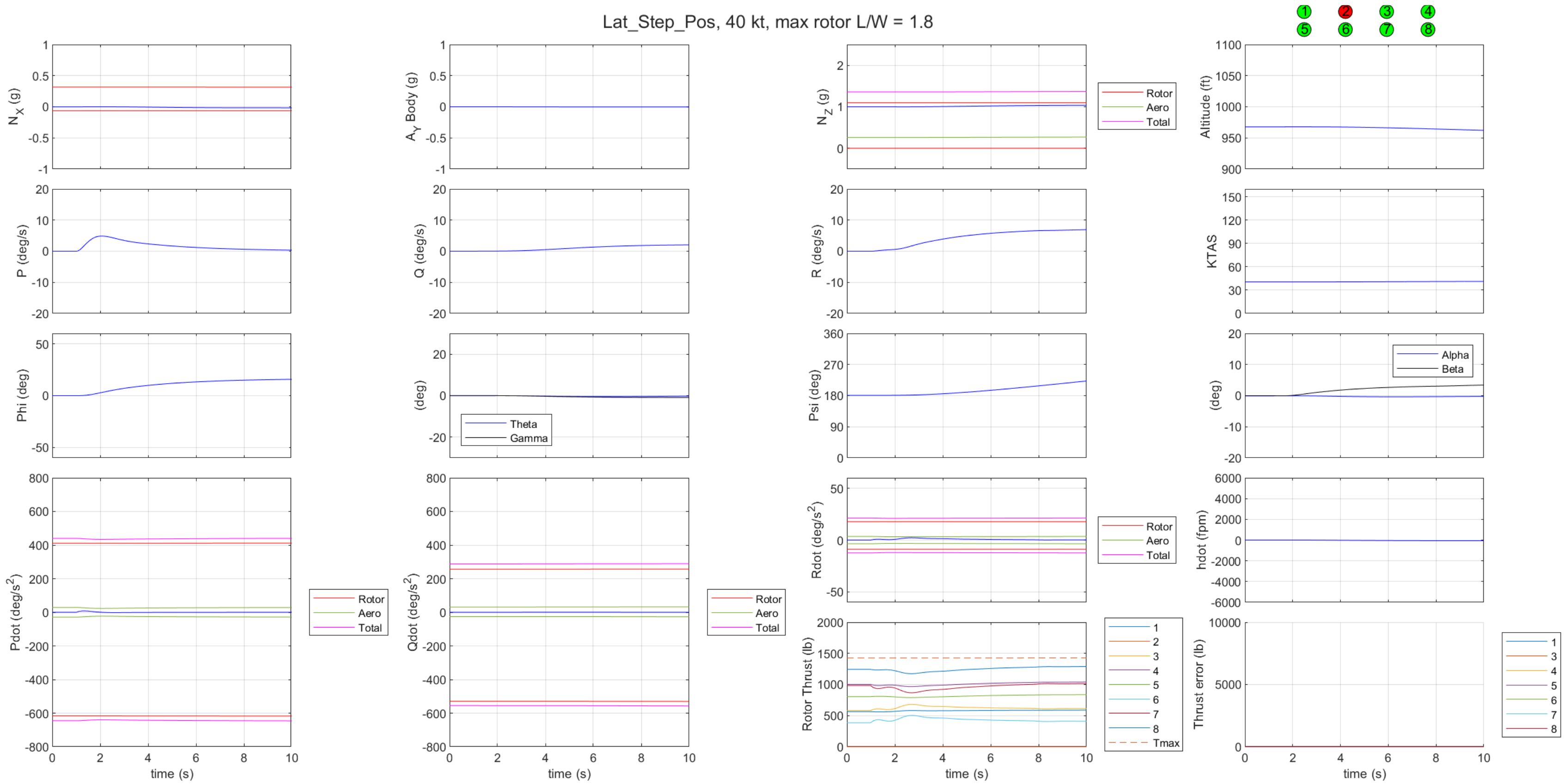

Figure A- 49. Max Pos. Lat. step trimmed at 40 KIAS with an L/Wmax = 1.8 g and rotor two failed

A.14 Maximum positive lateral step with rotor failures

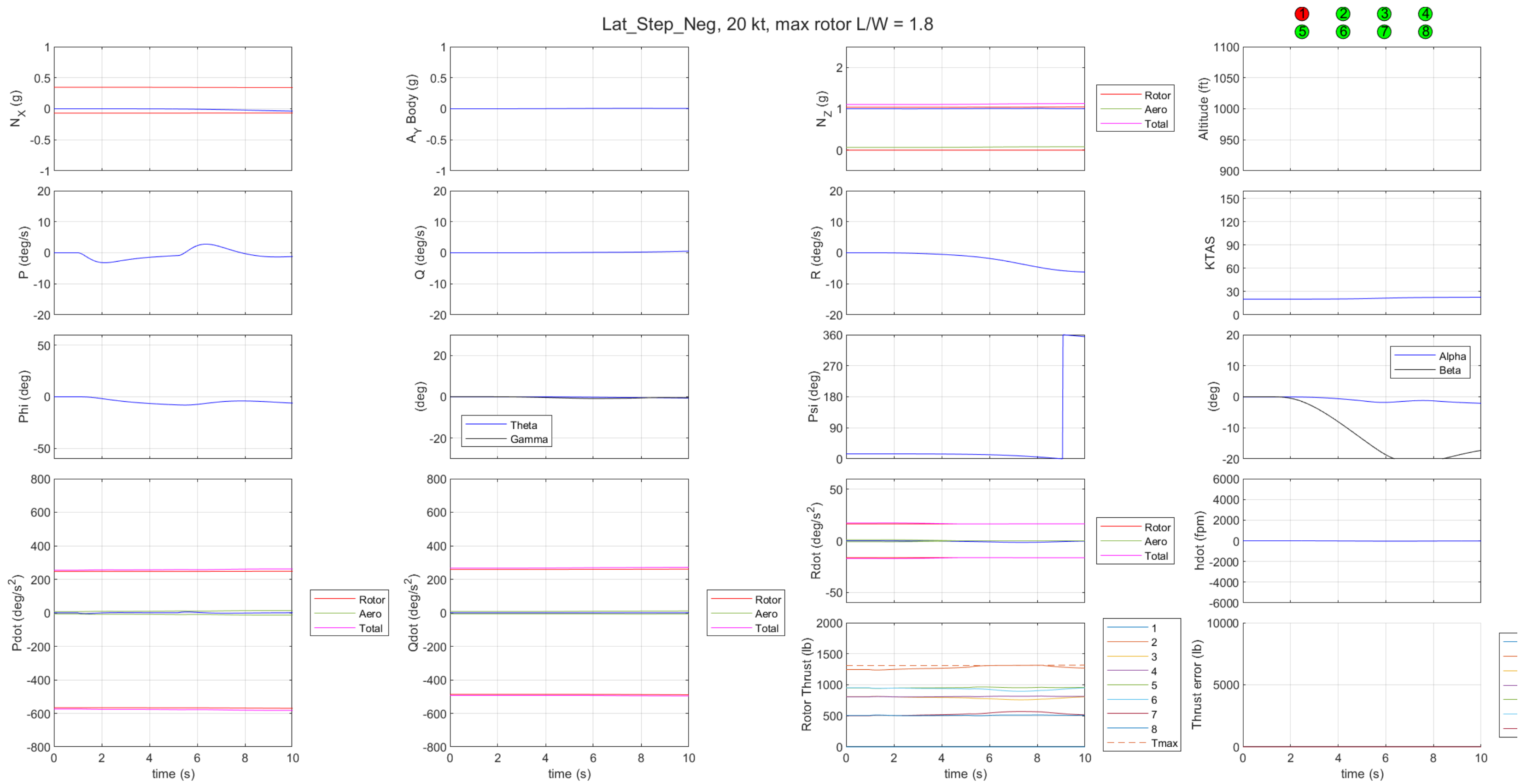

Figure A- 50. Max Neg. Lat. step trimmed at 20 KIAS with an L/Wmax = 1.8 g and rotor one failed

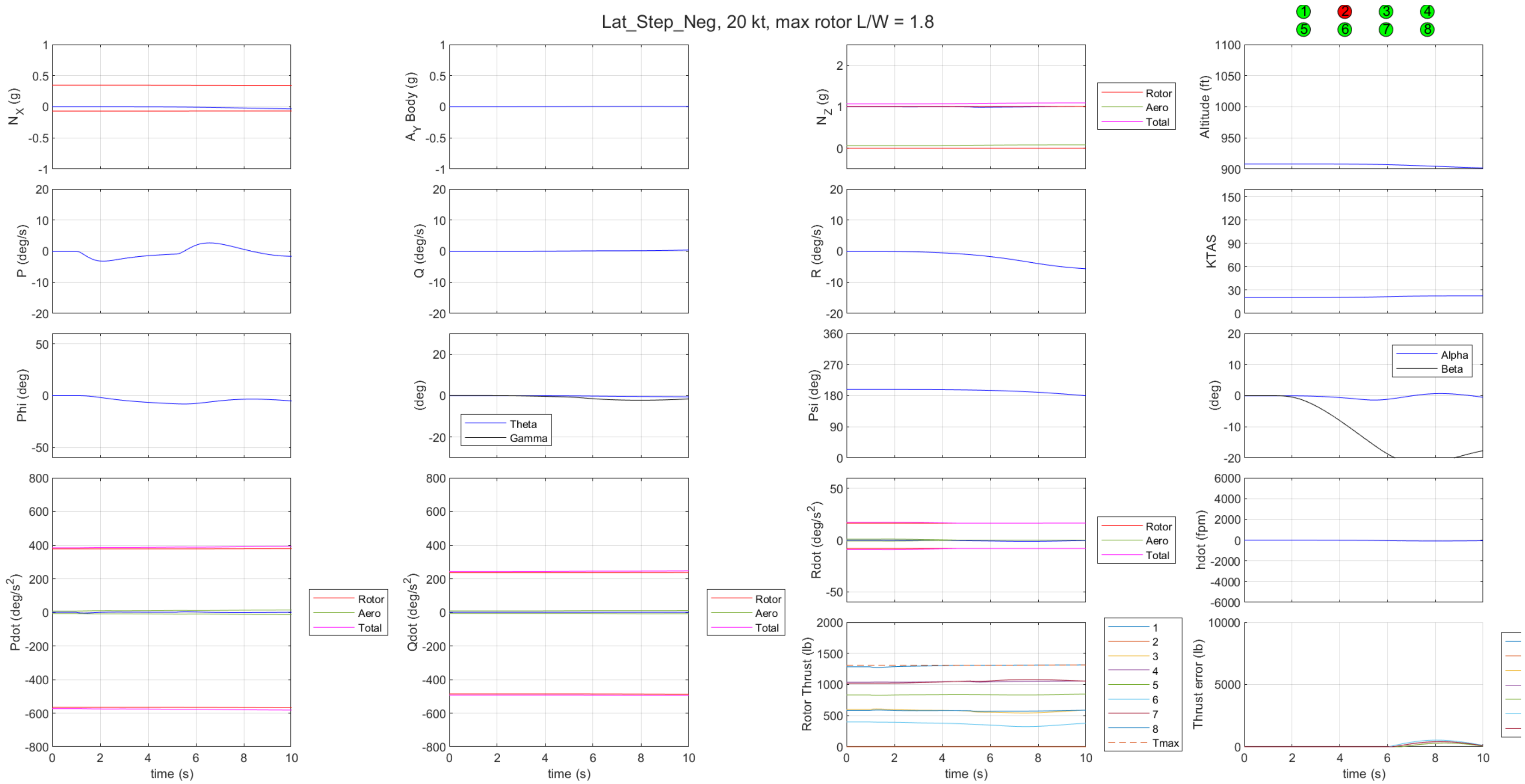

Figure A- 51. Max Neg. Lat. step trimmed at 20 KIAS with an L/Wmax = 1.8 g and rotor two failed

A.15 Maximum positive pedal step with rotor failures

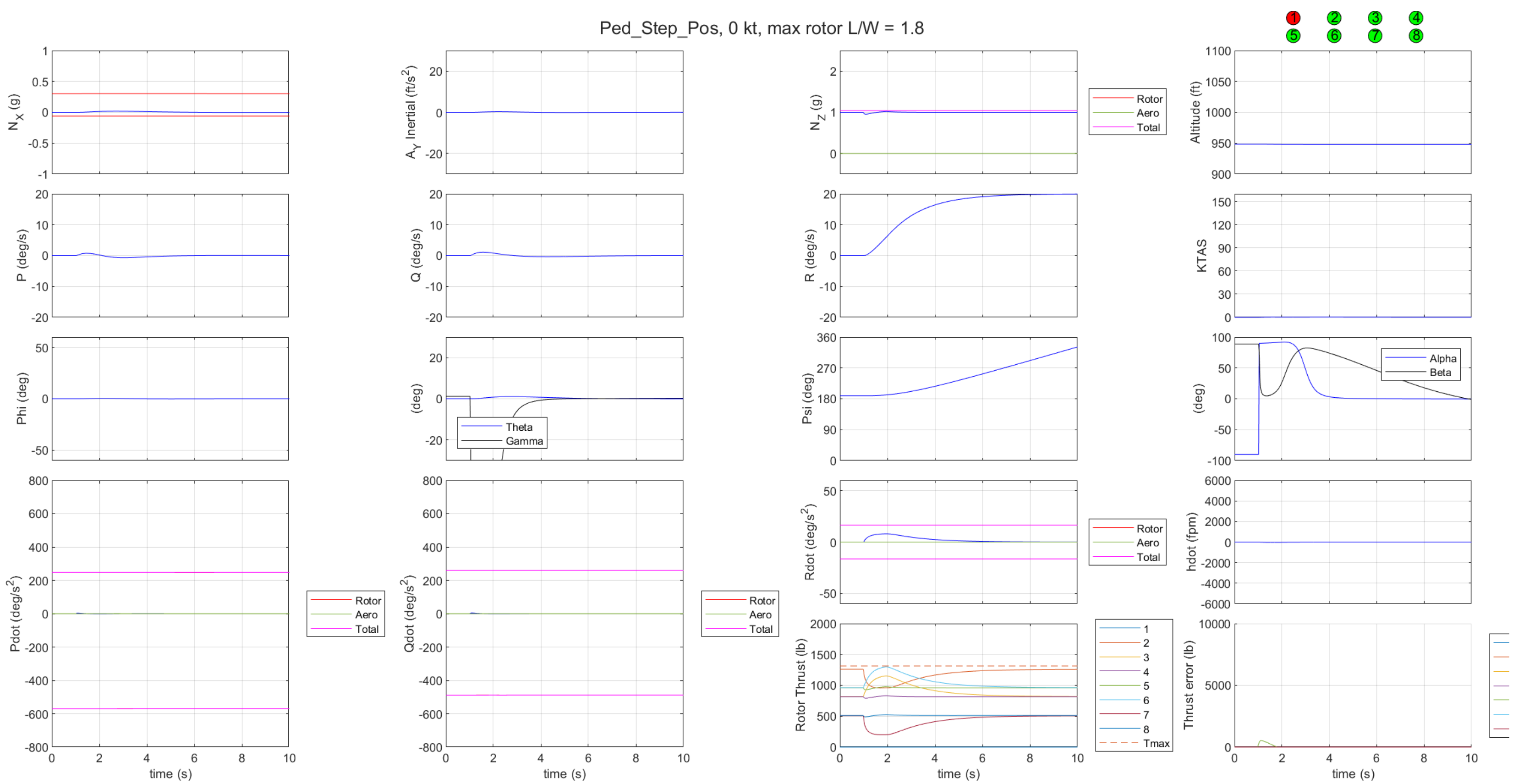

Figure A- 52. Max Pos. Ped. step trimmed at 0 KGS with an L/Wmax = 1.8 g and rotor one failed

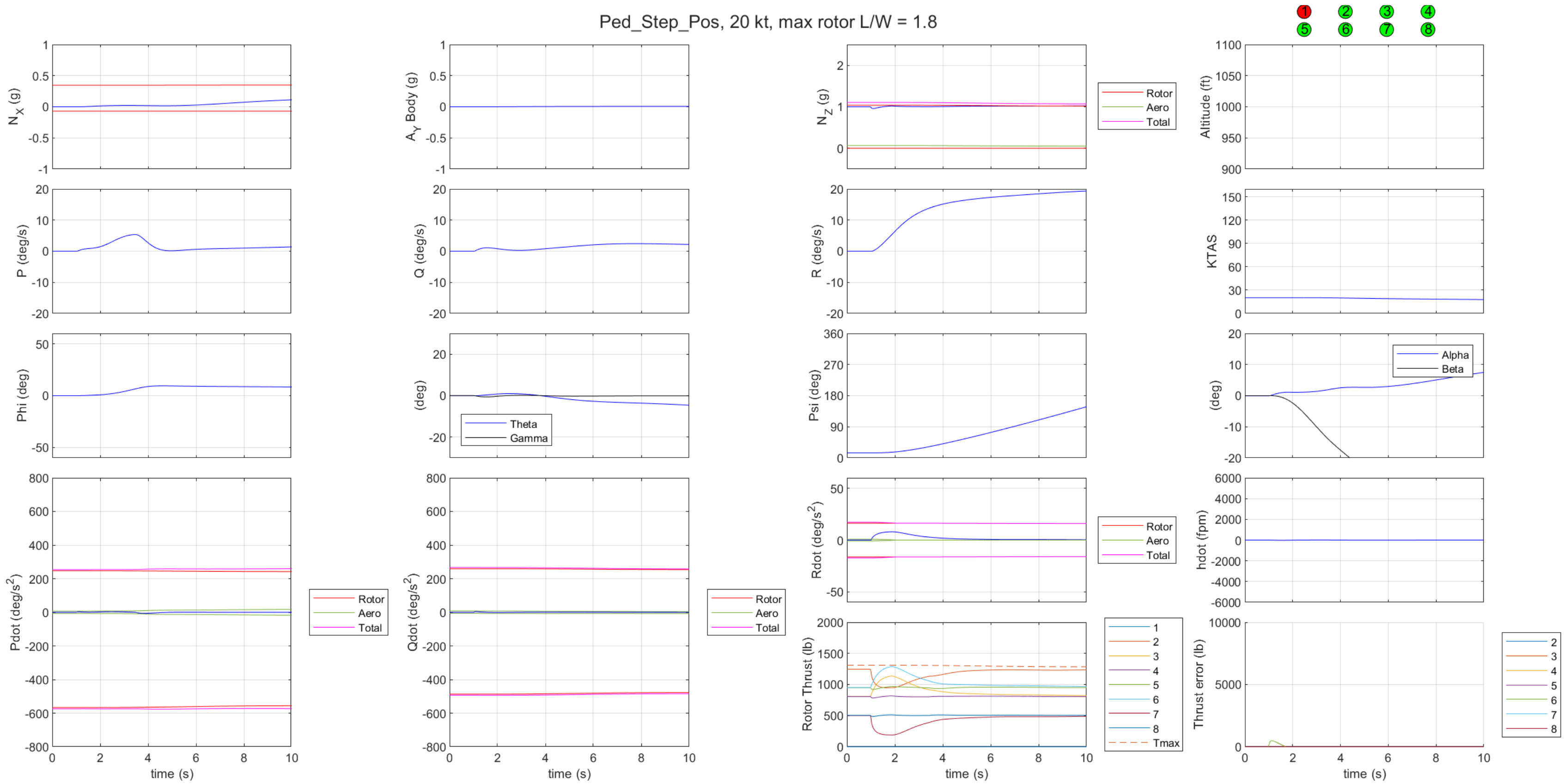

Figure A- 53. Max Pos. Ped. step trimmed at 20 KIAS with an L/Wmax = 1.8 g and rotor one failed

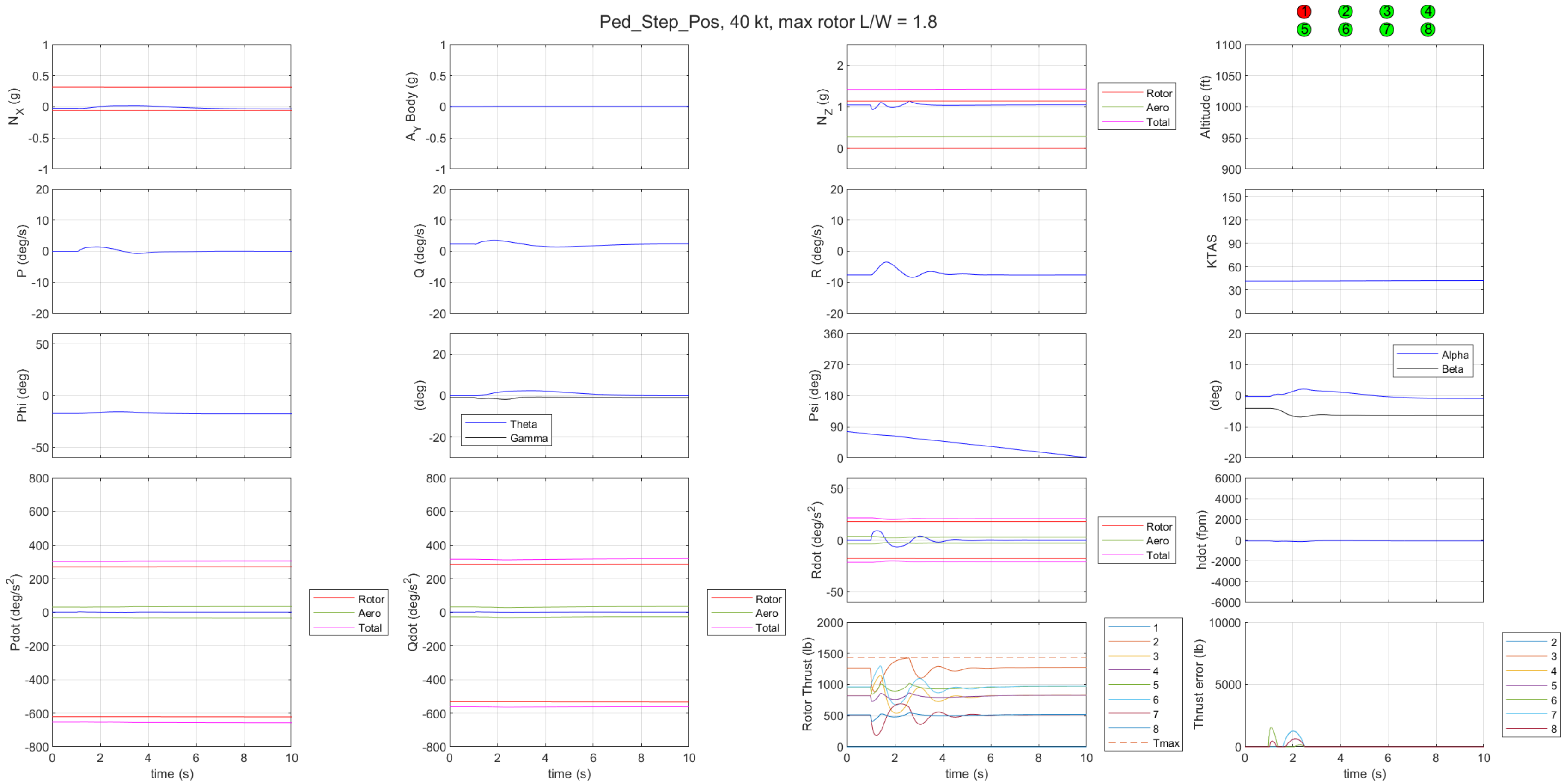

Figure A- 54. Max Pos. Ped. step trimmed at 40 KIAS with an L/Wmax = 1.8 g and rotor one failed

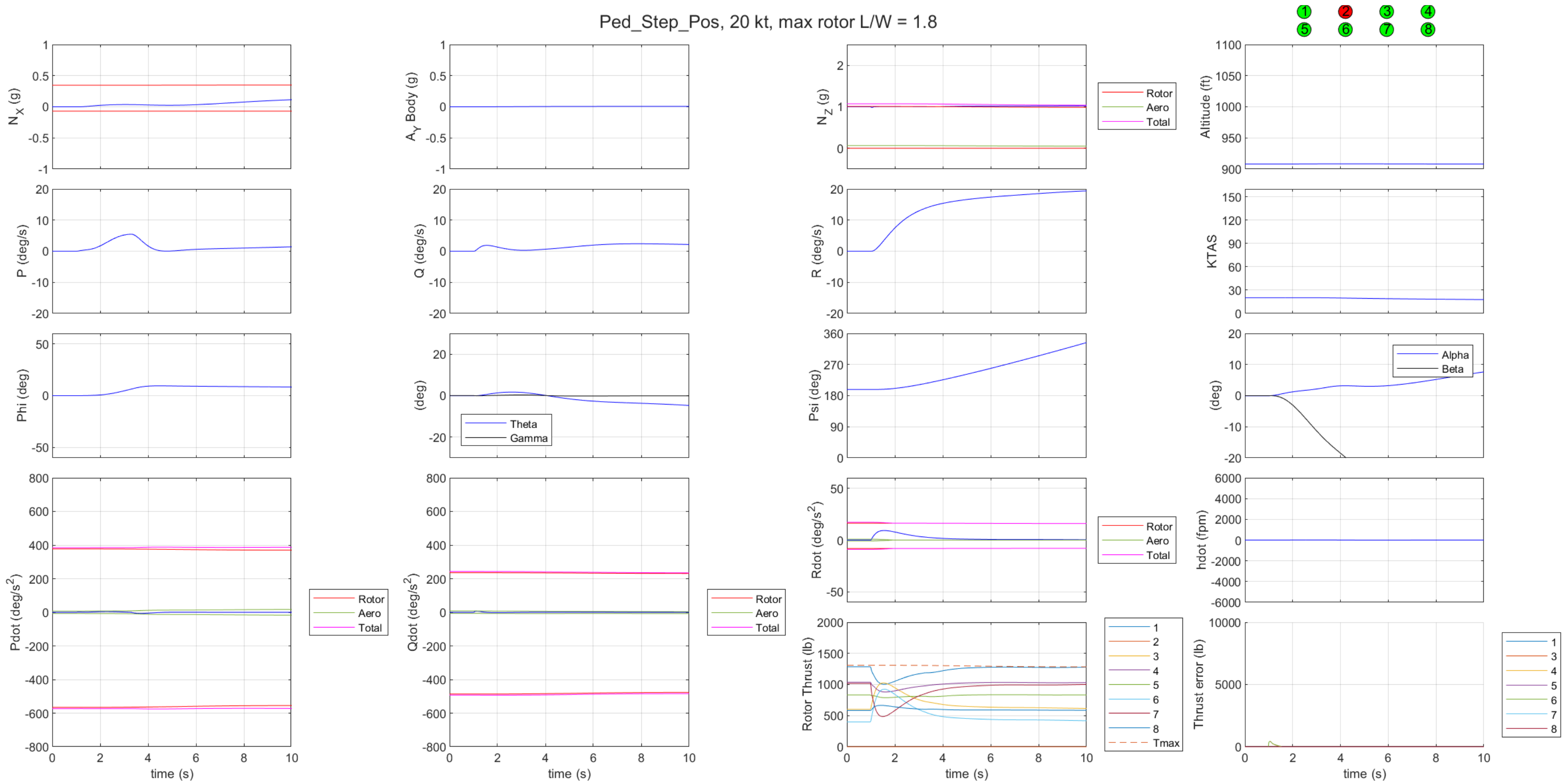

Figure A- 55. Max Pos. Ped. step trimmed at 20 KIAS with an L/Wmax = 1.8 g and rotor two failed

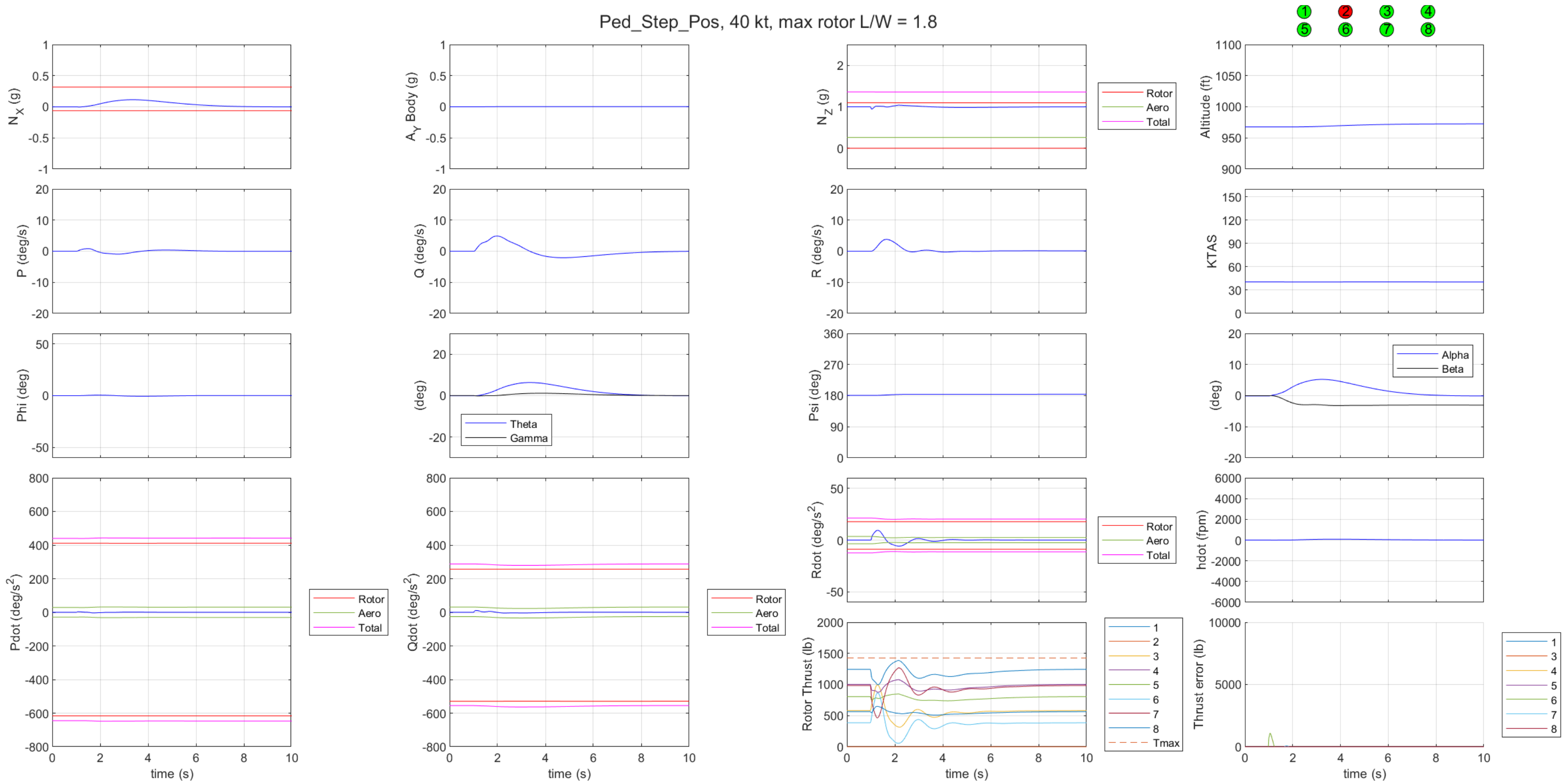

Figure A- 56. Max Pos. Ped. step trimmed at 40 KIAS with an L/Wmax = 1.8 g and rotor two failed

A.16 Maximum negative pedal step with rotor failures

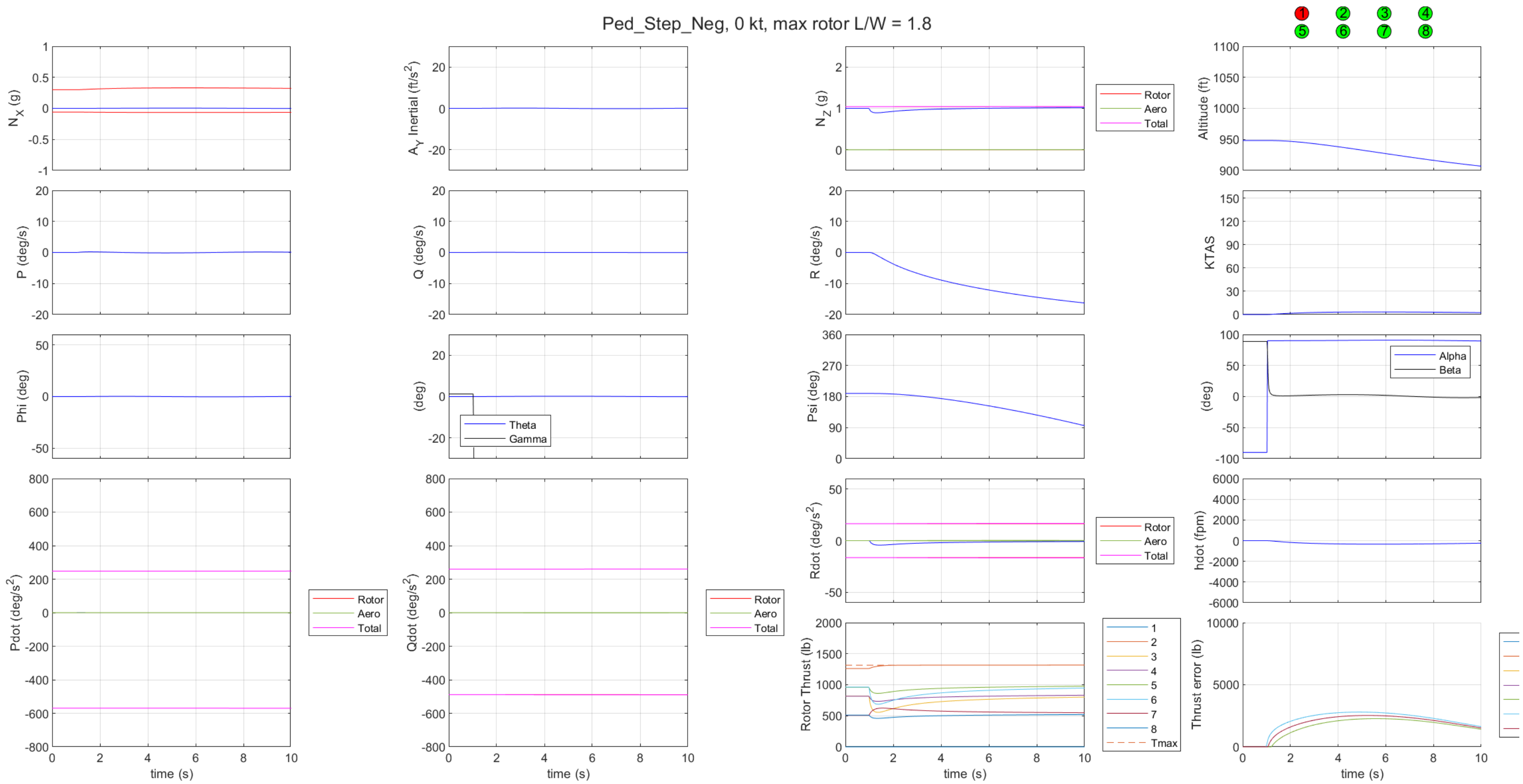

Figure A- 57. Max Neg. Ped. step trimmed at 0 KGS with an L/Wmax = 1.8 g and rotor one failed

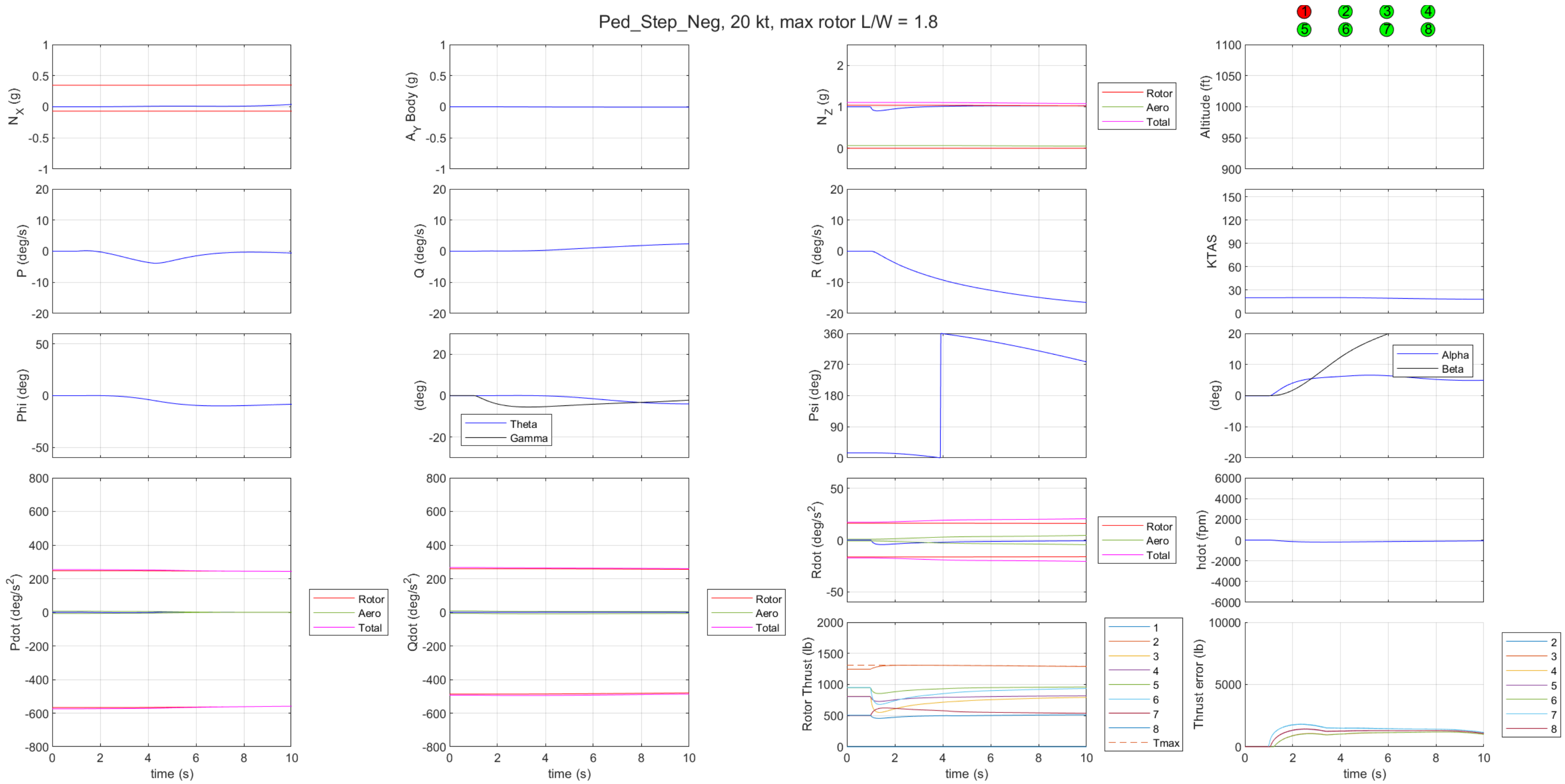

Figure A- 58. Max Neg. Ped. step trimmed at 20 KIAS with an L/Wmax = 1.8 g and rotor one failed

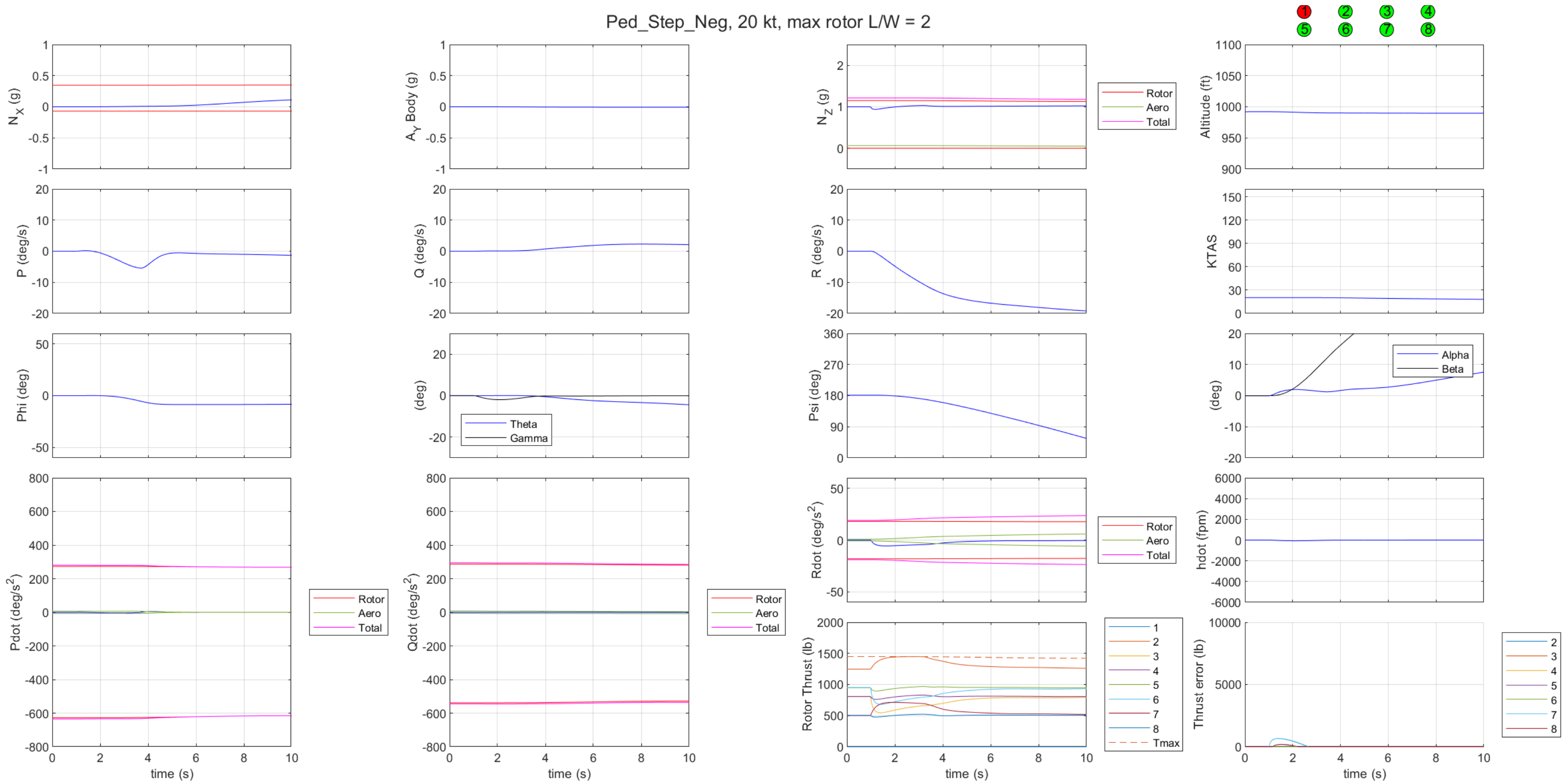

Figure A- 59. Max Neg. Ped. step trimmed at 20 KIAS with an L/Wmax = 2 g and rotor one failed

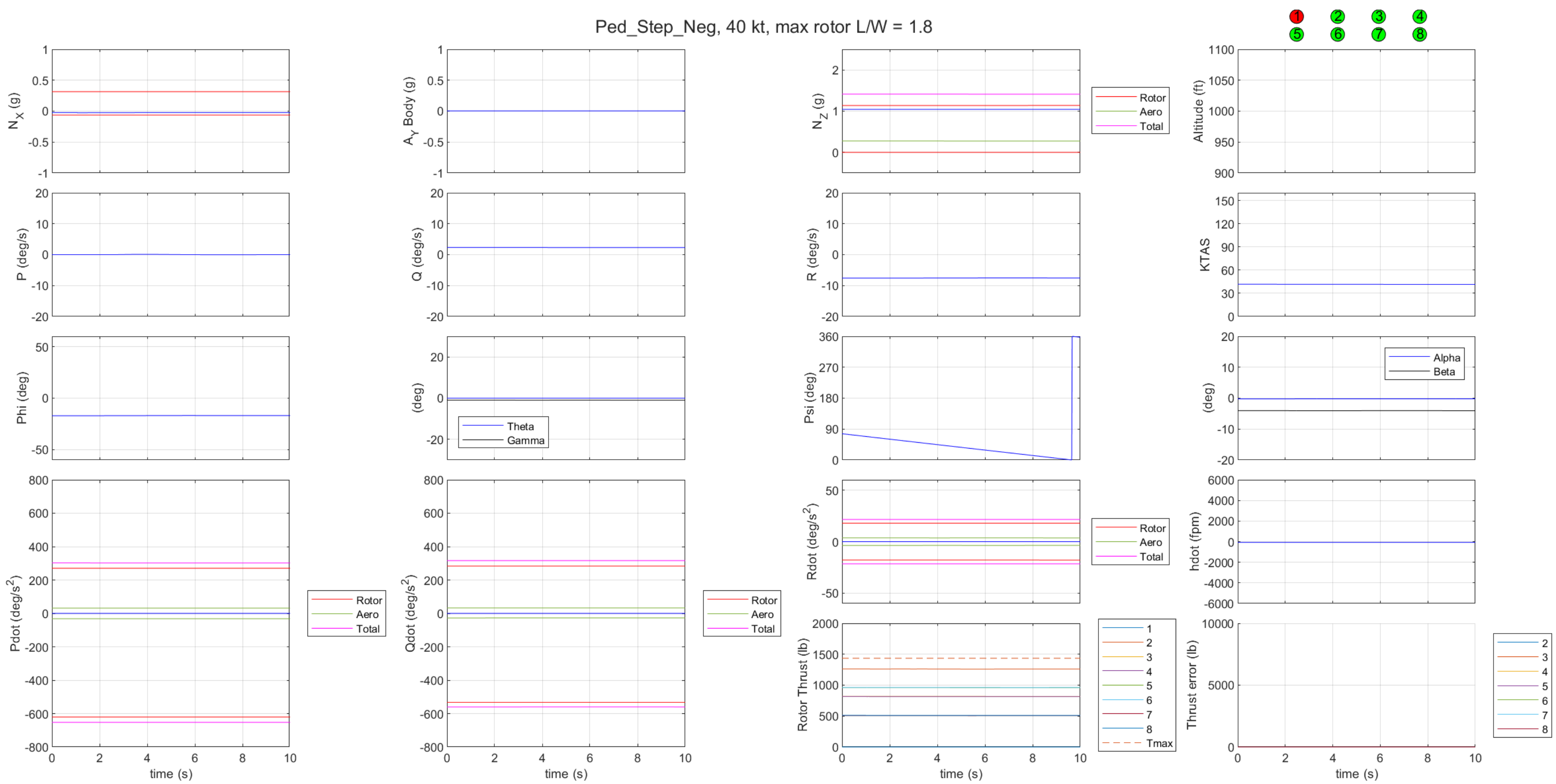

Figure A- 60. Max Neg. Ped. step trimmed at 40 KIAS with an L/Wmax = 1.8 g and rotor one failed

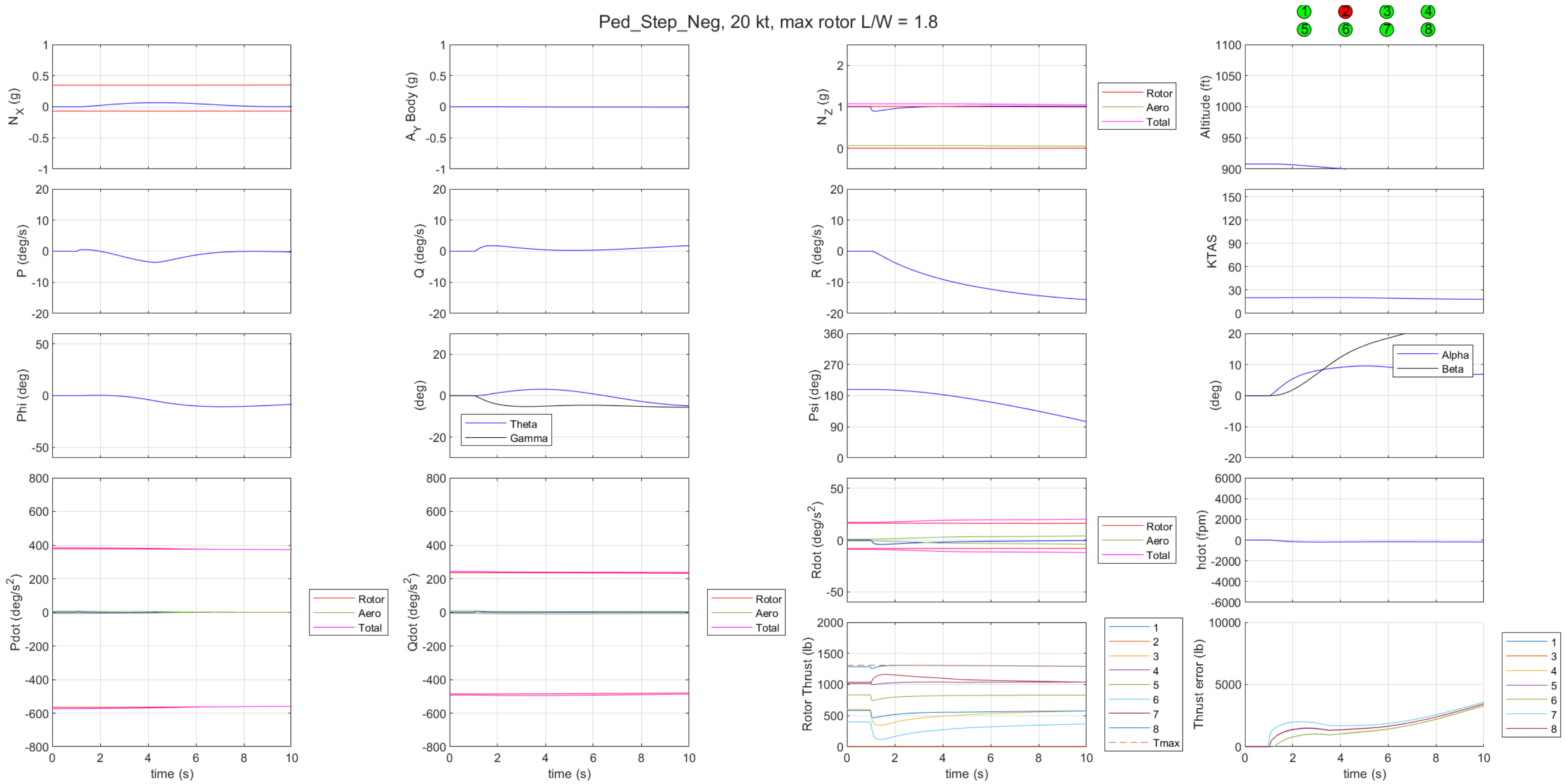

Figure A- 61. Max Neg. Ped. step trimmed at 20 KIAS with an L/Wmax = 1.8 g and rotor two failed

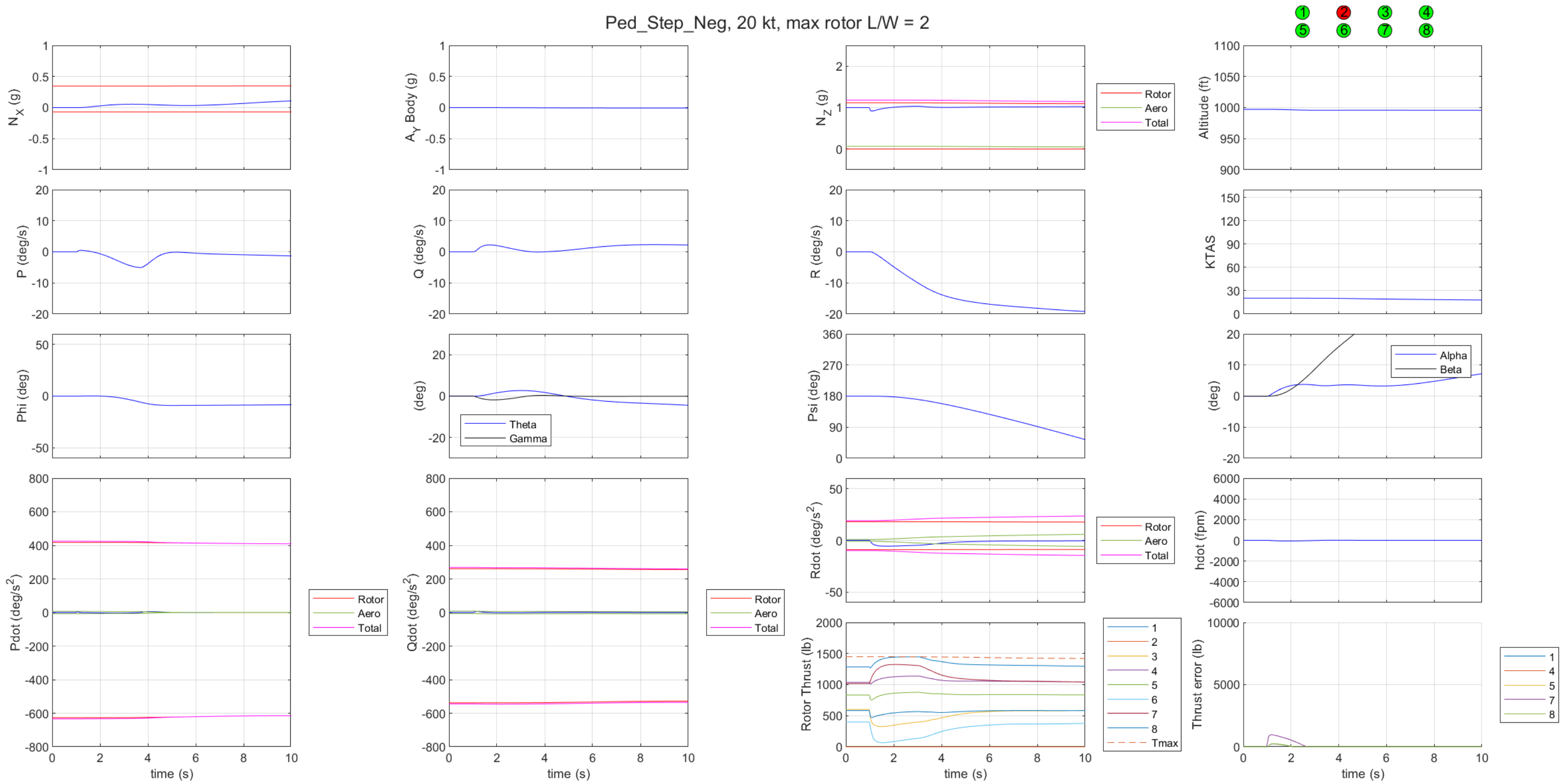

Figure A- 62. Max Neg. Ped. step trimmed at 20 KIAS with an L/Wmax = 2 g and rotor two failed

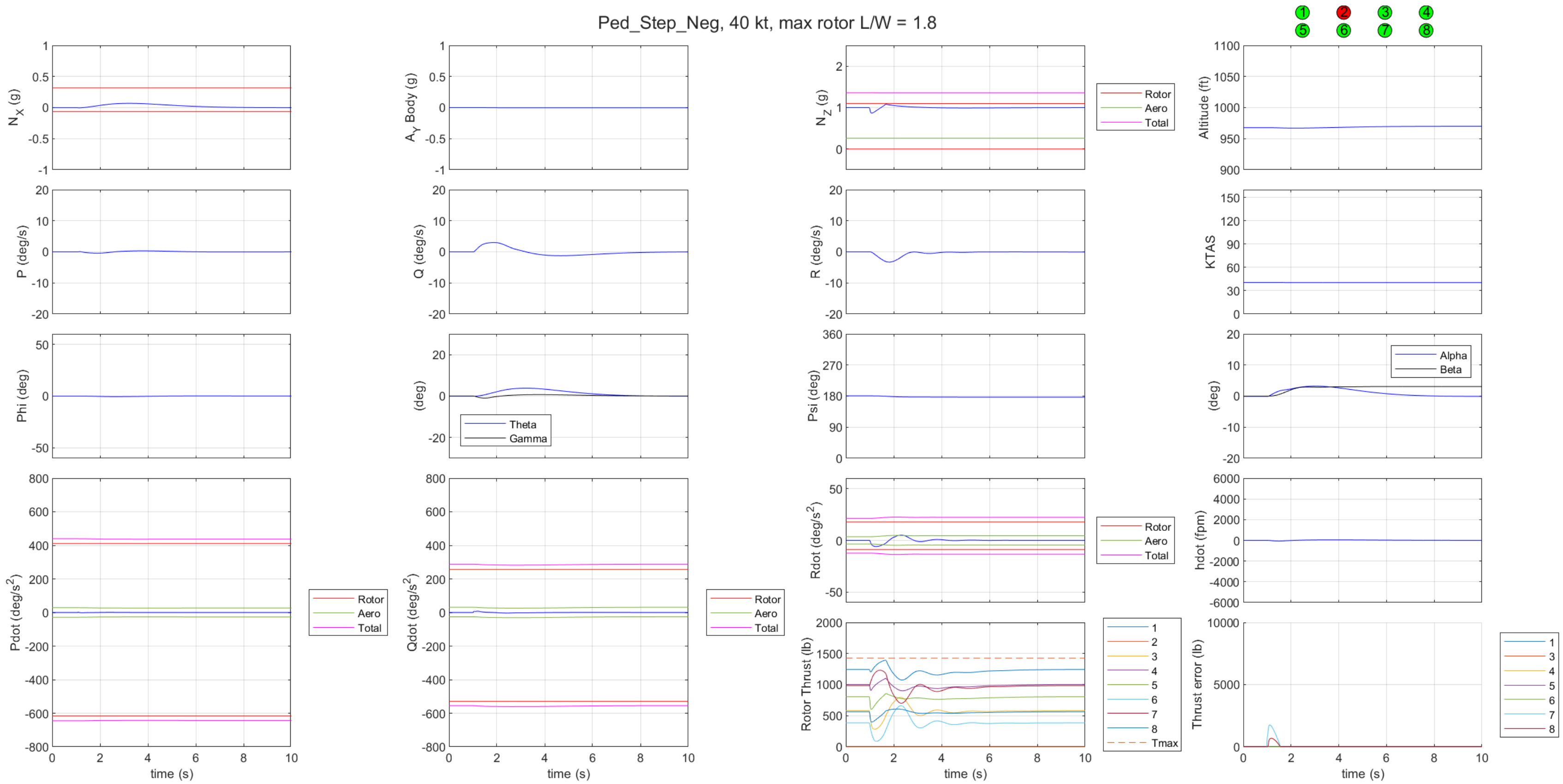

Figure A- 63. Max Neg. Ped. step trimmed at 40 KIAS with an L/Wmax = 1.8 g and rotor two failed

A.17 Maximum deceleration with rotor failures

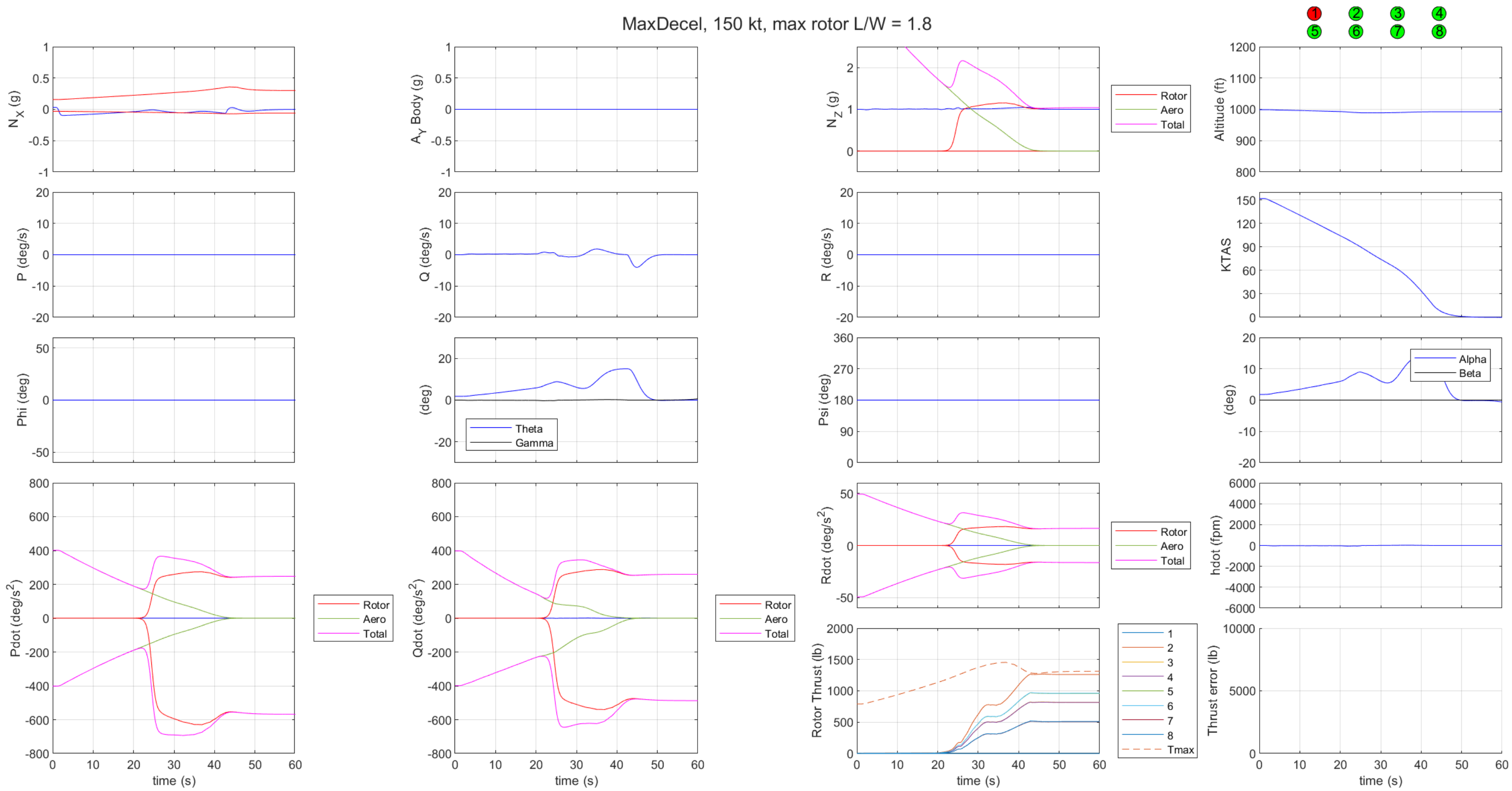

Figure A- 64. Max Decel. trimmed at 150 KIAS with an L/Wmax = 1.8 g and rotor one failed

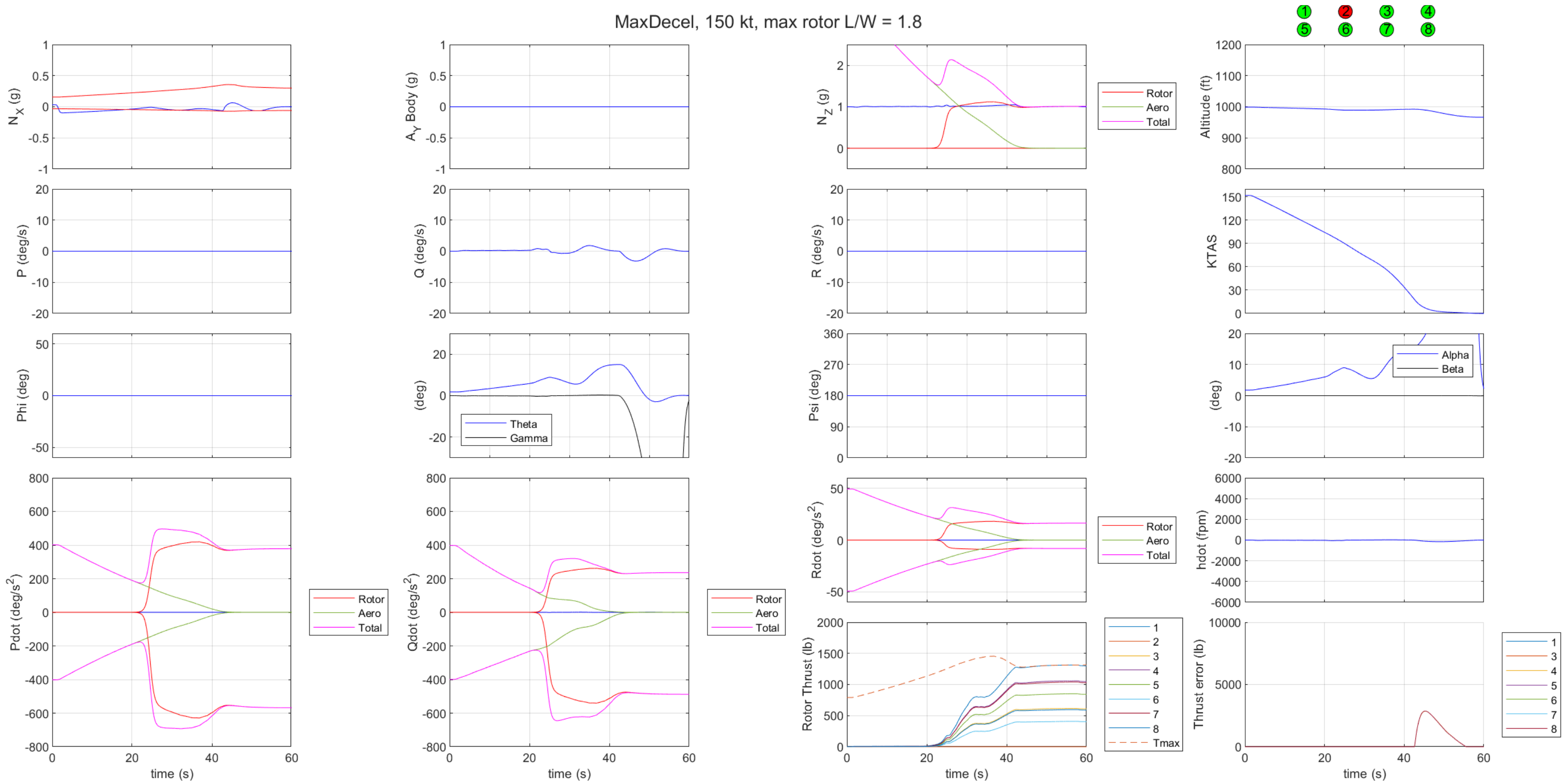

Figure A- 65. Max Decel. trimmed at 150 KIAS with an L/Wmax = 1.8 g and rotor two failed

A.18 Maximum acceleration with rotor failures

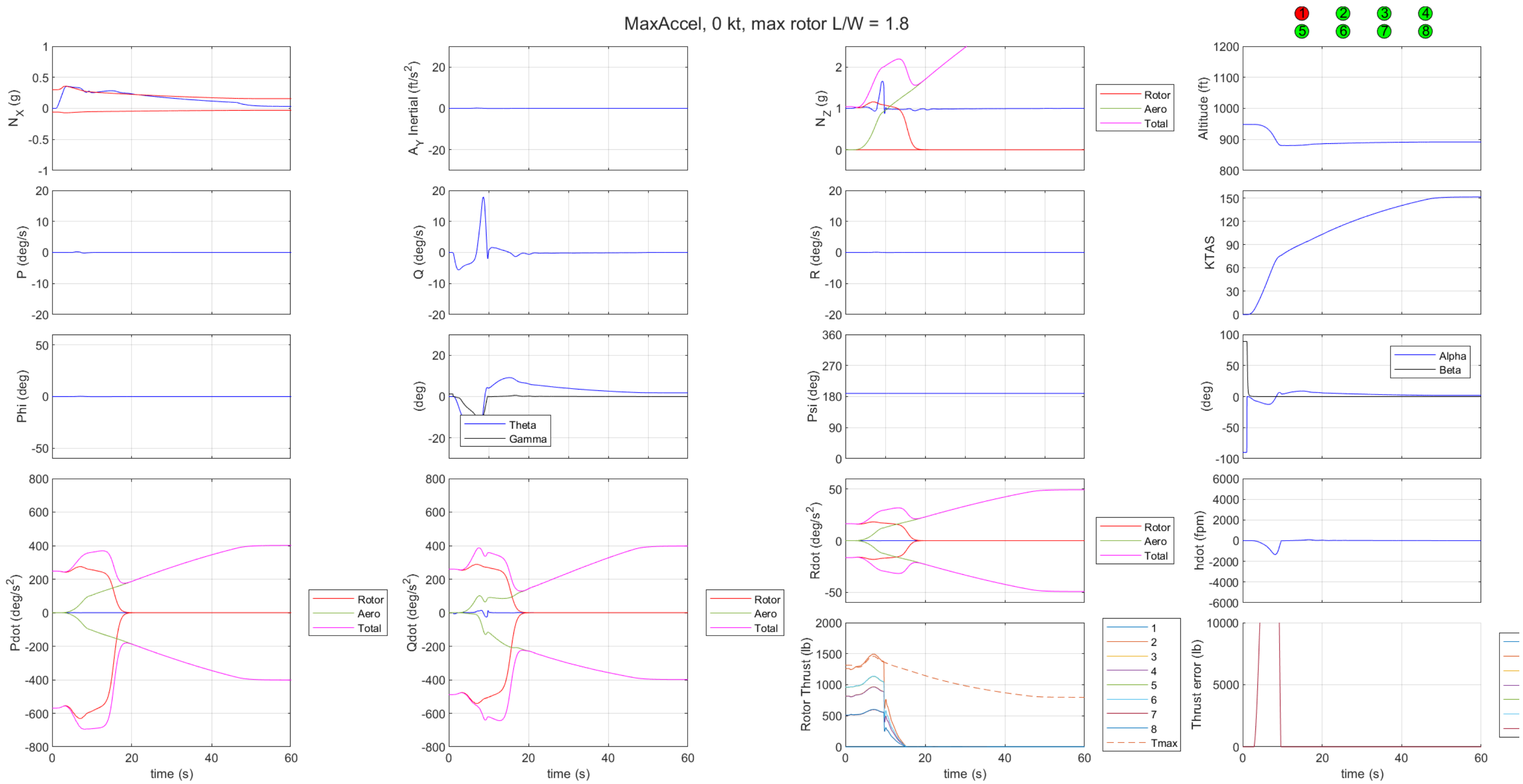

Figure A- 66. Max Accel. trimmed at 0 KGS with an L/Wmax = 1.8 g and rotor one failed

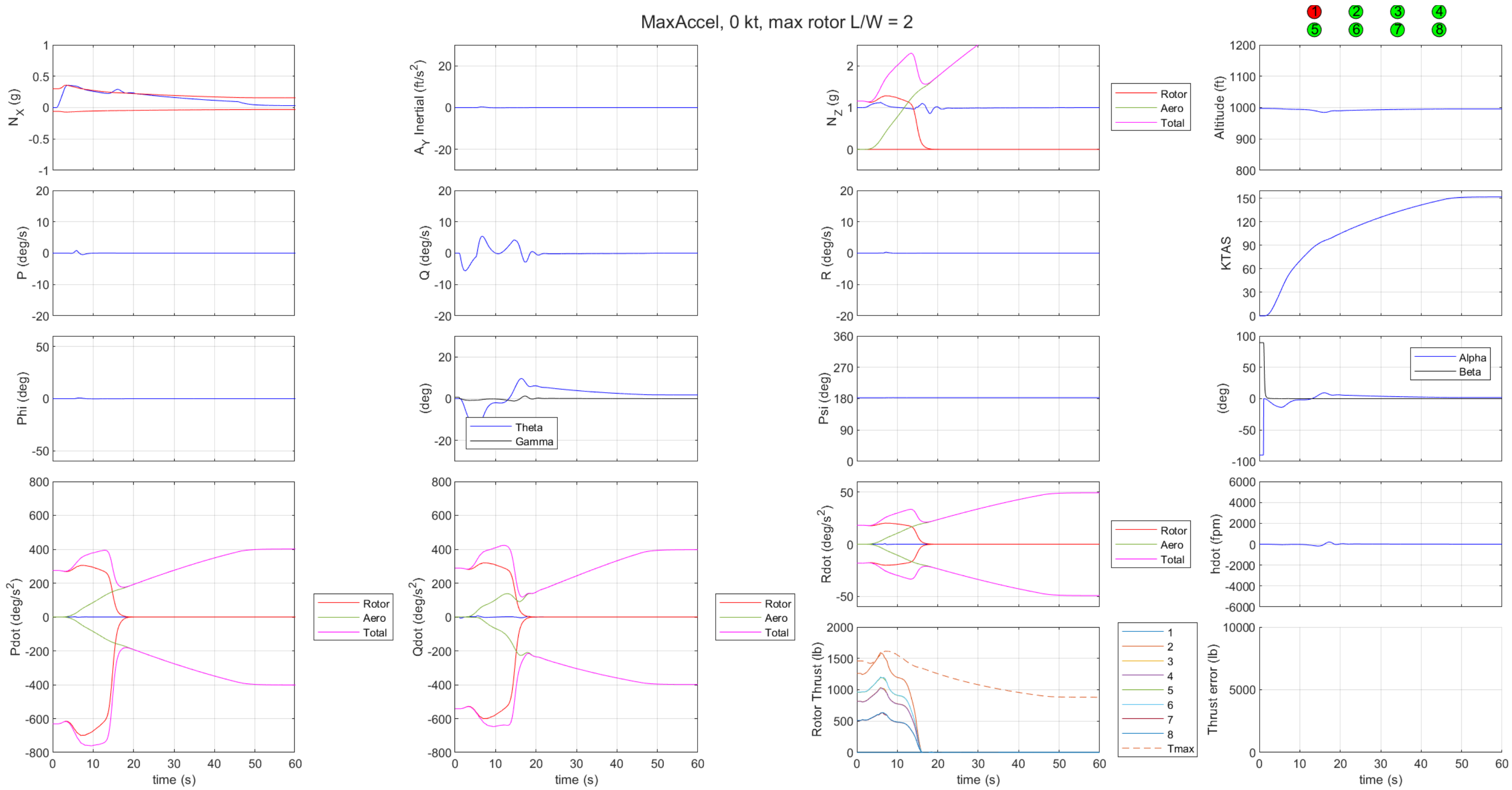

Figure A- 67. Max Accel. trimmed at 0 KGS with an L/Wmax = 2 g and rotor one failed

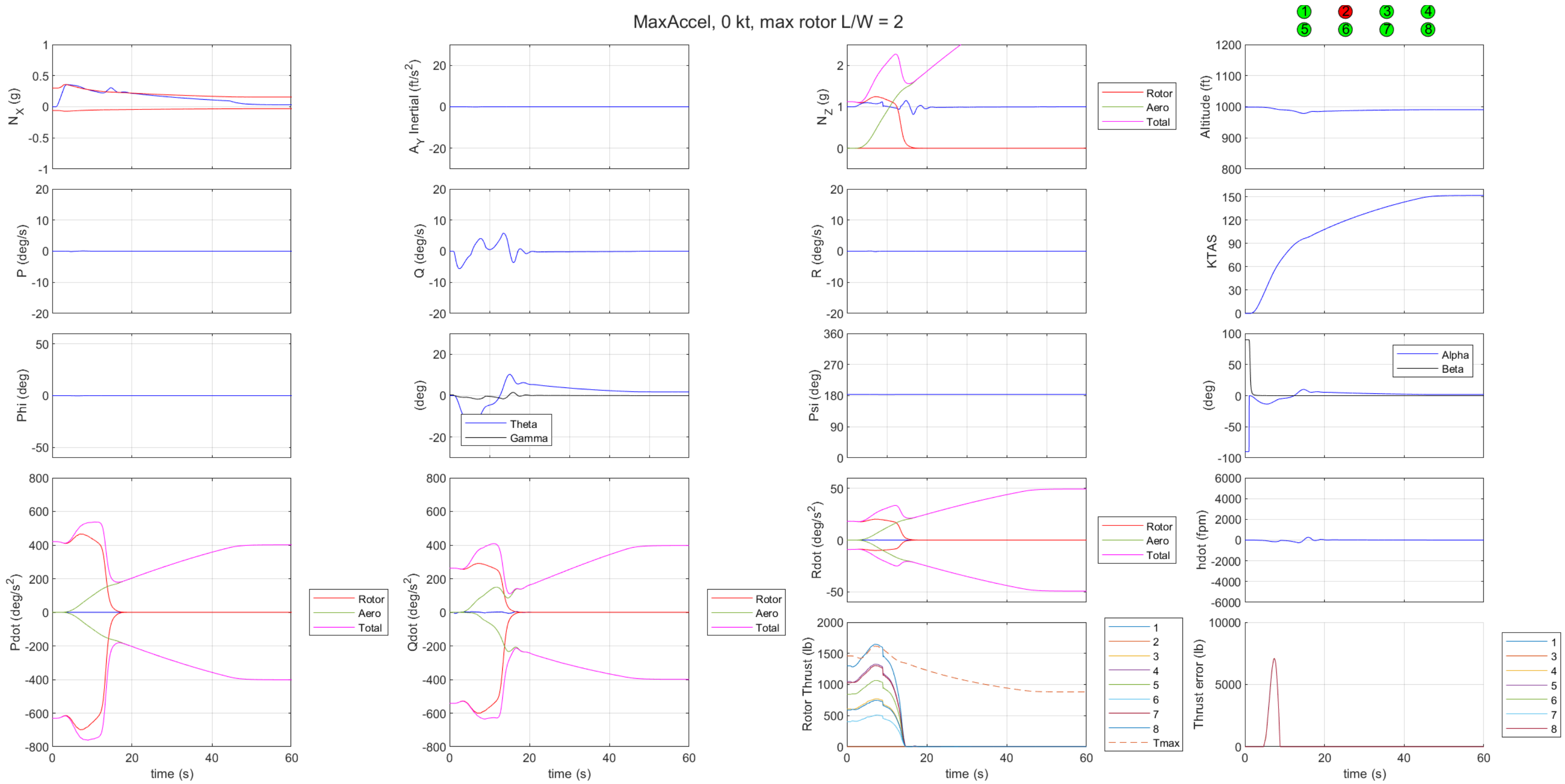

Figure A- 68. Max Accel. trimmed at 0 KGS with an L/Wmax = 2 g and rotor two failed

A.19 Maximum positive longitudinal step and negative pedal step with rotor failures

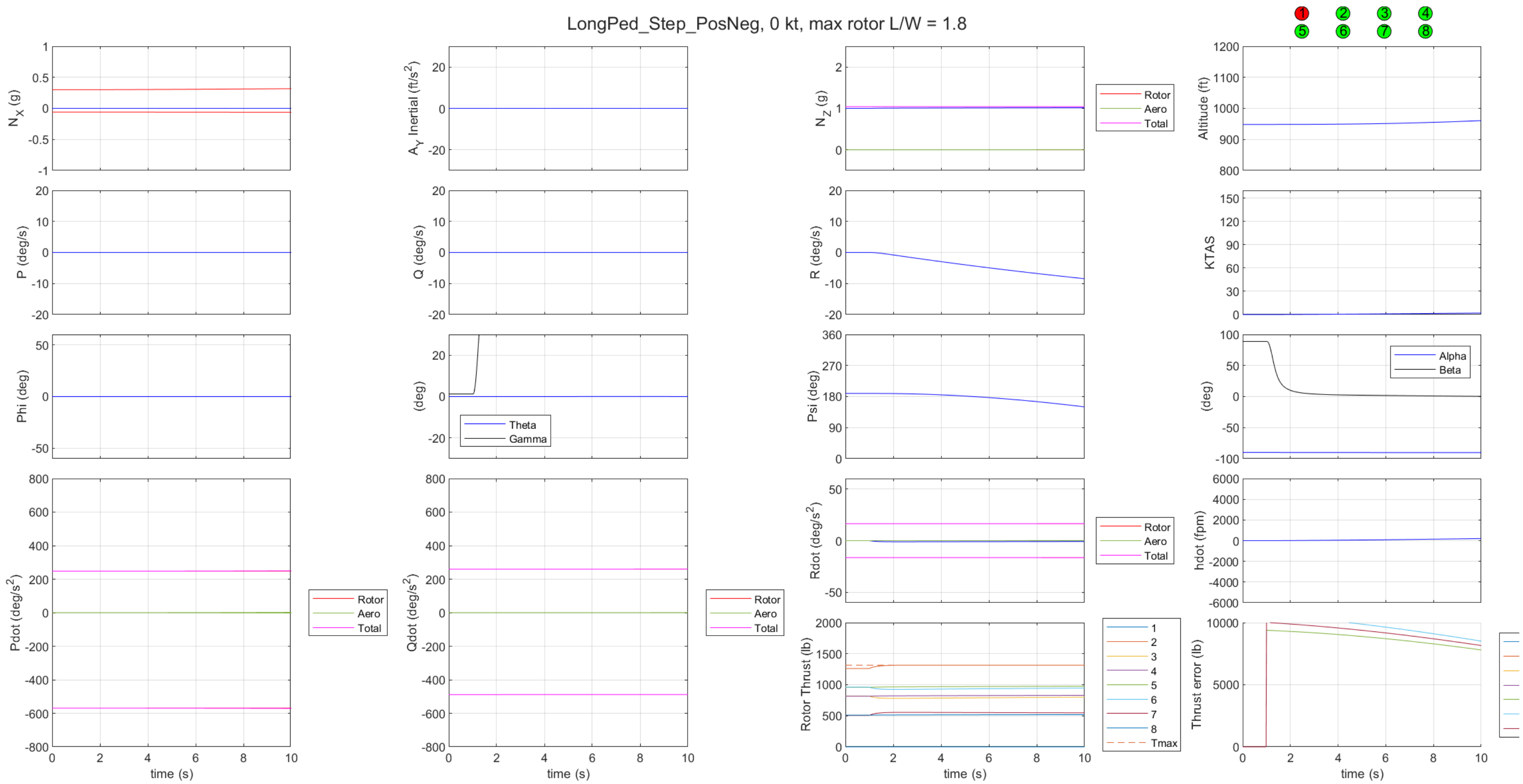

Figure A- 69. Max Pos. Long. and Neg. Ped. step trimmed at 0 KGS with an L/Wmax = 1.8 g and rotor one failed

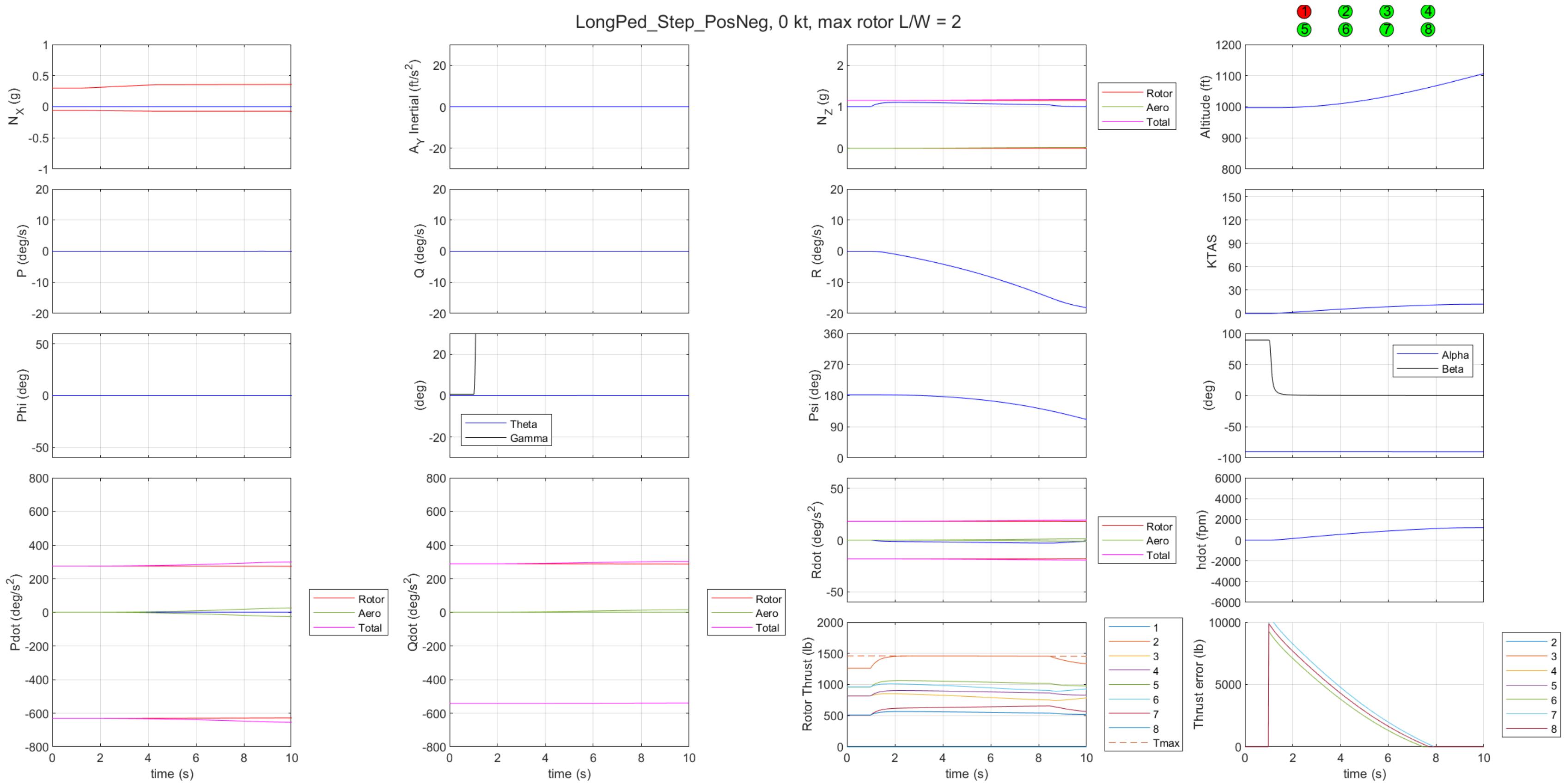

Figure A- 70. Max Pos. Long. and Neg. Ped. step trimmed at 0 KGS with an L/Wmax = 2 g and rotor one failed

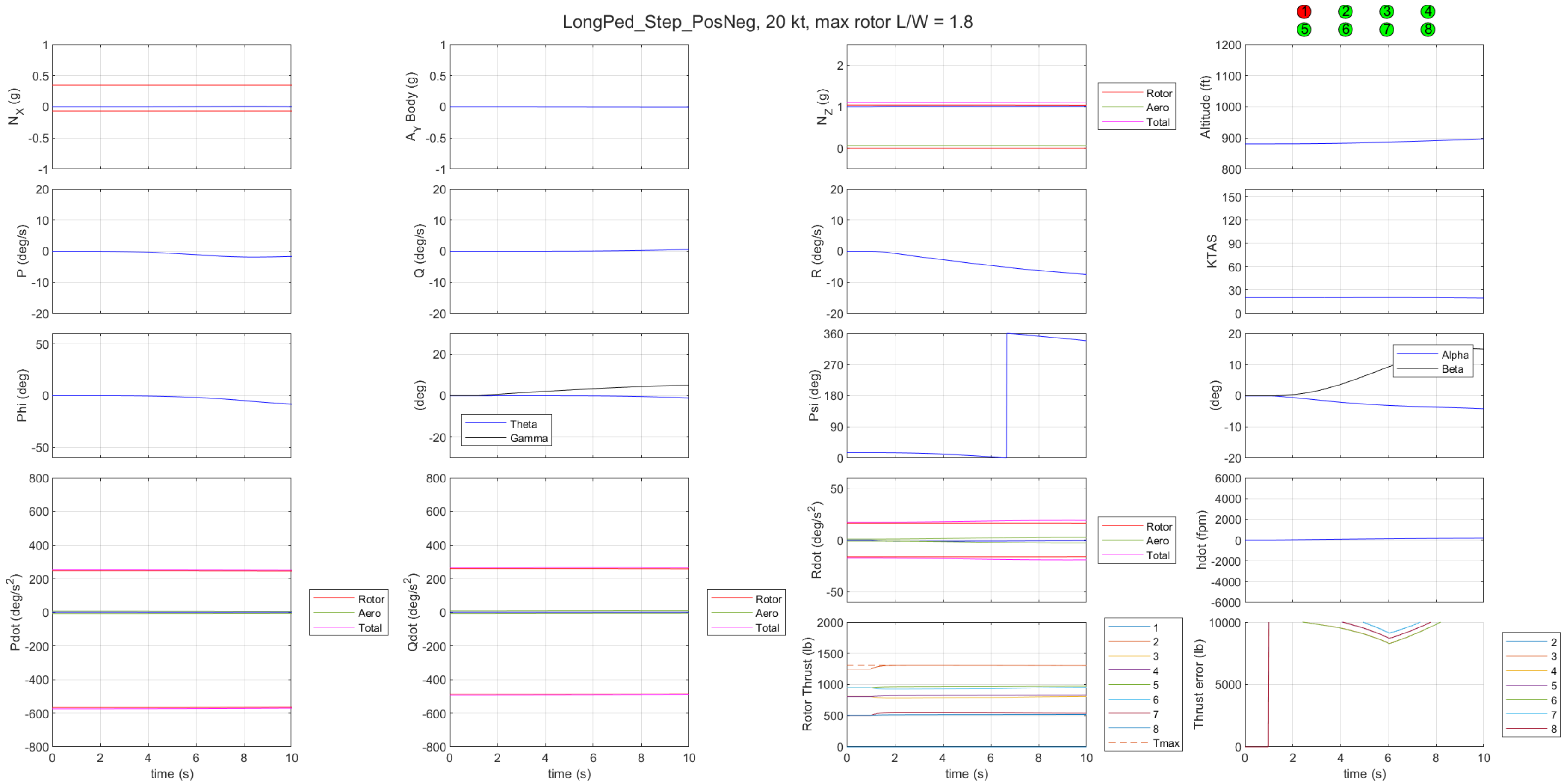

Figure A- 71. Max Pos. Long. and Neg. Ped. step trimmed at 20 KIAS with an L/Wmax = 1.8 g and rotor one failed

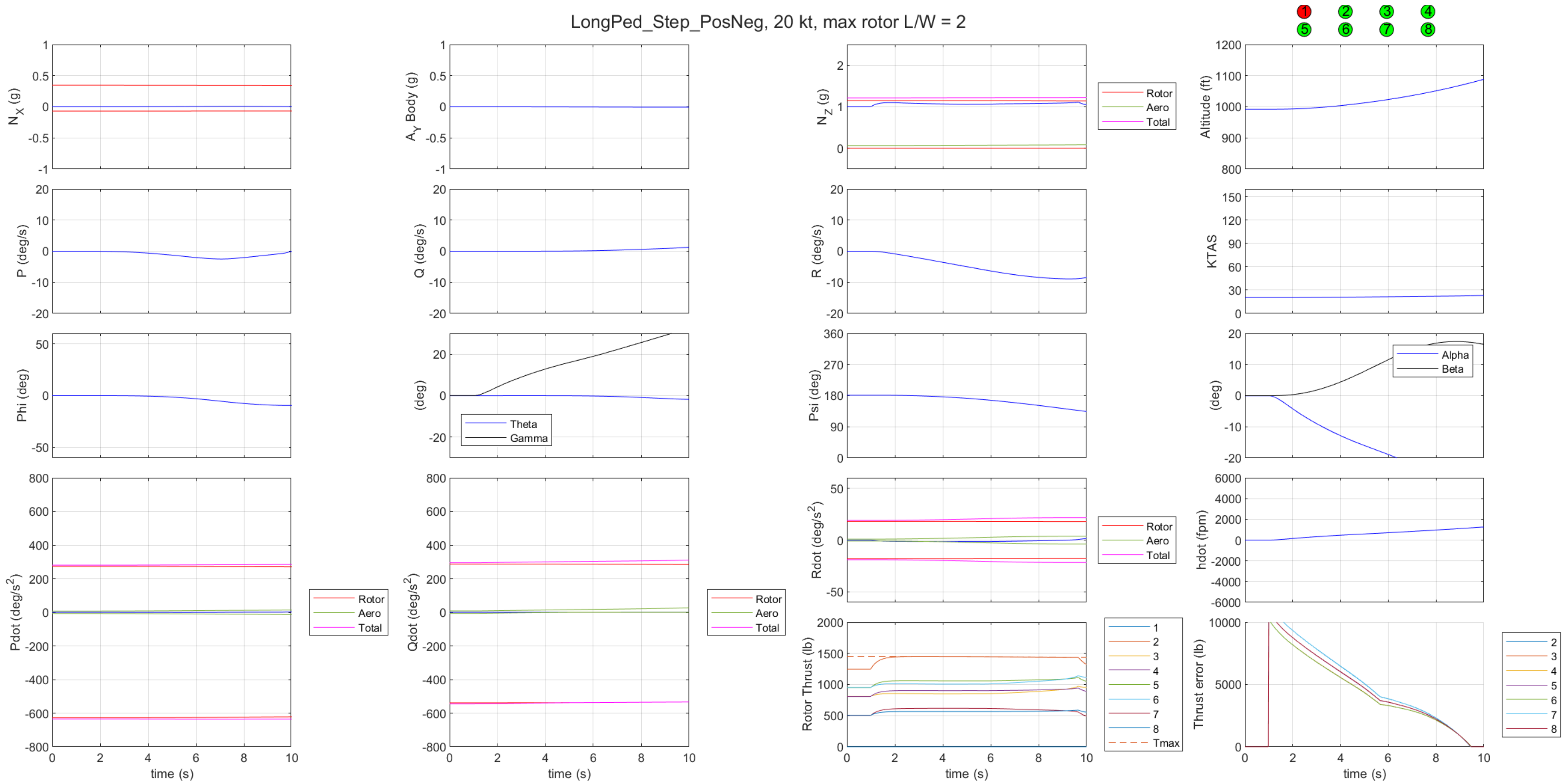

Figure A- 72. Max Pos. Long. and Neg. Ped. step trimmed at 20 KIAS with an L/Wmax = 2 g and rotor one failed

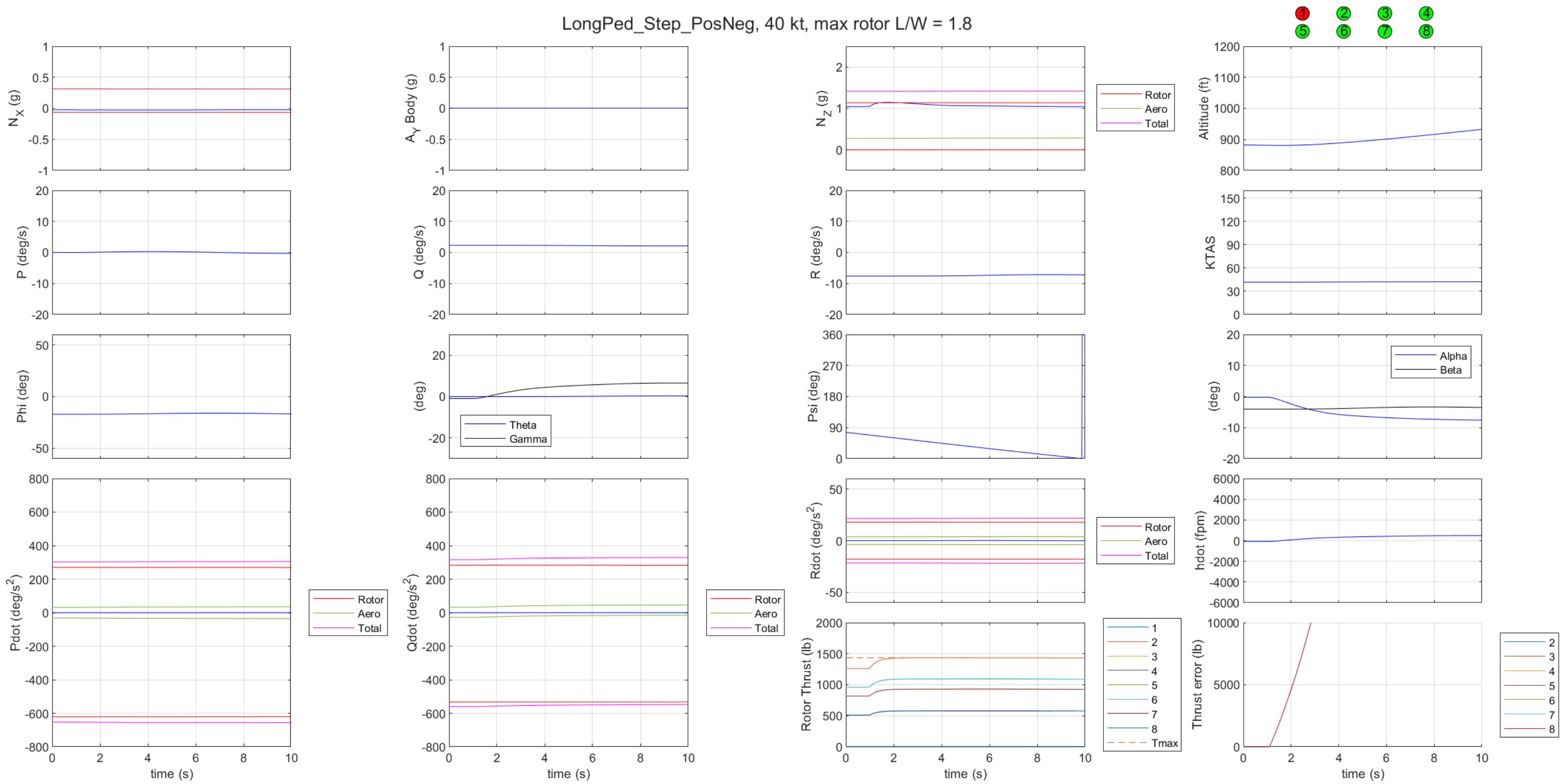

Figure A- 73. Max Pos. Long. and Neg. Ped. step trimmed at 40 KIAS with an L/Wmax = 1.8 g and rotor one failed

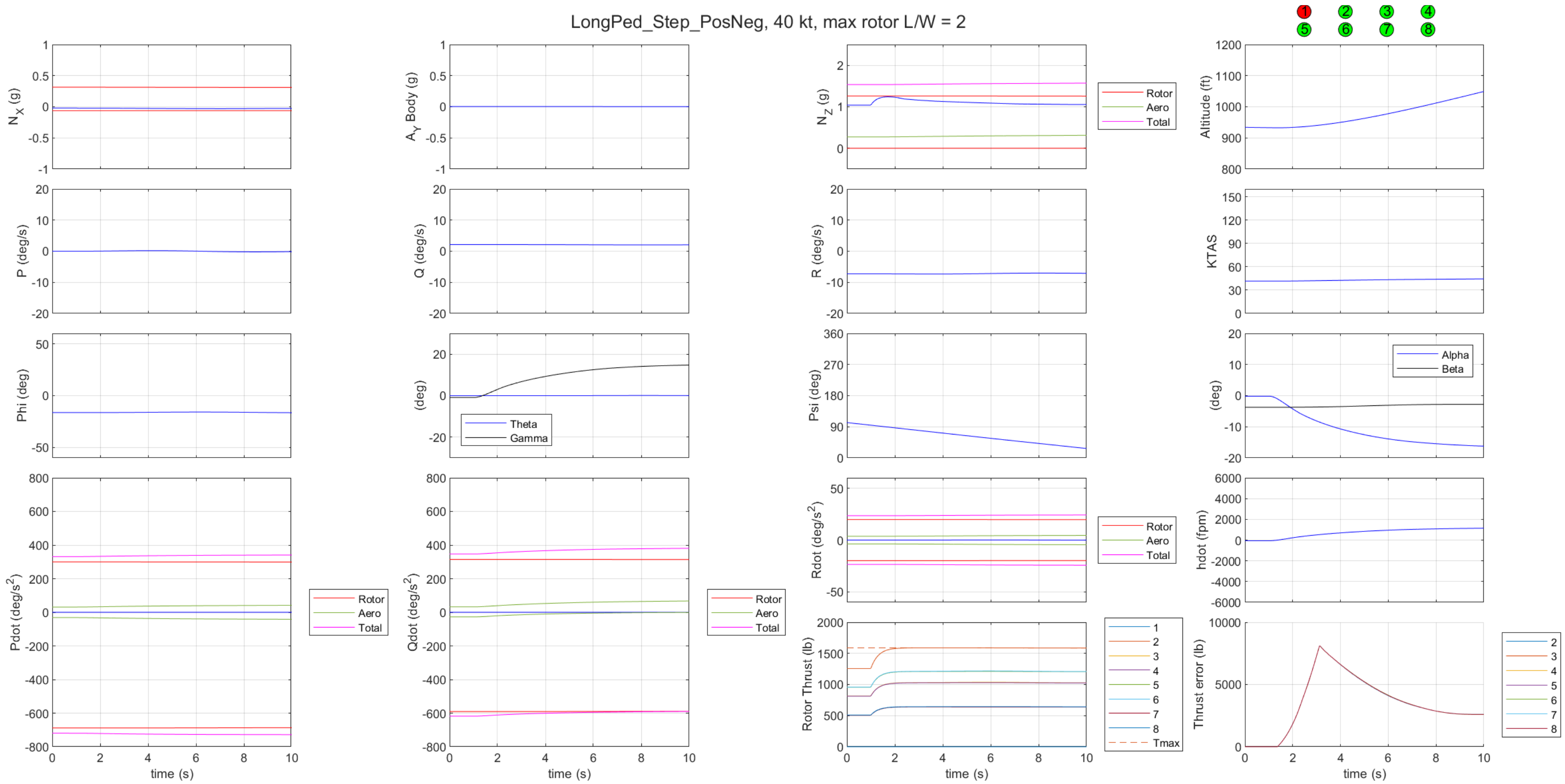

Figure A- 74. Max Pos. Long. and Neg. Ped. step trimmed at 40 KIAS with an L/Wmax = 2 g and rotor one failed

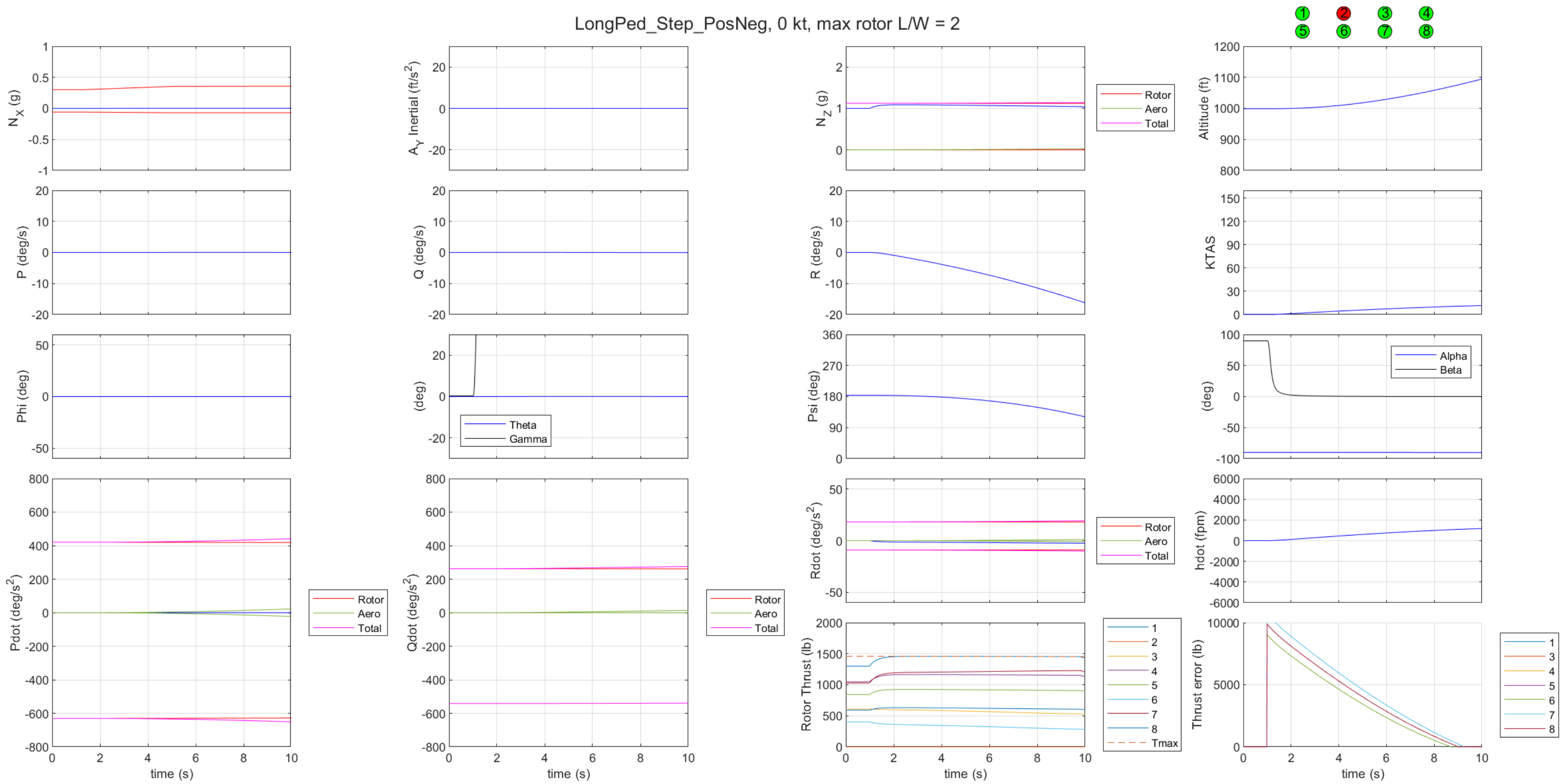

Figure A- 75. Max Pos. Long. and Neg. Ped. step trimmed at 0 KGS with an L/Wmax = 2 g and rotor two failed

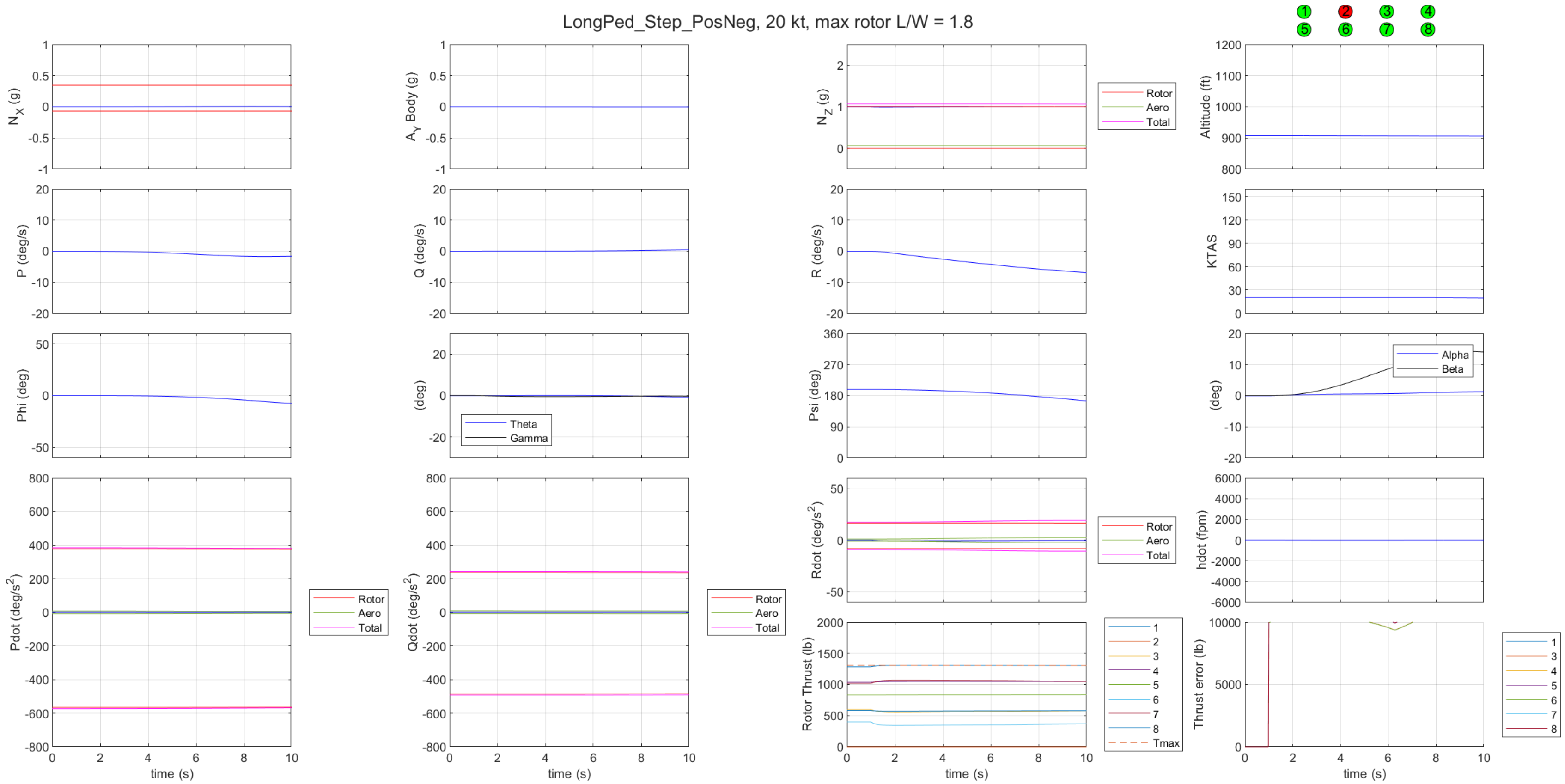

Figure A- 76. Max Pos. Long. and Neg. Ped. step trimmed at 20 KIAS with an L/Wmax = 1.8 g and rotor two failed

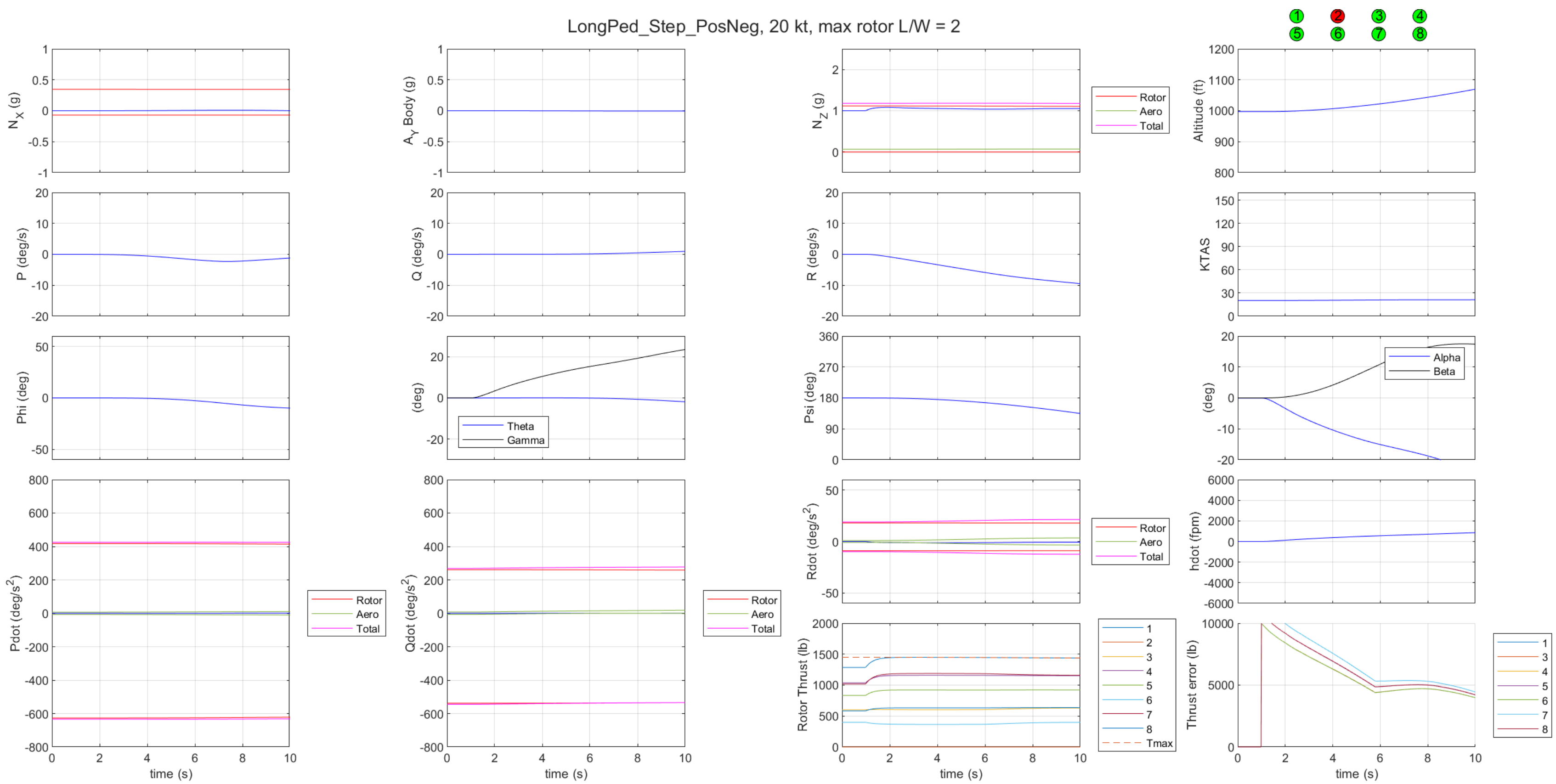

Figure A- 77. Max Pos. Long. and Neg. Ped. step trimmed at 20 KIAS with an L/Wmax = 2 g and rotor two failed

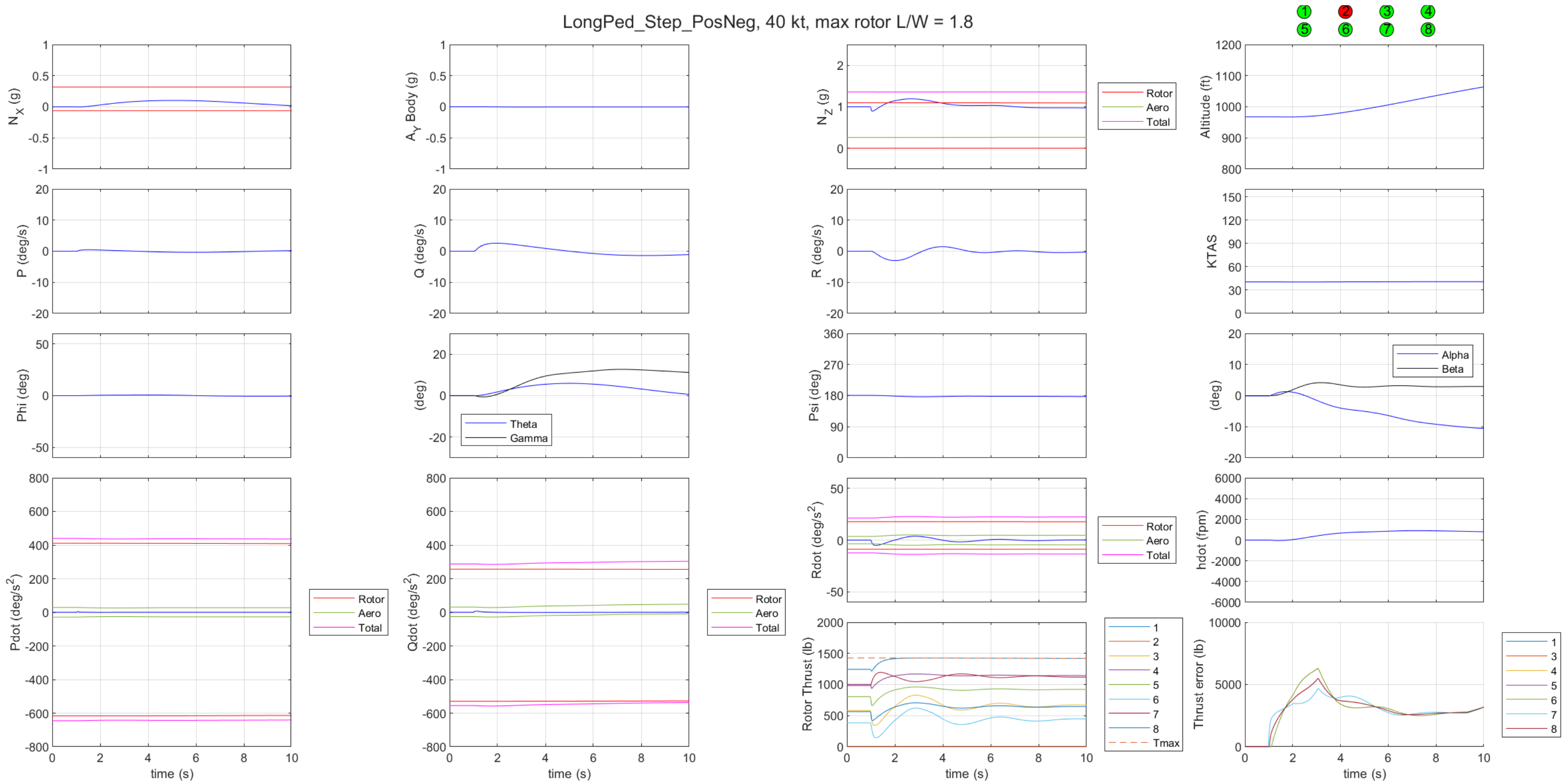

Figure A- 78. Max Pos. Long. and Neg. Ped. step trimmed at 40 KIAS with an L/Wmax = 1.8 g and rotor two failed

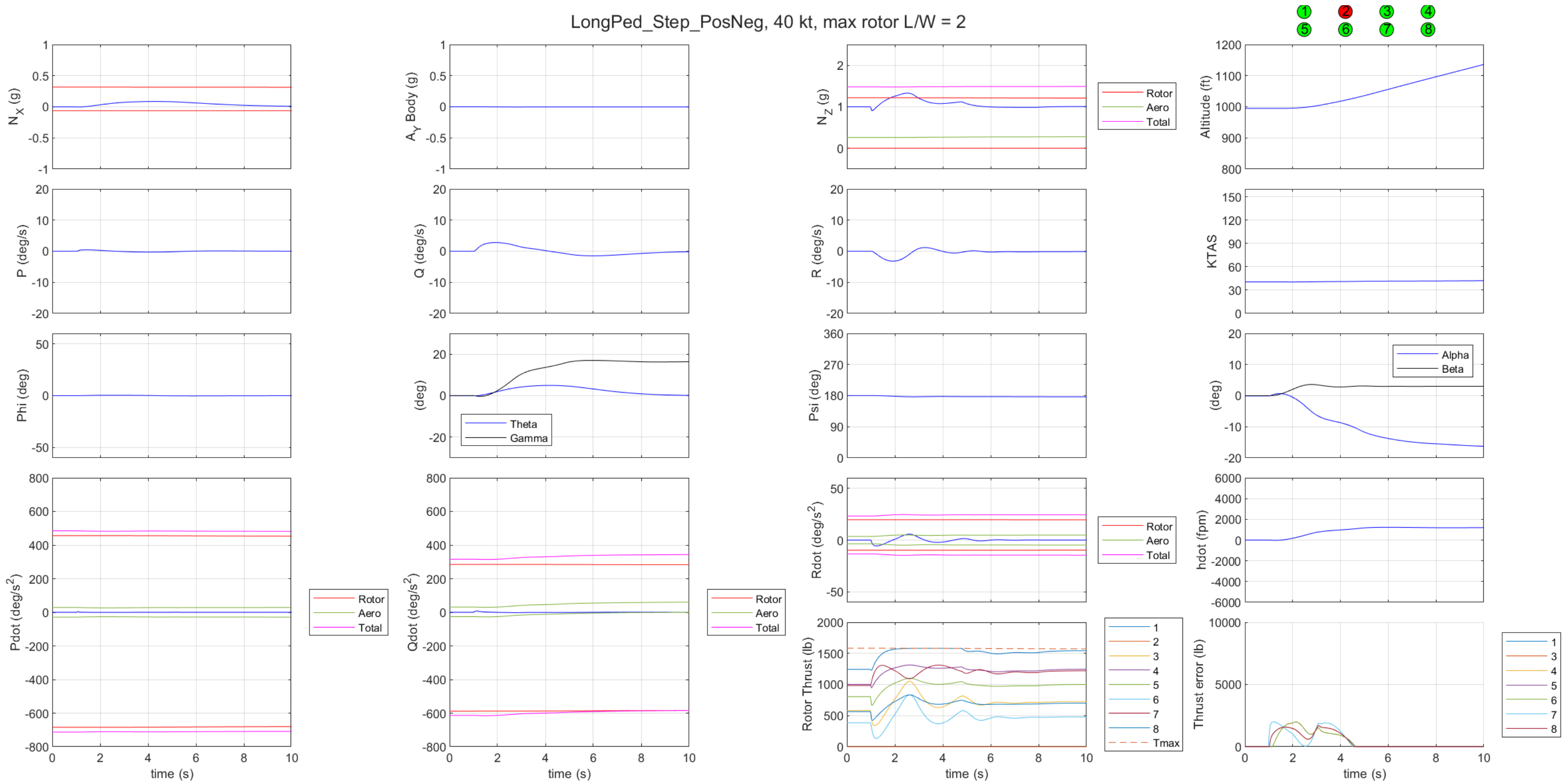

Figure A- 79. Max Pos. Long. and Neg. Ped. step trimmed at 40 KIAS with an L/Wmax = 2 g and rotor two failed

A.20 Maximum positive longitudinal and negative lateral step with rotor failures

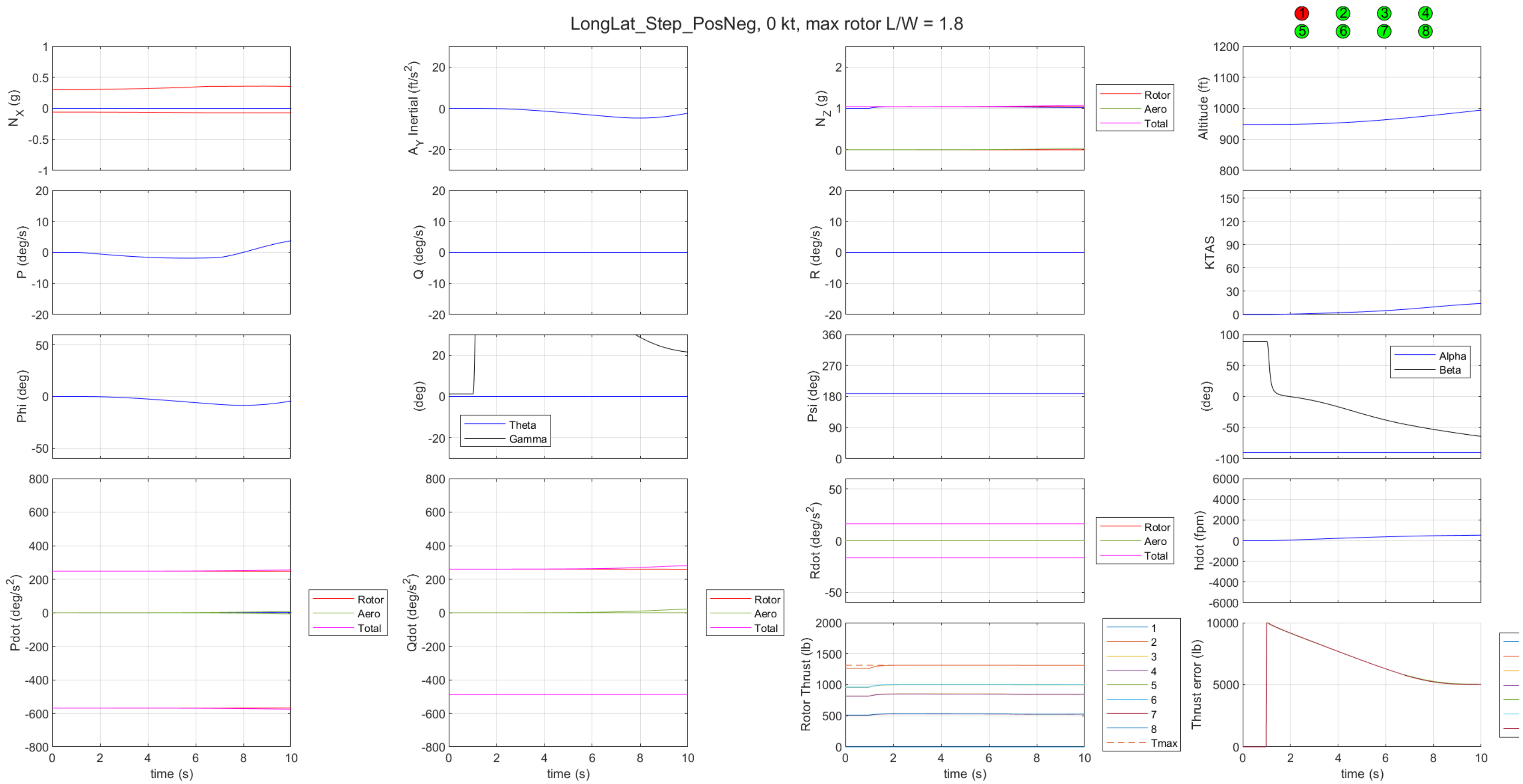

Figure A- 80. Max Pos. Long. and Neg. Lat. step trimmed at 0 KGS with an L/Wmax = 1.8 g and rotor one failed

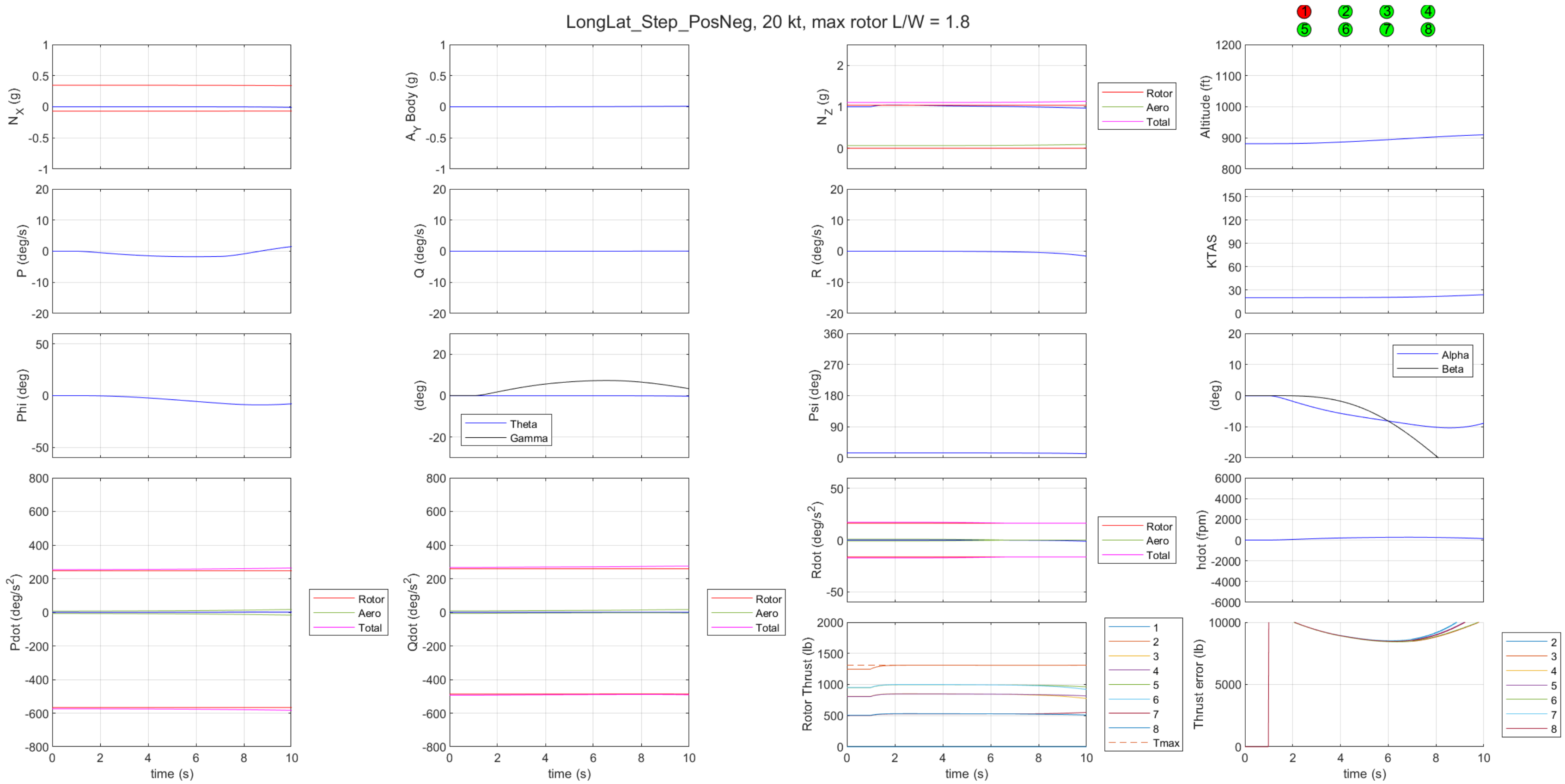

Figure A- 81. Max Pos. Long. and Neg. Lat. step trimmed at 20 KIAS with an L/Wmax = 1.8 g and rotor one failed

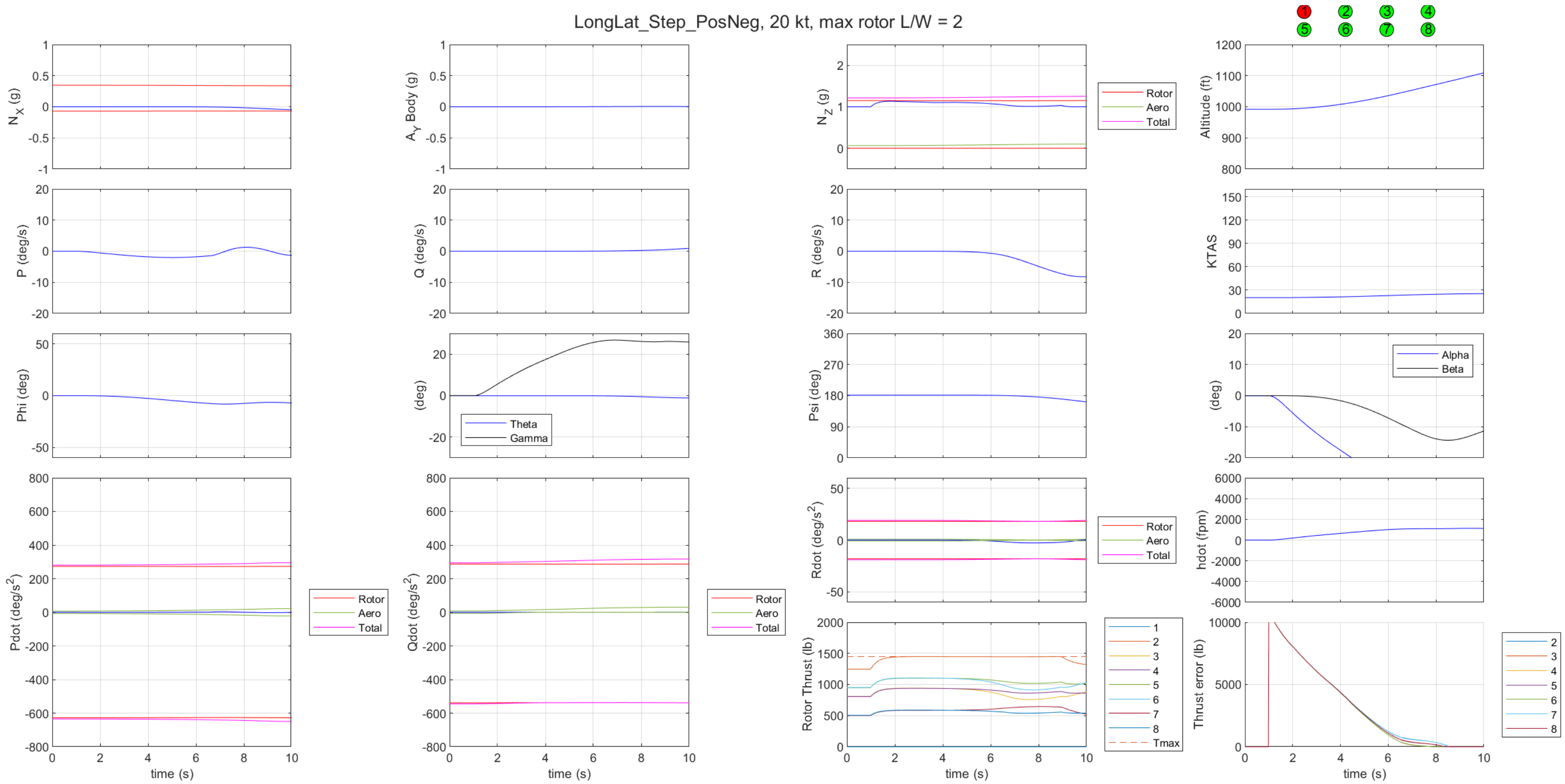

Figure A- 82. Max Pos. Long. and Neg. Lat. step trimmed at 20 KIAS with an L/Wmax = 2 g and rotor one failed

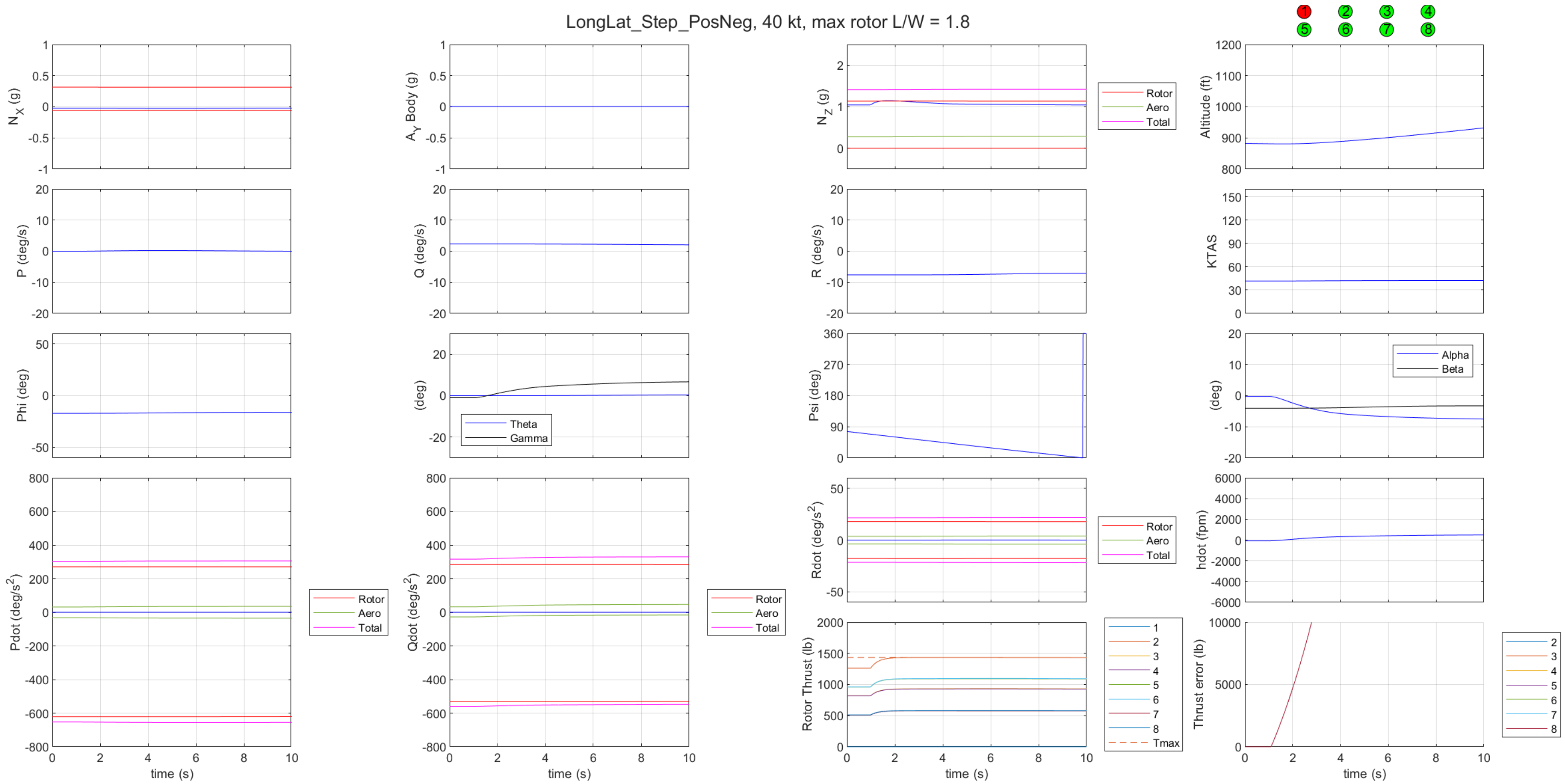

Figure A- 83. Max Pos. Long. and Neg. Lat. step trimmed at 40 KIAS with an L/Wmax = 1.8 g and rotor one failed

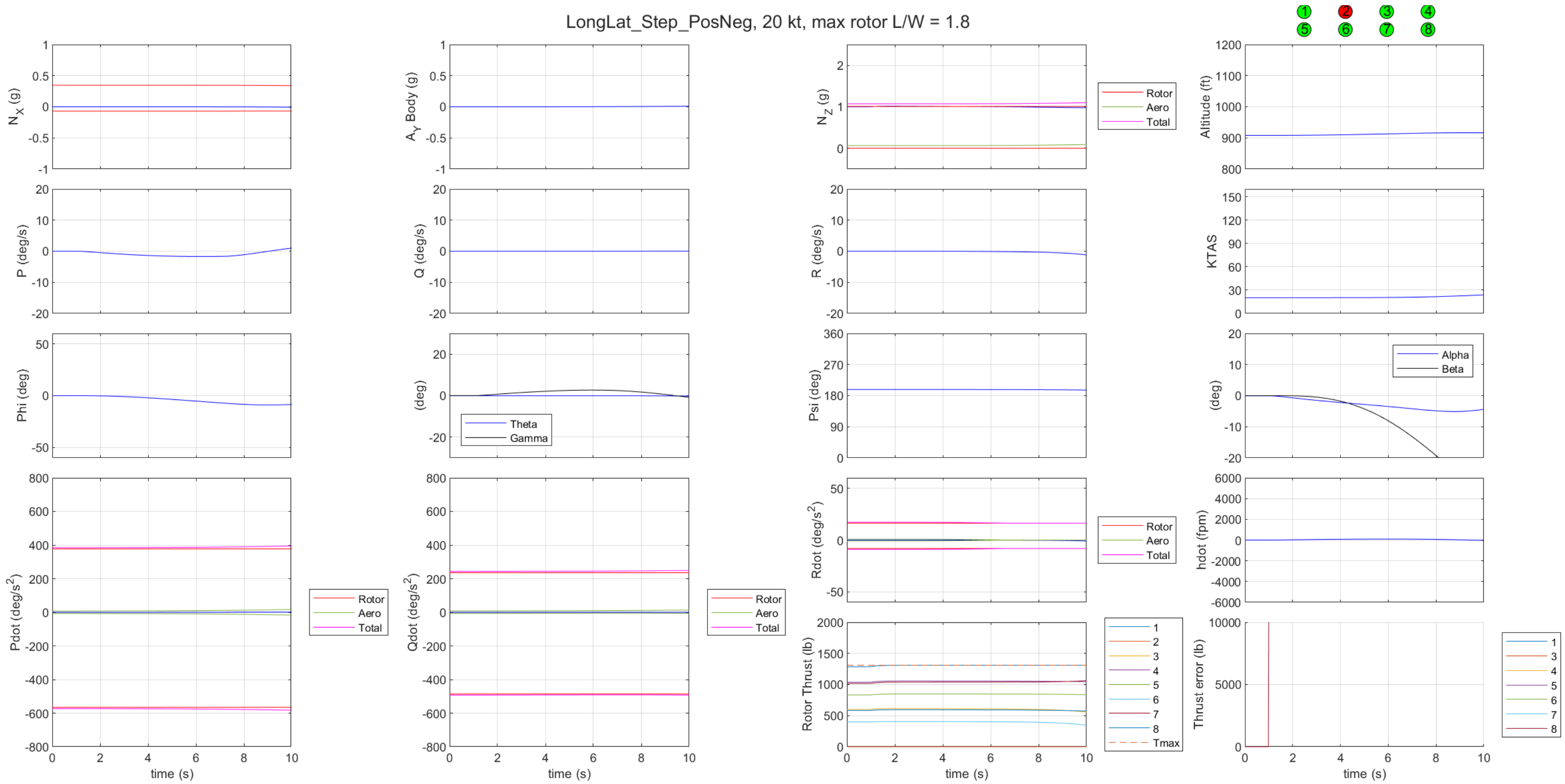

Figure A- 84. Max Pos. Long. and Neg. Lat. step trimmed at 20 KIAS with an L/Wmax = 1.8 g and rotor tow failed

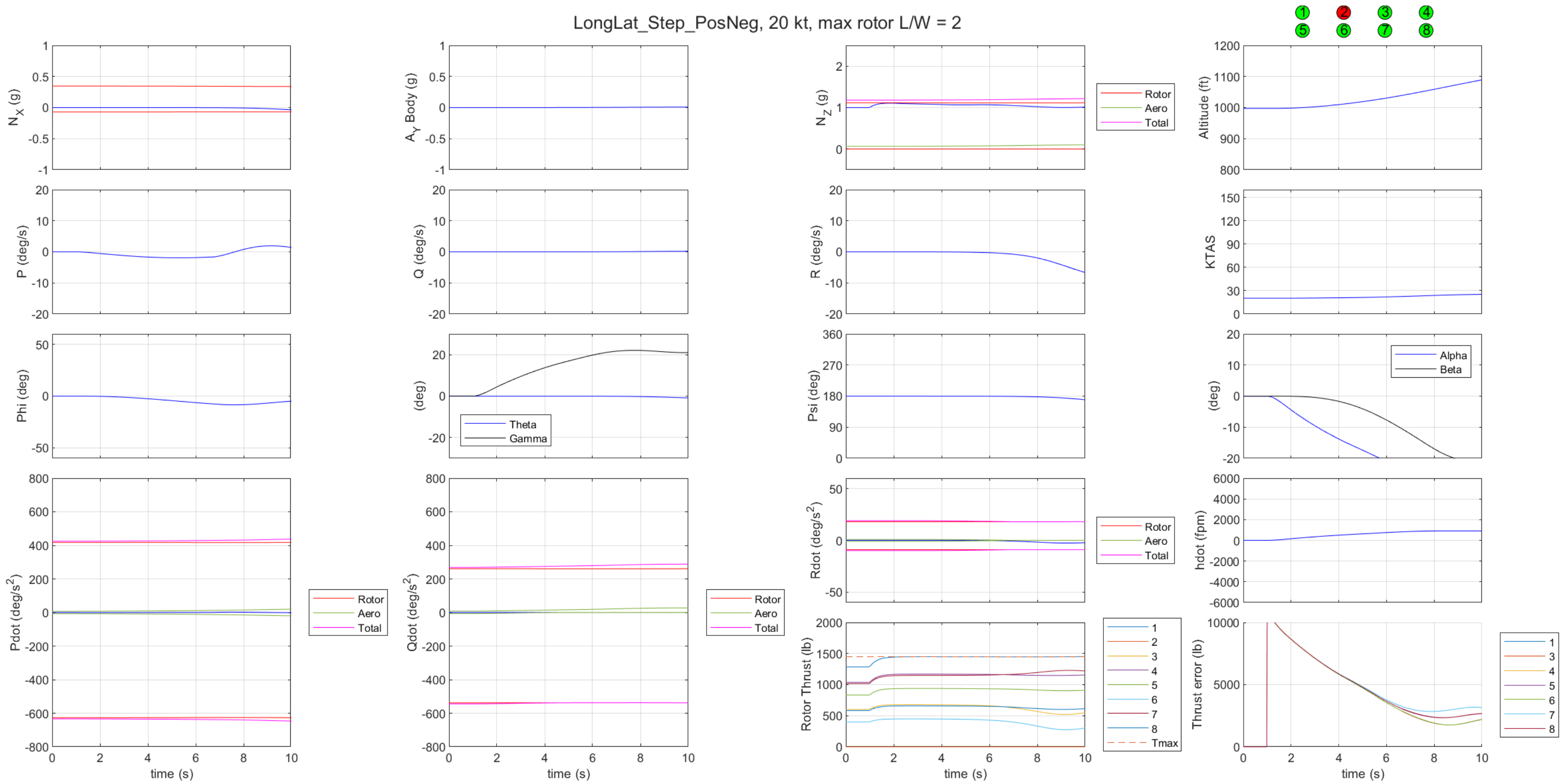

Figure A- 85. Max Pos. Long. and Neg. Lat. step trimmed at 20 KIAS with an L/Wmax = 2 g and rotor two failed

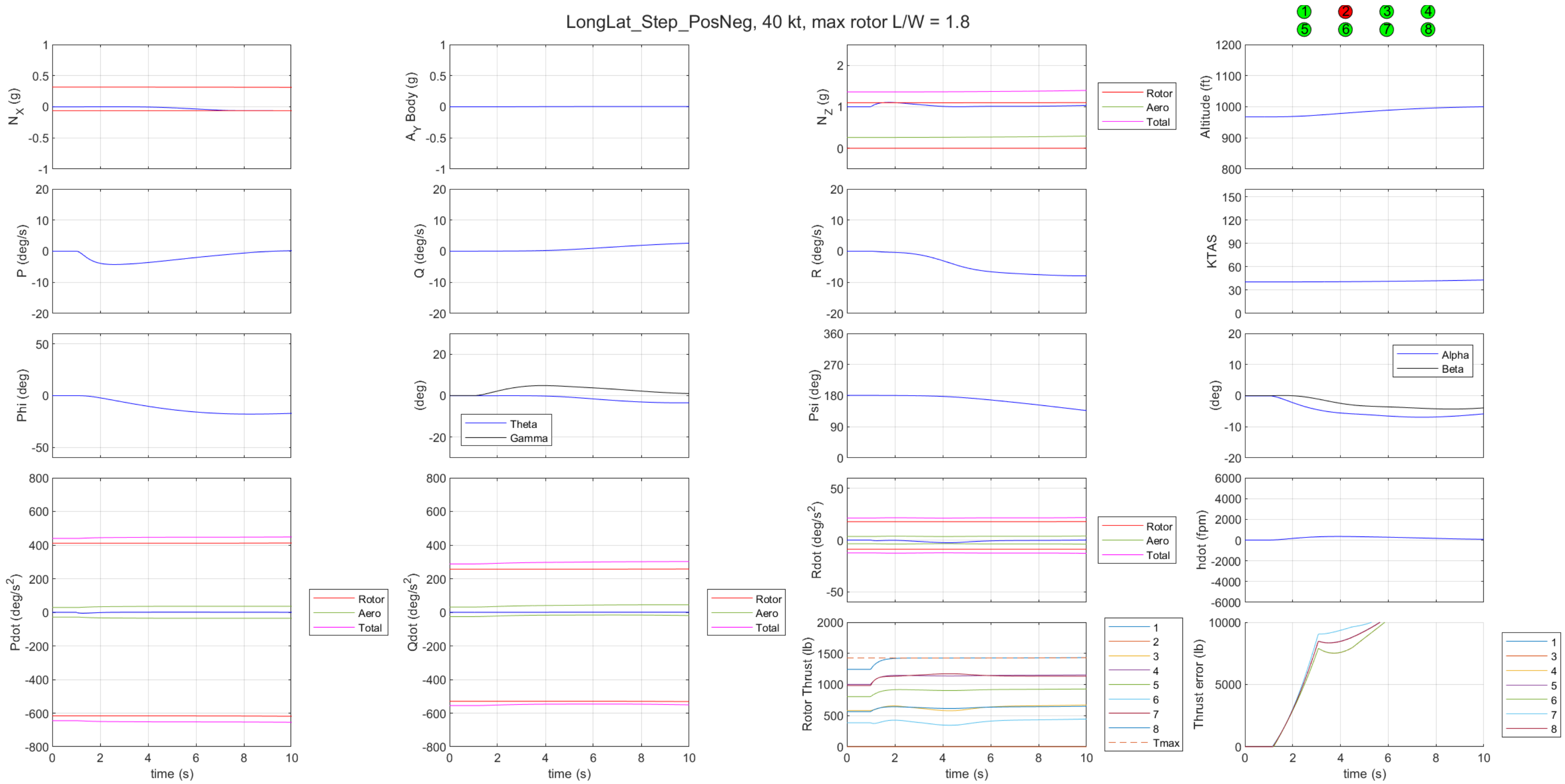

Figure A- 86. Max Pos. Long. and Neg. Lat. step trimmed at 40 KIAS with an L/Wmax = 1.8 g and rotor two failed

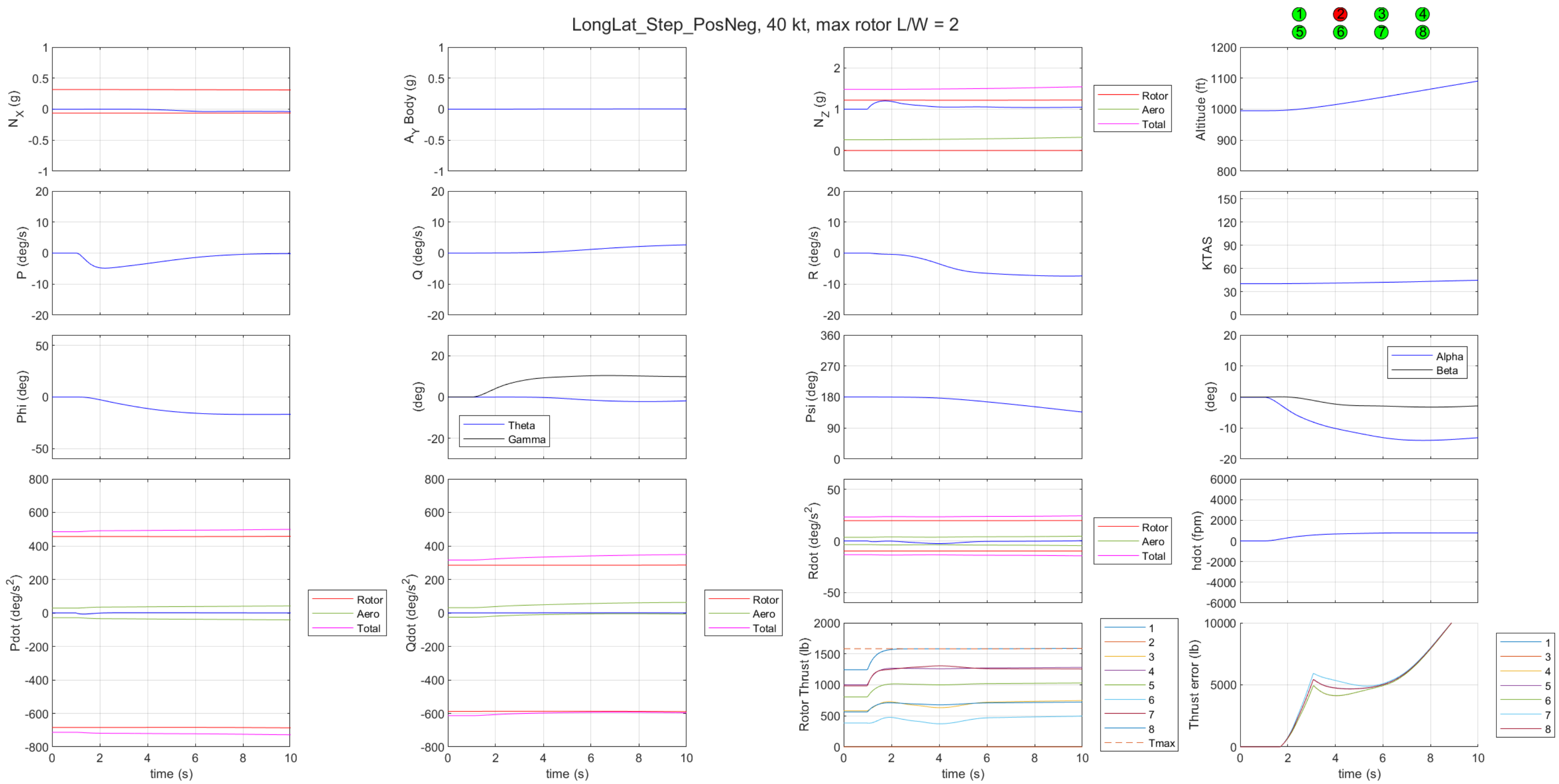

Figure A- 87. Max Pos. Long. and Neg. Lat. step trimmed at 40 KIAS with an L/Wmax = 2 g and rotor two failed

A.21 Maximum negative lateral and negative pedal step with rotor failures

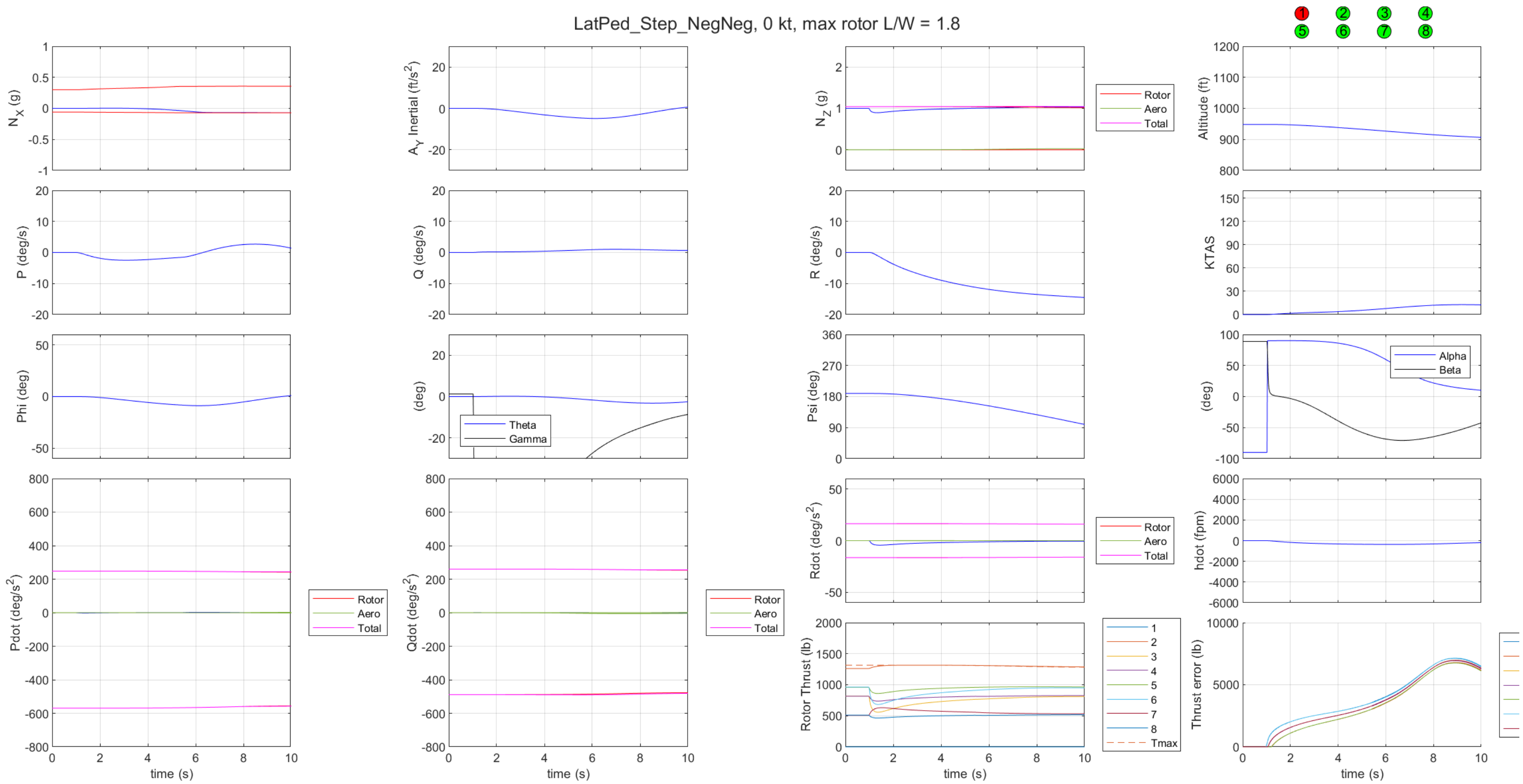

Figure A- 88. Max Neg. Lat. and Neg. Ped. step trimmed at 0 KGS with an L/Wmax = 1.8 g and rotor one failed

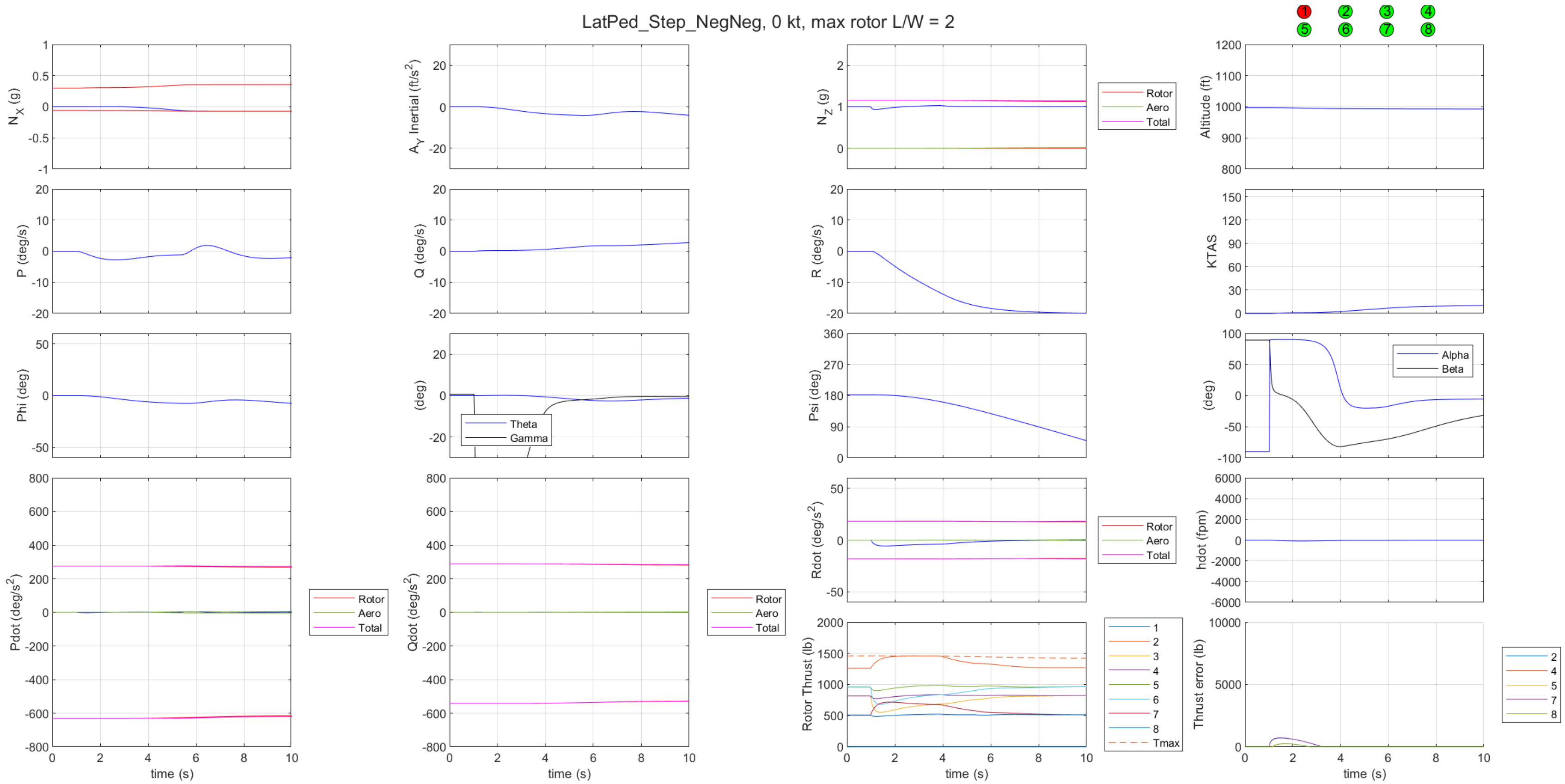

Figure A- 89. Max Neg. Lat. and Neg. Ped. step trimmed at 0 KGS with an L/Wmax = 2 g and rotor one failed

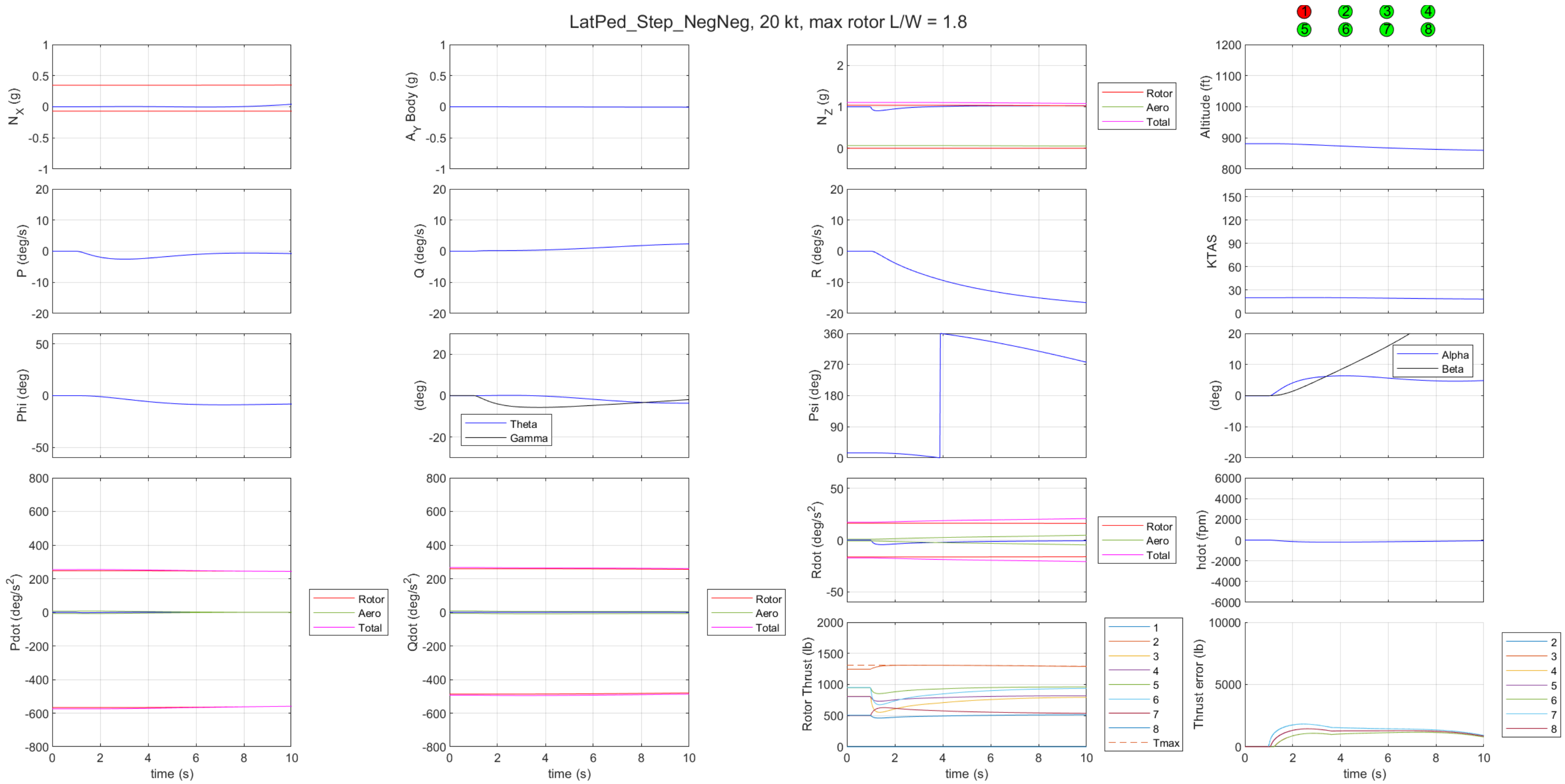

Figure A- 90. Max Neg. Lat. and Neg. Ped. step trimmed at 20 KIAS with an L/Wmax = 1.8 g and rotor one failed

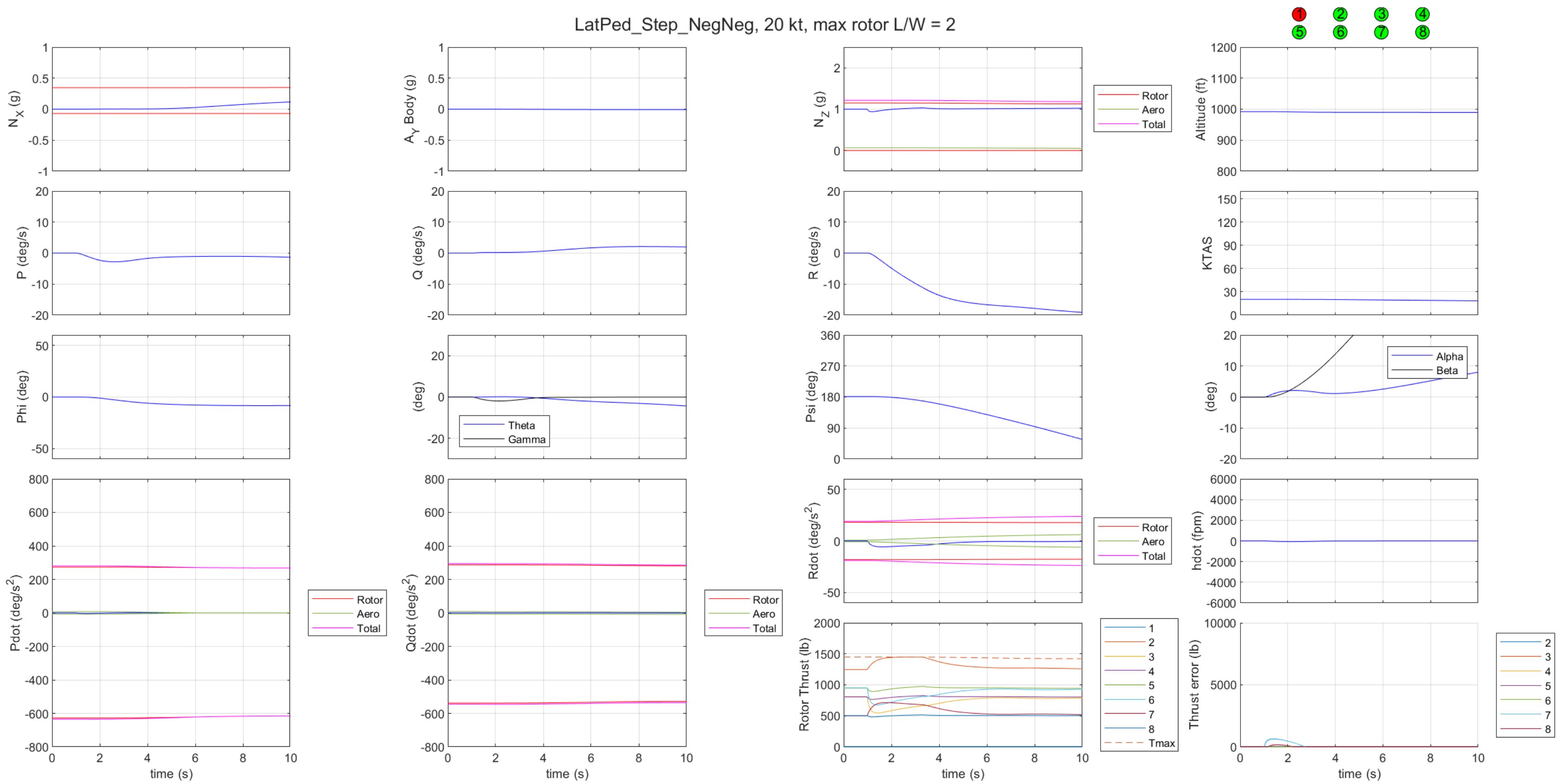

Figure A- 91. Max Neg. Lat. and Neg. Ped. step trimmed at 20 KIAS with an L/Wmax = 2 g and rotor one failed

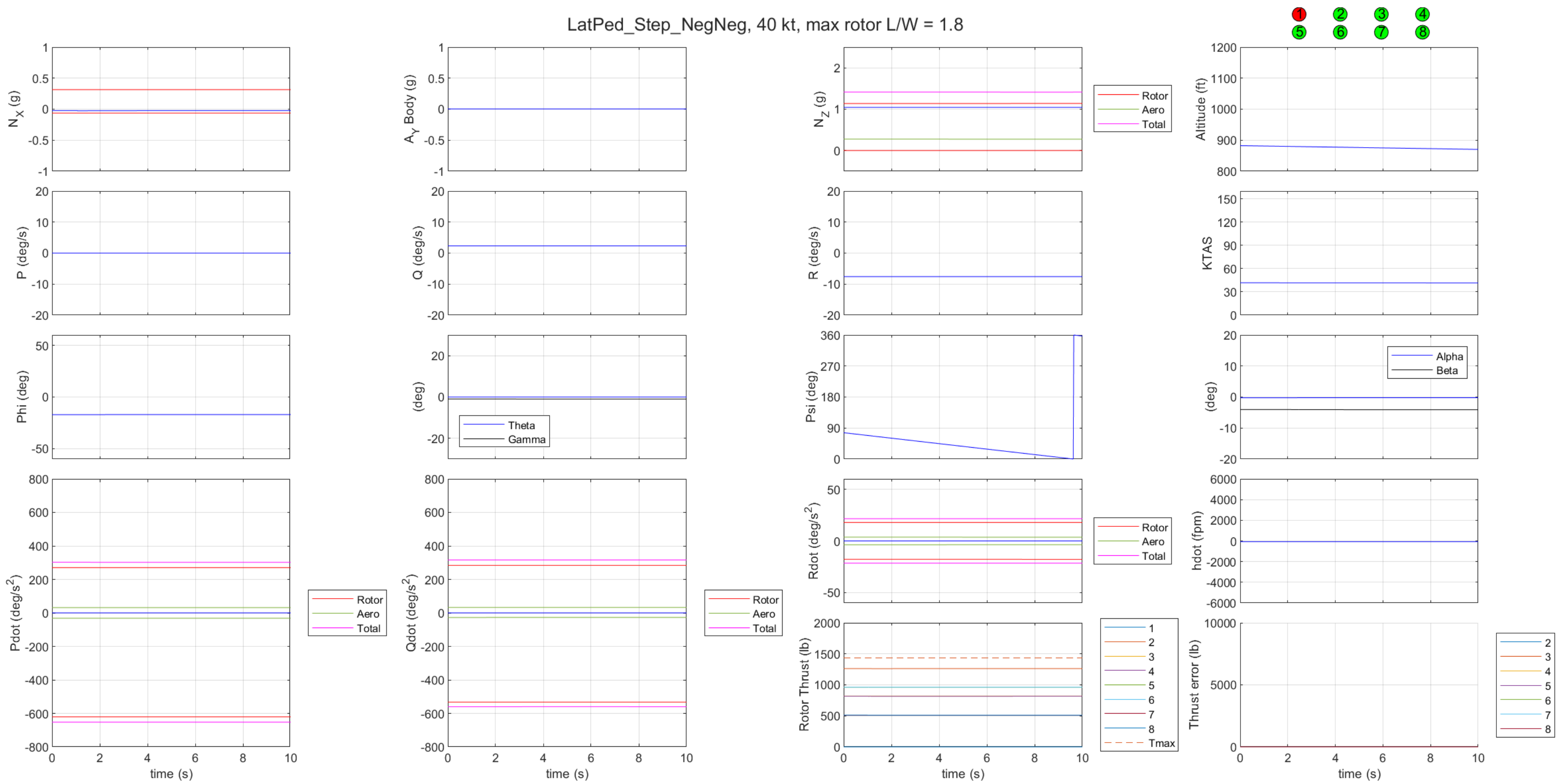

Figure A- 92. Max Neg. Lat. and Neg. Ped. step trimmed at 40 KIAS with an L/Wmax = 1.8 g and rotor one failed

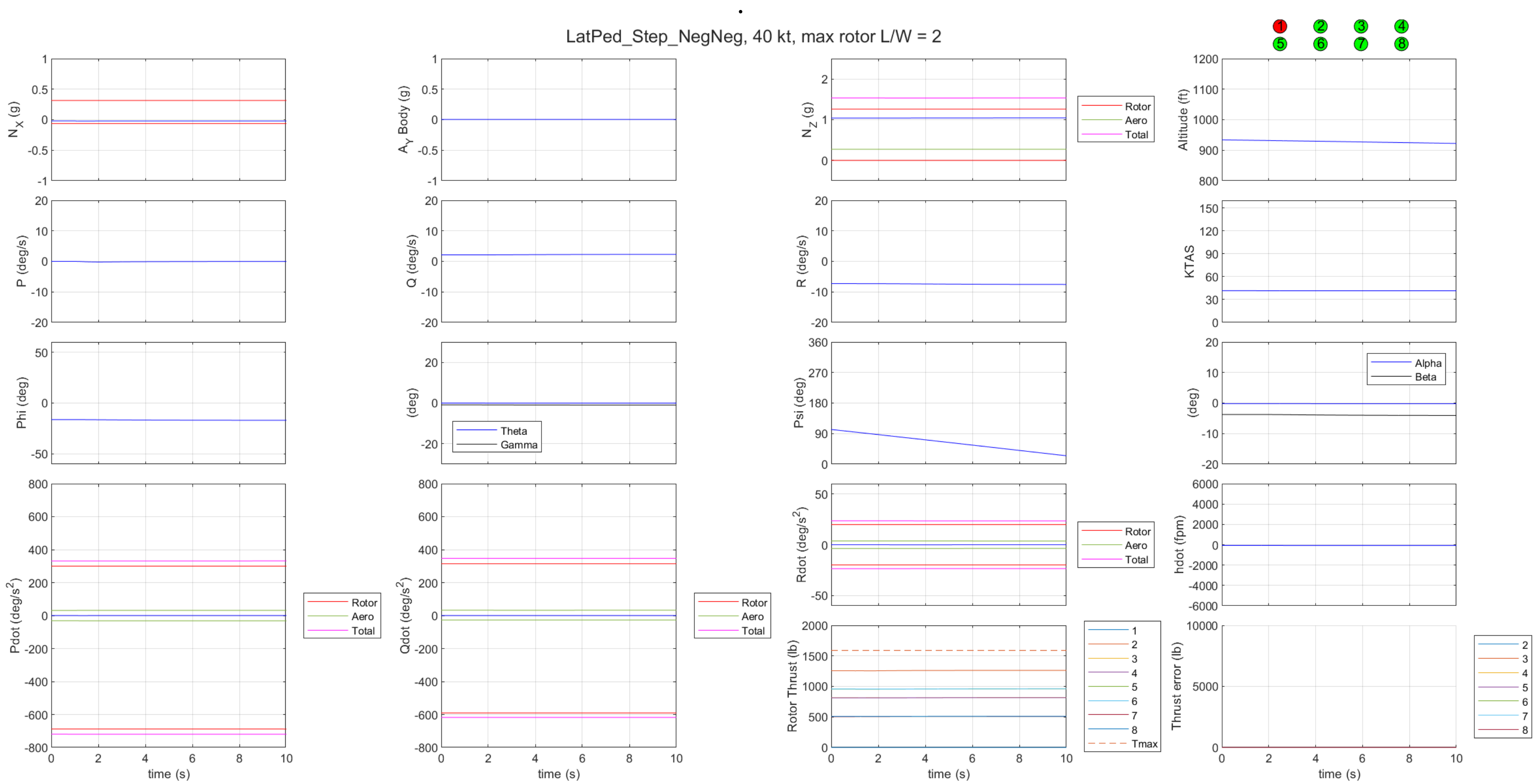

Figure A- 93. Max Neg. Lat. and Neg. Ped. step trimmed at 40 KIAS with an L/Wmax = 2 g and rotor one failed

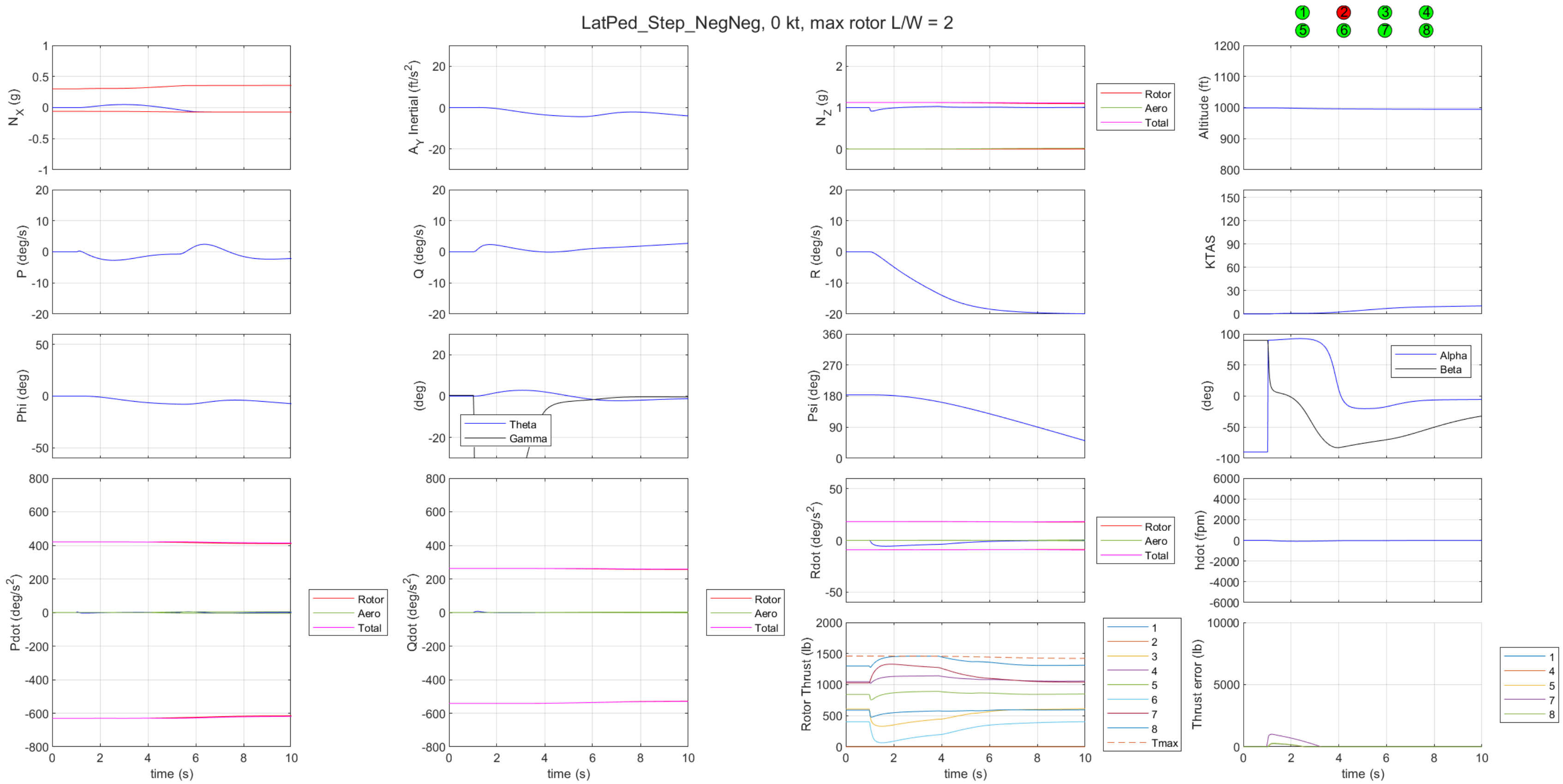

Figure A- 94. Max Neg. Lat. and Neg. Ped. step trimmed at 0 KGS with an L/Wmax = 2 g and rotor two failed

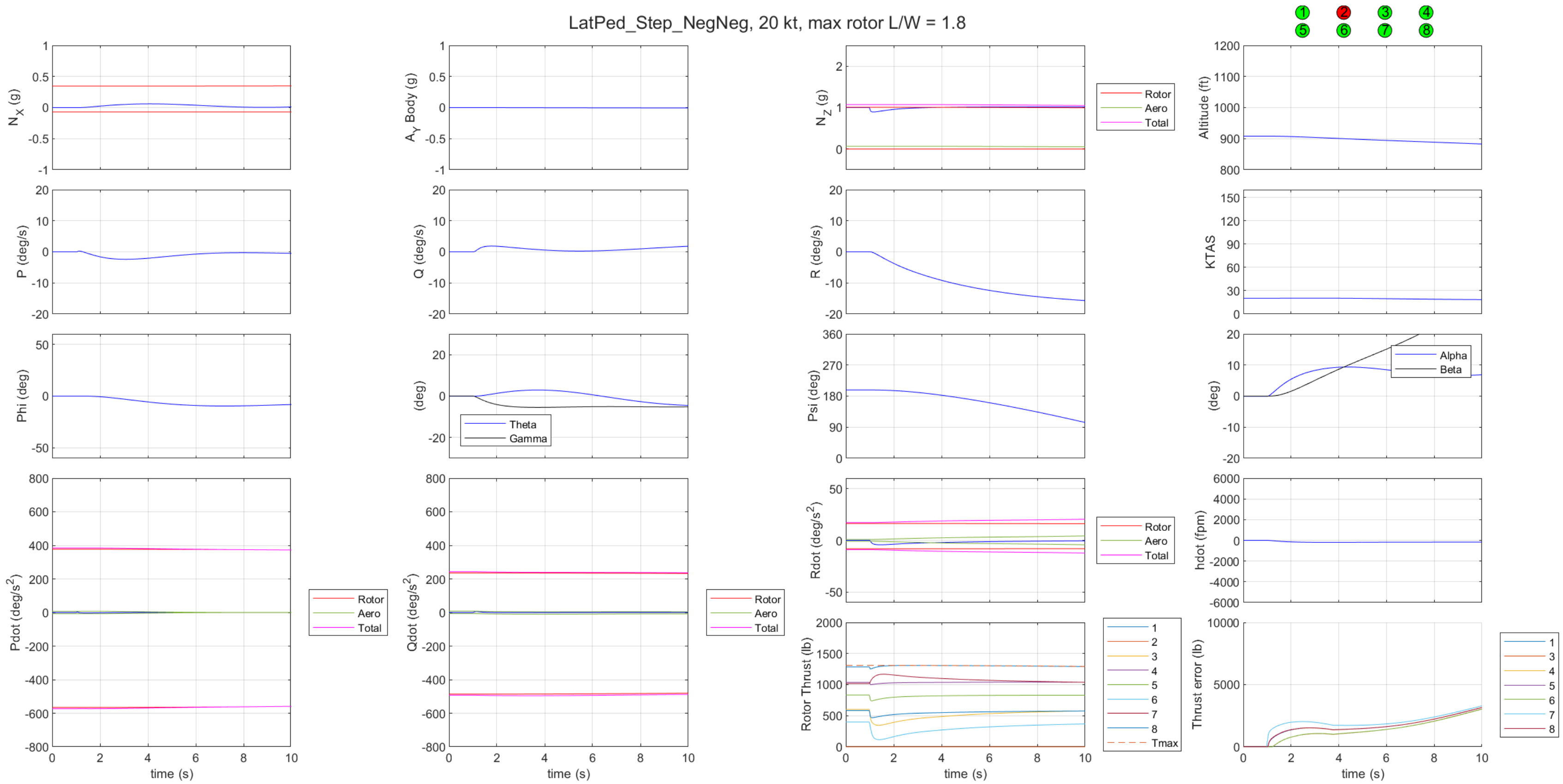

Figure A- 95. Max Neg. Lat. and Neg. Ped. step trimmed at 20 KIAS with an L/Wmax = 1.8 g and rotor two failed

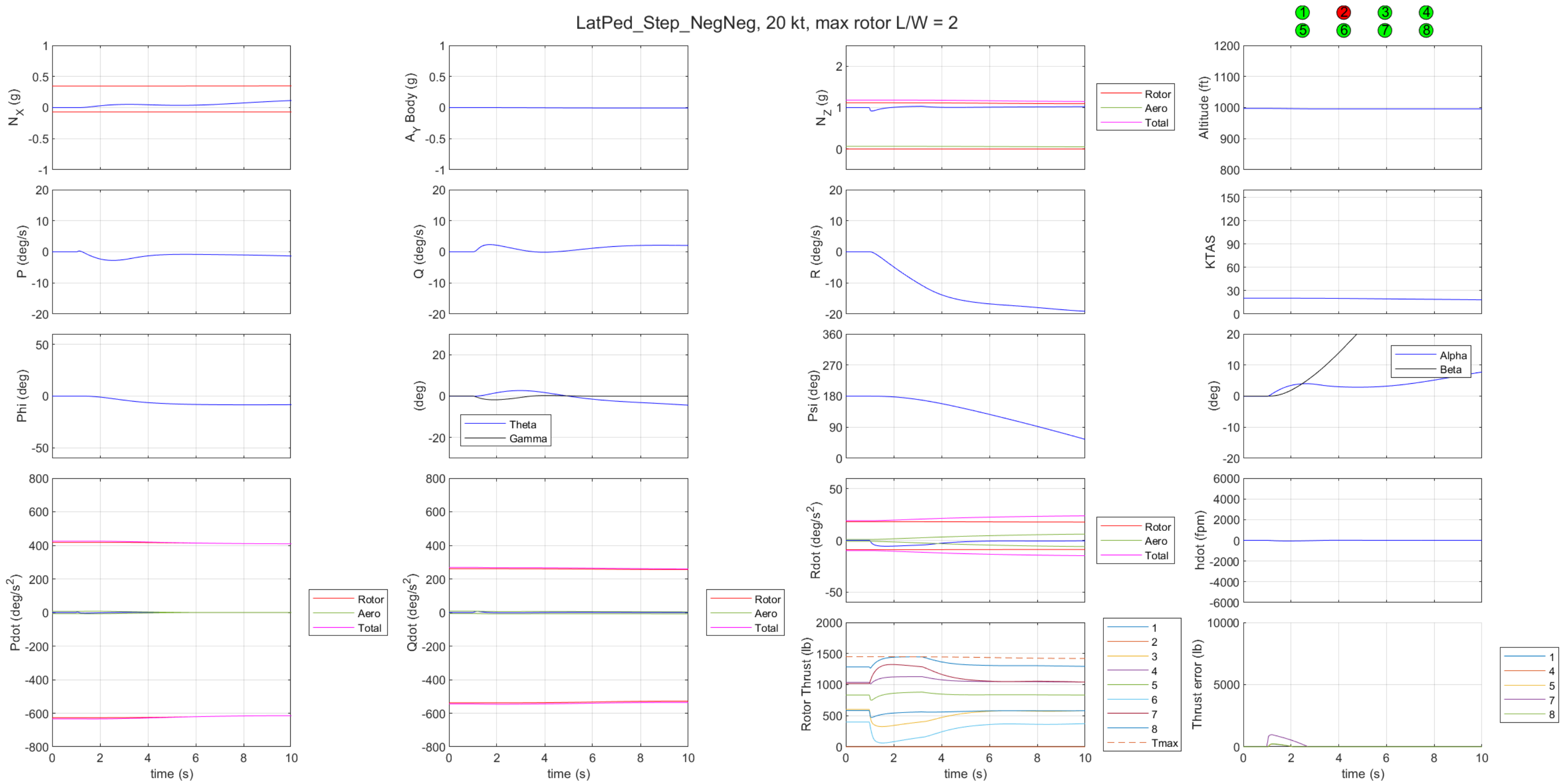

Figure A- 96. Max Neg. Lat. and Neg. Ped. step trimmed at 20 KIAS with an L/Wmax = 2 g and rotor two failed

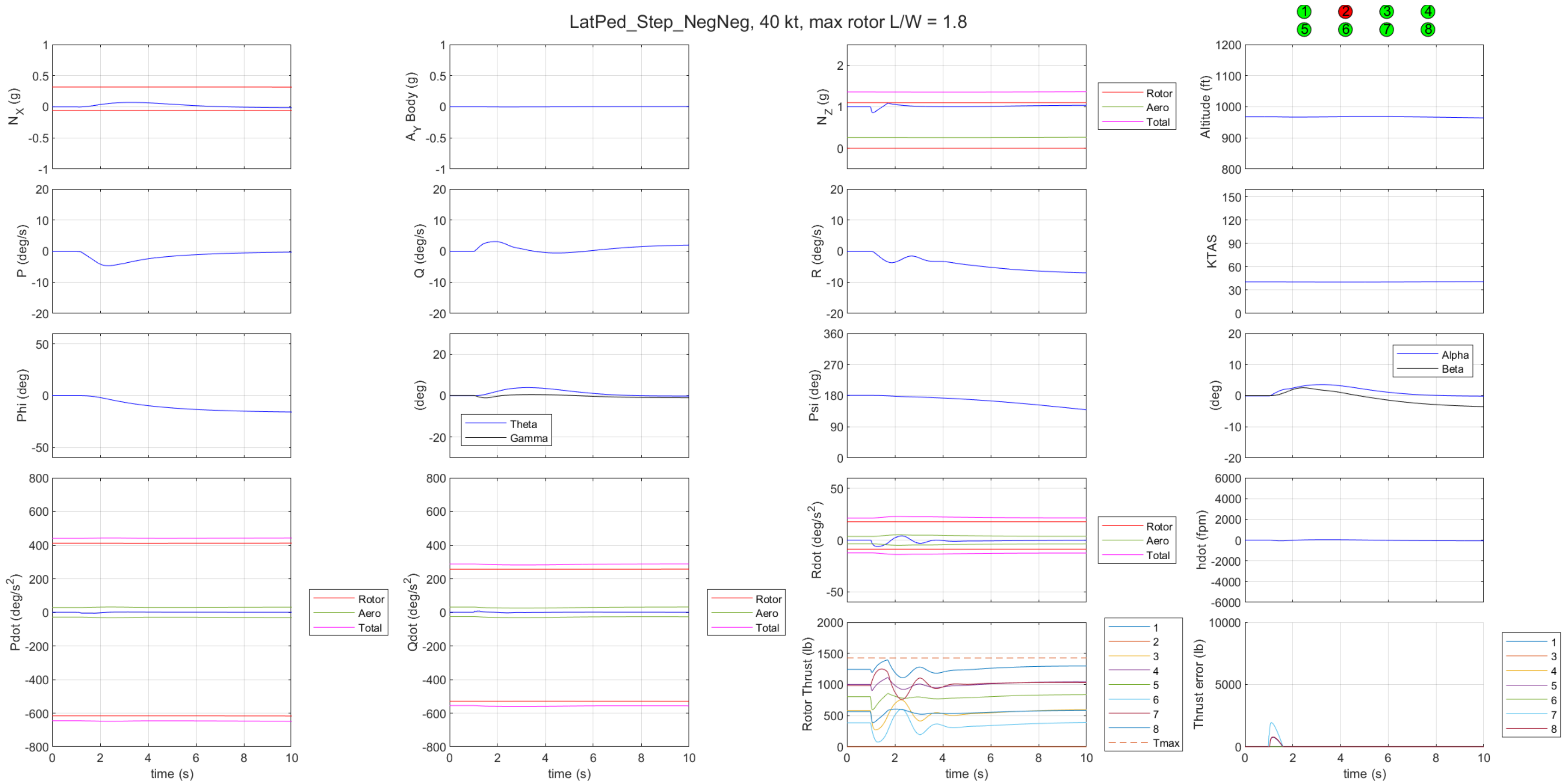

Figure A- 97. Max Neg. Lat. and Neg. Ped. step trimmed at 40 KIAS with an L/Wmax = 1.8 g and rotor two failed

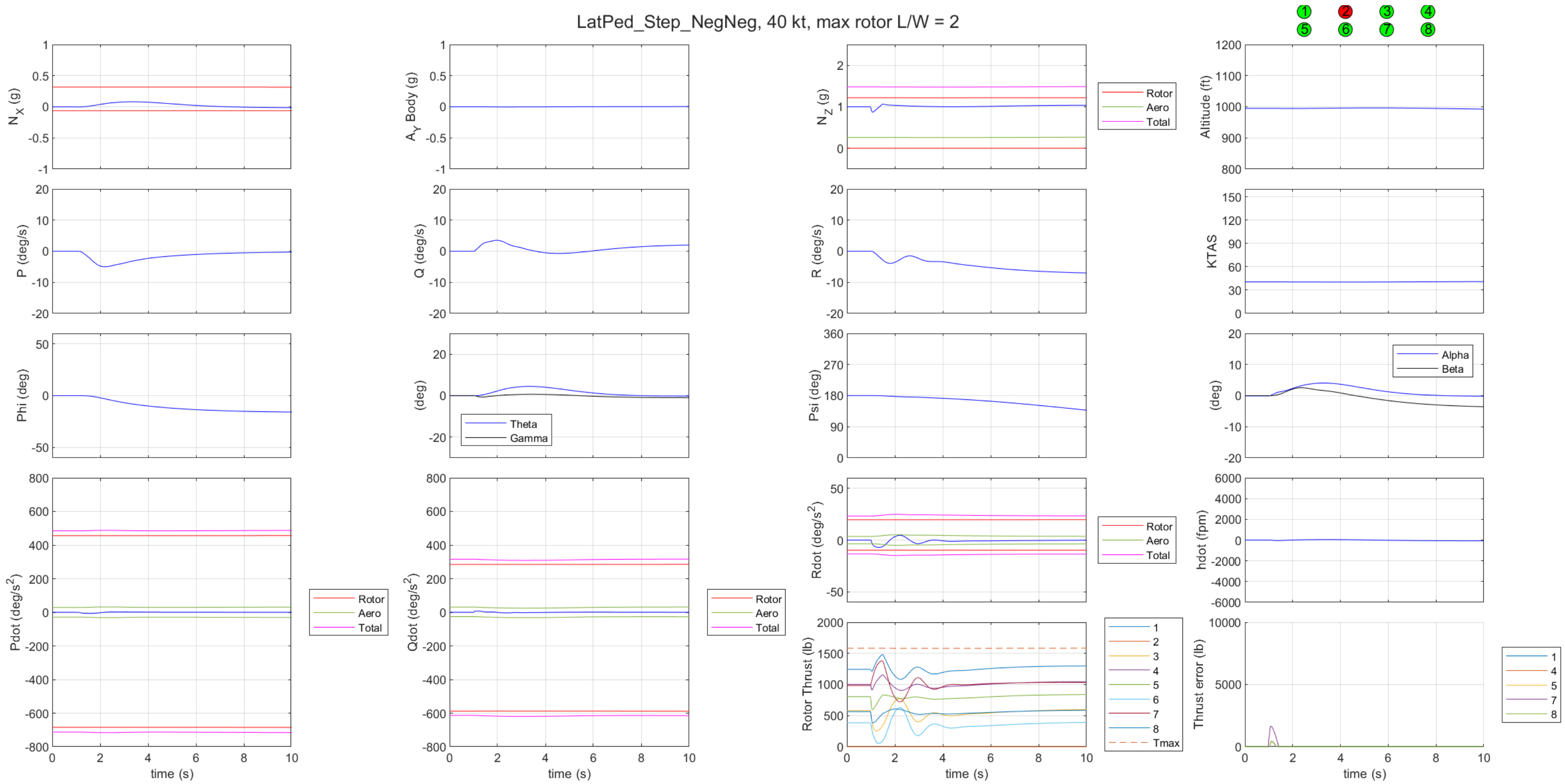

Figure A- 98. Max Neg. Lat. and Neg. Ped. step trimmed at 40 KIAS with an L/Wmax = 2 g and rotor two failed

B Results tables

The tables shown in this appendix are the remaining results tables not discussed in the results section either because they did not show severe control power limiting or were like results that were already discussed.

Table B- 1. Half pos. long. step results

Pilot Input	Trim Speed (kt)	Max Rotor L/W	Response Duration (s)	Primary Axis Rotor CP Status	Secondary Axis Rotor CP Status	Primary Axis Total CP Status	Secondary Axis Total CP Status
Long. Pos. Half Step	0	1.2	2.48	0.20	0.20	0.20	0.20
		1.4	1.94				
		1.6	1.78				
		1.8	1.76				
		2	1.70				
	20	1.2	2.92	0.20	0.20		
		1.4	2.06				
		1.6	1.84				
		1.8	1.72				
		2	1.68				
	40	1.2	1.16	0.40	0.40		
		1.4	1.16				
		1.6	1.16				
		1.8	1.16				
		2	1.16				
	60	1.2	1.46				
		1.4	1.06				
		1.6	1.06				
		1.8	1.06				
		2	1.06				
	80	1.2	1.36				
		1.4	1.36				
		1.6	1.36				
		1.8	1.36				
		2	1.36				

Completely Limited

Significantly Limited

Never Limited

L

Table B- 2. Max neg. long. step results

Pilot Input	Trim Speed (kt)	Max Rotor L/W	Response Duration (s)	Primary Axis Rotor CP Status	Secondary Axis Rotor CP Status	Primary Axis Total CP Status	Secondary Axis Total CP Status
Long. Neg. Step	0	1.2	2.30				
		1.4	2.30				
		1.6	2.30				
		1.8	2.30				
		2	2.30				
	20	1.2	2.12				
		1.4	2.12				
		1.6	2.12				
		1.8	2.12				
		2	2.12				
	40	1.2	0.92				
		1.4	0.92				
		1.6	0.92				
		1.8	0.92				
		2	0.92				
	60	1.2	0.84				
		1.4	0.84				
		1.6	0.84				
		1.8	0.84				
		2	0.84				
	80	1.2	0.78				
		1.4	0.78				
		1.6	0.78				
		1.8	0.78				
		2	0.78				

Completely Limited
Significantly Limited
Never Limited

Table B- 3. Max pos. lat. step results

Pilot Input	Trim Speed (kt)	Max Rotor L/W	Response Duration (s)	Primary Axis Rotor CP Status	Secondary Axis Rotor CP Status	Primary Axis Total CP Status	Secondary Axis Total CP Status
Lat. Pos. Step	0	1.2	4.24				
		1.4	4.24				
		1.6	4.24				
		1.8	4.24				
		2	4.24				
	20	1.2	1.12				
		1.4	1.12				
		1.6	1.12				
		1.8	1.12				
		2	1.12				
	40	1.2	1.06				
		1.4	1.06				
		1.6	1.06				
		1.8	1.06				
		2	1.06				
	60	1.2	0.62				
		1.4	0.62				
		1.6	0.62				
		1.8	0.62				
		2	0.62				
	80	1.2	0.56				
		1.4	0.56				
		1.6	0.56				
		1.8	0.56				
		2	0.56				

Completely Limited

Significantly Limited

Never Limited

Table B- 4. Pos. speed cmd. step results

Pilot Input	Trim Speed (kt)	Max Rotor L/W	Response Duration (s)	Primary Axis Rotor CP Status	Secondary Axis Rotor CP Status	Primary Axis Total CP Status	Secondary Axis Total CP Status
Speed Cmd. Step Pos.	0	1.2	3.48				
		1.4	3.48				
		1.6	3.48				
		1.8	3.48				
		2	3.48				
	20	1.2	>9				
		1.4	>9				
		1.6	>9				
		1.8	>9				
		2	>9				
	40	1.2	>9				
		1.4	>9				
		1.6	>9				
		1.8	>9				
		2	>9				
	60	1.2	>9				
		1.4	>9				
		1.6	>9				
		1.8	>9				
		2	>9				
	80	1.2	>9				
		1.4	>9				
		1.6	>9				
		1.8	>9				
		2	>9				

Completely Limited

Significantly Limited

Never Limited

Table B- 5. Neg. speed cmd. step results

Pilot Input	Trim Speed (kt)	Max Rotor L/W	Response Duration (s)	Primary Axis Rotor CP Status	Secondary Axis Rotor CP Status	Primary Axis Total CP Status	Secondary Axis Total CP Status
Speed Cmd. Step Neg.	0	1.2	>9				
		1.4	>9				
		1.6	>9				
		1.8	>9				
		2	>9				
	20	1.2	4.16				
		1.4	4.16				
		1.6	4.16				
		1.8	4.16				
		2	4.16				
	40	1.2	8.3				
		1.4	8.3				
		1.6	8.3				
		1.8	8.3				
		2	8.3				
	60	1.2	8.68				
		1.4	8.68				
		1.6	8.68				
		1.8	8.68				
		2	8.68				
	80	1.2	>9				
		1.4	>9				
		1.6	>9				
		1.8	>9				
		2	>9				

Completely Limited
Significantly Limited
Never Limited

Table B- 6. Max neg. long. and pos. ped. step results

Pilot Input	Trim Speed (kt)	Max Rotor L/W	Nz Response Duration (s)	Rdot Response Duration (s)	Primary Axis 1 Rotor CP Status	Primary Axis 2 Rotor CP Status	Secondary Axis Rotor CP Status	Primary Axis 1 Total CP Status	Primary Axis 2 Total CP Status	Secondary Axis Total CP Status
Neg. Long. & Pos. Ped Step	0	1.2	2.30	7.42	2.96	2.96	2.96	2.96	2.96	2.96
		1.6	2.30	5.82						
		2	2.30	5.78						
	20	1.2	1.74	>9	1.18	1.18	1.18	1.18	1.18	1.18
		1.6	1.74	>9						
		2	1.74	>9						
	40	1.2	0.70	1.56						
		1.6	0.70	1.46						
		2	0.70	1.40						

Completely Limited
Significantly Limited
Never Limited

Table B- 7. Max pos. long. and pos. lat. step results

Pilot Input	Trim Speed (kt)	Max Rotor L/W	Nz Response Duration (s)	Pdot Response Duration (s)	Primary Axis 1 Rotor CP Status	Primary Axis 2 Rotor CP Status	Secondary Axis Rotor CP Status	Primary Axis 1 Total CP Status	Primary Axis 2 Total CP Status	Secondary Axis Total CP Status
Pos. Long. & Pos. Lat Step	0	1.2	4.58	5.50	2.08	2.08	2.08	2.08	2.08	2.08
		1.6	2.36	4.78						
		2	1.98	4.62						
	20	1.2	6.00	3.68	5.06	5.06	5.06	5.06	5.06	5.06
		1.6	2.06	1.92						
		2	1.70	1.54						
	40	1.2	0.84	1.12	6.58	6.58	6.58			
		1.6	0.80	1.08						
		2	0.80	1.08						

Completely Limited
Significantly Limited
Never Limited

Table B- 8. Max neg. long. and pos. lat. step results

Pilot Input	Trim Speed (kt)	Max Rotor L/W	Nz Response Duration (s)	Pdot Response Duration (s)	Primary Axis 1 Rotor CP Status	Primary Axis 2 Rotor CP Status	Secondary Axis Rotor CP Status	Primary Axis 1 Total CP Status	Primary Axis 2 Total CP Status	Secondary Axis Total CP Status
Neg. Long. & Pos. Lat Step	0	1.2	2.36	4.40						
		1.6	2.36	4.40						
		2	2.36	4.40						
	20	1.2	2.18	1.24						
		1.6	2.18	1.24						
		2	2.18	1.24						
	40	1.2	0.98	1.04						
		1.6	0.98	1.04						
		2	0.98	1.04						

Completely Limited
Significantly Limited
Never Limited

Table B- 9. Max pos. lat. and neg. ped step results

Pilot Input	Trim Speed (kt)	Max Rotor L/W	Pdot Response Duration (s)	Rdot Response Duration (s)	Primary Axis 1 Rotor CP Status	Primary Axis 2 Rotor CP Status	Secondary Axis Rotor CP Status	Primary Axis 1 Total CP Status	Primary Axis 2 Total CP Status	Secondary Axis Total CP Status
Pos. Lat. & Neg. Ped Step	0	1.2	4.54	7.80	3.62	3.62	3.62	3.62	3.62	3.62
		1.6	4.50	5.80						
		2	4.44	5.72						
	20	1.2	1.78	>9	2.26	2.26	2.26	2.26	2.26	2.26
		1.6	1.20	>9						
		2	1.10	>9						
	40	1.2	1.30	3.54						
		1.6	1.12	3.44						
		2	1.06	3.40						

Completely Limited
Significantly Limited
Never Limited

Table B- 10. Max pos. lat. step rotor one failed results

Pilot Input	Trim Speed (kt)	Max Rotor L/W	Pdot Response Duration (s)	Primary Axis Rotor CP Status	Secondary Axis Rotor CP Status	Primary Axis Total CP Status	Secondary Axis Total CP Status
Lat. Pos. Step	0	1.8	4.24				
		2	4.24				
	20	1.8	1.12				
		2	1.12				
	40	1.8	Control system is bank angle hold. Bank angle does not return to wings level after rotor failure				
		2					

Rotor 1 Failure
Completely Limited
Significantly Limited
Never Limited

Table B- 11. Max pos. lat. step rotor two failed results

Pilot Input	Trim Speed (kt)	Max Rotor L/W	Pdot Response Duration (s)	Primary Axis Rotor CP Status	Secondary Axis Rotor CP Status	Primary Axis Total CP Status	Secondary Axis Total CP Status
Lat. Pos. Step	0	1.8	Doesn't Recover				
		2	4.22				
	20	1.8	1.12				
		2	1.12				
	40	1.8	1.06				
		2	1.06				

Rotor 2 Failure
Completely Limited
Significantly Limited
Never Limited

Table B- 12. Max neg. lat. step rotor one failed results

Pilot Input	Trim Speed (kt)	Max Rotor L/W	Pdot Response Duration (s)	Primary Axis Rotor CP Status	Secondary Axis Rotor CP Status	Primary Axis Total CP Status	Secondary Axis Total CP Status
Lat. Neg. Step	0	1.8	4.26				
		2	4.26				
	20	1.8	1.12	2.66	2.66	2.66	2.66
		2	1.12				
	40	1.8	Control system is bank angle hold. Bank angle does not return to wings level after rotor failure				
		2					

Rotor 1 Failure
Completely Limited
Significantly Limited
Never Limited

Table B- 13. Max neg. lat. step rotor two failed results

Pilot Input	Trim Speed (kt)	Max Rotor L/W	Pdot Response Duration (s)	Primary Axis Rotor CP Status	Secondary Axis Rotor CP Status	Primary Axis Total CP Status	Secondary Axis Total CP Status
Lat. Neg. Step	0	1.8	Doesn't Recover				
		2	4.26				
	20	1.8	1.12	>9	>9	>9	>9
		2	1.12				
	40	1.8	1.06				
		2	1.06				

Rotor 2 Failure
Completely Limited
Significantly Limited
Never Limited

Table B- 14. Max pos. ped. step rotor two failed results

Pilot Input	Trim Speed (kt)	Max Rotor L/W	Rdot Response Duration (s)	Primary Axis Rotor CP Status	Secondary Axis Rotor CP Status	Primary Axis Total CP Status	Secondary Axis Total CP Status
Ped. Pos. Step	0	1.8	Doesn't Recover				
		2	5.72				
	20	1.8	>9				
		2	>9				
	40	1.8	1.30				
		2	1.22				

Rotor 2 Failure
Completely Limited
Significantly Limited
Never Limited

Table B- 15. Max neg. ped. step rotor two failed results

Pilot Input	Trim Speed (kt)	Max Rotor L/W	Rdot Response Duration (s)	Primary Axis Rotor CP Status	Secondary Axis Rotor CP Status	Primary Axis Total CP Status	Secondary Axis Total CP Status
Ped. Neg. Step	0	1.8	Doesn't Recover				
		2	6.72	1.94	1.94	1.94	1.94
	20	1.8	>9	>9	>9	>9	>9
		2	>9	1.32	1.32	1.32	1.32
	40	1.8	1.64				
		2	1.54				

Rotor 2 Failure
Completely Limited
Significantly Limited
Never Limited

Table B- 16. Max decel. rotor one failed results

Pilot Input	Trim Speed (kt)	Max Rotor L/W	Response Duration (s)	Primary Axis Rotor CP Status	Secondary Axis Rotor CP Status	Primary Axis Total CP Status	Secondary Axis Total CP Status
Max Decel	150	1.8	49.48				
		2	49.48				

Rotor 1 Failure
Completely Limited
Significantly Limited
Never Limited

Table B- 17. Max decel. rotor two failed results

Pilot Input	Trim Speed (kt)	Max Rotor L/W	Response Duration (s)	Primary Axis Rotor CP Status	Secondary Axis Rotor CP Status	Primary Axis Total CP Status	Secondary Axis Total CP Status
Max Decel	150	1.8	52.80	15.54	15.54	15.54	15.54
		2	49.48				

Rotor 2 Failure
Completely Limited
Significantly Limited
Never Limited

Table B- 18. Max accel. rotor one failed results

Pilot Input	Trim Speed (kt)	Max Rotor L/W	Response Duration (s)	Primary Axis Rotor CP Status	Secondary Axis Rotor CP Status	Primary Axis Total CP Status	Secondary Axis Total CP Status
Max Accel	0	1.8	46.26	6.92	6.92	6.92	6.92
		2	47.16	1.24	1.24	1.24	1.24

Rotor 1 Failure
Completely Limited
Significantly Limited
Never Limited

Table B- 19. Max accel. rotor two failed results

Pilot Input	Trim Speed (kt)	Max Rotor L/W	Response Duration (s)	Primary Axis Rotor CP Status	Secondary Axis Rotor CP Status	Primary Axis Total CP Status	Secondary Axis Total CP Status
Max Accel	0	1.8	Doesn't Recover				
		2	44.92	5.38	5.38	5.38	5.38

Rotor 2 Failure
Completely Limited
Significantly Limited
Never Limited

Table B- 20. Max pos. long. and neg. ped step rotor one failed results

Pilot Input	Trim Speed (kt)	Max Rotor L/W	Nz Response Duration (s)	Rdot Response Duration (s)	Primary Axis 1 Rotor CP Status	Primary Axis 2 Rotor CP Status	Secondary Axis Rotor CP Status	Primary Axis 1 Total CP Status	Primary Axis 2 Total CP Status	Secondary Axis Total CP Status
Pos. Long. & Neg. Ped Step	0	1.8	>9	>9	>9	>9	>9	>9	>9	>9
		2	8.54	>9	6.62	6.62	6.62	6.62	6.62	6.62
	20	1.8	>9	>9	>9	>9	>9	>9	>9	>9
		2	>9	>9	7.78	7.78	7.78	7.78	7.78	7.78
	40	1.8	0.64	>9	>9	>9	>9	>9	>9	>9
		2	0.68	>9	>9	>9	>9	>9	>9	>9

Rotor 1 Failure
Completely Limited
Significantly Limited
Never Limited

Table B- 21. Max pos. long. and neg. ped. step rotor two failed results

Pilot Input	Trim Speed (kt)	Max Rotor L/W	Nz Response Duration (s)	Rdot Response Duration (s)	Primary Axis 1 Rotor CP Status	Primary Axis 2 Rotor CP Status	Secondary Axis Rotor CP Status	Primary Axis 1 Total CP Status	Primary Axis 2 Total CP Status	Secondary Axis Total CP Status
Pos. Long. & Neg. Ped Step	0	1.8	Doesn't Recover							
		2	>9	>9	>9	>9	>9	>9	>9	>9
	20	1.8	>9	>9	>9	>9	>9	>9	>9	>9
		2	>9	>9	>9	>9	>9	>9	>9	>9
	40	1.8	1.62	2.18	>9	>9	>9			
		2	1.50	1.78	2.60	2.60	2.60			

Rotor 2 Failure
Completely Limited
Significantly Limited
Never Limited

Table B- 22. Max pos. long. and neg. lat. step rotor one failed results

Pilot Input	Trim Speed (kt)	Max Rotor L/W	Nz Response Duration (s)	Pdot Response Duration (s)	Primary Axis 1 Rotor CP Status	Primary Axis 2 Rotor CP Status	Secondary Axis Rotor CP Status	Primary Axis 1 Total CP Status	Primary Axis 2 Total CP Status	Secondary Axis Total CP Status
Pos. Long. & Neg. Lat Step	0	1.8	>9	6.96	>9	>9	>9	>9	>9	>9
		2	5.44	5.60	2.88	2.88	2.88	2.88	2.88	2.88
	20	1.8	Begins Low Frequency Limit Cycle Oscillation							
		2	8.22	3.98	7.08	7.08	7.08	7.08	7.08	7.08
	40	1.8	Control system is bank angle hold. Bank angle does not return to wings level after rotor failure							
		2								

Rotor 1 Failure
Completely Limited
Significantly Limited
Never Limited

Table B- 23. Max pos. long. and neg. lat. step rotor two failed results

Pilot Input	Trim Speed (kt)	Max Rotor L/W	Nz Response Duration (s)	Pdot Response Duration (s)	Primary Axis 1 Rotor CP Status	Primary Axis 2 Rotor CP Status	Secondary Axis Rotor CP Status	Primary Axis 1 Total CP Status	Primary Axis 2 Total CP Status	Secondary Axis Total CP Status
Pos. Long. & Neg. Lat Step	0	1.8	Doesn't Recover							
		2	7.78	5.68	4.32	4.32	4.32	4.32	4.32	4.32
	20	1.8	Begins Low Frequency Limit Cycle Oscillation							
		2	7.70	4.26	>9	>9	>9	>9	>9	>9
	40	1.8	0.70	1.56	>9	>9	>9	>9	>9	>9
		2	0.72	1.20	>9	>9	>9	>9	>9	>9

Rotor 2 Failure
Completely Limited
Significantly Limited
Never Limited

Table B- 24. Max neg. lat. and neg. pos. rotor one failed results

Pilot Input	Trim Speed (kt)	Max Rotor L/W	Pdot Response Duration (s)	Rdot Response Duration (s)	Primary Axis 1 Rotor CP Status	Primary Axis 2 Rotor CP Status	Secondary Axis Rotor CP Status	Primary Axis 1 Total CP Status	Primary Axis 2 Total CP Status	Secondary Axis Total CP Status
Neg. Lat. & Neg. Ped Step	0	1.8	5.12	>9	>9	>9	>9	>9	>9	>9
		2	4.62	6.74	2.02	2.02	2.02	2.02	2.02	2.02
	20	1.8	2.00	>9	>9	>9	>9	>9	>9	>9
		2	1.62	>9	1.50	1.50	1.50	1.50	1.50	1.50
	40	1.8	Control system is bank angle hold. Bank angle does not return to wings level after rotor failure							
		2								

Rotor 1 Failure
Completely Limited
Significantly Limited
Never Limited

Table B- 25. Max neg. lat. and neg. ped. step rotor two failed results

Pilot Input	Trim Speed (kt)	Max Rotor L/W	Pdot Response Duration (s)	Rdot Response Duration (s)	Primary Axis 1 Rotor CP Status	Primary Axis 2 Rotor CP Status	Secondary Axis Rotor CP Status	Primary Axis 1 Total CP Status	Primary Axis 2 Total CP Status	Secondary Axis Total CP Status
Neg. Lat. & Neg. Ped. Step	0	1.8	Doesn't Recover							
		2	4.52	>9	2.20	2.20	2.20	2.20	2.20	2.20
	20	1.8	2.08	>9	>9	>9	>9	>9	>9	>9
		2	1.52	>9	1.34	1.34	1.34	1.34	1.34	1.34
	40	1.8	1.32	1.42						
		2	1.20	1.36						

Rotor 2 Failure
Completely Limited
Significantly Limited
Never Limited